UAB
Universitat Autònoma de Barcelona

It takes two to tango:
Transcriptome remodelling and mitochondrial metabolism during oocyte's meiotic maturation

Sara Pietroforte

UAB
Universitat Autònoma de Barcelona

It takes two to tango:

Transcriptome remodelling and mitochondrial metabolism during oocyte's meiotic maturation

Sara Pietroforte

Memoria presentada para optar al Grado de Doctora en Biología Celular en la Universidad Autónoma de Barcelona.

Tesis doctoral inscrita en el Departament de Biologia Cel·lular, Fisiologia i Immunologia, Facultat de Biociències, Universitat Autònoma de Barcelona.

Directores:

Dra. Rita Vassena

Dra. Elena Ibáñez de Sans (Tutor)

Dr. Filippo Zambelli

2023

La **Dra. Rita Vassena**, investigadora senior, Ex Directora Científica Global - Eugin Group y CEO Fecundis,

la **Dra. Elena Ibáñez de Sans**, profesora agregada del Departament de Biologia Cel·lular, Fisiologia i Immunologia de la Universitat Autònoma de Barcelona

y el **Dr. Filippo Zambelli,** investigador senior en el Departamento de Research and Development de Eugin Group en Barcelona

CERTIFICAN

Que **Sara Pietroforte** ha realizado bajo su dirección el trabajo de investigación que se expone en la memoria titulada "**It takes two to tango: Transcriptome remodelling and mitochondrial metabolism during oocyte's meiotic maturation**" para optar al Grado de Doctora por la Universitat Autònoma de Barcelona.

Y para que así conste, firmamos el presente certificado.

Bellaterra, 09 de julio de 2023

Dra. Rita Vassena Dra. Elena Ibáñez de Sans Dr. Filippo Zambelli

The project presented here has received funding from the European Union's Horizon 2020 research and innovation programme under the Marie Skłodowska-Curie grant agreement N. 860960. Sara Pietroforte was enrolled in this Marie Skłodowska-Curie ITN *EUROVA* programme, and her thesis project was carried out in collaboration between the Research and Development laboratory of Eugin Group in Barcelona and the Department of Cell Biology, Physiology and Immunology, of the Universitat Autònoma de Barcelona.

TABLE OF CONTENTS

ABBREVIATIONS AND ACRONIMS

5'Cap: 5' Capping

AC3: Adenylyl cyclase 3

ADP: Adenosine Diphosphate

AFC: Antral Follicular Count

Alt 3'/5': Alternative splice site at 3'/5'

AMA: Advanced Maternal Age

AMH: anti-Mullerian hormone

aMTOC: Acentriolar Microtubule Organization Centre

APA: Alternative polyadenylation

APC2: Adenomatosis Polyposis Coli 2

Arp2/3: Actin Related Protein 2/3

ART: Assisted Reproductive Technologies

AS: Alternative Splicing

ATP: Adenosine Triphosphate

AU: Arbitrary Unit

AUC: Area Under the Curve

AURKB: Aurora Kinase family

BMI: Body Mass Index

BMP15: Bone Morphogenetic Protein 15

BSA: Bovine Serum Albumin

BUB1B: BUB1 Mitotic Checkpoint Serine/Threonine Kinase B

Ca^{2+}: Calcium ion

cAMP: Cyclic Adenosine Monophosphate

CAST: Calpastatin

CBP20 (NCBP2): Nuclear Cap Binding Protein Subunit 2

CBP80 (NCBP1): Nuclear Cap Binding Protein Subunit 1

CCs: Cumulus cells

CDC25: Cell Division Cycle 25C

CDK1: Cyclin-Dependent Kinase 1

cDNA: complementary DNA

CDS: Coding sequence

CENP: Centromere Protein family

CENPE: Centromere Protein E

cGMP: cyclic guanosine monophosphate

CGs: Cortical Granules

CHEK1: Checkpoint Kinase 1

CNOT6L: CCR4-NOT Transcription Complex Subunit 6 Like

COC: Cumulus-Oocyte Complex

CoQ10: Co-enzyme Q10

CTRL: Control

DEGs: Differentially expressed genes

D-LAT: Dihydrolipoamide S-Acetyltransferase

DMSO: Dimethyl sulfoxide

DNA: Deoxyribonucleic Acid

dPSI: differential PSI

EGA: Embryonic Genome Activation

EGFP-MAP4: engineered Green Fluorescent Protein- Microtubule-associated protein 4

eIF4A3: Eukaryotic Translation Initiation Factor 4A3

eIF4F: Eukaryotic Translation Initiation Factor 4F

ER: Endoplasmic Reticulum

EX: Exon skipping

FAD+/FADH2: Flavine-adenine dinucleotide

FBXO43: F-box protein 43

FCCP: Carbonyl cyanide-p-trifluoromethoxyphenylhydrazone

FDR: False Discovery Rate

FLIM: Fluorescence Lifetime Imaging Microscopy

FMN2: Formin 2

FRG1: FSHD Region Gene 1

FSH: Follicle Stimulating Hormone

FSHR: Follicle Stimulating Hormone Receptor

FTM-GV: GV that failed to mature after IVM

GDP: Guanosine Diphosphate

GnRH: Gonadotropin-Releasing Hormone

GO: Gene Ontology

GRch38: Genome Reference Consortium Human Build 38

GSEA: Gene Set Enrichment Analysis

GTP: Guanosine Triphosphate

GV oocyte: Germinal Vesicle oocyte

GVBD: Germinal Vesicle Breakdown

H2B-mRFP1: Histone2B-monomeric Red Fluorescent Protein

H2O2: hydrogen peroxide

hCG: Human chorionic gonadotropin

HEPES: 4-(2-hydroxyethyl)-1-piperazineethanesulfonic acid

ICSI: Intracytoplasmic Sperm Injection

IF: Immunofluorescence

IR: Intron retention

IU: International Unit

IUI: Intrauterine insemination

IVF: In Vitro Fertilization

IVM: In vitro maturation

IVM-MII: In vitro matured Metaphase II oocytes

IVO-MII: In vivo matured Metaphase II oocytes

JMY: Junction Mediating And Regulatory Protein

k-fibers: Kinetochore Fibers

KIF23: Kinesin Family Member 23

KIFC1: Kinesin Family Member C1

KIT: KIT Proto-Oncogene, Receptor Tyrosine Kinase

LH: Luteinizing Hormone

lncRNA: long non-coding RNA

Log2FC: log2 Fold Change

MAGOH: Mago Homolog, Exon Junction Complex Subunit

MAPK: Microtubule Associated Proteins Kinase

MARDO: mitochondria-associated ribonucleoprotein domain

MEIOC: Meiosis Specific With Coiled-Coil Domain

MI oocyte: Metaphase I oocyte

MII oocyte: Metaphase II oocyte

MLH1: MutL Homolog 1

MPF: M-phase promoting factor

mRNA: messenger RNA

mtDNA: mitochondrial DNA

MTOC: Microtubule Organizing Centre

mTOR: Mammalian Target Of Rapamycin

MYT1: Myelin Transcription Factor 1

NADH: Nicotinamide adenine dinucleotide

NADPH: Nicotinamide adenine phosphate dinucleotide

NDJ: Non-disjunction

NIPBL: NIPBL Cohesin Loading Factor

NPR2: Atrial Natriuretic Peptide Receptor 2

NS: not significant

NSN: non-surrounded nucleolus

NUF2: NUF2 Component Of NDC80 Kinetochore Complex

O2-: superoxide ion

OH-: hydroxyl ion

OXPHOS: oxidative phosphorylation

PAPOLG: Poly(A) Polymerase Gamma

PAU: usage of alternative poly(A)

PB: Polar Body

PCA: Principal Component Analysis

PCM1: Pericentriolar Material 1

PDE3A: Phosphodiesterase 3A

PFA: Paraformaldehyde

PKA: Protein kinase A

POGZ: Pogo Transposable Element Derived with ZNF Domain

POI: Premature Ovarian Insufficiency

POI-like: similar to POI

poly(A) tail: polyadenylated tail

PRPF18: Pre-MRNA Processing Factor 18

PRPF8: Pre-mRNA Processing Factor 8

PSI: Percent Spliced-In Index

PSMC3IP: Proteasome 26S Subunit, ATPase 3 Interacting Protein

PSSC: Premature separation of sister chromatids

qPCR: quantitative Polymerase Chain Reaction

RanGAP: Ran GTPase Activating Protein

RER: Rough Endoplasmic Reticulum

RNA: Ribonucleic acid

RNASEH2A: Ribonuclease H2 Subunit A

RNF4: Ring Finger Protein 4

RNU5D: RNA, U5D Small Nuclear 1

ROS: Reactive oxygen species

RPP40: Ribonuclease P/MRP Subunit P40

rRNA: ribosomal RNA

RS: Reverse segregation

SAC: Spindle Assembly Checkpoint

scRNA-seq: Single cell RNA sequencing

SD: Standard Deviation

SER: Smoot Endoplasmic Reticulum

SF3B: Splicing Factor 3b

SIRT2: Sirtuin 2

SN: Surrounded nucleolus

SNX14: Sortin Nexin 14

SOHLH1: Spermatogenesis And Oogenesis Specific Basic Helix-Loop-Helix 1

SPDL1: Spindle Apparatus Coiled-Coil Protein 1

SPIN1: Spindlin 1

SREK1: Splicing Regulatory Glutamic Acid And Lysine Rich Protein 1

SRSF3: Serine and Arginine Rich Splicing Factor 3

STAG1: Stromal Antigen 1

STAG3: Stromal Antigen 3

STAR: Steroidogenic Acute Regulatory Protein

SYCE1: Synaptonemal Complex Central Element Protein 1

TCM-199: Tissue Culture Medium-199

TCSPC: time-correlated single photon counting

THOCs: THO Complexes

TNRC6A: Trinucleotide Repeat Containing Adaptor 6A

TOMM20: Translocase of outer mitochondrial membrane, 20

TREX: transcription-export complex

TUBB8: Tubulin Beta 8 Class VIII

TZPs: Transzonal Projection

U1-U6 snRNPs: U-rich small nuclear ribonucleoproteins

UTR: Untranslated Region

VastDB: *Vast-tools* database

WAVE (WASF1): Wiskott-Aldrich Syndrome Protein Family Member 1

WEE1B: WEE2 Oocyte Meiosis Inhibiting Kinase

WHO: World Health Organization

YTHDC1: YTH N6-Methyladenosine RNA Binding Protein C1

ZAR1: Zygote Arrest 1

ZP: Zona Pellucida

ΔPPAU: difference in average of proximal PAU

ABSTRACT

Meiotic maturation is a highly regulated process, key to produce competent oocytes and, consequently, successful embryo development after fertilization. Several studies have been conducted to understand the biological mechanisms driving oocyte maturation, with a strong interest for the transcriptome and mitochondrial metabolism. However, the exact role of these elements during oocyte maturation and their link with a successful meiosis progression still remains elusive. This thesis was aimed, first, at understanding the role of transcriptome remodelling and mitochondrial metabolism during final meiotic maturation of human oocytes and then, to clarify the effect of aging on these mechanisms.

In the first study, we aimed at elucidating the transcriptome of oocytes undergoing final meiotic maturation using single cell RNA-sequencing. The evaluation of oocytes from young women revealed abundant transcriptome remodelling, both in global gene expression and in specific mRNA processing, needed for meiosis progression. Interestingly, we found similar profiles between *in vitro* and *in vivo* matured oocytes, and we revealed that germinal vesicle (GV) oocytes that failed to mature *in vitro* had a similar transcriptional profile to GV oocytes at retrieval.

In the second study, we aimed at defining an animal model to study the decrease in oocyte quality associate with aging. We identified, by single cell RNA-sequencing, the failure to remodel the transcriptome as a possible cause of oocyte quality decay in a cow model of premature ovarian insufficiency.

In the final study, we focused on the identification of mitochondrial dynamics through oocyte's meiotic maturation and on changes induced by aging. We found mitochondria were distributed throughout the whole cytoplasm, but that active mitochondria specifically localized to the subcortical area of the oocyte. Moreover, we observed a dynamic reorganization of mitochondria through maturation. These distributions were confirmed with several techniques, both indirect, as immunofluorescence, and direct ones, as live dyes staining or non-invasive live imaging. We found that maturing oocytes need an increase in mitochondrial metabolism to reach the metaphase II stage and that oocytes from young women have a similar metabolic profile during maturation, while oocytes from advanced maternal age (AMA) women present higher metabolic oscillations. The comparison between young and AMA oocytes identified lower mitochondrial activity and lower mitochondrial metabolism in AMA oocytes, concordant

with a reduced ability of these oocytes to successfully accomplish meiotic maturation *in vitro*, compared to the young ones. Finally, a loss of function experiment in young oocytes with a mitochondrial inhibitor linked a poor mitochondrial metabolism with the decreased ability to mature, suggesting a key role of the correct range of metabolism through meiosis.

Overall, the present thesis has dissected transcriptome remodelling and mitochondrial metabolism during meiotic maturation of human oocytes, and elucidated the changes on these elements that can affect oocyte quality, meiotic progression and, ultimately, oocyte competence.

RESUMEN

La maduración meiótica es un proceso altamente regulado, clave para producir ovocitos competentes y, en consecuencia, un desarrollo embrionario exitoso tras la fecundación. Se han realizado varios estudios para comprender los mecanismos biológicos que impulsan la maduración oocitaria, con un gran interés por el transcriptoma y el metabolismo mitocondrial. Sin embargo, el papel exacto de estos elementos durante la maduración del ovocito y su relación con una progresión exitosa de la meiosis sigue siendo esquivo. El objetivo de esta tesis fue, en primer lugar, comprender el papel de la remodelación del transcriptoma y el metabolismo mitocondrial durante la maduración meiótica final de los ovocitos humanos y, a continuación, aclarar el efecto del envejecimiento sobre estos mecanismos.

En el primer estudio, nos propusimos dilucidar el transcriptoma de los ovocitos sometidos a maduración meiótica final mediante “single cell RNA sequencing”. La evaluación de ovocitos de mujeres jóvenes reveló una extensa remodelación del transcriptoma, tanto en la expresión génica global como en el procesamiento específico de mRNA, necesaria para la progresión de la meiosis. Curiosamente, encontramos perfiles similares entre los ovocitos madurados in vitro e in vivo, y revelamos que los ovocitos en vesícula germinal (GV) que no maduraron in vitro tenían un perfil transcripcional similar al de los ovocitos GV en el momento de la recuperación.

En el segundo estudio, nos propusimos definir un modelo animal para estudiar la disminución de la calidad ovocitaria asociada al envejecimiento. Identificamos, mediante “single cell RNA sequencing”, el fallo en la remodelación del transcriptoma como posible causa del deterioro de la calidad ovocitaria en un modelo vacuno de insuficiencia ovárica prematura.

En el estudio final, nos centramos en la identificación de la dinámica mitocondrial a lo largo de la maduración meiótica del ovocito y en los cambios inducidos por el envejecimiento. Encontramos que las mitocondrias se distribuían por todo el citoplasma, pero que las mitocondrias activas se localizaban específicamente en la zona subcortical del ovocito. Además, observamos una reorganización dinámica de las mitocondrias a lo largo de la maduración. Estas distribuciones se confirmaron con varias técnicas, tanto indirectas, como inmunofluorescencia, como directas, como tinción con colorantes vivos o imagen en vivo no invasiva. Observamos que los ovocitos en proceso de maduración

necesitan un aumento del metabolismo mitocondrial para alcanzar el estadio de metafase II y que los ovocitos de mujeres jóvenes tienen un perfil metabólico similar durante la maduración, mientras que los ovocitos de mujeres de edad materna avanzada (AMA) presentan mayores oscilaciones del perfil metabólicos. La comparación entre ovocitos jóvenes y AMA identificó una menor actividad mitocondrial y un menor metabolismo mitocondrial en los ovocitos AMA, concordante con una menor capacidad de estos ovocitos para llevar a cabo con éxito la maduración meiótica in vitro, en comparación con los jóvenes. Por último, un experimento de pérdida de función en ovocitos jóvenes con un inhibidor mitocondrial relacionó un metabolismo mitocondrial deficiente con la disminución de la capacidad de maduración, lo que sugiere un papel clave del rango correcto de metabolismo durante la meiosis.

En conjunto, la presente tesis ha diseccionado la remodelación del transcriptoma y el metabolismo mitocondrial durante la maduración meiótica de ovocitos humanos, y ha dilucidado los cambios en estos elementos que pueden afectar a la calidad ovocitaria, la progresión meiótica y, en última instancia, la competencia ovocitaria.

INTRODUCTION

According to Aristotle, the first embryologist known to history, science begins with wonder. “It is owing to wonder that people began to philosophize, and wonder remains the beginning of knowledge” (Aristotle, *Metaphysics*, ca. 350 BCE). The development of animals from a single egg has been a source of wonder throughout history. Aristotle observed a simple procedure of cracking open chick eggs, where a tiny pool of cells give rise to a bird. Anyone can wonder at this remarkable, even commonplace, phenomenon; however, it is the scientist who dedicates her life to discover how development actually occurs. And rather than dissipating wonder, new knowledge increases it.

1. “*Ex Ovo Omnia*”: THE OOCYTE

1.1 The oocyte’s journey

“*Omne Vivum Ex Ovo*“, “From the egg comes all” (William Harvey 1578-1657). The development of mature oocyte, from which all comes, is probably one of the most complicated and long processes in the human body, since it starts before birth with oogenesis and ends with ovulation, many years later.

1.1.1 Folliculogenesis

Folliculogenesis is the process of antral follicle formation, known as the spherical cyst, that encapsulates the maturing oocyte. It is a process that occurs within the cortex of the ovary in our species. The main purpose of this process is to produce a single dominant follicle from a pool of follicles in different growing stages.

Follicles in the ovary can be found in four different stages: primordial, primary, secondary and antral (**Figure 1**). All primordial follicles present in the fetal human ovaries reach the maximum number (four million on average) at 18-22 weeks post conception (Wallace and Kelsey, 2010). The total number of primordial follicles, which represents the ovarian reserve, decreases throughout the reproductive life until menopause.

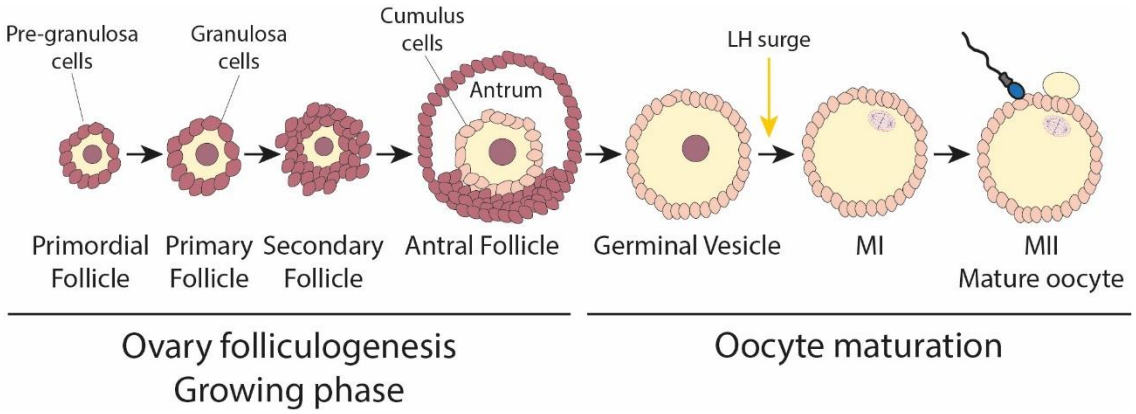

Figure 1. Folliculogenesis and oocyte maturation. Oocyte development is the process from folliculogenesis to Metaphase II oocyte formation. It is a complex process that involves several signalling cascades and crucial cell-to-cell communication between granulosa cells and oocyte. During the growing phase, the diameter of the oocyte increases more than 100 times to reach approximately 100 µm. Oocytes are already arrested at meiotic prophase I when they are in the stage of primordial follicles and will continue being arrested for most of their life cycle.

During human fetal life, the first step of folliculogenesis begins with the primordial follicle, a small dormant follicle of 0.03-0.05 mm in diameter, that contains a flattened layer of squamous granulosa cells surrounding the oocyte. Concomitant with the primordial follicle grow, the change of the granulosa cells from squamous to cuboidal structure, produces the primary or preantral follicle. The change in shape of the granulosa cells is followed by the expression of Follicle Stimulating Hormone (FSH) receptors and

the beginning of RNA synthesis and mitosis, a process controlled by autocrine/paracrine mechanisms (Yamoto et al., 1992; Oktay et al, 1997).

The transition from primary to secondary follicle is characterized by an increase in diameter of the follicle (from 0.1 mm to 1.2-0.4 mm) (Johnson and Everitt, 2003). This increase is due to the ongoing mitotic divisions of the granulosa cells, which end up forming six to nine layers around the oocyte. One of the most important events in the secondary follicle development is the condensation of the stromal cells surrounding the primary follicle to form the theca layer (Johnson and Everitt, 2003). The theca layer is formed around the basal lamina, and it undergoes cytodifferentiation into theca interna and theca externa. At the same time, an extensive network of capillary vessels is formed between these two layers and blood begins to bring hormones and nutrients.

The transition from secondary to antral follicle occurs only when a woman enters puberty. This transition begins with the appearance of a fluid-filled cavity in the granulosa cells, known as the antrum. This process is called cavitation and it is controlled by autocrine/paracrine mechanisms, such as growth factors and KIT (KIT Proto-Oncogene, Receptor Tyrosine Kinase) ligands (Li et al., 1995; Yoshida et al, 1997). At this stage of folliculogenesis, the basic structure of the follicle is established, and it will not change in appearance nor in complexity during final growth. Nevertheless, there are dramatic changes in the size of the antral follicle, explained in part by the high rate of mitotic divisions of the theca and the granulosa cells, only hampered by the availability of FSH and luteinising hormone (LH). These hormones are also crucial for follicular fluid formation, which leads to an increase in the antrum volume and, therefore, in the follicle size (Palermo, 2007). All these events lead to the formation of multiple antral follicles with same structure but that can vary in size, from 0.4 to 20 mm. The granulosa cells of the antral follicle are divided into four different regions, depending on their position within the follicle: the corona radiata, surrounding the zona pellucida (ZP), granulosa and periantral, and the cumulus oophorous, a cluster of cumulus cells (CCs) that connect the granulosa and corona radiata together and that are crucial for oocyte maturation.

Antral follicles have only two possible fates: continue development or undergo atresia. The one that continues development becomes progressively more differentiated, until it reaches the preovulatory stage. In contrast, atretic follicles are normally smaller than 10

mm in diameter since their granulosa cells arrest division and begin the expression of apoptotic genes (Johnson and Everitt, 2003).

The fate of antral follicles is determined by the increase in FSH levels. If the follicle is located in an area of the ovary with lower concentration of FSH or the follicle itself presents fewer FSH receptors in its CCs, it will not be able to develop further, becoming atretic (Palermo, 2007; Baerward et al., 2012).

At the end, only one follicle will be viable, the dominant follicle (Palermo, 2007). The granulosa cell of this dominant follicle begin division rapidly, leading to rapid growth of the follicle size up to 20 mm in diameter.

Finally, following the LH surge from the pituitary gland, an opening is formed in the preovulatory follicle, the oocyte surrounded by CCs is released to the oviduct and the oocyte exits dictyate arrest to resume meiosis (Hutt and Albertini, 2007). This final stage, known as ovulation, marks the end of folliculogenesis.

1.1.2 Menstrual cycle

The menstrual cycle is a complex sequence of events coordinated by female hormones that cause regular bleeding, and it is generally divided into four phases characterized by histological changes that take place in the uterine endometrium: proliferative phase, luteal or secretory phase, pre-menstrual or ischemic phase, and menstruation (Johnson and Everitt, 2003).

Considering the ovarian changes associated to this cycle, the first half of the menstrual cycle is called follicular phase. At the beginning of this phase, estrogen levels are low, and gonadotropin-releasing hormone (GnRH) starts stimulating the pituitary gland to secrete FSH and low levels of LH. These hormones cooperate to stimulate the growth of several follicles, each containing an oocyte. Around day seven of the menstrual cycle, estrogen levels in blood rise significantly and begin to inhibit the secretion of FSH. When FSH levels decrease, smaller follicles stop growing and undergo atresia. At the end of the follicular phase, midway of the menstrual cycle (around day 14), estrogen levels are sufficiently high to stimulate GnRH production, which in turn stimulates the pituitary gland to secrete FSH and LH. The sudden release of LH triggers the final maturation and

release of the mature oocyte from the follicle. After ovulation, the follicle transforms into the corpus luteum (Wallace & Kelsey, 2010).

With ovulation, the luteal phase begins. During this phase, the corpus luteum produces high amount of progesterone, in addition to estrogen, to prepare the lining of the endometrium for implantation. Under the influence of progesterone, the endometrium changes its histology in response to hormonal cues (Yamoto et al., 1992; Oktay et al., 1997; Johnson and Everitt, 2003; Palermo, 2007; Wallace & Kelsey, 2010).

If oocyte fertilization and embryo implantation occur, the corpus luteum continues to produce progesterone until about 10 weeks of gestation, preventing the flaking of the endometrium. Otherwise, if the implantation of the embryo does not occur, circulating levels of progesterone decrease as the corpus luteum degenerates and the endometrium is shed, leading to bleeding **(Figure 2**) (Yamoto et al., 1992; Oktay et al., 1997; Johnson and Everitt, 2003; Hutt & Albertini, 2007; Palermo, 2007; Wallace & Kelsey, 2010).

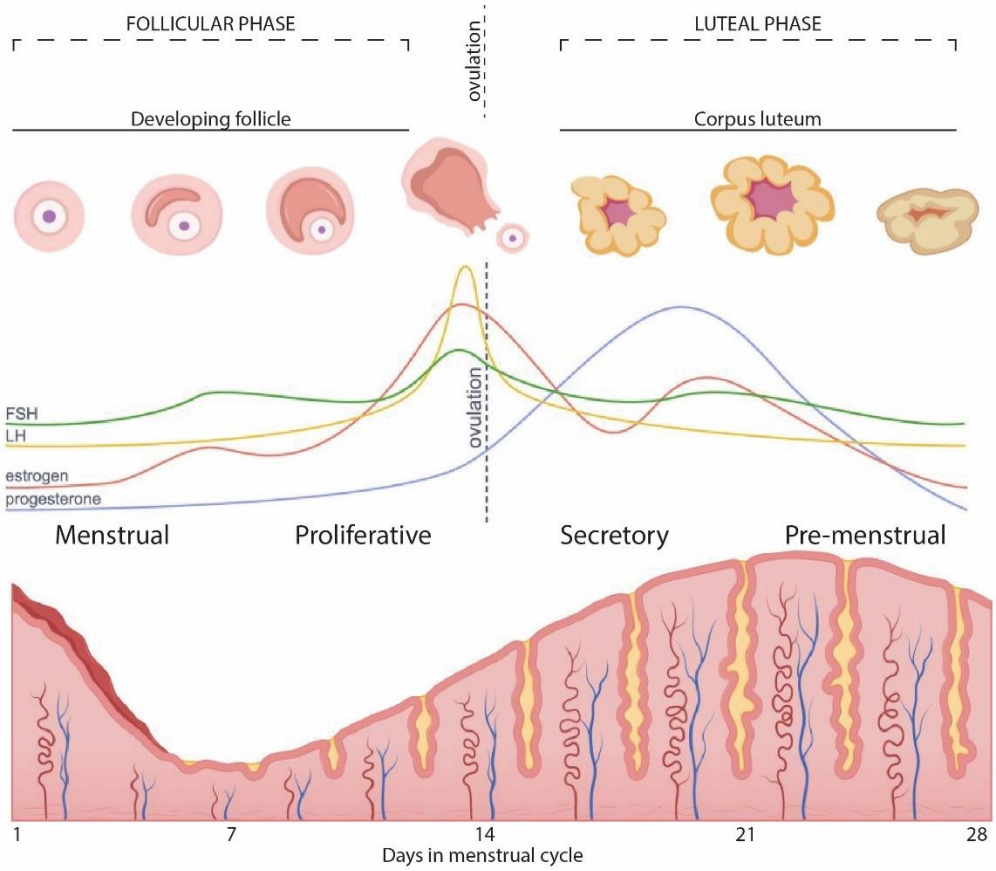

Figure 2. Menstrual cycle. Representation of the different phases of the menstrual cycle: menstrual, proliferative phase, luteal or secretory phase and pre-menstrual or ischemic phase. In different colours are reported the changes of the main hormones involved, FSH in green, LH in yellow, estrogen in red and progesterone in blue. The characterization of changes in follicles are reported divided into the two main phases, follicular and luteal. (*Different sections in part adapted from BioRender.com*)

1.1.3 Oocyte development

In the developing embryo, immediately after sex differentiation, female germ cells continue to proliferate through mitotic divisions with incomplete cytokinesis, to form oogonia cysts. In response to retinoic acid signals, oogonia start meiosis and differentiate into primary oocytes (Bowles et al., 2006; Koubova et al., 2006). Meiosis is initiated with prophase I between 12-16 weeks post-coitum (Zuccotti et al., 1998; Albertini et al., 2001; Zuccotti et al., 2011), and is divided into five sub-stages based on the conformation of chromosomes: leptotene (prophase begins, chromosome start to condense), zygotene (synapsis begins), pachytene (crossing over), diplotene (synapsis ends) and diakinesis

(prophase ends, nuclear membrane disintegrates) (**Figure 3**). Primary oocytes arrest at the dictyate stage, defined as the prolonged resting phase in oogenesis where oocytes remain quiescent until puberty (Revenkova et al., 2010), as they form the storage pool awaiting the hormonal signal for meiosis resumption (Jones, 2004; Jones, 2008). It is also during this time that most oocytes in the ovary undergo apoptosis, whereby less than 30% of them will continue their development. When meiosis resumes, the germ cell breaks down. Oocytes are then assembled into primordial follicles with pre-granulosa cells; the primordial follicles are essentially the accumulation of germ cells for the entire female reproductive life.

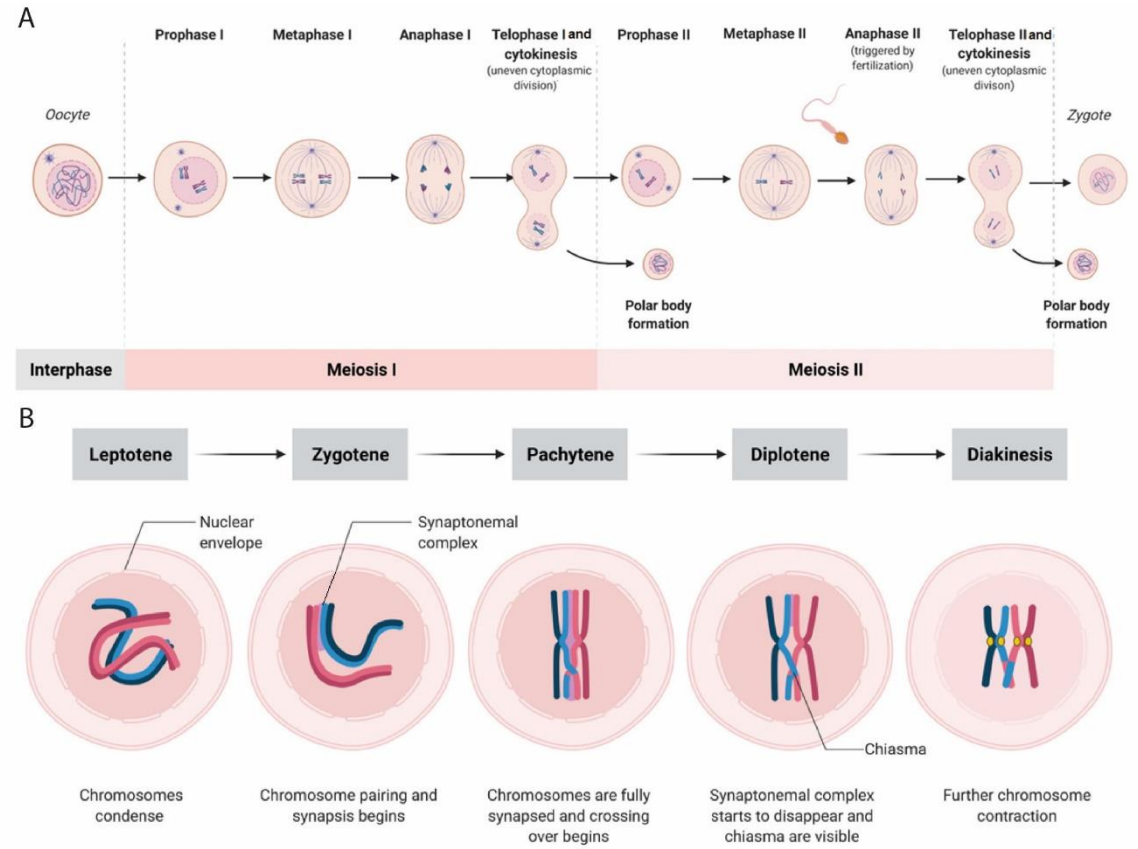

Figure 3. Female germ cell development. (**A**) Graphic representation of the processes of meiosis I and II of human oocyte and zygote formation after fertilization. (**B**) Focus on the physiological stages of prophase I (first meiotic division) in oocytes: leptotene, zygotene, pachytene, diplotene, and diakinesis stages. (*Adapted from Wasielak-Politowska and Kordowitzki, 2022*)

1.2 Oocyte structure

The human oocyte, the female gamete, can be divided into two main parts. The first part is the oocyte itself, that includes both the cytoplasm and the genetic material, and is surrounded by the oolemma and the ZP (**Figure 4**). The second part is the cumulus oophorous, composed of several layers of somatic granulosa cells that further surround the oocyte. The oocyte with its granulosa cells constitutes a functional unit called the Cumulus Oocyte Complex (COC) (Litscher et al., 2009; Zhang & Jiang, 2010; Claw & Swanson, 2012; Rienzi et al., 2012).

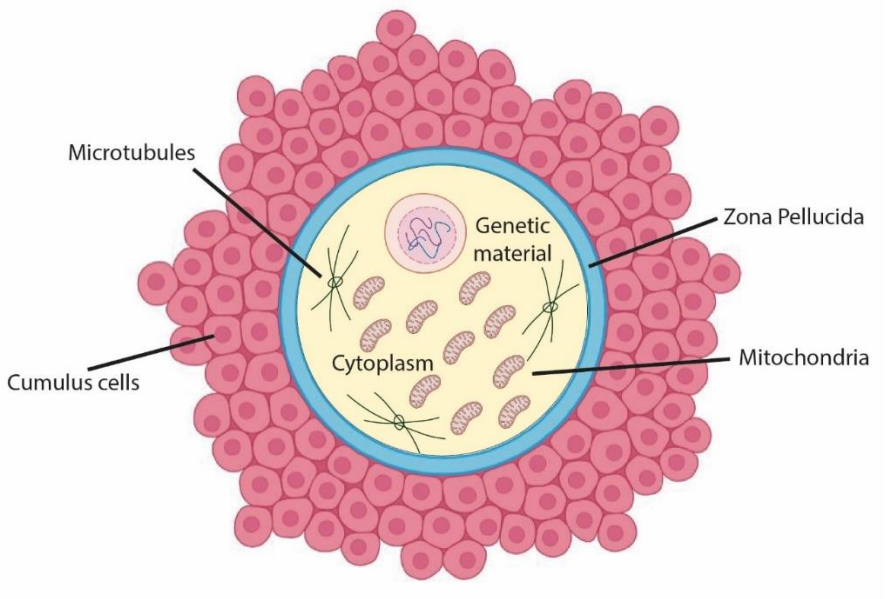

Figure 4. The oocyte. Oocyte structure can be divided into two main parts: the oocyte itself, composed of cytoplasm, the genetic material and the zona pellucida, and the cumulus oophorous mainly composed of cumulus cells.

The oocyte cytoplasm is enriched in maternally derived proteins and RNAs, and contains the maternal genetic material, mitochondria, and other organelles. The ZP is an extracellular glycoprotein matrix that surrounds and protects the oocyte, but its main function is to provide species-specific fertilization (Zhang & Jiang, 2010; Claw and Swanson, 2012; Rienzi et al., 2012) and to avoid polyspermy. In humans, four different ZP glycoproteins (ZPG 1 to 4) form a unique code recognizable by the spermatozoon

(Litscher et al., 2009; Pang et al., 2011). Upon fertilization, ZPG2 is cleaved, changing the three-dimensional structure of the ZPG complex. This conformational change will prevent fertilization by other spermatozoa (polyspermy).

The cumulus oophorous is formed by CCs (somatic granulosa cells). The CCs are necessary for a correct oocyte development since they directly communicate with the oocyte, mediating the bidirectional transmission of regulatory factors and nutrients through gap junctions (Van Soom et al., 2002; Huang & Wells, 2010a; Turathum et al., 2021a).

1.3 Microtubules

Microtubules are intracellular cylindric filaments of about 25 nm in diameter and one of the elements of the cytoskeleton, together with the actin fibers and the intermediate filaments (Burbank et al., 2006; Burbank and Mitchison, 2006).

Microtubules are hollow tubular polymers mainly composed of α- and β- tubulin dimers, very similar in structure and size (about 55kDa each) (Wade, 2009; Goodson & Jonasson, 2018). Moreover, the 450-residue-long peptides present an identity of 41% between them (Krauhs et al., 1981; Little et al., 1981; Ponstingl et al., 1981; Goodson & Jonasson, 2018). α- and β- tubulin are high conserved across all eukaryotic species with up to 60% homology (Little et al., 1981; Wade, 2009).

The self-assembly of the α- and β- tubulin dimers result in polarized protofilaments that form the microtubule through lateral interactions (Bryan and Wilsont, 1971; Luduena et al., 1977; Luduena & Little, 1981; Lu et al., 1999; Wade, 2009). In mammals, most of the microtubules are composed of 13 protofilaments, however, this number can vary between 12 and 17 depending on the species, and in *in vitro* assembled microtubules (Chretien and Wade, 1991; Chrétien & Fuller, 2000; Luchniak et al., 2023). In humans, microtubules are commonly constituted by 13 protofilaments, although microtubules with 14 and 15 protofilaments have been observed in platelets (Chaaban and Brouhard, 2017).

Regarding the structure, one end has an exposed α-tubulin (the minus end) whereas the other has an exposed β-tubulin (the plus-end). This feature provides different characteristics to each end and the polarity, which can be recognized by molecular motors.

In mammals, tubulins are intrinsically bound to GTP (Guanosine triphosphate) or GDP (Guanosine diphosphate). α- and β- tubulin dimers have two GDP/GTP binding sites, one in the α-tubulin subunit (N or non-interchangeable site) and another in the β-tubulin subunit (E or exchangeable site). Free tubulin dimers have GDP nucleoside in the E-site, and a non-interchangeable GTP at the N-site. The exchange of GDP to GTP in the β-tubulin at the E site, results in a competent dimer, ready for the addition to the microtubule plus-end (Alushin et al., 2014; Mitchison, 2014) (**Figure 5**).

Microtubules growth by addition of GTP-tubulin dimers, at temperatures higher than 30ºC and in the presence of magnesium ions (Wade, 2009). Furthermore, when they are added to the extending microtubules, subunits are hydrolysed to became GDP-tubulin, where GDP-tubulin is more stable in a "curved state". When the shrink process, i.e. catastrophe (**Figure 5**), begins, the GDP-tubulin is released and the microtubule shrinks rapidly (Burbank and Mitchison, 2006). Overall, this process is made by conformational changes within the microtubule structure, conferring instability to the growing microtubule while protecting it from depolymerization driven by the GTP cap (Alushin et al., 2014; Nogales, 2015; Nogales, 2016). In absence of a GTP-cap at the plus end, in fact, microtubules depolymerize rapidly.

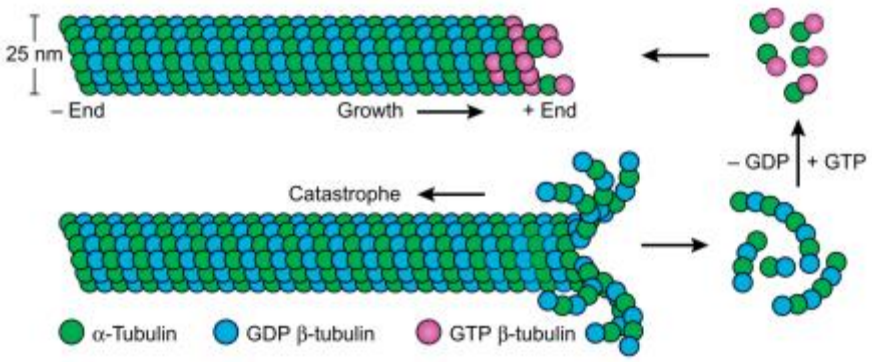

Figure 5. Microtubules dynamics. Graphical representation of the two main events occurring at the plus end, growth and catastrophe, known also as. (*Image obtained with permission from Elsevier license. Severson et al., 2016*)

The "*Search and capture*" theory (Kirschner and Mitchison, 1986) derives from the observation of a dynamic instability in the functioning of microtubules (Kirschner and Mitchison, 1986). In contrast to other cytoskeletal filaments, microtubules oscillate between periods of growth and shrinkage, and the balance between these two antagonistic reactions defines microtubule amount in the cell, with physiological fluctuations throughout the cell life cycle (Kirschner and Mitchison, 1986; Burbank and Mitchison, 2006). Fluctuations allow the rapid reorganization of the microtubule network in the cell (Burbank and Mitchison, 2006) so that the cytoskeleton and the cell adapt rapidly to external stimuli and internal signals. Indeed, in the oocyte, microtubules change their dynamics to support and sustain the final meiotic transition with nuclear and cytoplasmic maturation (Burbank and Mitchison, 2006). Moreover, the frequency of shrinkage seems to increase significantly when mitosis starts, specifically in the transition between longer and stable microtubules, typical of the interphase cytoskeleton, to two dynamic radial matrices of microtubules able to set they trajectory of several micrometres (Kirschner and Mitchison, 1986).

1.4 Spindle and spindle assembly

Mitotic and meiotic spindles are fascinating structures made from microtubules and able to arrange, move and segregate the genetic material into the daughter cells during nuclear division (Kirschner & Mitchison, 1986; Tournebize et al., 1997; Tirnauer et al., 2004). Since cell division is a intricated process that must be regulated in time and space to ensure functional cell development, the spindle is the central component orchestrating that (Coticchio et al., 2013; Coticchio et al., 2014; Coticchio et al., 2015).

The bipolar spindle is a complex macromolecular machine composed of three different classes of microtubules: astral, interpolar and kinetochore microtubules. First, the astral microtubules, only present in spindles with centrosomes, are nucleated from the centrosome and extend towards the cell cortex. Their main role is to orient the spindle and define the cleavage plane. Then, the interpolar microtubules, forming a robust mass of microtubules, are generated from one pole of the meiotic spindle and extended towards the other. They establish antiparallel interactions that provide support to the forces required for chromosome movements (congression and segregation). Finally, the

kinetochore microtubules (or k-fibers) are bundles of microtubules that connect the spindle poles with the kinetochores. These fibers mediate chromosome movement and, globally, they are more stable than the other classes of microtubules (Muller et al., 2019; Kiewisz et al., 2022; Matković et al., 2022).

During metaphase, the chromosomes are pulled back and aligned along the equatorial plane of the cell. Then the cell goes through an important cellular checkpoint known as Spindle Assembly Checkpoint (SAC) that is crucial to monitoring the correctness and integrity of the attachment of spindle microtubules to the kinetochores (Musacchio & Salmon, 2007; Gorbsky, 2015; Musacchio, 2015), as will be discussed in detail in the next sections.

The current model for spindle assembly encompasses both the centrosomal and non-centrosomal microtubule assembly pathways (Heal and Khodjakov, 2015). In this model, when the cell enters mitosis, the centrosomes act as the main microtubule-organizing centre (MTOC). The MTOC was first discovered in eukaryotic cells, with the main function of organizing flagella and cilia and mitotic and meiotic spindle apparatus, which segregates chromosomes during cellular divisions (Brinkley, 1985). The MTOC morphological characteristics can vary between different animals (Francis and Davis, 1999); however, one of the most important types of MTOC is the centrosome associated with spindle formation (Brinkley, 1985).

1.5 Spindle assembly in human oocytes

In eukaryotes, the microtubule spindle is the structure orchestrating chromosome alignment and segregation during nuclear division (Brinkley, 1985). However, the spindle in human oocytes is different from male germ cells and somatic cells, as oocytes generally lack canonical centrosomes. Moreover, in contrast with mouse oocytes, human oocytes also lack prominent acentriolar microtubule organizing centres (aMTOCs), which contain many of the components of canonical centrosomes and functionally replace centrosomes in mouse oocytes (Bennabi et al., 2016; Bennabi et al., 2018).

In human oocytes, the spindle is a barrel-shape structure and its size, compared to the cell itself (around 100-120 µm in the maximum diameter), is small, 11.8±2.6 µm in length and 8.9±1.7 µm in width, with the metaphase plate close to the oocyte's membrane (Coticchio et al., 2013; Coticchio et al., 2014; Coticchio et al., 2015). It was reported that human oocytes are able to cause the degeneration or otherwise eliminate their centrosome and any other aMTOC, and in fact typical spindle markers as pericentrin or γ-tubulin cannot be detected in human oocytes (Combelles and Albertini, 2001). In our species, meiotic spindle assembly is driven by the chromosome-mediated Ran dependent pathway (Holubcova et al., 2015). This pathway relies on a gradient of Ran-GTP concentrated around each chromosome. Ran-GTP locally releases spindle assembly factors, such as TPX2 (TPX2 Microtubule Nucleation Factor), from inhibitory binding to importins and thereby facilitates local microtubule polymerization and subsequent spindle assembly (Nachury et al., 2001; Kalab and Heald, 2008; Cavazza and Vernos, 2016). Therefore, RanGTP itself, collaborating with microtubule nucleation from pre-existing microtubules, is able to provide microtubule to assemble a functional spindle (Cavazza and Vernos, 2016).

The absence of a MTOC in spindle assembly seems to be specific for humans, while, in other species including mice, aMTOCs contribute to spindle assembly and bipolarization by a three-step aMTOC fragmentation and clustering mechanisms (Gueth-Hallonet et al., 1993; Palacios et al., 1993; Carabatsos et al., 2000; Schuh and Ellenberg, 2007; Clift and Schuh, 2015; Thomas et al., 2020).

Human oocytes assemble their spindle thought a slow, chromosome-dependent mechanism (Bennabi et al., 2018), that it takes around 7 hours (Holubcová et al., 2015), while mouse oocytes require only 3-5 hours (Dumont et al., 2007; Schuh and Ellenberg, 2007) to assemble a functional spindle. This long timeline and the reliance on chromosomes as nucleation points might explain why the meiotic spindle of human oocytes is prone to instability. Another factor contributing to spindle instability may be the size of the cytoplasm; larger cytoplasm decreases pole integrity, that result less focused, and spindle checkpoint stringency, as the spindle checkpoint factors are more diluted (Kyogoku and Kitajima, 2017).

1.6 Spindle assembly in human oocytes: when and where does it take place?

In human oocytes, at the time of germinal vesicle (GV) breakdown (GVBD), chromosomes cluster into a single mass, and microtubule assembly begins only 4-5 hours after GVBD (Holubcova et al., 2015) (**Figure 6**). Microtubules, at first, form a small aster inside the aggregated chromosomes and are mostly associated with kinetochores (Holubcova et al., 2015). As microtubules grow, chromosomes are spread outward on the aster surface with their kinetochores turned inwards. The microtubule aster begins to extend into an early bipolar spindle only 6-7 hours after GVBD (Thomas et al., 2020). Due to the high dynamism of these structures, the spindle poles are not well defined initially, therefore, alignment of the chromosomes in the metaphase plate does not occur until about 13-14 hours after GVBD. The alignment is often not permanent, as the chromosomes become stabilized and correctly aligned on the metaphase plate only about 16 hours after GVBD. Around 17 to 18 hours after GVBD the oocyte progresses through anaphase and the homologous chromosomes segregate (Holubcova et al., 2015; Thomas et al., 2020). Through asymmetric division, half of the genetic material is eliminated within the first polar body and the other half remains in the oocyte. Finally, 23-25 hours after GVBD, the oocyte has assembled the second metaphase spindle and is ready for fertilization (Holubcova et al., 2015; Thomas et al., 2020) (**Figure 6**).

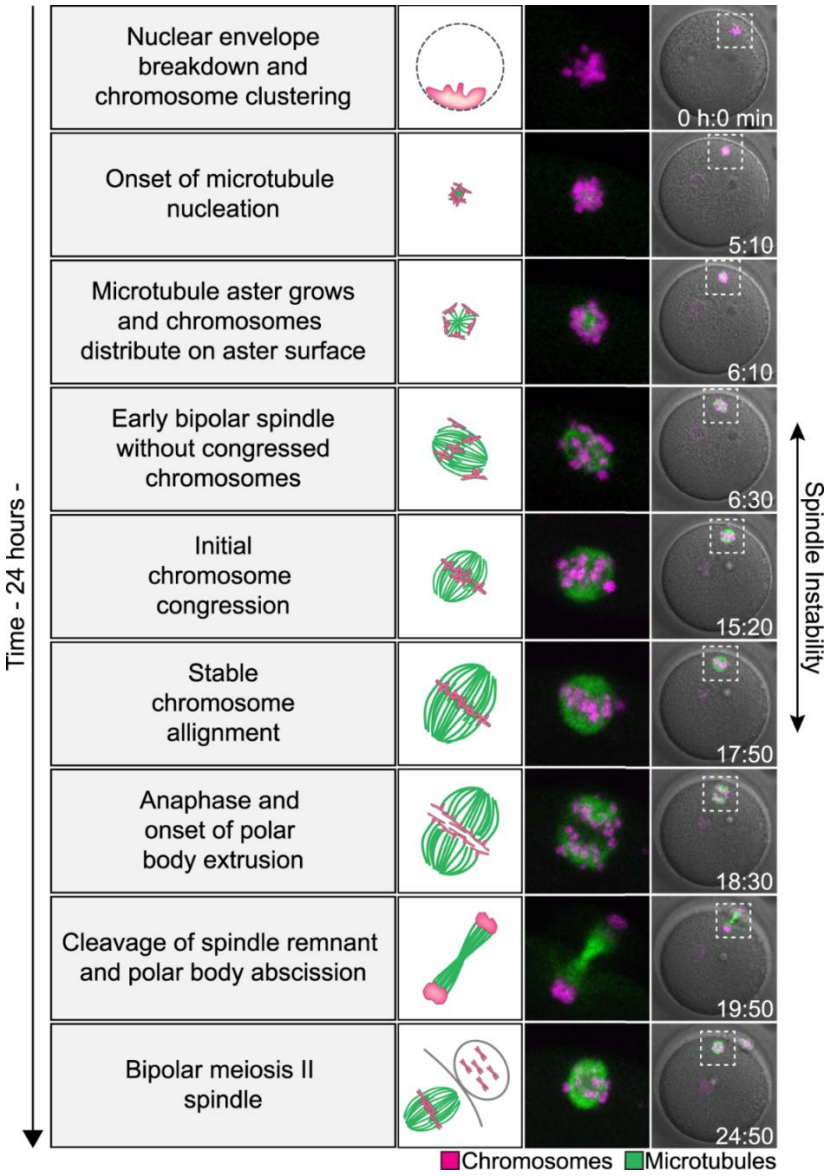

Figure 6. Meiosis in human oocytes. (Left) Schematic of chromatin organization and spindle assembly during human oocyte meiosis. Green, microtubules. Magenta, DNA. (Middle and right). Stills from a representative time-lapse movie of a human oocyte undergoing meiosis. Green, microtubules (EGFP-MAP4). Magenta, DNA (H2B-mRFP1). Merge with differential interference contrast in gray (right). Outlined regions magnified on the side (middle). Time, hours: minutes, 00:00 is nuclear envelope breakdown. Z-projections, 4 sections every 5 µm. Scale bar, 20 µm. (*Thomas et al., 2021*)

Oocyte maturation is also determined by the spatial positioning of the Metaphase I (MI) and Metaphase II (MII) spindles (Kincade et al., 2023). In mice, the MI spindle must be located in the central part of the cytoplasm, while later on it must migrate to the oocyte cortex to ensure the asymmetric division (one big cell and the polar body) and the

extrusion of half of the genetic material (Longo and Chen, 1985; Verlhac et al., 2000; EK and B, 2006; McCarthy and Goldstein, 2006; H. Li et al., 2008; Kincade et al., 2023).

In the human species, spindle to cell polarity is established before GVBD (Coticchio et al., 2015) and the MI spindle is positioned in proximity of the cortex (Coticchio et al., 2014; Coticchio et al., 2015).

1.7 Actin filaments in maturing oocytes

The spatial positioning of the spindle is of such importance, that actin filaments are also involved in this process, more so from anaphase I onward. In human oocytes, actin filaments promote chromosome congression and spindle stability during meiosis II, also suggesting a conserved mechanism across species (Thomas et al., 2020).

Nuclear (GV) positioning during meiosis defines the starting site of the spindle migration, which might affect the first asymmetric division, the extrusion of the first polar body, and the formation of a functional mature gamete (Coticchio et al, 2015; Coticchio et al., 2013; Duan and Sun, 2019). This is supported by the observation that MII oocytes have more abundant cortical actin close to the spindle and a slight increase, but of minor intensity, at the polar body (Coticchio et al, 2013).

The initial GV positioning and subsequent spindle positioning are indicators of meiotic competence (Metchat et al., 2015). Specifically, in mouse and rat, the GV is localized in the centre of the oocyte during meiosis (Duan and Sun, 2019). Oocytes with centrally positioned GV show a higher meiotic competence than those with side-positioned GV (Brunet and Maro, 2007; Bellone et al., 2009; Almonacid et al., 2018). A non-centric GV position in the oocyte is more common in aged mouse oocytes (Brunet and Maro, 2007; Bellone et al., 2009), concomitant with actin nucleator degradation, which is shown by decreases in Arp2/3, WAVE, and JMY expression, with aging (Sun et al., 2012) (**Figure 7**). This is further evidence that actin filaments are involved in GV positioning in mammalian oocytes (Coticchio et al., 2013; Coticchio et al., 2015; Almonacid et al., 2018).

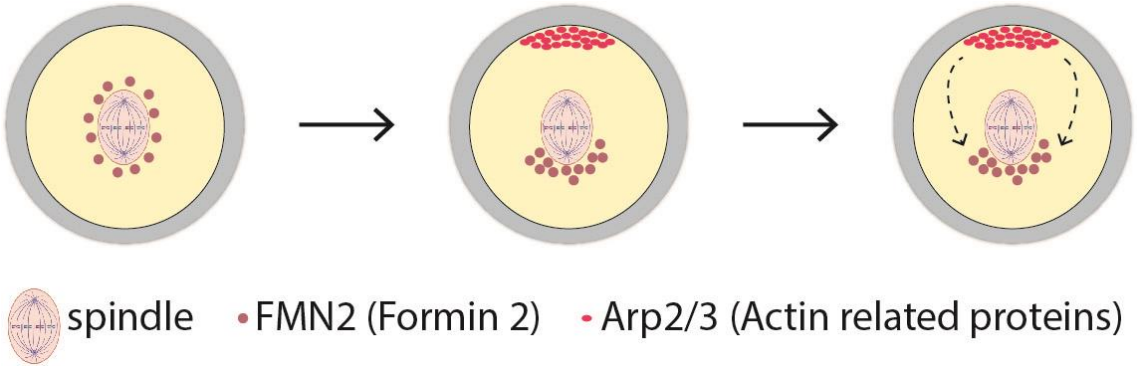

Figure 7. Schematic representation of forces in spindle repositioning prior to polar body extrusion. In the first image on the left the spindle moves spontaneously to the middle of the oocyte's cytoplasm as an effect of symmetric distribution of FMN2 (dark pink circle) and actin filaments. Afterwards, FMN2 accumulation and f-actin polymerization in the proximity of the spindle acquires a polarized distribution, causing the spindle to drift towards to the cortex. As the spindle moves close to the cell membrane, Arp2/3 (red circles) becomes progressively localized in front of that, in correspondence to the cortical domain. The dynamic polymerization caused by Arp2/3 promotes a flow of cytoplasmic material. As a whole, these collaborate to spindle positioning at the cortex. (*Graphical representation of the image obtained with permission from Oxford University press license. Coticchio et al., 2015*)

1.8 Mitochondria: general structure and function

Mitochondria are multi-functional cellular organelles, responsible for the production of adenosine triphosphate (ATP) through oxidative phosphorylation (OXPHOS) (**Figure 8**). They are also involved in several other processes, including calcium homeostasis, lipid and carbohydrate metabolism, apoptosis and several signalling pathways. Mitochondria vary in abundance and structure depending on cell size and energy requirements (Yan et al., 2021; Bhatti et al, 2016).

Mitochondria originated by endosymbiosis of a prokaryotic entity and still have their own small circular multicopy genome, residing in the inner matrix (Cavalier-Smith, 2006; Grey et al., 2012). The number of mitochondrial DNA (mtDNA) molecules in human cells varies between 500 to 10.000, with the exception of mature oocytes, where there are between 100.000 and 200.000 mtDNA copies (Boguszewska et al., 2020). Mitochondria have a double membrane that forms two compartments, an inner matrix and an intermembrane space (**Figure 8**). The inner membrane has low ion permeability and is folded into numerous cristae that protrude into the matrix. The protein complexes needed

for OXPHOS are located on the inner mitochondrial membrane and are composed of five subunits (I-V) and two electron carriers (coenzyme Q and cytochrome C) (**Figure 8**). The number, shape, and size of mitochondria in a cell are regulated by cycles of fission and fusion. During these processes, the organelles can exchange their membrane components between them, as well as their mtDNA (McBride et al., 2006; Tilokani et al., 2018). During fission, a single mitochondrion will divide in two by cleavage of both membranes, whereas these are joined during fusion (Scott and Youle, 2010). While the remodelling of the mitochondrial structure and the control of their numbers are not strictly connected to the replication of the mtDNA, both respond to physiological and environmental cues, and are crucial to adjust to the demands on mitochondrial function and activity during the different stages of development (Scott and Youle, 2010).

Two types of mitochondria can be identified based on their structure and metabolism (Almansa-Odonez et al., 2020). Orthodox mitochondria, that are usually present in glycolytic cells, and are spherical, with a large matrix volume, small intra-cristae volume and few lamellar cristae. In contrast, mitochondria that generate ATP through OXPHOS are indeed typical of cell with high respiratory activity and are characterized by a relatively small matrix volume and an expanded intra-cristae space (Almansa-Odonez et al., 2020). The production of ATP through OXPHOS is carried out through a series of reversible reactions of oxidation and reduction of nicotinamide adenine dinucleotide (NAD+/NADH) or flavine-adenine dinucleotide (FAD/FADH2) molecules by different protein complexes (Complexes I-IV), that allow the generation of a proton gradient across the inner membrane of the organelles, which is used by an ATP synthase (Complex V) to convert ADP and organic phosphate into ATP (Xiao et al., 2018; Amjad et al., 2021) (**Figure 8**). This process is fundamental to support the high energy requirements of oocyte maturation and embryo development, as it guarantees a higher yield of ATP compared to glycolysis. However, during the subsequent reactions of oxidation and reduction that characterize OXPHOS, reactive oxygen species (ROS) are produced, mainly in complex I and III (Chen et al., 2003; Onukwufor et al., 2019; Checa et al., 2020; Mailloux, 2020). ROS are reactive molecules and free radicals (molecules having one unpaired electron) containing oxygen. The most abundant ROS in biology are the hydroxyl ion (OH-), the superoxide ion (O2-) and hydrogen peroxide (H2O2). While ROS are key factors for several physiological processes, and finely regulated levels of ROS are required for the correct functioning of the organism, and alterations in the redox equilibrium are

deleterious for cells and can cause molecular damages at lipid, protein, and DNA levels (Schieber and Chandel, 2015; Onukwufor et al., 2019; Checa et al., 2020; Mailloux, 2020).

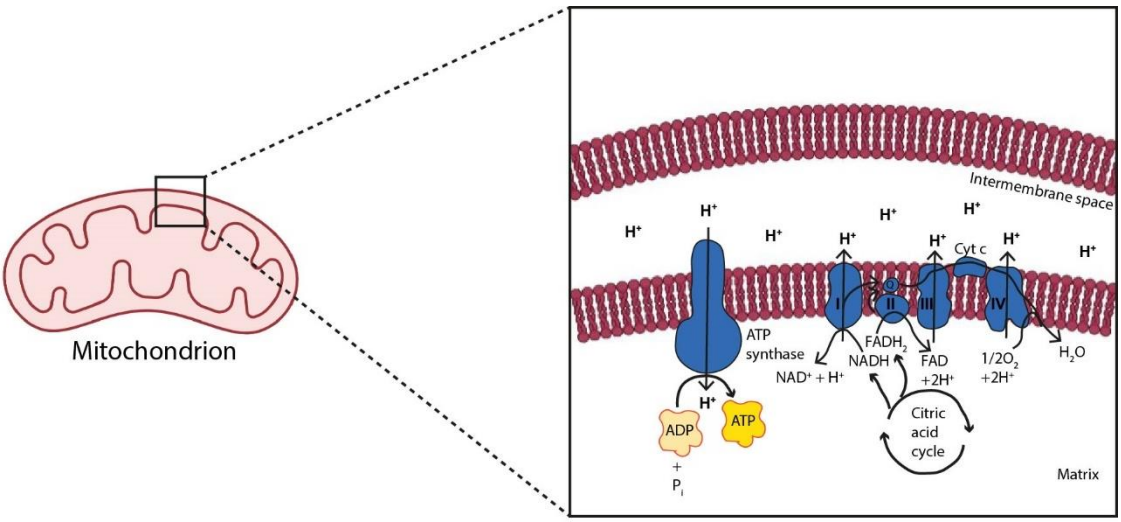

Figure 8. Schematic representation of mitochondrion and OXPHOS. Graphical illustration of a mitochondrion and zoom on the inner membrane (on the right). The chain of oxidation and reduction of the complexes I-IV causes the polarization of the membrane. The protons forced into the intermembrane space are used by the complex V (leftmost side in the box) to catalyse the production of ATP from ADP. (*In part adapted from BioRender.com*)

1.9 Mitochondria in oocytes

The metabolic regulation of developing oocytes in humans has not been extensively explored, with data only available from animal models such as mice, pigs, and cows. Mitochondria are generally inactive in primordial germ cells and early oocytes (before the antral phase) and with an immature morphology, a globular shape and few cristae with a non-polarized membrane (Pasquariello et al., 2019). In mice, when final oocyte maturation begins, mitochondria are located in the perinuclear area of the oocyte, and at the GVBD, they migrate towards the outer area of the ooplasm to finally reach the subcortical area in the mature MII oocyte (Takahashi et al., 2016; Kirillova et al., 2021).

In human oocytes, the mitochondria in the inner area are not polarized, and are considered inactive, while the subcortical ones have a polarized membrane. Overall, the membrane

potential of the oocyte will not increase significantly during final meiotic maturation, although an increase in ATP content has been observed in bovine oocytes during *in vitro* maturation. Also in the bovine model, a better COC morphology is associated to a higher ATP content and a specific mitochondrial distribution (Kirillova et al., 2021). The scarcity of material has contributed to limiting studies on mitochondria in human oocytes, and further research is needed to fully understand the mitochondrial regulation during human oocyte maturation and how they can influence oocyte quality.

2. THE DEVELOPMENT OF A MATURE OOCYTE

Oocyte maturation is one of the most complex, highly regulated, and long processes in the human body. The development of a mature oocyte starts before birth with oogenesis and ends when the oocyte is fertilized. In mammals, meiosis is a unique process aimed at generating haploid gametes, the basis of sexual reproduction, through meiosis.

Furthermore, successful fertilization and normal embryo development depend on the nuclear and cytoplasmic maturity of the oocyte.

2.1 The art of meiotic arrest and resumption

One of the features characterizing the development of a mature oocyte is the timing of its growth and maturation. As already discussed in the first section of the present thesis, during the variable but very extended period of quiescence in follicle development, the oocytes are arrested at prophase I of meiosis. Oocytes maintain their meiotic arrest through oogenesis and, during this time, they growth in size to support the completion of meiosis, fertilization, and early development (Sanchez and Smit, 2012, Pan and Li, 2019; Das and Arur, 2022).

Most information on the maintenance of meiotic arrest and its later resumption have been gathered from mouse models (Coticchio et al., 2015). The prophase I arrest is mainly maintained by high intra-oocyte cyclic adenosine monophosphate (cAMP) levels (Jaffe and Egbert, 2017). In the oocyte, cAMP concentration is regulated by the opposite actions of adenylyl cyclase 3 (AC3) and the oocyte-specific phosphodiesterase (PDE3A). AC3 produces cAMP, whereas PDE3A metabolizes it. In the granulosa cells, the NPR2 guanylyl cyclase produces cyclic guanosine monophosphate (cGMP) that diffuses into the oocyte and inhibits PDE3A, thus keeping the oocyte's cAMP levels high, maintaining meiotic arrest (Jaffe and Egbert, 2017).

The levels of cAMP modulate the arrest or resumption of meiosis (Vivarelli et al., 1983) by regulating the protein complex known as M-phase promoting factor (MPF), formed by the CDK1 kinase and cyclin B (Jones, 2004). High intra-oocyte concentrations of cAMP activate protein kinase A (PKA, types I and II) (Viste et al., 2005) and, as a

cascade, PKA phosphorylates the phosphatase CDC25 and the kinases WEE1B and MYT1, causing inactivation of the phosphatase and activation of the two kinases, respectively (Jones, 2004). Following the same cascade, tyrosine, and threonine residues of CDK1 are phosphorylated, MPF activity is repressed, and GVBD is inhibited (Coticchio et al., 2015). Finally, the reduction of cAMP levels in the oocyte reverses the balance, allowing for the activation of MPF and triggering the meiosis resumption (Jones, 2004; Coticchio et al., 2015; Das and Arur, 2022).

2.2 Oocyte maturation

Oocyte developmental competence is determined by two factors: nuclear and cytoplasmic maturation. Nuclear maturation, i.e. the ability to reach correctly the MII stage, can be influenced by several aspects, including the number and location of the crossing over during meiosis I. For instance, crossing over too close to telomeres or centromeres can have deleterious effects on oocyte and embryo development (Hassold et al., 2007). Cytoplasmic maturation is commonly defined as the acquisition of a global population of transcripts, proteins and organelles that will provide the required substrate for early preimplantation development (Gosden and Lee, 2010).

Appropriate maturation will determine the quality of the ovulated oocyte and its developmental competence, i.e. its ability to sustain early embryonic development. In fact, the store of molecules and organelles in the cytoplasm of the mature oocytes will sustain the embryo until the Embryonic Genome Activation (EGA), whose timing is species specific. In humans, EGA is detectable as early as the 4-cell stage, with a blip of activation at late 2-cell stage, while most embryonic protein expression occurs form the morula stage onwards (Vassena et al. 2011). In cows, EGA occurs between 4- and 8-cell stages (Graf et al., 2014), while in mouse EGA is earlier, at 2-cell stage (Schultz, 1993; Aoki, 2022).

2.2.1 Nuclear maturation

Oocyte growth and meiotic maturation are long and highly regulated processes since the oocyte journey starts during fetal development, arrests at the diplotene stage of prophase I (dictyate stage), where it presents the characteristic GV, and remains quiescent for several years, until puberty. After puberty, each month, with the LH surge, oocyte chromatin condenses, and GV breaks down in the fully grown follicle (Coticchio, Abertini and De Santis, 2013; Jaffe and Egbert, 2017), with the objective to reach nuclear maturation. This process is aimed at ultimately produce a haploid gamete, a cell with half of its DNA content. This reduction is crucial to ensure that, at the time of fertilization and unification of the haploid oocyte with a haploid sperm, a diploid zygote with the correct chromosome content is produced.

The oocyte then progresses from prophase I to metaphase I and the homologous chromosomes align on the metaphase plate, assembling the first meiotic spindle at late metaphase I (He et al., 2021; Pailas et al., 2022; Charalambous et al., 2023). Then, the homologous chromosomes separate at anaphase I. The oocyte undergoes an asymmetric cytokinesis where most of the cytoplasm remains in the oocyte and, in parallel, the first polar body (PB) is extruded from the oocyte. The PB contains a small portion of the cytoplasm and half of the oocyte's genetic material. The oocyte arrests again at metaphase II, successfully mature and competent, ready to be fertilized (Charalambous et al., 2023; Hutt & Albertini, 2007).

Central to an oocyte's ability to resume meiosis is the global silencing of transcription, crucial to sustain the change in DNA or chromatin structure occurring during these stages (Grover at el., 2018). The changes in chromatin configuration and transcriptional activity are conserved across mammals, specifically among human (Coticchio et al., 2015; Cornet-Bartolomè et al., 2020; Pietroforte et al., 2023) and cow (Lodde et al., 2007). When arrested at prophase I, the oocyte chromatin is in non-surrounded nucleolus (NSN) configuration, characterized by uncondensed chromatin, typical of smaller growing oocytes actively transcribing their DNA (De La Fuente, 2006). This phase is followed by an intermediate transitory phase of NSN-to-surrounded nucleolus (SN), and finally the SN configuration with chromosomes fully condensed and chromatin that forms a tight ring around the nucleolus. This SN configuration is typical of the fully grown oocyte that

is transcriptionally silent (De La Fuente, 2006; Lodde et al., 2007; Mihajlovic and FitzHarris, 2018; Cornet-Barragan et al., 2020).

When the chromosomes are fully condensed in SN configuration, an acentrosomal spindle forms and, subsequently, it migrates towards the oocyte cortex, closer to the oolemma. Anaphase I takes place while the spindle is located in the oocyte cortex, resulting in a highly asymmetric cytokinesis and the formation of a large oocyte and a small PB. Shortly after, the first PB is extruded and the oocyte arrests in MII until fertilization. The oocyte completes meiosis II and extrudes the second PB upon successful fertilization (Mihajlovic and FitzHarris, 2018).

The acquisition of the SN configuration normally occurs in oocytes that have almost reached the maximum of their growth curve (Chouinard, 1975; Parfenov et al., 1989; Mattson and Albertini,1990). Moreover, the SN configuration seems to be associated with human and mouse oocytes able to support the G2 to M phase transition (Mirre et al., 1980; Bouniol-Baly et al., 1999).

2.2.2 Cytoplasmic maturation

Cytoplasmic maturation can be divided into three sub-events: organelle distribution, cytoskeleton reorganization and molecular maturation. These processes are regulated by differences in the hormonal concentration secreted by CCs (Ferreira et al., 2009; Buratini et al., 2023).

Mitochondria

Organelle distribution begins at the time of LH surge and is characterized by an extensive redistribution of intracellular organelles in the oocyte, through the progression to MII. Mitochondria are responsible for producing the ATP required for oocyte maturation. Variations in ATP content in human oocytes and embryos affect oocyte quality and embryo development (Sanchez et al., 2019; Venturas et al., 2020). Higher ATP levels have been correlated with better reproductive results, whereas mitochondrial dysfunction decreases the quality of the oocyte (Zhao and Li, 2012; Kim et al., 2019; van der Reest,

2021; Khan et al., 2021). In the bovine model, during oocyte development, mitochondria are reorganized to areas of high energy consumption to provide local energy supply (Stojkovic et al., 2001; Lodde et al., 2021). In GV oocytes from mice and pigs, mitochondria are aggregated in large clusters around the germinal vesicles, and after GVBD the mitochondria clusters change shape and become more numerous, reorganizing throughout the cytoplasm in MII oocytes (Sathananthan et al., 1985; Motta et al., 2000; Trounson, 2000; Sanchez, Venturas, et al., 2019; Sanchez, Zhang, et al., 2019). Numerous studies have demonstrated that an aberrant mitochondrial distribution leads to oocytes with less developmental competence (Schon et al., 2000; Sun et al., 2001; Au et al., 2005; Zhao and Li, 2012; Kim et al., 2019; van der Reest, 2021; Khan et al., 2021; Venturas et al., 2022).

Endoplasmic reticulum

There are two types of endoplasmic reticulum (ER) in the maturing oocyte, smooth (SER) and rough (RER). The SER is involved in lipid synthesis and transport and is the main storage site of calcium ions (Ca^{2+}) (Machaty, 2015). At the GV stage, the ER forms a fine network uniformly distributed throughout the cortex and the cytoplasm (Machaty, 2015; Tucker et al., 2016; Grover et al., 2018), whereas at MII stage, the ER is accumulated in large clusters (Mann et al., 2010). This is different from the mouse, where the ER is located mainly in the cell cortex in MII oocytes (FitzHarris et al., 2007; Grover et al., 2018). The RER presents in general a punctuated shape, is associated with ribosomes and is involved in the production and transport of proteins and other biomolecules (Grover et al., 2018; Trebichalská et al., 2021).

Golgi apparatus

The Golgi apparatus in human oocytes is distributed throughout the cytoplasm (Sathananthan et al., 1985) and it is composed by stacks of membranous compartments or cisternae. The main localization of the Golgi apparatus is close to the nucleus and at the periphery of the cytoplasm (Grover et al., 2018). Its main role in the cell is the secretion and intracellular transport of proteins from the ER (Sathananthan et al., 1985, 2002) and, in the oocyte, it is also involved in generating other structures and organelles

essential for maturation (Sathananthan, 1994, 2002; Grover et al., 2018). For example, the Golgi apparatus is involved in the modifications of glycoproteins that form the ZP. Vesicles of hypertrophied Golgi can fuse and became multivescicular bodies of cortical granules (CGs) (Liu, 2011). Regarding CGs, these are specialized structure into the cytoplasm, critical for proper fertilization. Indeed, the CGs migrate towards the cortex to form a mono- to multi- layer sheath below the plasma membrane, where they remain stable until fertilization, when they act as a crucial blocker of polyspermy (Sathananthan, 1994).

The Golgi apparatus undergoes changes in structure, localization, and abundance through oocyte maturation (Moreno et al, 2002; Payne and Schatten, 2003; Y. jie Yang et al., 2009). Upon GVBD, the Golgi apparatus is no longer essential for maturation, and it is fragmented and dispersed through the oocyte (Sathananthan et al., 2002). In the fertilized oocyte, under the influence of a rise in intracellular calcium level, CGs, originated from Golgi membranes during oocytes growth, extrude their contents generating a cortical reaction (Li, 2011; Cheeseman et al., 2016). The CGs contain a protease, ovastacin, responsible for the fragmentation of the zona pellucida's proteins and changing its glycolytic composition, preventing polyspermy (Sathananthan, 1994; Cheeseman et al., 2016; Evans and Janice Evans, 2020).

Cytoskeleton

During cytoplasmic maturation, the cytoskeleton and its reorganization play an important role. The cytoskeleton is a dynamic structure that extends from the nucleus to the cell membrane and is composed of three types of cytoskeletal filaments (microtubules, microfilaments and intermediate filaments) that perform several functions. In the oocyte, the cytoskeleton ensures structural support, provides a scaffold to organize organelles in the cytoplasm, and mediates intracellular transport (Alberts et al., 2008). Oocyte growth, maturation and fertilization rely on the correct distribution of the cellular organelles, accomplished through the reorganization of microtubules and microfilaments (Sun and Schatten, 2006). Microfilaments consist of globular and compacted actin subunits, involved in the regulation of chromatin movements and CGs migration, while arranging meiotic spindle and first PB extrusion (Ruggeri et al., 2015). In GV oocytes, microtubules and microfilaments are distributed throughout the ooplasm, however, their dynamics

differ after GVBD. In MII oocytes microtubules are located around the condensed chromatin and migrate to the cortical region, while microfilaments are accumulated in the subcortical region of the oocyte and surrounding the spindle. Intermediate filaments are formed by tetramers of fibrous polypeptides subunits that provide mechanical integrity to the oocyte (Mao et al., 2014).

Transcription

Molecular maturation contributes to cytoplasmic maturation and occurs by the end of GV oocyte growth when transcription is almost silenced (as described also in the previous section). It includes all the events related to the processing and storage of transcripts and molecules that will be used for fertilization and early embryonic development. Global transcriptional silencing in the oocyte is needed for developmental competence and has been associated to chromatin condensation (Mattson and Albertini, 1990; Inoue et al., 2008; Cornet-Bartolomè et al., 2021). The number and profile of the accumulated transcripts prior the onset of transcriptional silencing can determine the oocyte developmental competence and its ability to sustain early embryonic development (De la Fuente and Epping, 2001).

Transcription is the process turning DNA into RNA and represents the crucial first step in the production of functionally active proteins. Generally, transcription occurs in the nucleus of the cell, i.e. the oocyte's GV, and the mRNAs that will be translated into proteins are transported through nuclear pores into the cell's cytoplasm or simply spilled into the cytoplasm due to GVBD (Susor et al., 2014; Grover et al., 2018; Pan and Li, 2019). In the oocyte, however, all processes from meiosis resumption to fertilization and beyond happen in absence of active transcription, through the use of previously stored maternal mRNAs (Winata et al., 2018; Sha et al., 2020; Tora and Vincet, 2021). Maternal mRNAs are produced and stored in the cytoplasm of the growing oocyte. Since transcription is all but silenced after the fully grown stage, these mRNAs are the source of protein translation (Tora and Vincent, 2021). Alterations in the abundance of maternal transcripts can affect oocyte maturation, impairing its ability to complete meiosis, the health of the developing embryo and its ability to activate its own embryonic genome (Sha et al., 2021; Tora and Vincent, 2021).

In mouse oocytes, a 300% increase has been reported during the growth phase of oocytes with active transcription, while the fully grown oocyte has been estimated to contain about 200 times as much RNA as a typical somatic cell (about 0.6 ng of total RNA) (Eichenlaub-Ritter and Peschke, 2002). Regulation of transcript abundance in the oocyte is a tightly controlled process that ultimately will lead the transcript to be either used, degraded or stored. Some of the mRNAs are immediately recruited and translated into proteins and some undergo selective processing (Vassena et al., 2011; Sha et al., 2021; Tora and Vincen, 2021). The mRNAs in the first category are needed to support all the nuclear and cytoplasmic modifications through to the MII stage. In mice, it was observed that the fate of mRNA is partially defined by the length of its polyadenylated (Poly(A)) tail in its 3' untranslated region (Eichenlaub-Ritter and Peschke, 2002). Similar observations were made in pigs, cows (Leppek et al., 2018; Mignone et al., 2002; Reyes et al., 2017; Yung et al., 2020) and recently in humans (Hu et al., 2022).

The absence of transcription during the final phases of meiotic maturation highlights the importance of co- and post-translational modifications. Most regulatory factors interact with specific sequences at the 3'- and 5'- untranslated regions (UTRs) of RNA and regulate its stability through several processes. First, polyadenylation, where a poly(A) tail of 150-250 residues in length is added to the 3'-end of transcripts, conferring stability and protection from degradation. Second, deadenylation, which shortens the poly(A) tail of the transcript, affecting its stability. Concomitant with modifications at the 3' end, it is the association with cap binding complexes (CBP20/CBP80) and initiation factors at the 5' end. These contribute to export mRNA to the cytoplasm, confer protection from degradation and are crucial for the initiation of translation. Moreover, long non-coding RNAs (lncRNAs) and proteins interact to mask the RNA, to avoid translation and association with small non-coding RNAs, such as micro-RNA (miRNAs) that silence the target RNAs by the RNA-induced silencing complex (RISC) (Chu and Rana, 2008). Finally, splicing and the related mechanism of alternative splicing (AS) generate mature mRNA. Specifically, by AS, several transcript isoforms from a given gene can be generated, increasing transcriptome and proteome complexity.

During human and mouse oocyte maturation there is a selective degradation of maternal transcripts, which causes around 30% of the genes to decrease their abundance in mice. Alterations in all these mechanisms could directly affect oocyte developmental competence and embryo quality (Sha et al., 2021; Tora and Vincent, 2021).

Translation

Finally, translation is the process of mRNA conversion into proteins, occurring in the cell cytoplasm and mediated by ribosomes. Ribosome biogenesis and protein synthesis during oocyte growth are crucial features of cytoplasmic competence.

In order to sustain the production of a high number of proteins, the oocytes synthesize and accumulate high number of ribosomal RNA (rRNA), that are key elements of ribosome biogenesis. rRNA synthesis in the growing oocyte is higher than in other cell types, and rRNA constitutes about 60-70% of the total RNA in oocytes. For example, mouse oocytes accumulate ribosome rapidly during the initial growing phase, 95% of the ribosomal pool is already established when the oocyte is still growing (Eichenlaub-Ritter and Peschke, 2002).

2.3 Chromosome segregation in meiosis

When the oocyte is close to be ovulated from its follicle, the first meiotic division happens.

During the replication of each chromosome, the diploid cell genetic content is increased from 2N to 4N. Once the DNA replicates, each chromosome consists of two parallel strands or chromatids joined together at the centromere. Each chromatid contains a single DNA molecule, which is itself double stranded (**Figure 3**) (Huskins, 1933; Clift and Schuh, 2013).

Next, during prophase I, the chromosomes condense and homologous chromosomes pair to form the bivalents or tetrads, composed of four chromatids, two centromeres and two chromosomes. Bivalent formation allows the exchange of large segments of DNA through crossing over between two homologous chromosomes. The resulting recombination of the genetic material on homologous maternal and paternal chromosomes is largely random and contributes to increase the genetic variability of the next generation. The primary oocyte enters a phase of meiotic arrest during the first meiotic prophase (Huskins, 1933; Clift and Schuh, 2013; Charalambous et al., 2023).

During metaphase I, the bivalents are organized on the equator of a spindle apparatus. During anaphase I, the homologous chromosomes are pulled apart to opposite ends of the cell. The centromeres of the chromosomes do not separate; therefore, the two chromatids of each chromosome remain together. Immediately after, the oocyte undergoes asymmetric cytokinesis, producing a secondary oocyte and a first PB. The resulting daughter nuclei thus are haploid but 2N: they contain the same amount of DNA as the parent germ cell, but half the number of chromosomes (Clift and Schuh, 2013; Thomas et al., 2020; Charalambous et al., 2023).

During the second meiotic division DNA replication does not occur. The twenty-three double-stranded chromosomes in human condense during the second meiotic prophase and line up individually on the spindle equator during the second meiotic metaphase. The oocyte enters a second phase of meiotic arrest during the second meiotic metaphase and meiosis does not resume unless the oocyte is fertilized (Thomas et al., 2020; Charalambous et al., 2023).

When the spermatozoa enters the oocyte, meiosis II resumes. The chromosomal centromeres then separate during anaphase, and the double-stranded chromosomes pull apart into two single-stranded chromosomes, where one is distributed to each of the daughter nuclei. The second meiotic division, as the first, is asymmetrical and produces a large mature oocyte and the second PB (Huskins, 1933; Clift and Schuh, 2013; Thomas et al., 2020; Charalambous et al., 2023).

2.4 Chromosome segregation errors

The accurate segregation of homologous chromosomes during meiosis I and of sister chromatids during meiosis II is essential for the formation of euploid embryos. However, errors do occur through these processes (Handyside, 2012; Mihajlovic et al., 2018; Gottlieb et al., 2021; Lodge et al., 2020; Wasielak-Politowska & Kordowitzki, 2022). The majority of meiotic errors have been observed to occur in meiosis I (Thomas et al., 2020).

Three main classes of errors might occur during meiosis I in human oocytes: (I) mis-segregation of entire homologous chromosomes; (II) mis-segregation of one chromatid;

or (III) chromosomes segregating like in mitosis with two sister chromatids moving towards opposite spindle poles, also known as reverse segregation. In meiosis II the only error that can occur is the mis-segregation of sister chromatids (**Figure 9**).

Chromosome segregation errors are common during human oocyte meiosis and increase further as women approach 40 years (Charalambous et al., 2023).

Aneuploidy rates in human oocytes are much higher than in either sperm or most mitotically dividing somatic cells (Thomas et al., 2020; Wartosch et al., 2021; Charalambous et al., 2023; Samura et al., 2023). Recent studies focused on age-independent causes of chromosome segregation errors found that the architecture of the meiotic spindle itself and the absence of MTOCs promote errors during segregation. Other features that influence the occurrence of aneuploidy include the level of cortical tension at the oocyte surface and weakness of surveillance mechanism of chromosome segregation, such as the SAC (Thomas et al., 2020). The SAC function is to ensure accurate chromosome segregation by surveying of the proper attachment of chromosomes to spindle microtubules, including the block of mitotic progression whenever assembly is erroneous or absent (Chenevert et al., 2020; Thomas et al., 2020). In human, SAC appears less stringent than in mice, and only severe disruption of the spindle arrests the oocyte in meiosis I (Rémillard-Labrosse et al., 2020).

In human oocytes, the spindle forms through a long process (Holubcová et al., 2015; Haverfield et al., 2017). In this extended process, the spindles can take incorrect forms, for example in meiosis I spindles often collapse into a ball-shaped form or can became multipolar (Holubcová et al., 2015). Meiosis II spindles can be also unstable, albeit less frequently (Roeles and Tsiavaliaris, 2019). These instabilities can resolve before chromosome segregation in anaphase, and indeed spindle assembly allows for self-correction of mis-aligned spindles (Charalambous et al., 2023). Nevertheless, human oocytes show higher spindle instability compared to oocytes of other mammals, for instance through the mediation of lower levels of KIFC1 (Kinesin Family Member C1), a member of the microtubule motor protein superfamily (So et al., 2022; Xue et al., 2013; Wu et al., 2018), known to crosslink microtubules (She and Yang, 2017), stabilizing the bipolar spindle (Charalambous et al., 2023). Administration of exogenous KIFC1 to human oocytes improves spindle stability and reduces the frequencies of lagging chromosomes in anaphase (So et al., 2022).

Recent studies on age-dependent aneuploidy demonstrate that women in both young (<20 years) and advanced age groups (>37 years) can be substantially more at risk of chromosome segregation errors than women aged between 20 and 37 years (Gruhn et al., 2019; Wartosch et al., 2021). Indeed, aneuploidy exhibits a U-shape curve according to age (Gruhn et al., 2019; Wartosch et al., 2021). The features involved in age-dependent chromosome segregation errors seem to correlate with decreased cohesin levels, unpairing of sister kinetochores during meiosis I and eventual kinetochore fragmentation, increased DNA damage, epigenetic deregulation and telomere shortening and mitochondrial dysfunctions (Wartosch et al., 2021).

Interestingly, (**Figure 9B**) in spite of the similarly high level of meiotic errors between young and old women, the type of the most abundant error is different across ages: non-disjunction in MI (MI NDJ, blue bar in **Figure 9B**) in young oocytes and premature separation of sister chromatids (PSSC, orange bar in **Figure 9B**) and reverse segregation (RS, yellow bar in **Figure 9B**) in older oocytes. Specifically, MI NDJ, i.e. the gain or loss of a whole chromosome, decreases with age, while PSSC, in which sister chromatids of one homolog separate in meiosis I, increases linearly with age (Gruhn et al., 2019).

These phenomena support the theory that cohesion weakening acts as a "molecular clock", limiting women's reproductive capacity through the predisposition of specific meiotic errors (Gruhn et al., 2019). The more abundant MI NDJ in the youngest group could be due to the high force and cohesion involved into maintaining chromosomes pairs, that remain robust in teenagers. Therefore, when meiosis resumes in these young women, the chromosomes are too stabilized and cannot segregate properly. On the contrary, the extensive cohesion loss, i.e. fully-inverted and deteriorated bivalents (univalent), where both sets of sister kinetochores form bipolar attachments in meiosis I (**Figure 9**) (Angell, 1995; Kouznetsova, 2007; Zielinska et al., 2015), correlates with a higher incidence of PSSC and RS in women of advanced maternal age (Gruhn et al., 2019).

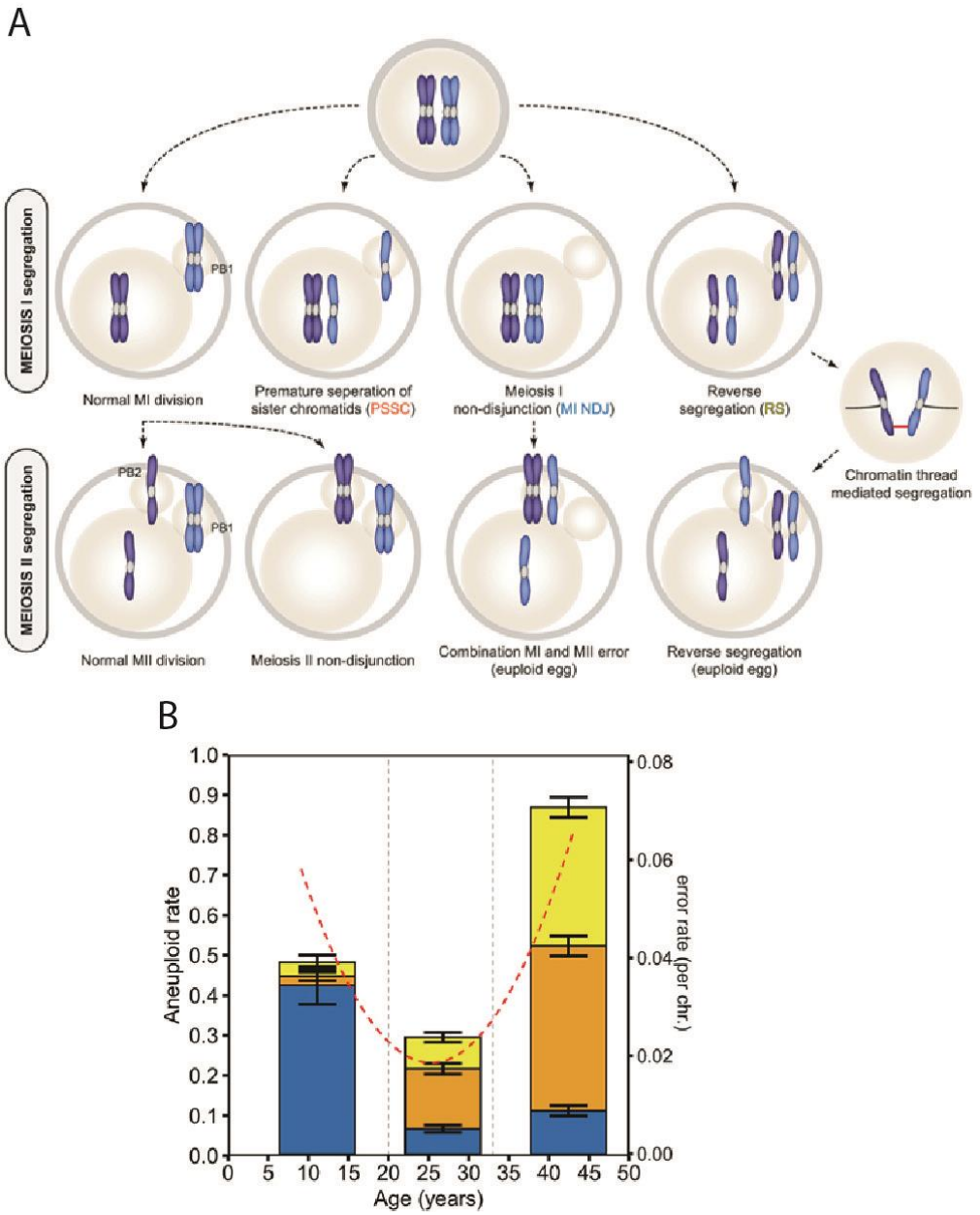

Figure 9. Meiosis I and meiosis II segregation errors and their age dependency in human oocytes. (**A**) Chromosome segregation patterns in meiosis I and meiosis II. (**B**) The U-curve of aneuploidy in human oocytes (dotted red line) is a compilation of all three chromosome missegregation events—MI non-disjunction (NDJ; blue), premature separation of sister chromatids (PSSC; orange), and reverse segregation (RS; yellow)—and acts in an age dependent manner. (*Wartosch et al., 2021*)

2.5 Transcriptional control in meiosis

Meiosis in human oocytes entails an intricate regulation of the transcriptome to support late oocyte growth and early embryo development. Progression to meiosis I and meiosis II in human oocytes is under transcriptional control at the level of gene expression and mRNA processing.

During oocyte growth, transcripts are accumulated, and in the fully grown oocyte transcription stops and remain silenced during final meiotic maturation, fertilization and initial embryo development, as confirmed in mice, pigs, cows (Mamo et al., 2011; Luciano et al., 2012; Yang et al., 2020; Wu et al., 2022) and humans (Cornet-Bartolomè et al., 2021). Specifically, transcription in human oocytes is still active in those immature GV oocytes with an open chromatin configuration, resembling the mouse NSN, while it arrests when the chromatin condenses around the nucleolus, similar to the mouse SN state (Cornet-Bartolomè et al., 2021). Since the transcriptional activity during the final phase of oocyte growth and meiotic maturation is reduced to basal levels and the oocyte needs the accumulated maternal mRNAs to accomplish all the subsequent events to reach the MII stage, the role of co- and post- transcriptional modifications is crucial as the oocyte's ability to properly store mRNAs.

Membrane-free compartments for RNA storage are observed in non-mammalian oocytes: P granules in *Caenorhabditis elegans* oocytes (Brangwynne et al., 2009; Seydoux, 2018), polar granules in *Drosophila* oocytes (Kistler et al., 2018; Trcek and Lehmann, 2019; Bose et al., 2022) and Balbiani body in *Xenopus* and zebrafish oocytes (Boke et al., 2016; Jamieson-Lucy and Mullins, 2019). However, similar structures have not been described in human oocytes until recently, even though a type of Balbiani body has been long observed in the early stages of oocyte development (Hertig and Adams, 1967). At the end of 2022, the existence of a mitochondria-associated domain related to the storage of mRNA was reported in several mammalian oocytes, including human (Cheng et al., 2022). Since this domain was different from all known compartments containing RNA, it was named "*mitochondria-associated ribonucleoprotein domain*", or "*MARDO*" (Cheng et al., 2022). MARDO seems to assemble around mitochondria, especially to the most active ones, during oocyte growth, and progressively store the mRNA produced. Zygote Arrest 1 (ZAR1) was identified as one of the main RNA-binding proteins involved in MARDO assembly (Cheng et al., 2022).

2.6 Co- and post- transcriptional modifications

In somatic cells, the pre-mRNA undergoes 5' capping, 3' polyadenylation and RNA splicing in the cell nucleus before being exported to the cytoplasm and translated.

The first step is the addition of the 5' Cap (Capping), then transcripts are cleaved and polyadenylated at the 3'-end by specific RNA binding proteins which interact with regulatory RNAs motifs contained in the 3'UTRs (Matoulkova et al., 2012). However, in oocytes, polyadenylation occurs later on, in the cytoplasm, and influences specific transcripts degradation/translation potential, as shown in mice and pigs (Yang et al., 2020; Wu et al., 2022). Over 80% of mammalian mRNA genes present multiple polyadenylation sites, resulting in alternative polyadenylation (APA) isoforms with different 3'UTR lengths (Derti et al., 2012). Alternative 3'UTR isoforms can lead to different mRNA subcellular localization, stability, and translation timing (Leppek et al., 2018). Finally, splicing is a co-transcriptional mechanism able to modify the pre-mRNA into a mature transcript ready to be translated. This process is mainly performed by the spliceosome, a complex machinery composed of five U-rich small nuclear ribonucleoproteins (U1, U2, U4, U5, U6 snRNPs), NineTeen complex, NineTeen complex-related and several other factors, including serine/arginine-rich proteins and hetero-nuclear ribonucleoproteins, and proteins stably bound within the building mRNAs, like the Exon-Junction Complex (EJC) and the TRanscription-EXport (TREX) complex (Dias et al., 2010; Pühringer et al., 2020).

AS is a tightly regulated mechanism mediated by the spliceosome (**Figure 10**), a molecular machine assembled from small RNAs and approximately 80 proteins that removes introns from a transcribed pre-mRNA (Modrek and Lee, 2002; Wang et al., 2008). AS is a crucial process to obtain different proteins from the same gene, through several mechanisms, like exon skipping, intron retention and alternative splice sites (**Figure 10**). Although they originate from the same transcript, these proteins can have different functions. AS plays a vital role in transcriptome complexity (Braunschweig et al., 2013) and its dysregulation can lead to aberrant phenotypes and diseases (Cooper et al., 2009). While some reports show a differential expression of spliceosome related transcripts (Zhao et al., 2019; Llonch et al., 2021) and differentially spliced genes (Cornet-Bartolomè et al., 2021; Li et al., 2020) during human oocyte maturation, a lack of deep information on the transcriptomic regulation during human meiosis still persists.

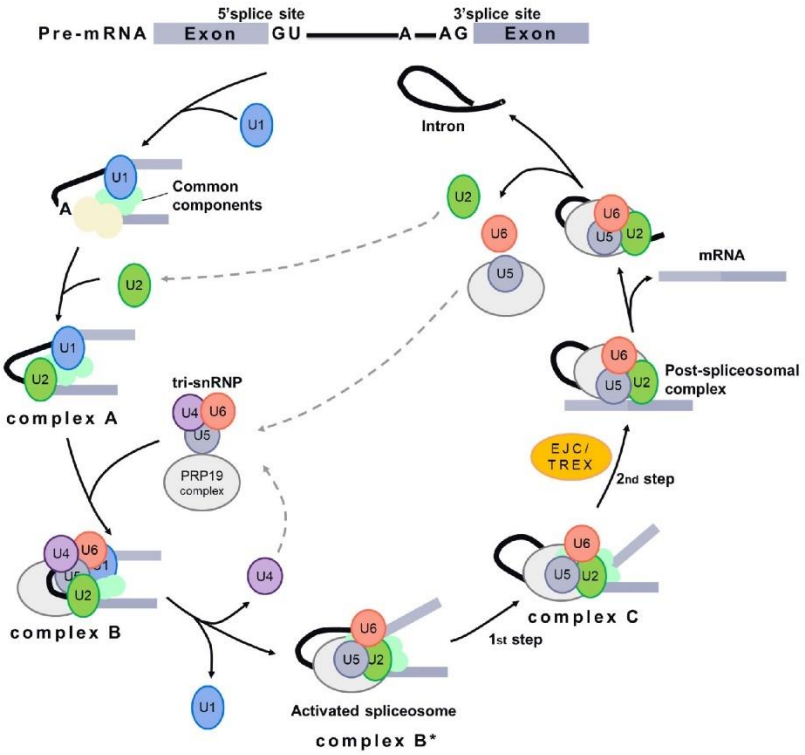

Figure 10. The spliceosome machinery. Graphical representation of the spliceosome machinery and how the subsequent events cooperate to process the pre-mRNA to obtain a mature intronless mRNA.

AS generates different isoforms by five mechanisms, while three are the major AS events (**Figure 11**). The first and most common is the exon skipping. This event is also known as cassette-exon, and it is the event of exon retention or skipping from the nascent transcript (**Figure 11**). Then, it is possible that some exons can be mutually excluded, when two or more regions are spliced or retained in a coordinated manner. Alternative splice site at 5' donor site or 3' acceptor site defines changes of the upstream and downstream exon, respectively (**Figure 11**). Finally, intron retention is the event when the intron is not removed and is retained in the nascent transcript. This splicing event can change the reading frame, altering the function and localization of the resulting protein isoforms (**Figure 11**).

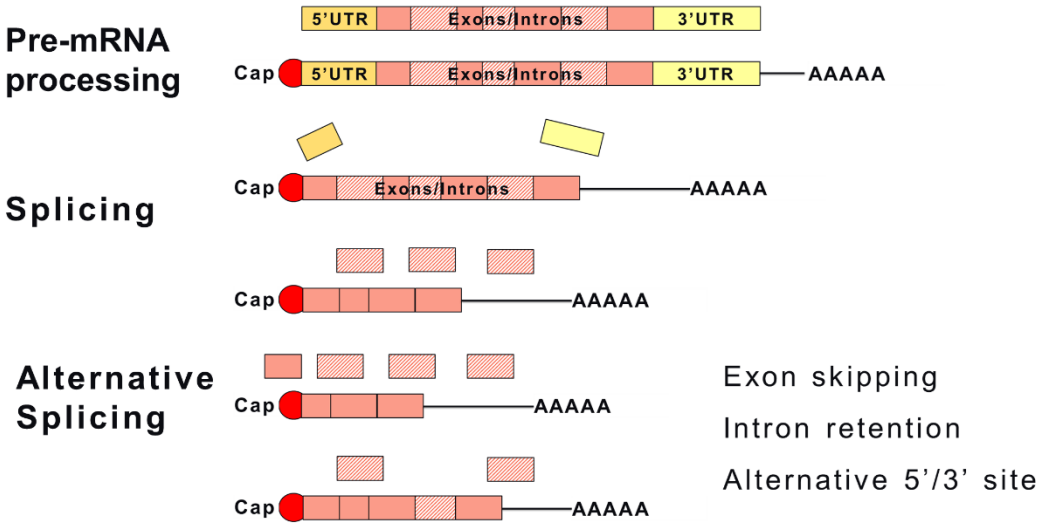

Figure 11. mRNA processing and splicing events. Graphical representation of the cascade events of pre-mRNA processing and subsequent splicing events. The different major types of alternative splicing are reported: exon skipping, intron retention and alternative 5'/3' splice sites.

3. OOCYTE QUALITY IN ASSISTED REPRODUCTION

3.1 Assisted reproduction

According to the World Health Organization (WHO), infertility is a "disease of the reproductive system defined by the failure to achieve a clinical pregnancy after 12 months of more of regular unprotected sexual intercourse" (WHO-ICMART glossary). Infertility has an impact not only on clinical, but also psychological, social, and financial aspects (Mascarenhas et al., 2012), affecting 1 in 6 couples of reproductive age worldwide (WHO Guidelines, 2023). Infertility can be related to female factors (35-40% of couples), male factors (20-40% of couples), both (20-30% of couples) or can remain unexplained. In women, it is commonly caused by ovulatory dysfunction, tubal obstructions and/or endometriosis. In men, it is often a result of abnormalities in sperm production and/or function or of sperm duct obstructions (Nardelli et al., 2014).

Most couples affected by infertility will only achieve pregnancy through assisted reproductive techniques (ART), where the gametes are manipulated outside the human body to increase the chance of a pregnancy. The management of these couples includes fertility counselling, lifestyle modifications, medical/surgical treatments, fertility medications and the adaption of the appropriate ART, such as intrauterine insemination (IUI), *in vitro* fertilization (IVF) and intracytoplasmic sperm injection (ICSI). In recent years, the most common *in vitro* fertilization technique used worldwide has been ICSI, followed by IVF (Nardelli et al., 2014).

In couples undergoing ART, there are three commonly used ovarian stimulation protocols: agonist "down regulation" protocol, also called Luteal Lupron protocol; antagonist protocols that involve the use of the GnRH antagonists to suppress the pituitary function; and the short protocol, also called Microdose Lupron Co-Flare protocol, generally used for patients expected to have low response to ovarian stimulation (Pacchiarotti et al., 2016).

The stimulation generally involves the use of medication to stimulate development of multiple follicles to grow by controlled ovarian hyperstimulation with FSH, in order to obtain more oocytes to fertilize. After 10-12 days approximately, when the follicles growing on the ovary reach trigger size, controlled ovarian hyperstimulation is interrupted, and the GnRH antagonist is generally administered to prevent premature

ovulation. Then, the ovulatory trigger hCG (human Chorionic Gonadotropin) or GnRH agonist is administered, and the oocytes are retrieved 32-36h later. In the case of IVF, the sperm sample is collected, and the spermatozoa are selected for motility and morphology, and incubated with the oocyte. Alternatively, with ICSI, a spermatozoon is directly injected into the oocyte's ooplasm. Finally, the oocytes successfully fertilized are incubated for 5-7 days and then transferred to the uterine cavity (Pacchiarotti et al., 2016).

While several improvements have been made in the past few decades in the field of assisted reproduction, no method has been able to achieve 100% pregnancy rates. This is due to the many variables that could affect the outcome of assisted reproductive cycles, and one of the most important is indeed the quality of the embryo transferred to the woman's uterus. In order to have a fully functional and properly developing embryo, both sperm and oocyte must be of adequate quality (Krisher, 2004). Specifically, the oocyte must be able to resume meiosis after being meiotically quiescent for an extended period of time, cleave after fertilization, and develop into a good quality embryo that can give rise to a normally developing pregnancy (Sirard et al., 2006).

3.2 Factors affecting oocyte quality

Oocyte quality is defined by the ability to undergo meiotic maturation, fertilization, proper embryo development and, finally, give rise to a successful pregnancy. However, several damages can occur altering the oocyte and its cellular content, including oxidative stress and DNA damage. Overall, damage or deregulation in the process impairs the possibility to obtain high quality oocytes, increasing the chance of chromosome segregations errors, aneuploidy and, ultimately, infertility.

Poor oocyte quality is commonly reported in reproductively aged women, with several causes investigated, including mitochondrial dysfunction, telomere and cohesin errors, and spindle assembly alterations (Cimadomo et al., 2018). Recently, it was also observed in women in their 20s and early 30s that more than 20% of their oocytes are aneuploid (Gruhn et al., 2019). Some causes of poor oocyte quality are age-independent (Charalambous et al., 2023).

3.2.1 Age-dependent oocyte quality decay

In human oocytes, meiosis is a long and highly regulated process involving regulation of cell cycle, and it is coupled to the acquisition of developmental competence to support fertilization and early embryonic development. As discussed in the previous chapter, in oocyte meiosis, DNA replication and meiotic recombination are completed during fetal development and the cell arrests at the dictyate (diplotene) stage of prophase I. At this stage, homologous chromosomes are tethered in a bivalent configuration due to crossing over recombination between homologous chromosomes and cohesion between sister chromatids. This bivalent configuration is maintained for decades until final maturation prior to ovulation, when the GV breaks down and meiosis resumes. This extended dictyate arrest as well as the vulnerable recombination configurations are two main reasons for the increased chromosome segregation errors in human oocytes compared to sperm. Moreover, after meiosis resumption, organelles need to reorganize inside the cytoplasm to support meiosis progression, including mitochondria fission and fusion, and mitochondrial activity boost in the subcortical area of the oocyte.

Errors in meiosis I and even meiosis II during chromosome segregation were found not only in oocytes from advanced maternal age (AMA) women, but also in women younger than 20 years old. Indeed, missegregation events were identified in human oocytes spanning the entire reproductive life span (9-43 years) following a U-shape curve (Gruhn et al., 2019). As discussed extensively in the section about "Chromosome segregation errors" (Introduction 2.4), this phenomenon may be due to a "metabolic clock" (Gruhn et al., 2019) finely regulated by the reproductive system, resulting in the ovulation of damaged oocytes in the extreme times of the reproductive life (i.e. too early, teenage, and too late, advanced maternal age).

Several factors have been explored to elucidate the molecular mechanisms behind the decline of oocyte quality in AMA women, and its inability to reach meiotic competence. Some are the loss of active DNA repair apparatus, bioenergetic status and mitochondrial damage of the oocyte (Titus et al., 2013), together with the reduced capacity to dispose of ROS.

3.2.2 Age-independent oocyte quality decay

Oocytes of poor quality are not exclusive to women approaching the end of their reproductive life, but also to women between late 20s and early 30s. Indeed, 1-10% of reproductive age women (Shestakova et al., 2016; McGlacken-Byrne & Conway, 2022) show a reduced number of follicles accompanied by alteration in hormonal levels, diminished ovarian function and poor oocyte quality, overall impairing their ability to conceive (Alviggi et al., 2009). Women affected by Premature Ovarian Insufficiency (POI) present complex systemic symptoms such as amenorrhea, hypoestrogenism, high serum FSH levels, low anti-Mullerian hormone (AMH) levels, and a reduction of estradiol concentration in blood. Furthermore, POI is characterised by accelerated ovarian senescence with a reduction in follicle size and number and, overall, hypofertility (De Vos et al., 2010; Nelson, 2009). This condition was defined as early ovarian aging or POI and it is found in several mammals including humans, mice and, recently, cows (Goswami et al., 2007; Jagarlamudi and Daumè, 2010; Lodde et al., 2021).

Two main hypotheses have been proposed to explain the onset of POI: (1) failure to acquire an adequate number of initial primordial follicles during fetal life, and (2) excessive clearance of primordial follicles, together with the suppressed activation and further development of primordial follicles (Jagarlamudi et al., 2010; Tucker et al., 2016). However, the aetiology of the majority of POI cases remains idiopathic. This condition seems to have a heterogeneous background, and in the past decade an increasing number of genes have been associated with POI, including *STAR* (Steroidogenic Acute Regulatory Protein) important for hormonal support, *STAG3* (Stromal Antigen 3) subunit of cohesion and required for proper pairing and segregation of chromosomes during meiosis, *SYCE1* (Synaptonemal Complex Central Element Protein 1) and *PSMC3IP* (Proteasome 26S Subunit, ATPase 3 Interacting Protein) involved in homologous recombination, and *SOHLH1* (Spermatogenesis And Oogenesis Specific Basic Helix-Loop-Helix 1), *BMP15* (Bone Morphogenetic Protein 15) and *FSHR* (Follicle Stimulating Hormone Receptor) involved in follicular activation, development or maturation (Tucker et al., 2022). At first, POI was considered only a monogenic condition, but recent data also support its polygenic aetiology, suggesting a synergistic effect of several genes for arising the phenotype (Tucker et al., 2022). Overall, most genes mutated in patients affected by POI are associated to biological processes as folliculogenesis, metabolic support/ROS control, DNA damage repair, cell death and apoptosis, meiosis and DNA

replication, immune function and hormonal signalling (Tucker et al., 2016; Lodde et al., 2021; Tucker et al., 2022).

3.3 Animal models to study the mechanisms of oocyte quality decay

Several animal models have been developed to study the mechanisms of oocyte competence acquisition and the causes of oocyte quality decay. Cows are an attractive species to investigate oocyte growth and maturation, including the alterations and errors of this process.

A phenotype similar to POI has been described in young adult cows since the late 1990s. However, it has been characterized in detail in terms of morphological and functional aspects only recently (Malhi et al., 2005; Lodde et al., 2021). The poor ovary phenotype reported in cows presents itself with high FSH serum levels, low AMH, reduced estradiol and increased progesterone in follicular fluid, reduced antral follicle count (less than 10 in both ovaries) and small ovary size (length on the major axis), and overall reduced fertility. These animals are also characterized by normal oocyte meiotic progression rates but reduced developmental competence, with about 6% blastocyst and high aneuploidy rates (60%) in embryos (Luciano et al., 2013). As a whole, these features are actually comparable with the ones noted in young women affected by early ovarian ageing, as deeply discussed in the previous "Age-independent oocyte quality decay" section (Introduction 3.4).

Specifically, Lodde and colleagues studied a model of low-quality oocytes obtained from young adult cows and observed several alterations in nuclear and cytoplasmic maturation, such as mitochondria distribution and activity, histone modifications, DNA damage, glutathione content and communications between oocyte and CCs. These alterations were linked to oocyte developmental competence (Lodde et al., 2021).

4. WHAT THE OOCYTE NEEDS TO BE COMPETENT

4.1 How the oocyte must look like: morphology

The first parameter used for oocyte selection was the morphological evaluation (De Vos et al., 1999; Balakier et al., 2002; Rosenbush et al. 2002) at the time of retrieval, as common practice in ART clinics. The use of morphological criteria can provide valuable information to identify oocytes with the highest quality, that must be competent and that will potentially generate viable embryos (Wang et al., 2007).

Due to the high subjectivity of the evaluation, guidelines have been developed (ESHRE Atlas of Human embryology, 2023) to standardize the assessment of several elements commonly evaluated, including COC, oocyte cytoplasm, PB size, shape, and localization, ZP and perivitelline space.

Cumulus-oocyte complex

The COC is formed by an oocyte surrounded by specialized granulosa cells, the CCs. These CCs are in direct contact with the oocytes, expanding through oocyte maturation (Coticchio et al., 2004), and are therefore critical for oocyte maturation, ovulation and fertilization, providing energy and protecting the oocyte itself against the damaging effects of ROS. The COC is crucial in maintaining communications between the oocyte and the CCs by directly affecting gene expression and protein synthesis (Huang and Wells, 2010; Turathum et al., 2021). This mutual connection in the COC is maintained by high specialized trans-zonal cytoplasmic projections that penetrate through the ZP and contain gap junctions (Albertini et al., 2001; Li and Albertini, 2013). Moreover, the general function of CCs is to support the growth of the oocyte, produce hyaluronic acid, and undergo expansion in response to FSH (Turathum et al., 2021). Following oocyte growth and maturation, CCs undergo proliferation, and the gap junctions are gradually released from the ooplasm (Huang and Wells, 2010; Turathum et al., 2021).

Cytoplasm

At the time of retrieval, the oocyte's cytoplasm is evaluated, including the size and distribution of the vacuoles and granules in the cytoplasm (**Figure 12**).

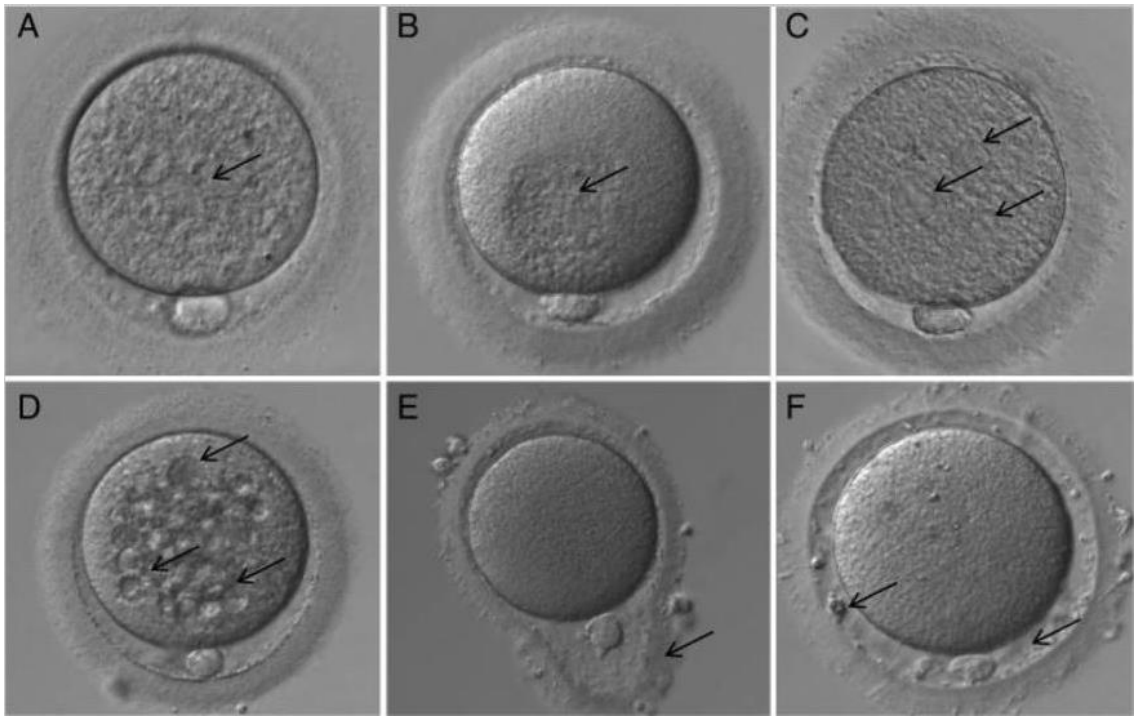

Figure 12. Denuded human MII oocytes with different morphological abnormalities. Images acquired using light microscopy (400X magnification). The morphological abnormalities are marked (arrows). (**A**) Diffuse cytoplasmic granularity, (**B**) centrally located cytoplasmic granular area, (**C**) smooth endoplasmic reticulum clusters, (**D**) vacuoles, (**E**) abnormal zona pellucida, (**F**) large perivitelline space with fragments. (*Image obtained with permission from Oxford University press license. Rienzi et al., 2011*)

Best quality human oocytes are usually transparent, turgid and with a homogeneous cytoplasm without abnormalities or granules in the cytoplasm (Balaban and Urman, 2006; Ebner et al., 2006; Rienzi et al., 2008; Figueira et al., 2010). Nevertheless, CGs seem to be fundamental characteristic of competent oocytes and are known to be crucial in the early steps during fertilization (Coticchio et al., 2015). CGs are small membranous organelles distributed close to the oolemma in mature oocytes and appear as secretory small vesicles measuring 0.2-0.6 µm in diameter (Szollosi, 1967) (while the oocyte is about 100-120 µm in diameter). Furthermore, CGs are associated with the modifications

occurring at the time of fertilization, where intracellular Ca2+ signalling drives activation events. CGs fuse their membrane with the oolemma spilling their content into the perivitelline space, i.e. the space between the ZP and the plasma membrane of the oocyte (Hassa et al., 2014). These events together with the changes in the ZP contribute to prevent polyspermic fertilization (Coticchio et al., 2015).

Perivitelline space

Perivitelline space abnormalities, i.e. large space between ZP and the surface of the egg and granularity, have been reported associated with increased oocyte degeneration (Mikkelsen and Lindenberg, 2001) and lower fertilization rates (Plachot et al., 2002; Hassa et al., 2014; Ferrarini Zanetti et al., 2018). However, several studies failed to found a direct correlation between shape and size of perivitelline space and successful fertilization and/or embryo development (Ebner et al., 2006; de Cássia S Figueira et al., 2010) and the argument is still controversial. On the contrary, the perivitelline space granularity significantly correlates with embryo quality (Hassa et al., 2014; de Cássia S Figueira et al., 2010) (**Figure 12F**).

Zona pellucida

Oocytes are moreover classified based on the thickness and the colour of the ZP (**Figure 12E**). Best quality human oocytes are the ones with a birefringent ZP of about 20 µm (Rama Raju et al., 2007). However, there are studies reporting that the thickness of the ZP has no influence on embryo development after ICSI (Laisiene et al., 2009). A thinner ZP might be associated with higher fertilization rates, as it appears to facilitate sperm penetration (Ozturk, 2020). As a whole, the available information does not allow the ZP to be used to assess oocyte quality and competence (Lemseffer et al., 2022).

Polar body

The presence of one PB is evaluated to assess the meiotic stage of the retrieved oocyte and, therefore, to determine whether it is potentially competent (Sirard et al., 2006). Several studies in animal models but also in humans (Coticchio et al., 2004, 2015;

Hoshino et al, 2018; Yang et al., 2022) supported the positive correlation between PB extrusion, its morphology, and positioning with oocyte competence, contributing to include PB as common hallmark of achieved meiotic maturation, i.e. oocyte at MII stage. Oocytes with intact and normal PB have high fertilization rates, while those displaying PB characterized by fragmentation, large size, irregular shape, rough surface, are considered poor quality oocytes. Moreover, oocytes with PB alterations are developmentally less competent after fertilization, yielding low pregnancy rates after embryo transfer (Ebner et al., 1999; Ebner et al., 2002; Coticchio et al, 2015; Hoshino et al, 2018). However, the extrusion of the first PB alone does not provide information regarding the oocytes' cytoplasmic competence, and there is still a dispute on whether this can be sufficient to assess the MII stage (Patrizio and Sakkas, 2007; Hoshino et al, 2018; Lemseffer, 2022).

Meiotic spindle

The meiotic spindle is fundamental for the correct alignment and segregation of chromosomes through meiosis (Coticchio et al., 2015; Thomas et al., 2021; Charalambous et al., 2023). Several studies conducted with polarized light (**Figure 13**), suggest that oocytes with a birefringent spindle had better embryonic development than those without (Wang and Sun, 2007; Lemseffer et al., 2022).

In good quality oocytes, spindles display a vertical orientation relative to the oolemma, to form a compact bipolar spindle. Furthermore, the correct alignment of chromosomes at the meiotic spindle is fundamental for their proper segregation during meiosis and later for fertilization. As already discussed in the previous sections, alterations in spindle localization and/or positioning are associated with errors in chromosome segregation and, ultimately, aneuploidy (Thomas et al., 2021; Charalambous et al., 2023).

The parameters of the meiotic spindle used to determine the quality of oocytes are usually location and refraction. Nevertheless, some studies have reported absence of relationship between spindle location and oocyte developmental competence (Wang et al., 2001; Moon et al., 2003; Rienzi et al., 2003). Conversely, oocytes with birefringent spindles have been associated with higher developmental potential after fertilization (Wang et al., 2001; Moon et al., 2003; Rienzi et al., 2003).

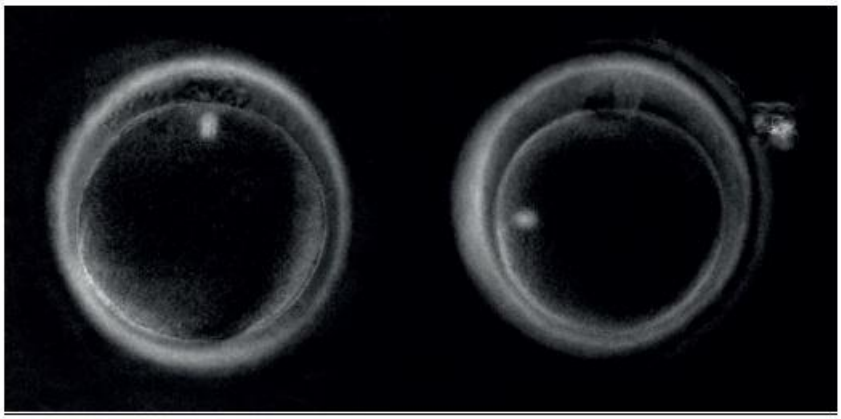

Figure 13. Polscope imaging of two human oocytes. The meiotic spindle is observed in both panels. On the left, the spindle is in the correct alignment, in correspondence to the first polar body. On the contrary, in the image on the right, the spindle is offset 90º. (*Clinical embryology notebook, ASEBIR*).

4.2 Global gene expression

In the previous sections, it was discussed that oocyte growth and maturation are associated with dynamic transcriptional changes, featured by high transcriptional activity of growing oocytes and transcriptional silencing of mature oocytes. Elucidating the differences in transcriptomic profiles in individual oocytes might allow for the prediction of their meiotic competence and potential to develop into viable embryos. Several microarray and massive parallel sequencing-based studies have been performed in mouse, rabbit, cow, monkey (Su et al., 2007; Kues et al., 2008; Ruebel et al., 2018; Ruebel et al., 2021) and also in human oocytes (Ruebel et al., 2021; Llonch et al., 2020; Cornet-Bartolomè et al., 2021). Collectively, these studies confirmed that oocytes at different stages of maturation have distinct molecular profiles and that alteration in gene expression profile can lead to lower oocyte quality. Nevertheless, robust and reliable biomarkers of oocyte quality and embryo development in human oocytes are still lacking.

4.3 The role of non-coding RNA

Most transcriptomic studies on cells and tissues, including oocytes and embryos, are focused on protein-coding mRNA transcripts (Vassena et al., 2007; Vassena et al., 2011). However, non-coding RNAs play a central role in eukaryotic gene regulation: mRNA polyadenylation is driven by events regulated by small nuclear and nucleolar RNAs; mRNA translation is mediated by ribosomal RNAs and transfer RNAs and it is negatively regulated by micro RNAs. Finally, small-interfering RNAs and piwi-interacting RNAs regulate mRNA abundance (Siomi et al., 2011; Wang et al., 2012). Moreover, a new class of non-coding RNA has been identified (Mercer et al., 2009; Hangauer et al., 2013). This class of non-coding RNAs (lncRNAs) have been detected at different stages of human preimplantation development, suggesting an additional level of regulation of oocyte maturation and embryo early development (Caley et al., 2010; Hangauer et al., 2013; Fatica et al., 2014; Xu et al., 2014; Taylor et al., 2015).

4.4 mRNA processing, splicing and alternative splicing

Another approach that might provide information of the molecular mechanisms influencing the oocyte quality, its competent status and, finally, the subsequent early embryo development is the analysis of alternative pre-mRNA splicing (AS).

Until recent years, transcriptomic analysis were focused on gene expression to identify genes involved in the control of oocyte maturation and embryo development (Evsikov et al., 2009). The oocyte's transcripts are mostly accumulated inside the GV. The accumulated transcripts are crucial to support the final steps of oocyte maturation and the initiation of cell division in the nascent embryo, where transcription is at a basal level, mostly undetectable, until the embryonic genome activation at the 8-cell stage (Gosden and Lee, 2010; Vassena et al., 2011). Among the possible mechanisms, selective degradation of mRNA transcripts is the best explored one (Lequarre et al., 2004; Bettegowda et al., 2006; Su et al., 2007). Moreover, AS is also involved in human oocyte transcript regulation (Salisbury et al., 2009; Tang et al., 2011; Li et al., 2020; Cornet-Bartolome et al; 2021).

In fact, it was recently reported that a fine control of the isoform balance is necessary for proper development and adult tissue homeostasis (Yan at al., 2013; Baralle and Giudice, 2017). Furthermore, in Xenopus eggs, Grenfell and colleagues observed that spliceosome components were involved in the correct formation of an appropriate spindle and non-coding mis-spliced transcripts could act on AURK and CENP proteins to induce incorrect spindle formation (Grenfell, Heald, & Strzelecka, 2016). Moreover, an imbalance between protein isoforms induces chromosome mis-segregation during mitosis in cancer cell lines. Sororin and APC2, both involved in chromosome segregation, show mis-spliced variants that can induce incorrect spindle formation when the spliceosome activity is deregulated in HeLa cells (Lelij et al., 2014; Oka et al., 2014; Sundaramoorthy, Vázquez-Novelle, Lekomtsev, Howell, & Petronczki, 2014; Watrin, Demidova, Watrin, Hu, & Prigent, 2014). In mice, the deletion of the Serine and Arginine Rich Splicing Factor 3 (SRSF3) that plays critical roles in the regulation of pre-mRNA splicing, alters GVBD (Do et al., 2018). These data suggest that AS is crucial for GVBD in mice. Besides, these studies in animal models indicate that the oocyte requires a controlled AS mechanism to acquire not only the correct transcripts abundance but also the correct transcript isoforms.

4.5 Mitochondria

Mitochondria regulate numerous metabolic, redox, epigenetic and calcium signalling processes that are essential for oocyte function, and emerging studies highlight mitochondrial dysfunction as key contributor of poor quality in oocytes, associated or not with aging.

Mitochondria have a crucial role in supplying the energy to sustain the nuclear and cytoplasmic changes occurring during oocyte maturation, that are essential for meiotic competence (Krisher and Bavister, 1998; Krisher, 2004; Stojkovic et al., 2001; van der Reest et al., 2021; Kirillova et al., 2021). Recently, mitochondrial dysfunction has been associated with meiotic spindle damage, chromosome misalignment, and aneuploidy (Mikwar, MacFarlane, & Marchetti, 2020), but the functional link between these phenomena has not been established yet.

There are two main aspects that can influence oocyte developmental competence, mtDNA number and energy basal capacity. In several species there is an association between mtDNA copy number and an oocyte ability to be fertilized (Santos et al., 2006; Reynier et al., 2001). Moreover, oocytes from AMA women or women with diminished ovarian reserve have lower levels of mtDNA (Duran et al., 2011; May-Panloup et al., 2005).

There is a known cooperation between the oocyte and the surrounding CCs, where the CCs are responsible for the conversion of glucose to pyruvate, which is finally transported into the oocyte. Despite being present in an immature shape and function, mitochondria in the oocyte participate in ATP production. Moreover, in animal models and humans it was recently reported that higher ATP levels positively correlate with better reproductive outcomes, and that oocytes that fail to fertilize are usually characterized by lower amount of ATP (Zhao et al., 2012). Indeed, in mice, the inhibition of oocyte's OXPHOS negatively affects the blastocyst rates of the derived embryo (Almansa-Ordonez et al., 2020).

The distribution and reorganization of mitochondria during oocyte maturation are extremely dynamic, and these changes might be related to mitochondrial function. Oocytes with higher concentrations of ATP show higher fertilization and blastocyst rates (Stojkovic et al., 2001; Nagano et al., 2006; Kirillova et al., 2021). On the other hand, inhibition of OXPHOS in mouse oocytes leads to a compromised ability to correctly assemble spindle, progress in meiosis, distribute mitochondria and, overall, the ability to form blastocysts (Almansa-Ordonez et al., 2020).

With aging and age-related changes in oocytes, mitochondrial abnormalities such as reduced mtDNA content, reduced mitochondrial membrane potential (and consequent bioenergetic capacity) (Pasquariello et al., 2019), increased oxidative stress and frequency of mtDNA mutation and deletions, have been related to poor quality or low oocyte competence (Rong-Hong Hsieh et al., 2002; Eichenlaub-Ritter et al., 2004; Bentov et al., 2011; Duran et al., 2011; Tilly and Sinclair, 2013; Simsek-Duran et al., 2013; Woods et al., 2018; Hoshino et al., 2018; van der Reest et al., 2021).

Overall, recent studies demonstrated the connection between mitochondrial metabolism, AS and spindle assembly, and this interplay could explain the mechanisms through which mitochondrial activity influences oocyte developmental competence.

5. NOVEL NON-INVASIVE METHODS FOR OOCYTE ASSESMENT

The selection of high-quality oocytes is crucial to obtain embryos with high developmental potential (Gardner and Sakkas, 2003; Kirkegaard et al., 2015; Kovacs and Lieman, 2019; Zaninovic and Rosenwalks, 2010). The most common method used to assess oocytes quality is to evaluate their morphology at different stages through meiotic maturation, as previously discussed (Introduction 4.1). Recently, novel microscopy techniques were developed to evaluate oocytes, CCs and embryo quality non-invasively (Venturas et al., 2023).

Some intracellular molecules like nicotinamide adenine phosphatase dinucleotide (NADPH), nicotinamide adenine dinucleotide (NADH) and flavine adenine dinucleotide (FAD+) are autofluorescent (Heikal et al., 2010). These molecules are endogenous electron carriers that play important roles in the electron transport chain, glycolysis and fermentation. NAD(P)+ and FADH2, on the contrary, are not autofluorescent (Heikal et al., 2010). These coenzymes have a diagnostic potential as non-invasive biomarkers for cellular metabolic state and mitochondrial abnormalities (Heikal et al., 2010; Dumollard et al., 2004; Tan et al., 2022). NADH and NADPH fluorescence spectra is almost indistinguishable (Ghukasyan and Heikal, 2014), therefore the fluorescence of both NADH and NADPH is often combined and called NAD(P)H. Both NAD(P)H and FAD+ two photon fluorescence spectra is quite distinct, allowing for simultaneous detection (Heikal et al., 2010) (**Figure 14**). Although FAD+ is only located in the mitochondria (Dumollard et al., 2009), NAD(P)H can also be located in the cytoplasm (Stein and Imai, 2012).

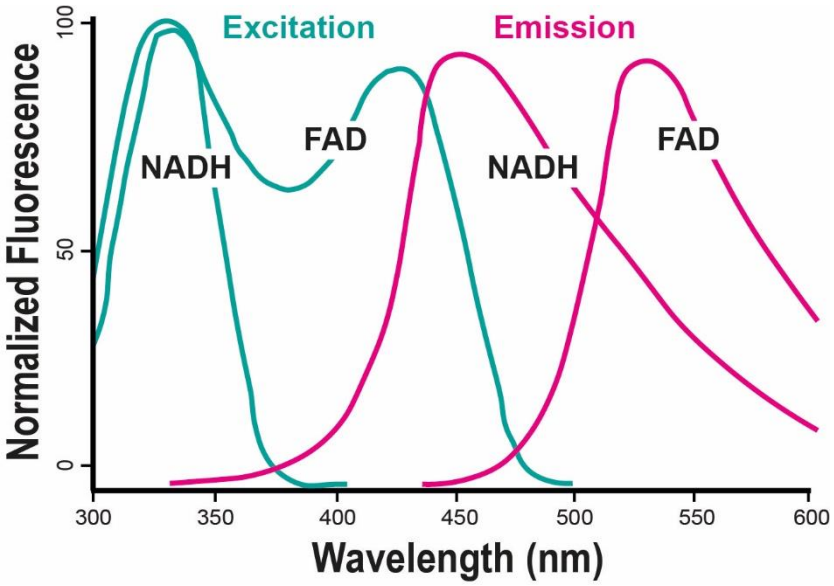

Figure 14. Excitation (green) and emission (pink) spectra of NADH and FAD.

Fluorescence lifetime imaging microscopy (FLIM) of NAD(P)H and FAD+ autofluorescence is a novel non-invasive technique that can provide direct quantitative measurements of concentration and fluorescence lifetimes (Sanchez et al., 2018; Ghukasyan and Heikal, 2014; Becker, 2012; Ma et al., 2019). The fluorescence intensity of a molecule correlates with its concentration and its molecular conformation, which can be altered by the surrounding environment, such as pH, oxygen concentration or temperature. Both NAD(P)H and FAD+ have a short and long lifetime component, depending on whether they are free or bound to an enzyme (Lakowicz, 2006). For NAD(P)H, the short lifetime corresponds to its free state and the long lifetime to its enzyme-bound state (Skala et al., 2007; Lakowicz, 2006). On the contrary, for FAD+ the longer lifetime component corresponds to free FAD+ and the shorter component to protein bound FAD+ (Skala et al., 2007).

FLIM uses a two-photon pulsed-laser microscopy (Becker, 2012), which is based on nonlinear excitation of molecules where two photons are then needed to excite a single molecule of NAD(P)H or FAD+. Moreover, FLIM uses the time-correlated single photon counting (TCSPC) technique. With TCSPC, the sample is scanned by a focused beam of a pulsed laser and single photons of fluorescent light emitted from both NADH and FAD+ can be detected. Two-photon pulsed-laser microscopy and TCSPC offer several

advantages compared to standard confocal microscopy, including high resolution, while minimizing the potential photodamage to the sample and offering great penetration depth, reducing laser scattering (Beaurepaire and Mertz, 2019). Additionally, FLIM can measure cellular and subcellular metabolic heterogeneity with high spatiotemporal resolution.

Overall, the fluorescence lifetimes of NADH and FAD+ provide a sensitive tool to characterize variations in the metabolic state of oocytes and embryos (Venturas et al., 2023). A single FLIM image provides eight quantitative measures to non-invasively assess the metabolic state of the cell. Additionally, the redox ratio can also be computed from the mean intensity of NADH divided by the mean intensity of FAD+. The use of FLIM to directly quantify mitochondrial activity and measure metabolism, introduce a potential new tool for the non-invasive assessment of oocytes.

OBJECTIVES

The main objective of the present thesis is the characterization of the final phases of human oocyte maturation, with a special focus on the transcriptional/post transcriptional profiles, and metabolic function. The knowledge acquired will be then translated to the most common reproductive conditions of altered meiotic competence, in both human and bovine species.

Specifically, the sub-objectives are:

1. To identify transcriptomic changes during oocyte final meiotic maturation, by evaluating differences in gene expression, mRNA processing and splicing pattern among GV oocytes, GV oocytes that fail to mature, *in vitro* matured MII oocytes (IVM-MII) and *in vivo* matured MII oocytes (IVO-MII) from young healthy women.
2. To define an animal model to study poor oocyte quality, by identifying the transcriptomic profile of GV and IVM-MII oocytes from young healthy cows and compare it to that of GV and IVM-MII oocytes from young cows with compromised oocyte and ovarian quality.
3. To evaluate mitochondrial activity, localization and metabolism during final meiotic maturation of oocytes obtained from young, healthy women and compare this profile with oocytes from AMA women.

RESULTS

1. mRNA PROCESSING DURING HUMAN OOCYTE MATURATION

Title: Specific processing of meiosis related transcript is linked to final maturation in human oocytes

Authors: Sara Pietroforte [1,2], Montserrat Barragan Monasterio [1], Anna Ferrer-Vaquer [1], Manuel Irimia[3,4,5], Elena Ibáñez [2], Mina Popovic [1], Rita Vassena [1], Filippo Zambelli [1]

Affiliations:

1 - Basic Research Laboratory – Eugin Group, Barcelona 08006, Spain.

2 - Departament of Cell Biology, Physiology and Immunology, Universitat Autònoma de Barcelona, 08193 Bellaterra, Barcelona, Spain.

3 - Center for Genomic Regulation, Barcelona Institute of Science and Technology, Barcelona, 08003, Spain.

4 - Universitat Pompeu Fabra, Barcelona, 08002, Spain.

5 - Catalan Institution for Research and Advanced Studies (ICREA), Barcelona 08010, Spain.

Manuscript published in *Molecular Human Reproduction*, doi:10.1093/molehr/gaad021.

ABSTRACT

Human meiosis in oocytes entails an intricate regulation of the transcriptome to support late oocyte growth and early embryo development, both crucial to reproductive success. Currently, little is known about the co- and post-transcriptional mRNA processing mechanisms regulating the last meiotic phases, which contribute to transcriptome complexity and influence translation rates. We analysed gene expression changes, splicing and pre-mRNA processing in an RNA sequencing set of 40 human oocytes at different meiotic maturation stages, matured both *in vivo* and *in vitro*. We found abundant untranslated region (UTR) processing, mostly at the 3' end, of meiosis-related genes between the germinal vesicle (GV) and metaphase II (MII) stages, supported by the differential expression of spliceosome and pre-mRNA processing related genes. Importantly, we found very few differences among GV oocytes across several durations of IVM, as long as they did not reach MII, suggesting an association of RNA processing and successful meiosis transit. Changes in protein isoforms are minor, although specific and consistent for genes involved in chromosome organization and spindle assembly. In conclusion, we reveal a dynamic transcript remodelling during human female meiosis, and show how pre-mRNA processing, specifically 3'UTR shortening, drives a selective translational regulation of transcripts necessary to reach final meiotic maturation.

Keywords: Human oocytes, meiosis, oocyte competence, 3' untranslated regions, 3' untranslated region processing, splicing, gene expression, alternative splicing

INTRODUCTION

Progression to metaphase of the second meiotic division (MII) in human oocytes is error-prone and the main cause of embryonic aneuploidy. Incorrect chromosomal segregation affects 20-30% of oocytes in young women and 70-80% in women of advanced reproductive age, with most alterations occurring during meiosis I (Hassold and Hunt, 2001; Wartosch et al., 2021). Nuclear and cytoplasmic maturation of the oocyte, key for successful fertilization and normal embryo development (Coticchio et al., 2013), start during fetal development, pause in the fetal ovary at the diplotene stage of prophase I, and resume after puberty (Jaffe and Egbert, 2017). An oocyte arrested in prophase I contains a large nucleus, called a germinal vesicle (GV), with a visible nucleolus (de la Fuente, 2006). The LH surge induces chromatin condensation and GV breakdown (GVBD), driven by the mTOR-eIF4F pathway (Susor et al., 2015; Jansova et al., 2018). When chromosomes are fully condensed, an acentrosomal spindle forms and migrates towards the oocyte cortex, where anaphase I takes place. The asymmetric cytokinesis that ensues produces a large oocyte and a small polar body (PB), which is extruded while the oocyte arrests in MII until fertilization (Mihajlović and FitzHarris, 2018).

The regulation of transcription during oogenesis is conserved across several mammalian species, including mice, pigs, bovines (Yang et al., 2020; Wu et al., 2022; Mamo et al., 2011; Luciano et al., 2012) and, as recently shown, also in humans (Cornet-Bartolomè et al., 2021). During oocyte growth, transcripts are first accumulated, then transcription stops in the fully grown oocyte and remains silenced during fertilization and initial embryo development. Specifically, transcription in human oocytes is active in those GVs that have an open chromatin configuration, resembling the mouse non-surrounded nucleolus (NSN), while it arrests when the chromatin condenses around the nucleolus, similar to the mouse surrounded nucleolus status (SN).

The role of co- and post-transcriptional regulation, conversely, remains poorly characterized (Jansova et al., 2018). In somatic cells, the pre-mRNA undergoes 5' capping, 3' polyadenylation and RNA splicing in the cell nucleus before being exported to the cytoplasm and translated. Capping occurs first, then transcripts are cleaved and polyadenylated at the 3'end by RNA binding proteins, which interact with regulatory RNAs motifs contained in the 3' untranslated regions (UTRs) (Matoulkova et al., 2012). In oocytes, however, polyadenylation occurs later on, in the cytoplasm, and influences

specific transcripts' degradation/translation potential, as shown in mice and pigs (Yang et al., 2020; Wu et al., 2022). Over 80% of mammalian mRNA genes present multiple polyadenylation sites, resulting in alternative polyadenylation (APA) isoforms with different 3'UTR lengths (Derti et al., 2012). Alternative 3'UTR isoforms can lead to different mRNA subcellular localization, stability, and translation timing (Leppek et al., 2018). Finally, splicing is a co-transcriptional mechanism that processes the pre-mRNA to a mature transcript ready to be translated. This process is mainly performed by the spliceosome, which is composed of five U-rich small nuclear ribonucleoproteins (U1, U2, U4, U5, U6 snRNPs), NineTeen complex, NineTeen complex-related and several other factors, including serine/arginine-rich proteins and hetero-nuclear ribonucleoproteins, and proteins stably bound within the building mRNAs, like the exon-junction complex and the transcription-export (TREX) complex (Dias et al., 2010; Pühringer et al., 2020).

Alternative splicing (AS) is a crucial process to obtain different proteins from the same gene, through exon skipping, intron retention and alternative splice sites. Although they originate from the same transcript, these proteins can have different functions. AS is involved in almost every aspect of protein function, including protein-ligand binding, and structural changes (Kelemen et al., 2020). AS contributes to transcriptome complexity (Braunschweig et al., 2013) and its dysregulation can lead to aberrant phenotypes and diseases (Cooper et al., 2009). While some reports show a differential expression of spliceosome related transcripts (Zhao et al., 2019; Llonch et al., 2021) and differentially spliced genes (Cornet-Bartolomè et al., 2021; Li et al., 2020) during human oocyte maturation, clear information on transcriptomic regulation during human meiosis is lacking.

Here, we present a detailed investigation of transcriptome remodelling in human oocytes from GV to MII, with a particular focus on expression and splicing patterns.

MATERIALS AND METHODS

Ethical approval

Approval to conduct this study was obtained from the Ethics Committee for Clinical Research (CEIm) of Clinica Eugin and all research was performed in accordance with relevant guidelines and regulations. All women participating in this study gave their written informed consent prior to inclusion.

Study population

Thirty-six oocyte donors at Clinica Eugin (Barcelona, Spain) from December 2018 until June 2019 were included in the study. Inclusion criteria were age 18-34 years, BMI<33, normal karyotype, and absence of systemic or reproductive conditions. For single-cell RNA sequencing analysis, 40 oocytes were collected: 10 of them were included in the study as GV immediately after oocyte retrieval, 10 as MII after IVM (IVM-MII), 10 as GV that failed to mature after IVM (FTM-GV) and 10 *in vivo* matured MII (IVO-MII) were included in the study after vitrification/warming. To lower the impact of the high genetic variability of human oocytes on our results, no more than two oocytes were collected from the same donor (Supplementary Table S1).

Ovarian stimulation, oocyte retrieval and IVM

All participants had normal ovarian morphology at transvaginal ultrasound, an ovarian reserve of more than eight antral follicles in both ovaries and a progressive increase in follicular size in response to ovarian stimulation. All women were stimulated with daily injections of 150 to 300 IU of highly purified hMG (Menopur®, Ferring, Saint-Prex, Switzerland) or follitropin alpha (Gonal®, Merck Serono, Darmstadt, Germany), as previously described (Blazquez et al., 2014). Pituitary suppression was performed with a GnRH antagonist (0.25 mg of cetrorelix acetate, Cetrotide®; Merck Serono, Darmstadt, Germany; or 0.25 mg of ganirelix, Orgalutran®; Merck Sharp & Dohme, Kenilworth, New Jersey, USA) administered daily from day 7 of stimulation (Olivennes et al., 1995). When three or more follicles of ≥18 mm of diameter were observed, final oocyte

maturation was triggered with 0.2 mg of the GnRH agonist triptorelin (Decapeptyl®; Ipsen Pharma, Paris, France).

Oocyte retrieval was performed by ultrasound-guided transvaginal follicular aspiration, strictly 36 hours after trigger. Oocytes were denuded 30 minutes after retrieval with 80 IU/ml hyaluronidase (Hyase-10x, Vitrolife, Gothenburg, Sweden) in G-MOPS (Vitrolife, Gothenburg, Sweden) by gentle pipetting. Once denuded, oocytes were checked for the presence of a polar body, and GVs were either processed immediately as GV or matured *in vitro* in 30 µL of G2-plus (Vitrolife, Gothenburg, Sweden) covered by Ovoil (Vitrolife, Gothenburg, Sweden) in a humidified atmosphere of 6% CO_2 at 37°C for 32 hours. After IVM, if the first PB was extruded, the oocyte was considered as IVM-MII, whereas if the GV was still present, the oocyte was considered as GV that failed to mature (FTM-GV). *In vivo* matured MII (IVO-MII) oocytes were vitrified/warmed according to the Cryotop vitrification method using the Cryotop vitrification open system (Kitazato BioPharma Co., Ltd, Fuji, Japan) (Kuwayama, 2007).

Single-cell RNA sequencing and raw data processing

The collection of samples for the four experimental groups (GV, IVM-MII, FTM-GV and IVO-MII) was performed in the same timeframe, distributing the oocytes evenly amongst the groups. The same operator performed all oocyte scoring, handling and collection. Oocytes' zona pellucida was removed with pronase (Roche Diagnostics, Basel, Switzerland) and zona-free oocytes were lysed individually in 20µL of Extraction Buffer (PicoPure RNA Isolation Kit, Thermo Fisher, Waltham, Massachusetts, USA), incubated at 42°C for 30 min and stored at -80°C. In the case of MIIs, the PB was removed after the zona digestion, and only the oocyte was lysed. Total RNA extraction was performed on the same day for all the oocytes, following manufacturer's specifications and two batches were created with equal representation of the four experimental groups in each batch.

Single oocyte cDNA libraries were constructed in two batches using the Ovation SoLo RNA-Seq System (NuGEN, TECAN, Männedorf, Switzerland). Sequencing of libraries was carried out using a HiSeq 2500 (Illumina, San Diego, California, USA) with 2x150 bp paired-end reads, with 30 million reads per sample. Sequencing was performed in one run but split in two flow cells, where each flow cell had shuffled samples representing the

four experimental groups. FastQC (Babraham Bioinformatics, Cambridge, UK) was used to perform the quality control of the sequencing.

Gene expression and splicing analysis

After quality control of raw reads, the remaining clean reads for each sample were aligned to the GRch38 human reference genome and bam files were generated. Subsequently, reads belonging to whole genes or single exons were counted using the function SummarizeOverlaps of the Bioconductor/R package Genomic Features (Lawrence et al., 2013) DESeq2 (Love et al., 2014) was then used to detect differentially expressed genes (DEGs) between experimental groups with an adjusted p-value <0.1, while DEXSeq (Anders et al., 2012) and edgeR (function: topSpliceDGE) (Robinson et al., 2010) detect the differential exon usage for genes in which global expression is not significantly different, and all exons with an adjusted p-value<0.05 for DEXseq and an FDR of 0.1 for edgeR were considered differentially expressed. When comparing the differentially expressed exons by Fold Change, we considered as similar those who showed similar trend (up- or down-regulated) and the same order of magnitude. Furthermore, qapa v1.3.3 (Ha et al., 2018) was adopted to identify alternative poly(A) sites that result in alternative 3'UTR isoforms. Following instructions provided by the developers, we generated a 3'UTR library from the annotations and extracted indexed sequences by transcript quantification tools. Finally, we calculated the relative usage of alternative poly(A) (PAU) for each oocyte only in the genes with two alternative UTR isoforms and used a ranked Wilcoxon paired test to evaluate significant alternative poly(A) site usage between stages. Significant alternative 3'UTR isoform usage was reported with a difference in average of proximal PAU of |10| (ΔPPAU) and a p-value <0.05. Adapting the method of Ha and colleagues (Ha et al., 2018), "lengthen" was defined for events with ΔPPAU >10, "shorten" was defined for events with ΔPPAU < -10 and no-change was defined with |ΔPPAU ≤10|. The statistical significance of the differential usage of poly(A) sites was calculated by a one-side Binomial test. The significance of the overlap between gene lists obtained in different comparisons or by different software was determined using the hypergeometric test followed by Fisher's exact test.

The AS profiles of known events were identified using vast-tools (Irimia et al., 2014), an RNA-seq pipeline developed for the systematic discovery and analysis of all classes of

AS events, using the developer's recommendation. Briefly, reads were aligned to the GRch38 human reference genome using Bowtie (Langmead et al., 2009) and to a series of databases containing known events of exon skipping, intron retention, alternative 5' and 3' transcription sites, and micro-exons (command: tidy –min_N 10, --noVLOW). The Percent Spliced-In Index (PSI) was then calculated, and significant differences between groups obtained by performing a ranked Wilcoxon test and selecting events with PSI differences over 8 and p-value <0.05.

Gene ontology analysis

Pathways enrichment analysis was performed by the ToppGene Suite tool (Chen et al., 2009), and biological processes of the differentially expressed, spliced and AS events were assessed statistically with an adjusted p-value <0.05.

Gene set enrichment analysis

Gene set enrichment analysis (GSEA) was performed by WebGestalt (Liao et al., 2019), using the gene ontology (GO) database for biological function and selecting the following parameters: Organism: *hsapiens*; Enrichment Categories: *geneontology Biological Process noRedundant*; ID type: *ensemble gene id*; Minimum number of IDs in the category: *3*. We then selected the top 20 pathways sorted by False Discovery Rate (FDR)

Target validation by qPCR

Quantitative PCR (qPCR) was performed on the CFX96 Real-Time PCR system (Bio-Rad) with SYBR green (Bio-Rad) chemistry. Fourteen genes were chosen as targets and two primer pairs were used for the relative quantification for each gene. Three GV and three IVO-MIIs were used per gene. The constant exon was used as a normalizer and the relative expression of target/control was obtained by the ΔΔCt method.

RESULTS

Study population

The average age of women included in the study was 26 years, with a SD ± 4.3, BMI of 22.5 ± 6.8 and antral follicle counts of 20.27 ± 7.3. Demographic characteristics of the women and the corresponding oocytes collected are shown in detail in Supplementary Table S1.

Table S1. Demographic characterization of the patients involved in the study and the related oocytes processed.

Donor ID	AGE	BMI (kg/cm)	AFC	GV (n)	FTM-GV (n)	IVM-MII (n)	IVO-MII (n)
D1	32	24	26 (OR 15 + OL 11)	0	1	0	0
D2	22	22.86	24 (OR 8 + OL 16)	1	0	0	0
D3	21	24.97	14 (OR 8 + OL 6)	1	0	0	0
D4	23	25.1	16 (OR 10 + OL 6)	1	0	0	0
D5	22	21.93	20 (OR 11 + OL 9)	0	1	0	0
D6	33	29	14 (OR 8 + OL 6)	0	0	1	0
D7	25	21.6	33 (OR 16 + OL 17)	0	0	1	0
D8	21	24.68	34 (OR 16 + OL 18)	0	0	1	0
D9	24	24.03	28 (OR 12 + OL 16)	1	0	0	0
D10	24	24.8	25 (OR 15 + OL 10)	0	2	0	0
D11	34	22.23	19 (OR 9 + OL 10)	0	0	1	0
D12	24	24.8	25 (OR 15 + OL 10)	0	0	1	0
D13	30	20.37	10 (OR 5 + OL 5)	1	0	0	0
D14	30	20.12	14 (OR 8 + OL 6)	0	1	0	0
D15	30	20.12	10 (OR 5 + OL 5)	0	1	0	0
D16	33	21.5	9 (OR 3 + OL 6)	0	0	1	0
D17	25	29.87	22 (OR 12 + OL 10)	1	0	0	0
D18	22	23	25 (OR 12 + OL 13)	0	1	0	0
D19	25	20.12	20 (OR 11 + OL 9)	0	1	0	0
D20	22	30	19 (OR 8 + OL 11)	0	0	1	0
D21	33	20.17	23 (OR 10 + OL 13)	1	0	0	0
D22	19	17	32 (OR 15 + OL 17)	0	1	0	0
D23	21	22.49	23 (OR 12 + OL 11)	0	1	0	0
D24	33	23.18	13 (OR 6 + OL 7)	0	0	1	0
D25	27	20.12	23 (OR 13 + OL 10)	1	0	0	0
D26	23	24.95	17 (OR 7 + OL 10)	1	0	0	0
D27	22	21.5	17 (OR 10 + OL 7)	0	0	1	0
D28	25	20	19 (OR 12 + OL 7)	0	0	1	0
D29	27	22.03	11 (OR 4 + OL 7)	0	0	0	1
D30	24	25.8	12 (OR 17 + OL 5)	1	0	0	0
D31	32	20.12	32 (OR 17 + OL 15)	0	0	0	1

D32	29	21.3	24 (OR 16 + OL 8)	0	0	0	1
D33	29	22.5	14 (OR 7 + OL 7)	0	0	0	2
D34	25	20.12	32 (OR 17 + OL 15)	0	0	0	2
D35	24	22.24	22 (OR 13 + OL 9)	0	0	0	1
D36	22	23.2	9 (OR 3 + OL 6)	0	0	0	2

Women enrolled in the study are numbered from D1 to D36 and corresponding age, body mass index (BMI) and Antral Follicle Count (AFC) are reported. The number of germinal vesicle (GV), failed to mature GV (FTM-GV), *in vitro* matured MII (IVM-MII) and *in vivo* ovulated MII (IVO-MII) is indicated.

Spliceosome and mRNA processing related genes are differentially expressed during meiotic progression

We identified 1675 DEGs between GV and *in vivo* matured MII (IVO-MII) (Supplementary Table S2, **Figure 1A**), 874 up-regulated and 801 down-regulated in IVO-MII (**Figure 1B**). Selecting for log2 Fold Change > |±1|, we found 122 up-regulated (30%) and 280 down-regulated (70%) DEGs in IVO-MII. In IVM-MII versus GV, fewer DEGs were identified (Supplementary Table S3, **Figure 1D**), with 17 up-regulated and 56 down-regulated (**Figure 1C**). Interestingly, only five DEGs were found between GV and failed to mature GV (FTM-GV) (**Figure 1F**), suggesting that differential gene expression is linked to meiotic progression. GSEA highlighted pathways related to translation initiation, protein transport and several pathways related to RNA metabolism, RNA transport, splicing and microtubule organization within the genes upregulated in MII, while less specific pathways enriched in the subset of genes upregulated in MII (**Figure 1E**). We identified 27 genes amongst the DEGs involved in the spliceosome machinery, such as *PRPF8* (Pre-mRNA Processing Factor 8), involved in the pre-mRNA capping and processing, and splicing factors such as *SF3B* and *SRFS* (**Figure 2**). Moreover, we found genes involved in other RNA regulatory processes and nuclear export of maturing mRNA, such as the TREX complex factors *MAGOH* (Mago Homolog, Exon Junction Complex Subunit) and *THOCs* (THO Complexes), as well as *eIF4A3* (Eukaryotic Translation Initiation Factor 4A3) (Supplementary Table S2). We also observed several genes strongly associated with protein processing and metabolism pathways. In IVM-MII versus GV, the most affected pathways were related to mitochondrial metabolism and protein targeting/stability (**Figure 1G**), but several genes associated with RNA

processing were also found, such as *RNASEH2A* (Ribonuclease H2 Subunit A), *RNU5D* (RNA, U5D Small Nuclear 1) and *RPP40* (Ribonuclease P/MRP Subunit P40) (Supplementary Table S3).

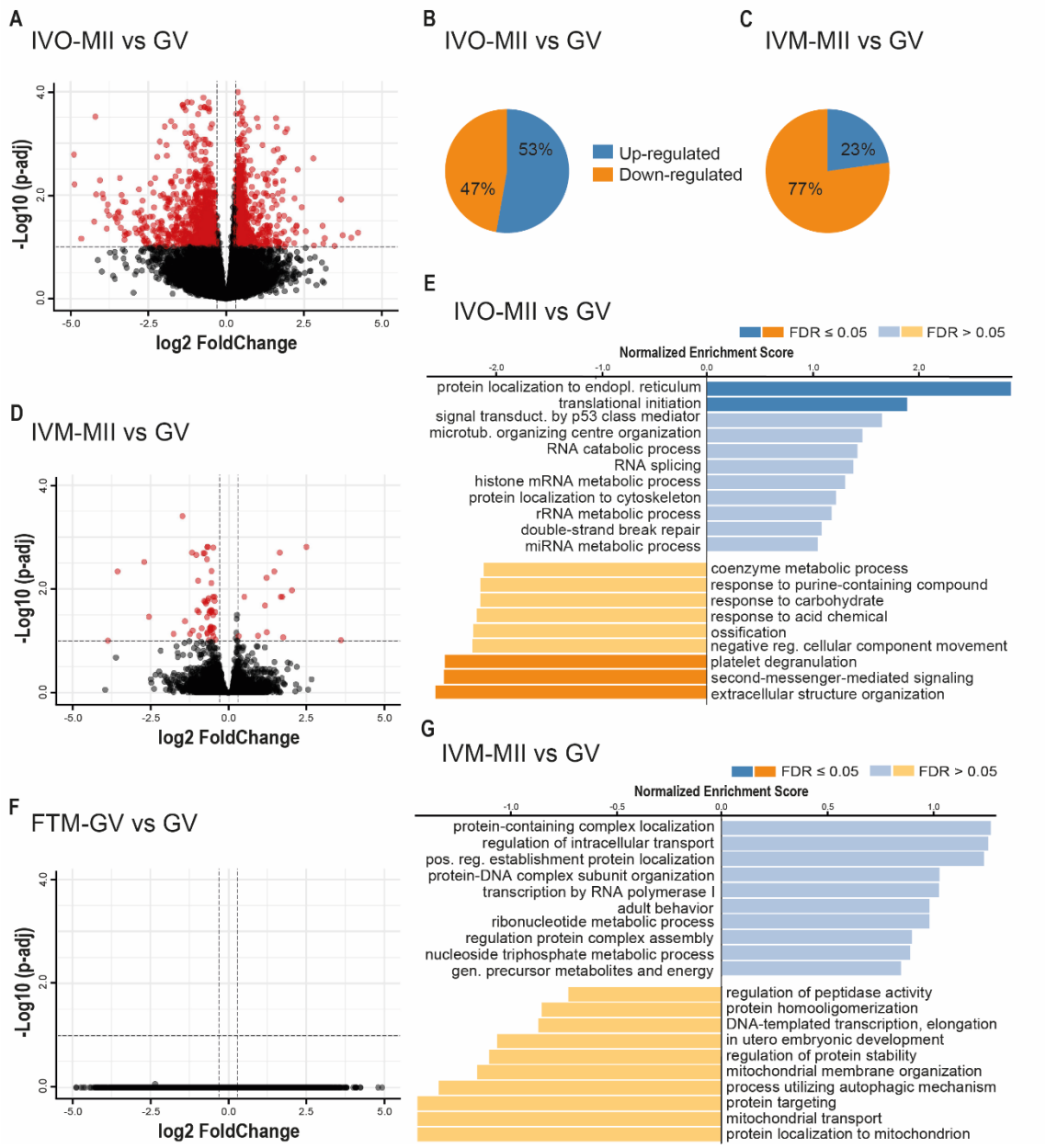

Figure 1. Differentially expressed genes during human oocyte final meiotic maturation. (A) Volcano plot of the differentially expressed genes found with p-adjusted<0.1 (red dots) in the comparison IVO-MII versus GV, in the comparison (**D**) IVM-MII versus GV, and in the comparison (**F**) FTM-GV versus GV. (**B**) Proportion of up- (blue) and down-regulated (orange) genes in the IVO-MII versus GV and (**C**) IVM-MII versus GV comparisons, respectively. (**E**) Gene Set Enrichment Analysis of the most affected pathways in the IVO-MII versus GV

comparison and (**G**) IVM-MII versus GV comparison. The affected pathways with FDR ≤ 0.05 are reported in orange and blue and the ones with FDR > 0.05 are in light orange and light blue.

IVO-MII = *in vivo* matured MII oocytes; IVM-MII = *in vitro* matured MII oocytes; GV = germinal vesicle oocytes; FTM-GV = GV that failed to mature after IVM; FDR = False Discovery Rate. (*Image obtained with permission from Oxford University press license. Pietroforte et al., 2023*)

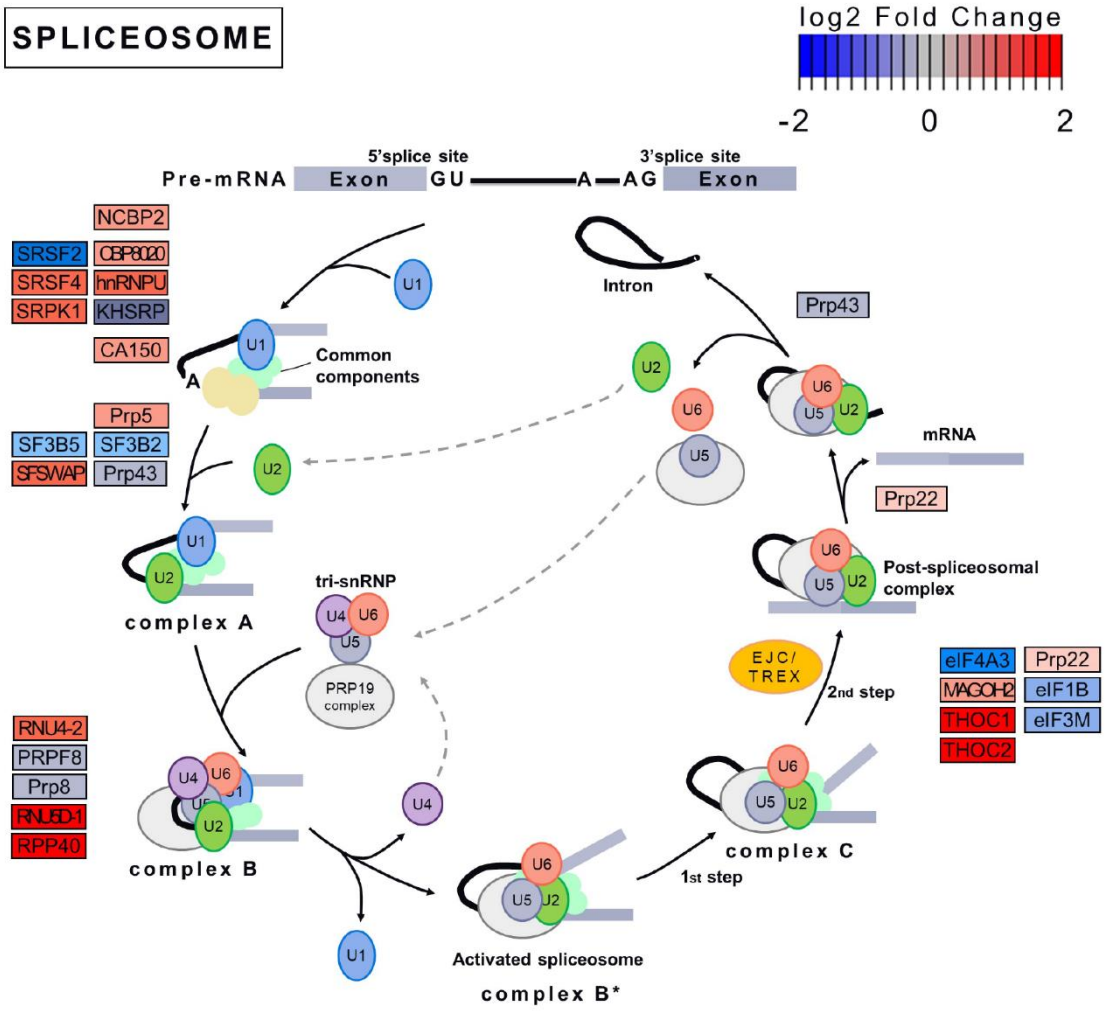

Figure 2. Genes involved in the spliceosome machinery differentially expressed in the comparison between immature germinal vesicle and *in vivo* matured MII.

Schematic representation of the spliceosome, from pre-mRNA to mature intronless mRNA, with all the different complexes involved, including five major U-rich small nuclear ribonucleoproteins (U1/U2/U4/U5/U6 snRNPs), common components and other factors exemplified by serine/arginine-rich (SR) proteins and hetero-nuclear ribonucleoproteins (hnRNPs). The DEGs we identified in IVO-MII versus GV related to these complexes are located next to them and color-coded based on their expression levels. Genes with positive log2 Fold Change are shown in shades of red, while those with negative log2 Fold Change are in shades of blue.

DEGs = differentially expressed genes; IVO-MII = *in vivo* matured MII oocytes; GV = germinal vesicle oocytes. (*Image obtained with permission from Oxford University press license. Pietroforte et al., 2023*)

Abundant processing of 5'/3'UTR during the maturation from GV to MII

We first performed a differential exon usage analysis with DEXseq to detect the relative abundance of exons and UTR variants and found 2292 exons/UTRs belonging to 1610 genes that were differentially used in IVO-MII versus GV (Supplementary Table S4), 771 exons/UTRs from 551 genes in IVM-MII versus GV (Supplementary Table S5), and again, none in FTM-GV versus GV. Remarkably, most of the differentially used exons/UTRs were down-regulated in IVO-MIIs and IVM-MIIs with respect to GV (87%, 1986/2292 in IVO-MII, and 86%, 663/771 in IVM-MII, respectively, **Figure 3A**). We further characterized exons longer than 5bp, with a p-adjusted <0.05 and an absolute log2 Fold Change (log2FC) ≥1. This led to the identification of 880 events from 688 genes in the IVO-MII versus GV comparison (Supplementary Table S4) and 312 events from 248 genes in IVM-MII versus GV (Supplementary Table S5). The majority of these events targeted UTRs of the transcript, suggesting the processing of pre-mRNA forms. In the IVO-MII versus GV comparison, 61 (7%) of the genes had processing events in their 5'-UTRs and 468 (53.2%) in their 3'UTR. The remaining 351 (39.8%) had changes in the coding exons or introns (**Figure 3B**). We found a very consistent overlap between events in IVO-MII versus GV and IVM-MII versus GV ($p < 0.00001$, Fisher's exact test), where a total of 159 exons out of the 312 found in IVM-MII versus GV were also found in the comparison IVO-MII versus GV (**Figure 3C**), with similar fold changes, indicating their robust association with the successful transition through meiotic maturation, irrespective of oocyte quality and maturation conditions. We then performed the same comparisons with a similar tool for exon usage detection, edgeR, to strengthen our analysis. Once again, we found no differences in the comparison of FTM-GV versus GV and found 286 exons from 195 genes and 207 exons from 138 genes differentially expressed in IVO-MII versus GV and IVM-MII versus GV, respectively (Supplementary Table S6). Of the genes affected by differential exon usage in the edgeR analysis, we found 140 out of 195 and 84 out of 138 to be also identified in the DEXseq dataset, highlighting the high degree of similarity of the two software packages used, above 60% in both comparisons (Supplementary Table S6).

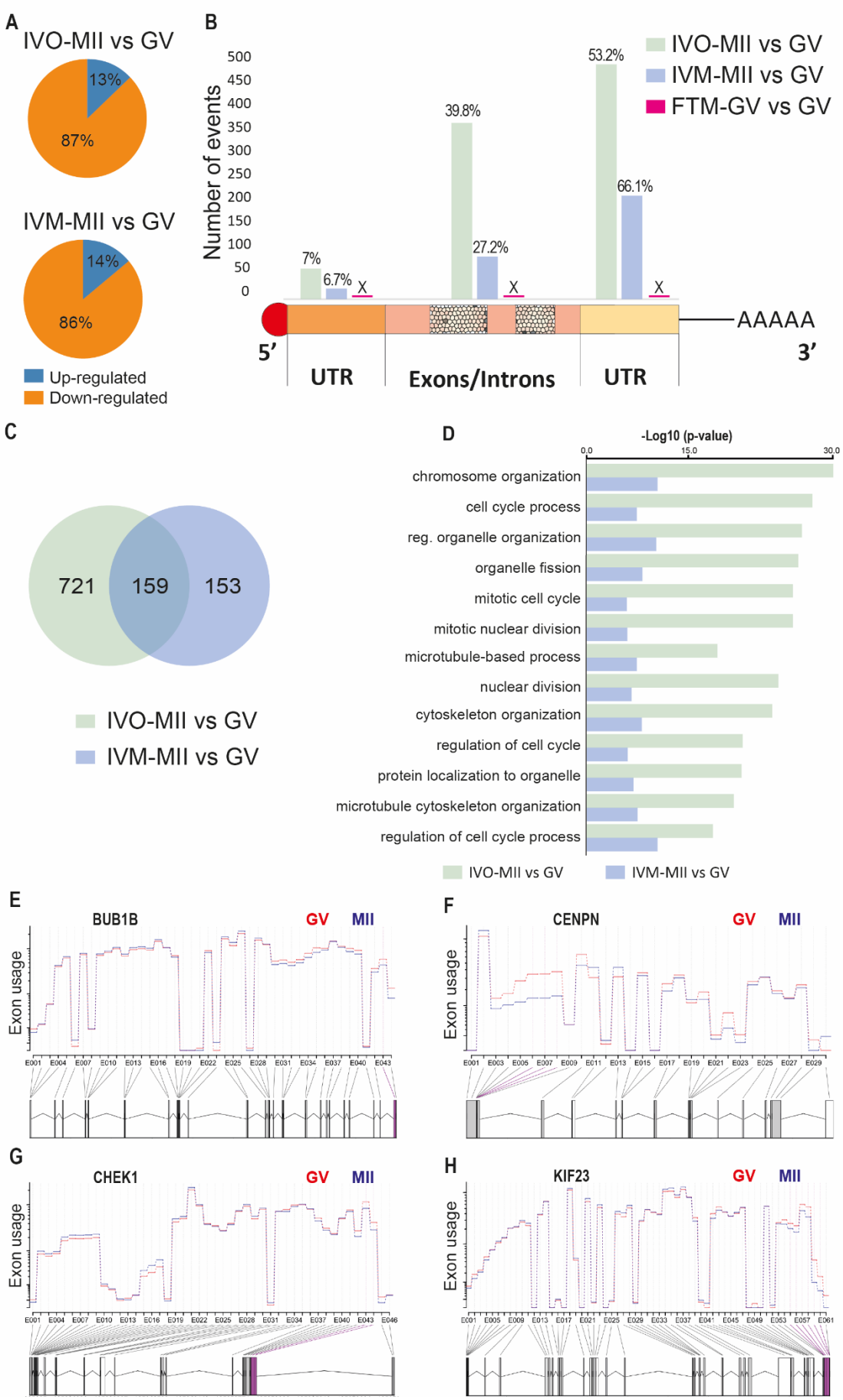
A
IVO-MII vs GV
13%
87%
IVM-MII vs GV
14%
86%
Up-regulated
Down-regulated
B
Number of events
500
450
400
350
300
250
200
150
100
50
0
IVO-MII vs GV
IVM-MII vs GV
FTM-GV vs GV
7%
6.7%
X
39.8%
27.2%
X
53.2%
66.1%
X
5'
UTR
Exons/Introns
UTR
AAAAA
3'
C
721
159
153
IVO-MII vs GV
IVM-MII vs GV
D
-Log10 (p-value)
0.0
15.0
30.0
chromosome organization
cell cycle process
reg. organelle organization
organelle fission
mitotic cell cycle
mitotic nuclear division
microtubule-based process
nuclear division
cytoskeleton organization
regulation of cell cycle
protein localization to organelle
microtubule cytoskeleton organization
regulation of cell cycle process
IVO-MII vs GV
IVM-MII vs GV
E
BUB1B
GV
MII
Exon usage
F
CENPN
GV
MII
Exon usage
G
CHEK1
GV
MII
Exon usage
H
KIF23
GV
MII
Exon usage

Figure 3. Differential exon usage profiles between immature and mature oocytes.

(A) Proportion of up- (blue) and down-regulated (orange) exons with higher and lower expression in the IVO-MII versus GV and IVM-MII versus GV. **(B)** Exons with differential usage identified by DEXseq (log2 Fold Change >|1|, p-adj<0.05, > 5bp) in the three different comparisons (IVO-MII versus GV is reported in light green, IVM-MII versus GV in light blue and FTM-GV versus GV in purple) and their distribution on the gene structure (5'UTR, exons/introns or 3'UTR) (**C**) Overlap between the exons with differential usage found in the comparisons IVO-MII versus GV (light green) and IVM-MII versus GV (light blue). **(D)** Most significant pathways affected by differential exon usage from the comparison IVO-MII versus GV (light green) and IVM-MII versus GV (light blue). (**E-H**) Examples of specific processed genes found in the IVO-MII versus GV comparison. The bars represent the levels of expression of the single exons as identified by DEXseq, and the different colours are related to the GV or MII group. The gene structure is represented in the bottom part of each graph, and the differentially processed exon/exons is/are represented in purple.

IVO-MII = *in vivo* matured MII oocytes; IVM-MII = *in vitro* matured MII oocytes; GV = germinal vesicle oocytes; FTM-GV = GV that failed to mature after IVM; UTR = Untranslated region. (*Image obtained with permission from Oxford University press license. Pietroforte et al., 2023*)

mRNA processing affects genes related to meiosis, chromosome organization and spindle assembly

Pathway over-representation analysis of the DEXseq dataset provided very similar results for genes containing differentially used exons in IVO-MII versus GV and in IVM-MII versus GV, in line with the high level of overlap in the single events, also confirmed by the same analysis conducted in the pathways obtained by edgeR (Supplementary Table S6, sheet 2 "pathways comparison"). In IVO-MII versus GV, we found that the majority of differentially processed genes had functions related to chromosome and organelle organization, mitotic cell cycle and nuclear division (**Figure 3D** and Supplementary Table S4). Similarly, from the exons showing differential usage identified in IVM-MII versus GV, we found chromosome and microtubule organization, organelle assembly and spindle organization (**Figure 3D** and Supplementary Table S5). Moreover, in the two comparisons we found specific genes known to be necessary for cell cycle regulation, such as *CDC25C* (Cell Division Cycle 25C), *SIRT2* (Sirtuin 2), *CHEK1* (Checkpoint Kinase 1), *POGZ* (Pogo Transposable Element Derived With ZNF Domain) and *RNF4* (Ring Finger Protein 4), or genes involved in spindle assembly and chromosome segregation, like *SPIN1* (Spindlin 1), *BUB1B* (BUB1 Mitotic Checkpoint

Serine/Threonine Kinase B), *SPDL1* (Spindle Apparatus Coiled-Coil Protein 1), *AURKA* (Aurora Kinase A), *CENP-L, -U, -Q, -N, -C* (Centromere Proteins), *KIF23* (Kinesin Family Member 23), *NUF2* (NUF2 Component Of NDC80 Kinetochore Complex), and genes that participate in chromosome cohesion and recombination like *STAG1* (Stromal Antigen 1), *MEIOC* (Meiosis Specific With Coiled-Coil Domain) and *MLH1* (MutL Homolog 1) (Supplementary Table S4 and Table S5 and examples in Fig. 3E-H). These processes related to meiotic resumption and cell progression, suggest that the pre-mRNA processing of specific transcripts is linked, and perhaps necessary for, successful completion of meiosis I and transit through metaphase II. Finally, data obtained from FTM-GV strongly suggest that this process is independent of time in culture or oocyte *in vitro* aging.

Alternative poly(A) usage between GV and MII oocytes

Given that most genes exhibited different processing of the 3'end, we characterized the APA sites in more detail using qapa (Ha et al., 2018). Analysis of the genes with only two possible alternative UTRs confirmed our previous observations, as several genes showed a differential usage of PAU sites: 238, 149 and 95 in IVO-MII versus GV, IVM-MII versus GV and FTM-GV versus GV, respectively (Supplementary Tables S7, S8 and S9 and **Figure 4A, 4C** and **4E**). Specifically, we found a higher number of shortened UTRs in all comparisons: 154/238 (64.7%, p = 3.3e-06, one-side Binomial test) in IVO-MII versus GV, 105/149 (70.4%, p = 3.1e-07, one-side Binomial test) in IVM-MII versus GV and 72/95 (75.8%, p = 2.4e-07, one-side Binomial test) in FTM-GV versus GV (**Figure 4B**, examples of affected genes are provided in **Figure 4D** and **4F**). We then performed separate GO analysis of the genes with shortened and lengthened UTRs. This analysis revealed that genes with 3'UTR isoforms shortening during oocyte maturation (IVO-MII versus GV and IVM-MII versus GV) were functionally linked to chromosome and chromatin organization and cell cycle process, while the genes with lengthened UTRs were not associated with any specific pathway.

Within the genes with the highest difference in poly(A) usage, we found significant overlap with both genes identified as DEGs (81/399, p<0.0001 in IVO-MII versus GV, and 7/306, p=0.0017 in IVM-MII versus GV) and genes with differential exon usage (112/399 in IVO-MII versus GV, p<0.00001, and 37/306 in IVM-MII versus GV,

p=0.115) confirming that this phenomenon affects both classes of genes (Supplementary Figure S1).

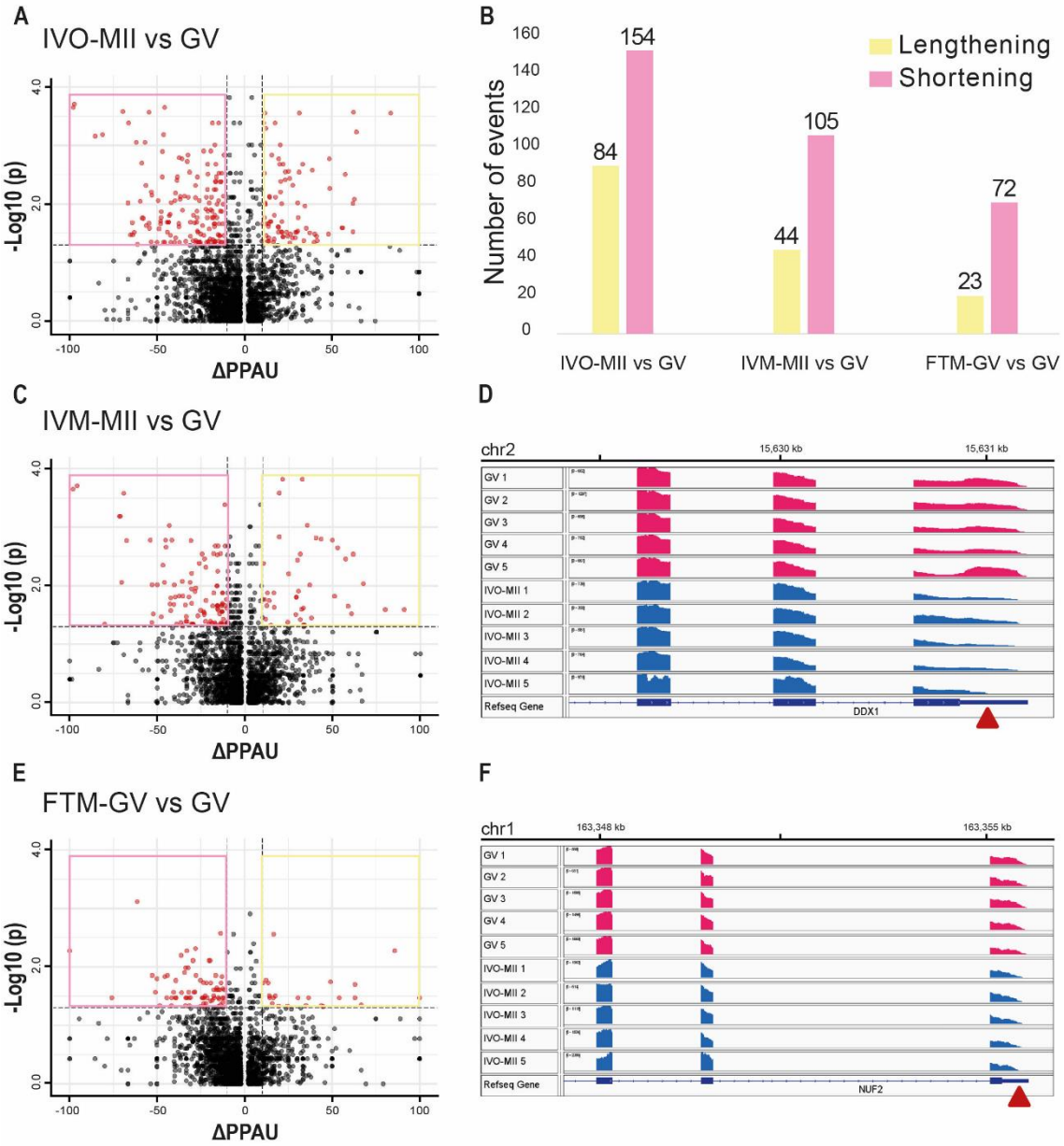

Figure 4. Differential usage of poly(A) sites during the final stages of oocyte meiosis. (**A, C, E**) Volcano plot of the poly(A) site differential usage in the three comparisons IVO-MII versus GV, IVM-MII versus GV and FTM-GV versus GV). ΔPPAU lengthening and shortening are shown in yellow and pink windows, respectively. (**B**) Alternative poly(A) sites (ΔPPAU=|10| and p-value <0.05, ranked Wilcoxon paired test) in the three different comparisons and their distribution between lengthening (light yellow) and shortening (light pink). (**D, F**) Examples via genome-browser visualization of shortening UTR events between GV (pink) and MIIs (blue). Red arrows are pointing to the region shortened in IVO-MIIs compared to GVs.

IVO-MII = *in vivo* matured MII oocytes; IVM-MII = *in vitro* matured MII oocytes; GV = germinal vesicle oocytes; FTM-GV = GV that failed to mature after IVM; ΔPPAU = difference in Proximal poly(A) usage; UTR = Untranslated region. (*Image obtained with permission from Oxford University press license. Pietroforte et al., 2023*)

Alternative splicing events target meiosis associated pathways during oocyte maturation

Finally, to investigate AS in further detail, including all major types of events (exon skipping, intron retention and alternative 5'/3' transcription sites), we used an exon junction-based tool, vast-tools (Irimia et al., 2014), to perform the same group comparisons. We found 136 differentially spliced AS events (p-value <0.05 and |ΔPSI| ≥8) affecting 104 genes in IVO-MII versus GV (Supplementary Table S10), 82 AS events affecting 62 genes in IVM-MII versus GV (Supplementary Table S11) and 68 AS events affecting 54 genes in FTM-GV versus GV (Supplementary Table S12). Most AS events detected involved exon skipping (44%, 54% and 51%), followed by 5' (ALT5') (21%, 18% and 24%), 3' alternative transcription sites (ALT3') (20%, 16% and 18%), and intron retention (IR) (15%, 12% and 7%) in IVO-MII, IVM-MII and FTM-GV, respectively (**Figure 5A, 5B** and **5C**). GO analysis in IVO-MII versus GV found mitosis, nuclear division, meiosis, and chromosome formation and segregation as most affected pathways (**Figure 5D**), while in IVM-MII versus GV more generic pathways were identified (**Figure 5E**). In the FTM-GV versus GV comparison, we found no significantly affected pathways.

Moreover, in the IVO-MII versus GV comparison, we identified the presence of key players in the process of meiotic spindle formation such as *CENPE* (Centromere Protein E), *NIPBL* (NIPBL Cohesin Loading Factor), and *TUBB8* (Tubulin Beta 8 Class VIII) (**Table 1** and **Figure 5F, 5G, 5H**). We further validated expression of these genes by qPCR (**Figure 5I, 5J, 5K**).

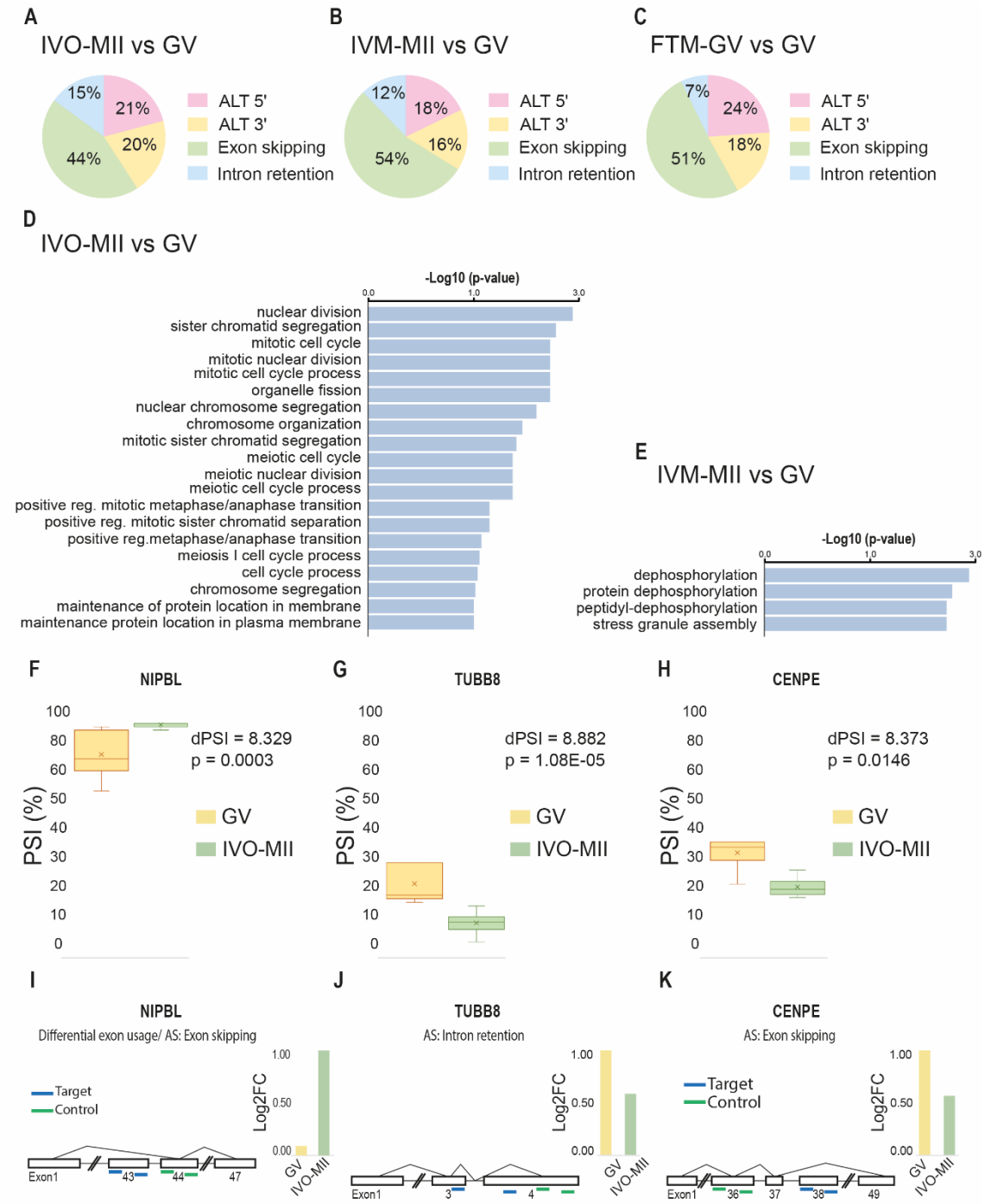

Figure 5. Alternative splicing profile between IVO-MII versus GV, IVM-MII versus GV and FTM-GV versus GV. (**A**) Frequencies of alternative splicing event types, Alternative 5'/3' transcription sites (Alt 5'/3', pink and yellow), exon skipping (green) and intron retention (blue), in all the three comparisons IVO-MII versus GV, (**B**) IVM-MII versus GV and (**C**) FTM-GV versus GV. (**D**) Top affected pathways identified from the two comparisons, IVO-MII versus GV and (**E**) IVM-MII versus GV. (**F, G, H**) Examples of specific alternative splicing isoforms (present in minimum 8/10 samples per group, dPSI >|8|, p-value<0.05, ranked Wilcoxon paired test) identified in IVO-MII versus GV and their Percentage Spliced In (PSI) values, differential PSI and p-value and validated by qPCR (**I, J, K**).

IVO-MII = *in vivo* matured MII oocytes; IVM-MII = *in vitro* matured MII oocytes; GV = germinal vesicle oocytes; FTM-GV = GV that failed to mature after IVM; PSI = differential Percentage Spliced In; dPSI = differential PSI; AS = alternative splicing; Log2FC = Log2 Fold Change. (*Image obtained with permission from Oxford University press license. Pietroforte et al., 2023*)

Table 1. Alternative splicing genes in human germinal vesicle versus *in vivo* ovulated metaphase II oocytes.

Gene Name	Original Symbol	p-value	Type of AS	Alternative isoform impact (VastDB)	dPSI
ERCC6	ERCC excision repair 6, chromatin remodeling factor	0.043	Alt 3'	5' UTR	9.075
CENPE	centromere protein E	0.014	EX	Alternative protein isoforms	8.373
RAD54B	RAD54 homolog B	0.035	EX	Alternative protein isoforms, Alt stop	8.961
ANAPC11	anaphase promoting complex subunit 11	0.017	Alt 5'	5'UTR	10.424
SYCP3	synaptonemal complex protein 3	0.035	Alt 3'	5'UTR	10,34
MPHOSPH8	M-phase phosphoprotein 8	0.027	EX	CDS	12.199
POGZ	pogo transposable element derived with ZNF domain	0.027	EX	Alternative protein isoforms	8.818
SMC2	structural maintenance of chromosomes 2	0.026	Alt 5'	5'UTR	15.969
ESPL1	extra spindle pole bodies like 1, separase	0.03	Alt 5'	5'UTR	9.721
NCAPG2	non-SMC condensin II complex subunit G2	0.005	EX	Alternative protein isoforms	14.518
NIPBL	NIPBL cohesin loading factor	0.0003	EX	Alternative protein isoforms	8.329
CDC25C	cell division cycle 25C	0.039	EX	ORF disruption upon sequence exclusion	9.243
TUBB8	tubulin beta 8 class VIII	1.08E-05	IR	Alternative protein isoforms	8.882
CNTRL	centriolin	0.005	Alt 3'	Protein isoform when splice site is used	11.064
ARID1B	AT-rich interaction domain 1B	0.027	EX	Alternative protein isoforms	12.111
SREK1	splicing regulatory glutamic acid-lysine rich protein 1	0.001	Alt 3'	Protein isoform when splice site is used	9.262
PCM1	pericentriolar material 1	0.002	Alt 5'	Protein isoform when splice site is used	11.535
CNOT6	CCR4-NOT transcription complex subunit 6	0.013	EX	5'UTR	10.850
TAOK3	TAO kinase 3	0.023	Alt 5'	5'UTR	14.512
FBXO43	F-box protein 43	0.002	Alt 5'	Protein isoform when splice site is used	17.808

List of selected genes found statistically significant (p-value <0.05, calculated with ranked Wilcoxon test), dPSI >8 and involved in nuclear division and chromosome organization pathways and relevant in mRNA processing, meiosis and spindle assembly and presenting different isoforms levels in the comparison of germinal vesicle versus *in vivo* ovulated metaphase II (IVO-MII).

Alt 3'/5' = Alternative splice site at 3'/5'; AS = Alternative Splicing; CDS = coding sequence; dPSI = differential Percentage Spliced In; EX = exon skipping; IR = intron retention; UTR = Untranslated region; VastDB = *Vast-tools* database.

IVM affects mRNA processing during the transition from GV to MII

To evaluate the effect of IVM on mRNA processing we compared IVO-MII versus IVM-MII with all tools (Supplementary Table S13). We found 147 DEGs between IVM-MII and IVO-MII (**Figure 6A**); 51.7 % (75/147) down-regulated and 48.3% (72/147) up-regulated (**Figure 6B**) in IVO-MII. GSEA highlighted pathways related to biosynthetic/metabolic processes, but none specific to oocyte maturation (**Figure 6C**). We then found 69 events related to 63 genes in the exon usage analysis (**Figure 6D**), where most of those were down-regulated (80%, 55/69) and fewer (20%, 14/69) up-regulated (**Figure 6E**) in IVO-MII. The small number of identified genes did not allow the detection of significantly affected pathways, but we could identify several genes related to oocyte meiosis (**Figure 6F**). The comparison IVO-MII versus IVM-MII of the alternative poly(A) usage showed 107 genes with differential usage of the APA sites (**Figure 6G**) and specifically, we found a high number of shortened UTRs (54%, 59/109) in IVO-MII (**Figure 6G**, pink window). Here, we identified genes related mainly to protein catabolic processes, not specific to oocyte maturation. The AS analysis showed 43 differentially spliced AS events affecting 37 genes. The majority of the AS events were Exon skipping (20/43, 46.6%) followed by Alternative splice site at 5' and 3' (11/43, 25.5% and 7/43, 16.3%, respectively) and intron retention (5/43, 11.6%) (**Figure 6H**). We observed important genes associated with female germ cell differentiation such as *FBXO43* (F-box protein 43) that is required for the establishment and maintenance of the second meiosis metaphase arrest until fertilization, *PCM1* (Pericentriolar Material 1) required for centrosomal assembly, *SNX14* (Sortin Nexin 14) and *CAST* (Calpastatin) involved in intracellular trafficking and membrane-fusion events during cellular reorganization, as well as *CNOT6L* (CCR4-NOT Transcription Complex Subunit 6 Like) and *TNRC6A* (Trinucleotide Repeat Containing Adaptor 6A) specifically involved in nuclear-transcribed mRNA poly(A) shortening.

Overall, these data support the hypothesis that IVM-MII oocytes have an incomplete transcriptional profile compared to *in vivo* matured MII.

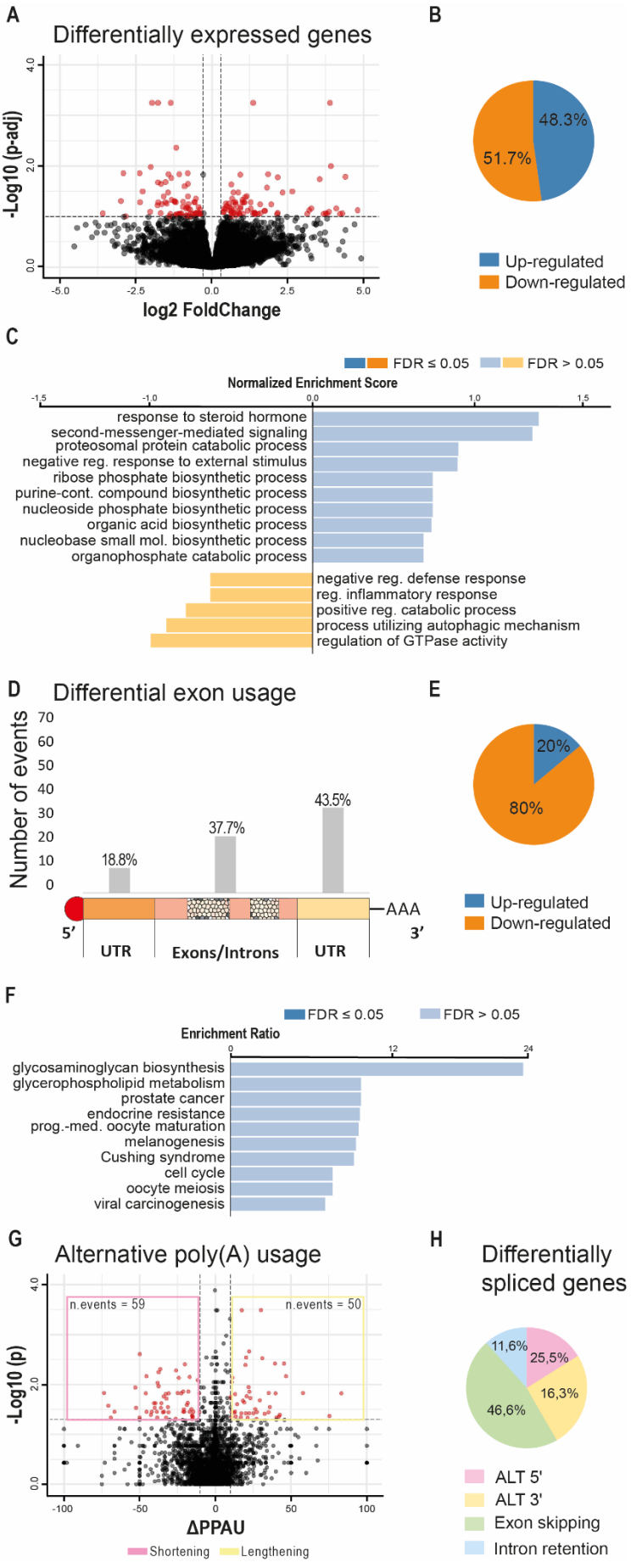
A
Differentially expressed genes
-Log10 (p-adj)
log2 FoldChange
B
48.3%
51.7%
Up-regulated
Down-regulated
C
FDR ≤ 0.05
FDR > 0.05
Normalized Enrichment Score
response to steroid hormone
second-messenger-mediated signaling
proteosomal protein catabolic process
negative reg. response to external stimulus
ribose phosphate biosynthetic process
purine-cont. compound biosynthetic process
nucleoside phosphate biosynthetic process
organic acid biosynthetic process
nucleobase small mol. biosynthetic process
organophosphate catabolic process
negative reg. defense response
reg. inflammatory response
positive reg. catabolic process
process utilizing autophagic mechanism
regulation of GTPase activity
D
Differential exon usage
Number of events
18.8%
37.7%
43.5%
5'
UTR
Exons/Introns
UTR
AAA
3'
E
20%
80%
Up-regulated
Down-regulated
F
FDR ≤ 0.05
FDR > 0.05
Enrichment Ratio
glycosaminoglycan biosynthesis
glycerophospholipid metabolism
prostate cancer
endocrine resistance
prog.-med. oocyte maturation
melanogenesis
Cushing syndrome
cell cycle
oocyte meiosis
viral carcinogenesis
G
Alternative poly(A) usage
-Log10 (p)
n.events = 59
n.events = 50
ΔPPAU
Shortening
Lengthening
H
Differentially spliced genes
11,6%
25,5%
16,3%
46,6%
ALT 5'
ALT 3'
Exon skipping
Intron retention

Figure 6. Differences in RNA processing between *in vitro* and *in vivo* matured MIIs

(**A**) Volcano plot of the differentially expressed genes found with p-adjusted <0.1 (red dots) in the comparison IVO-MII versus IVM-MII. (**B**) Proportion of up- (blue) and down-regulated (orange) genes and (**C**) Gene Set Enrichment Analysis of the most enriched affected pathways in the IVO-MII versus IVM-MII (FDR ≤ 0.05 are in blue and orange and FDR > 0.05 are in light blue and light orange). **(D)** Exons with differential usage identified by DEXseq (log2 Fold Change >|1|, p-adj<0.05, > 5bp) in the comparison IVO-MII versus IVM-MII and their distribution on the gene structure (5'UTR, exons/introns or 3'UTR). **(E)** Proportion of up- (blue) and down-regulated (orange) exons with higher and lower expression in IVO-MII versus IVM-MII. (**F**) Most significant pathways affected by differential exon usage in the comparison IVO-MII versus IVM-MII (FDR ≤ 0.05 are in blue and FDR > 0.05 are in light blue). (**G**) Volcano plot of the poly(A) site differential usage. ΔPPAU lengthening (number of events = 50) and shortening (number of events = 59) are in yellow and pink windows, respectively. (**H**) Frequencies of alternative splicing event types, Alternative 5'/3' transcription sites (Alt 5'/3', pink and yellow), exon skipping (green) and intron retention (blue) found in IVO-MII versus IVM-MII.

IVO-MII = *in vivo* matured MII oocytes; IVM-MII = *in vitro* matured MII oocytes; FDR = False Discovery Rate; ΔPPAU = difference in Proximal poly(A) usage; UTR = Untranslated region. (*Image obtained with permission from Oxford University press license. Pietroforte et al., 2023*)

qPCR validation of the identified targets

To strengthen our conclusions and rule out the possible bias of the sequencing process and the bioinformatic analysis, we further performed qPCR on the sequencing libraries (Supplementary Table S14, Supplementary Fig. S2). We chose targets identified with the three different software packages, some of them identified as differentially processed by more than one. We could validate our findings in 14 targets, where we observed a concordant pattern of decrease/increase in the isoforms detected (Supplementary Fig. S2, "target"), while finding no differences in exons identified also in the bioinformatic analysis as invariant (Supplementary Fig. S2, "control").

DISCUSSION

The complex remodelling of the transcriptome in maturing oocytes has been mostly analysed in terms of mRNA abundance. There seems to be a consensus on the expression profiles that characterize the transition between the GV and MII stage, which includes genes involved in the cell cycle, organelle biogenesis and maintenance, spliceosome, transport to cytoplasm and mitochondrial metabolism (Cornet-Bartolomè et al., 2021; Llonch et al., 2021; Li et al., 2020; Reyes et al., 2017). However, to date, the remodelling of transcript isoform diversity has not been fully addressed.

As a whole, we detected significant changes in isoform composition between the GV and MII stages, which were conserved between *in vivo* and *in vitro* matured MII. These results indicate that the changes detected are tightly associated with the successful meiotic progression from GV to MII, while being mostly independent of factors such as time in culture or overall oocyte quality. Nevertheless, we observed a smaller number of changes in the *in vitro* matured MII, which may be related to some of the analyzed oocytes not having properly completed the maturation process (as we measured successful maturation only by PB extrusion). Moreover, our data revealed little to no difference between GVs at collection and GVs that failed to mature after 30 hours in culture and retained their GV.

Through the analysis of mRNA dynamics, we identified abundant remodelling of UTR isoforms, mostly at the 3'end, of several genes involved in the meiotic progression from GV to MII, related to chromosome organization, microtubule dynamics and spindle assembly. These results were confirmed by different bioinformatic tools, and the very high level of concordance between the software we chose adds consistency to the results, ruling out bioinformatic artifacts. This was accompanied by a differential expression of genes associated with pre-mRNA processing, splicing and RNA transport. Both exon-level and APA analyses revealed a general shortening of the 3'UTR of a subset of genes.

RNAseq datasets with short reads are not amenable to identifying the lengthening or the shortening of poly(A) tails, but assumptions can be made by the processing of their 3'UTR, as the length of the UTR and its processing at the 5' and at the 3'end usually represent signals for translation (Leppek et al., 2018; Mignone et al., 2002). The variety of regulatory elements involved in UTR-mediated translation efficiency, such as polyadenylation signals and cytoplasmic polyadenylation elements, makes it difficult to develop a common rule for the transcriptome-wide translation of mRNAs. However,

recent evidence in vertebrate oocytes indicates that the translation of mRNAs increases when UTRs are shorter and poly(A)s are longer (Yang et al., 2020). We hence speculate that the generalized 3'UTR shortening of meiosis-related transcripts is a signal for their immediate translation, reinforced by the fact that most of them are involved in chromosome packing, microtubules dynamics and spindle assembly. These pathways are needed for progression through meiosis I and the extrusion of the first PB to obtain competent MIIs. Among the targets spliced after the GV stage we found several meiosis-related genes, such as *BUB1B*, *MEIOC*, *POGZ*, *STAG1*, *AURKA* and *CENP* family members (Fig. 7). A recent report described the simultaneous analysis of the human transcriptome and translatome and showed that genes with higher translational efficiency in MII are involved in processes similar to those affected by UTR processing in our study, such as chromosome segregation, chromosome centromeric regions, chromatin modification, nuclear speck, transcriptional co-regulator activity, DNA repair histone modification and DNA methylation (Hu et al., 2022).

While transcription is reported to be silenced in fully grown GV stage oocytes, we observe an abundant processing of RNA transcripts in these samples, which is normally performed while transcription is active. This apparent contradiction can be explained in different ways: we could be observing the last steps of transcription in GVs that have not yet reached full maturity, and therefore are still transcriptionally active. This is in agreement with a recent study showing that a significant proportion of GVs collected after hormonal stimulation and oocyte retrieval still possess transcriptional activity (Cornet-Bartolomè et al., 2021). If so, our data would imply that the processing of meiosis-related transcripts happens during the latest phases of transcription. Alternatively, we could be detecting selective degradation of certain transcripts, in a similar fashion to the maternal mRNA clearance, which is involved in the oocyte to embryo transition. If this was the case, the observed differential abundance of spliceosome and RNA processing genes may be related to later steps of embryo development, as speculated previously (Yang et al., 2020).

Regardless of the mechanism responsible for the observed changes, our findings are supported by analogous observations in pigs (Wu et al., 2022) and mice (He et al., 2021), where the same phenomenon was observed. In pigs, the transcript processing during final oocyte maturation generates higher levels of UTR shortening in genes involved cell cycle, kinetochore, chromosome and spindle organization (Wu et al., 2022). In mice, pervasive

3'UTR isoform switches during the GV to MII oocyte transition were observed, with a global abundance of genes with longer 3'UTR isoforms in MII (He et al., 2021). Our data also indicate a specific abundant processing of the UTR regions but with higher levels of shortening. The discrepancy with mouse data can be explained by the methodology for RNA capture, based on poly(A)-capture (He et al., 2021) versus total RNA-isolation in our study. Accordingly, genes that did not undergo polyadenylation at the GV stage may have been missed by the capture method, which would influence the results on UTR shortening/lengthening. Interestingly, the analysis of the genes affected by longer 3'UTR by He and colleagues, shows similar biological processes with those affected by 3'UTR shortening in IVO-MII versus GV, including RNA processing, translation, chromosome organization and splicing (He et al., 2021). Similarly, genes affected by shorter 3'UTR were related to pathways such as DNA replication and mitotic cell cycle (He et al., 2021), as we observed in genes with 3'UTR lengthening.

After fertilization, during the initial embryonic cell divisions, the stored maternal mRNAs are also degraded and gradually consumed. In particular, the degradation of maternal mRNA in mouse oocytes is selective, particularly involving genes related to oxidative phosphorylation, energy production and protein synthesis (He et al., 2021). At the two-cell stage of early mice embryos, 90% of the maternal mRNA is degraded (Schellander et al., 2007). In human, transcripts with a decreased expression between MII oocytes and two- and four-cell stage embryos are related to biological processes such as nucleic acid metabolism, protein trafficking, cell cycle and protein metabolism. This suggests that the first burst of protein production occurring immediately after embryonic genome activation is mainly dedicated to building the translation machinery (Vassena et al., 2011). In our study, we found no evidence of differential expression/processing of such classes of transcripts, confirming the specificity of our findings.

We did not find an exclusive process associated with meiotic progression and AS, since AS events were also detected in the comparison between immature oocytes and oocytes that failed the IVM. However, again, we found specific genes involved in chromosome condensation, microtubule dynamics and spindle assembly only affected by AS in MII oocytes. AS regulates the growing oocytes at multiple levels, at least in mice, where it maintains transcriptome integrity in growing oocytes (Do et al., 2018). However, the changes in protein isoform that we and others (Cornet-Bartolomè et al., 2021; Li et al., 2020) have found are minor, though specific and consistent, and their effect might be

reduced, especially compared to the more pervasive pre-mRNA processing. Within the most consistently observed splicing of such proteins, we identified *SYCP3*, *SMC2*, *NIBPL*, *CDC25*, *TUBB8* and *CENPE* (**Figure 7**) genes crucial for meiotic progression, as recently reviewed by Biswas and colleagues (Biswas et al., 2021).

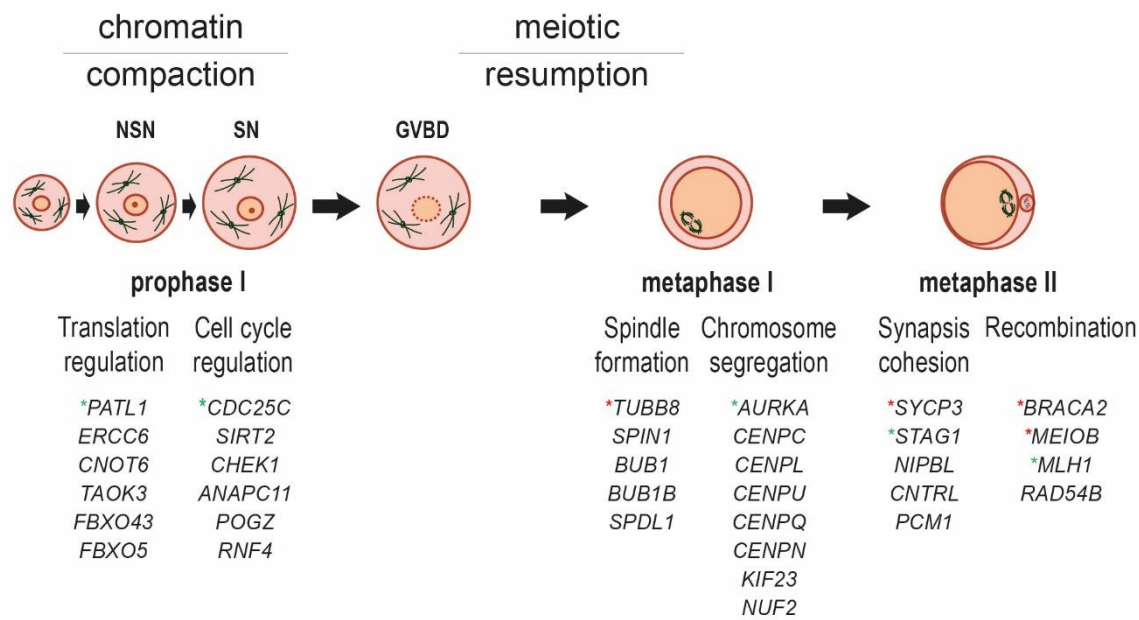

Figure 7. Oocyte meiotic maturation driven by the processing of specific genes.

Graphical representation of human oocyte meiotic maturation from the immature GV, with different chromatin status (NSN, non-surrounding nucleus, and SN, surrounding nucleus), through germinal vesicle breakdown (GVBD) and metaphase I to mature metaphase II oocyte. The differentially remodelled genes found in the two comparisons, *in vivo* matured MII oocytes versus GV and *in vitro* matured MII oocytes versus GV, and undergoing UTRs processing and/or alternative splicing, are involved in specific regulatory phases of the described meiotic maturation, such as translation or cell cycle regulation, and processes, such as spindle formation or chromosome segregation. Genes marked with an asterisk are those reviewed by Biswas and colleagues (Biswas et al., 2021) and either perfectly matched (red) or present in different isoforms or located in the same complex (green).

GV = germinal vesicle oocytes; UTR = Untranslated region. (*Image obtained with permission from Oxford University press license. Pietroforte et al., 2023*)

Cornet-Bartolomè et al. identified several differentially spliced genes when comparing GV and IVO-MII, associated with mRNA splicing and regulation of transcription and translation, including *DIAPH2* and *TAF6* (Cornet-Bartolomè et al., 2021). Owing to the technique used, they could not detect pre-mRNA processing. Nevertheless, some differentially spliced genes, such as *EPAS1* and *TRIO*, were also observed in our analysis. The study of Li et al. (2020) analysed the splicing patterns of oocytes that were able to mature *in vitro* but did not differentiate between immature oocytes that exited the GV block and those that simply did not reach MII after undergoing GVBD. However, we found some correspondence in terms of general pathways, such as oocyte meiosis and cell cycle, and in terms of specific genes involved. In particular, we identified 476 genes in our list of GV versus IVO-MII, and 173 genes in GV versus IVM-MII that were also reported in the study of Li et al. (2020), although we could not confirm whether the genes underwent the same splicing event.

Finally, the comparison of *in vivo* matured MII and MII obtained after IVM showed small but significant differences in terms of RNA processing, pointing towards an incorrect profile of RNA modification in IVM-MII, likely associated with lower developmental competence. The genes identified as differentially expressed/processed did not allow for a robust pathway detection, but we found several genes involved in oocyte meiosis progression, especially in the transcript subjected to RNA processing. This might indicate the failure to achieve some important milestones of oocyte maturation, such as spindle assembly and chromosome condensation, and could be reflecting their partially matured state, despite being morphologically similar to competent MIIs. The lower quality of this group does not come as a surprise, as it is known from older reports that "rescue" MII (i.e. GV obtained after LH priming, denuded from cumulus cells and matured *in vitro*) have low developmental competence, with a fertilization rate below 50%, versus ~80% observed in *in vivo* matured MII (Faramarzi et al., 2018).

In conclusion, our findings reveal a previously unknown level of dynamic transcript remodelling in human female meiosis, demonstrating how key meiosis genes change isoform composition after meiosis resumption, mostly on their 3'UTR, to reach the MII stage and assemble a functional meiotic spindle. This remodelling mostly generates shorter 3'UTR isoforms in mature oocytes, possibly a key feature of transcriptome regulation. Future investigations are needed to confirm the functional involvement of the targets, addressing both their translation levels and function during maturation.

Data availability

The data underlying this article are available in the Gene Expression Omnibus (GEO) at https://www.ncbi.nlm.nih.gov/geo, and can be accessed with GEO accession number: GSE213267.

Acknowledgements

We would like to thank the laboratory staff from EUGIN (Barcelona, Spain) for their help in sample handling and the IRB Barcelona Functional Genomics Core Facility (Barcelona, Spain) for the technical support.

Authors' roles

SP contributed to design the study, processed the samples, analysed and interpreted the data and drafted the manuscript; AFV contributed to samples collection; MI contributed to the interpretation and analysis of data; MBM, MP and EI revised the manuscript; RV designed the study, contributed to the interpretation of the data and substantially revised the manuscript; FZ designed the study, collected the samples, analysed and interpreted the data and substantially revised the manuscript.

Funding

This project received intramural funding from the Eugin Group and funding from the European Union's Horizon 2020 research and innovation program under the Marie Skłodowska-Curie grant agreement No 860960.

Conflict of interest

The authors declare that they have no competing interests.

REFERENCES

Anders S, Reyes A, Huber W. Detecting differential usage of exons from RNA-seq data. *Genome Res*. *2012*;22(10):2008-17. doi: 10.1101/gr.133744.111.

Biswas L, Tyc K, El Yakoubi W, Morgan K, Xing J, Schindler K. Meiosis interrupted: the genetics of female infertility via meiotic failure. *Reproduction*. *2021*; 161(2):R13-R35. doi: 10.1530/REP-20-0422.

Blazquez A, Guillén J J, Colomé C, Coll O, Vassena R, Vernaeve V. Empty follicle syndrome prevalence and management in oocyte donors. *Hum Reprod*. *2014*; 29(10):2221-7. doi: 10.1093/humrep/deu203.

Braunschweig U, Gueroussov S, Plocik A M, Graveley B R, Blencowe B J. Dynamic integration of splicing within gene regulatory pathways. *Cell*. *2013*; 152(6):1252-69. doi: 10.1016/j.cell.2013.02.034.

Chen J, Bardes E E, Aronow B J, Jegga A G. ToppGene Suite for gene list enrichment analysis and candidate gene prioritization. *Nucleic Acids Res*. *2009*; 37:W305-11. doi: 10.1093/nar/gkp427.

Cheng S, Altmeppen G, So C, Welp L M, Penir S, Ruhwedel T, Menelaou K, Harasimov K, Stützer A, Blayney M, Elder K, Möbius W, Urlaub H, Schuh M. Mammalian oocytes store mRNAs in a mitochondria-associated membraneless compartment. *Science*. *2022*; 378(6617):eabq4835. doi: 10.1126/science.abq4835.

Cooper T A, Wan L, Dreyfuss G. RNA and disease. *Cell*. *2009*; 136(4):777-93. doi: 10.1016/j.cell.2009.02.011.

Cornet-Bartolomé D, Barragán M, Zambelli F, Ferrer-Vaquer A, Tiscornia G, Balcells S, et al. Human oocyte meiotic maturation is associated with a specific profile of alternatively spliced transcript isoforms. *Mol Reprod Dev*. *2021*; ;88(9):605-617. doi: 10.1002/mrd.23526.

Coticchio G, Albertini D F, de Santis L. Oogenesis. *Oogenesis*. *2013*; 1;1–353. doi: 10.1007/978-0-85729-826-3.

de La Fuente R. Chromatin modifications in the germinal vesicle (GV) of mammalian oocytes. *Developmental Biology*. *2006*; 292(1):1-12 doi: 10.1016/j.ydbio.2006.01.008.

Derti A, Garrett-Engele P, MacIsaac K D, Stevens R C, Sriram S, Chen R, et al. A quantitative atlas of polyadenylation in five mammals. *Genome Res. 2012*; 22(6):1173-83. doi: 10.1101/gr.132563.111.

Dias A P, Dufu K, Lei H, Reed R. A role for TREX components in the release of spliced mRNA from nuclear speckle domains. *Nat Commun. 2010;* 1:97 doi: 10.1038/ncomms1103.

Do D V, Strauss B, Cukuroglu E, Macaulay I, Wee K B, Hu T X, et al. SRSF3 maintains transcriptome integrity in oocytes by regulation of alternative splicing and transposable elements. *Cell Discov*. *2018*; 4:33. doi: 10.1038/s41421-018-0032-3.

Faramarzi A, Khalili MA, Ashourzadeh S, Palmerini MG. Does rescue in vitro maturation of germinal vesicle stage oocytes impair embryo morphokinetics development? *Zygote. 2018*; 26(5):430-434. doi: 10.1017/S0967199418000515.

Ha K C H, Blencowe B J, Morris Q. QAPA: a new method for the systematic analysis of alternative polyadenylation from RNA-seq data. *Genome Biol*. *2018*; 19(1):45. doi: 10.1186/s13059-018-1414-4.

Hassold T & Hunt P. To err (meiotically) is human: the genesis of human aneuploidy. *Nat Rev Genet. 2001;* 2(4):280-91 doi: 10.1038/35066065.

He Y, Chen Q, Zhang J, Yu J, Xia M, Wang X. Pervasive 3'-UTR Isoform Switches During Mouse Oocyte Maturation. *Front Mol Biosci*. *2021*; 8:727614. doi: 10.3389/fmolb.2021.727614.

Hu W, Zeng H, Shi Y, Zhou C, Huang J, Jia L, et al. Single-cell transcriptome and translatome dual-omics reveals potential mechanisms of human oocyte maturation. *Nat Commun. 2022*; 13(1):5114. doi: 10.1038/s41467-022-32791-2.

Irimia M, Weatheritt R J, Ellis J D, Parikshak N N, Gonatopoulos-Pournatzis T, Babor M, et al. A highly conserved program of neuronal microexons is misregulated in autistic brains. *Cell*. *2014*; 159(7):1511-23. doi: 10.1016/j.cell.2014.11.035.

Jaffe L A, Egbert J R. Regulation of Mammalian Oocyte Meiosis by Intercellular Communication Within the Ovarian Follicle. *Annu Rev Physiol*. *2017*; 79:237-260. doi: 10.1146/annurev-physiol-022516-034102.

Jansova D, Tetkova A, Koncicka M, Kubelka M, Susor A. Localization of RNA and translation in the mammalian oocyte and embryo. *PLoS One*. *2018*; 13(3):e0192544. doi: 10.1371/journal.pone.0192544.

Kelemen O, Convertini P, Zhang Z, Wen Y, Shen M, Falaleeva M, et al. Function of alternative splicing. *Gene. 2013*; 514(1):1-30. doi: 10.1016/j.gene.2012.07.083.

Kuwayama M. Highly efficient vitrification for cryopreservation of human oocytes and embryos: the Cryotop method. *Theriogenology*. *2007*; 67(1):73-80. doi: 10.1016/j.theriogenology.2006.09.014.

Langmead B, Trapnell C, Pop M, Salzberg S L. Ultrafast and memory-efficient alignment of short DNA sequences to the human genome. *Genome Biol*. *2009*; 10(3):R25. doi: 10.1186/gb-2009-10-3-r25.

Lawrence M, Huber W, Pagès H, Aboyoun P, Carlson M, Gentleman R, Morgan M T, Carey V J. Software for computing and annotating genomic ranges. *PLoS Comput Biol*. *2013*; 9(8):e1003118. doi: 10.1371/journal.pcbi.1003118.

Leppek K, Das R, Barna M. Functional 5' UTR mRNA structures in eukaryotic translation regulation and how to find them. *Nat Rev Mol Cell Biol. 2018*; 19(3):158-174. doi: 10.1038/nrm.2017.103.

Li J, Lu M, Zhang P, Hou E, Li T, Liu X, Xu X, Wang Z, Fan Y, Zhen X, et al. Aberrant spliceosome expression and altered alternative splicing events correlate with maturation deficiency in human oocytes. *Cell Cycle*. *2020*; 19(17):2182-2194. doi: 10.1080/15384101.2020.1799295.

Liao Y, Wang J, Jaehnig EJ, Shi Z, Zhang B. WebGestalt 2019: gene set analysis toolkit with revamped UIs and APIs. *Nucleic Acids Res*. *2019*; 47(W1):W199-W205. doi: 10.1093/nar/gkz401.

Llonch S, Barragán M, Nieto P, Mallol A, Elosua-Bayes M, Lorden P, Ruiz S, Zambelli F, Heyn H, Vassena R, Payer B. Single human oocyte transcriptome analysis reveals distinct maturation stage-dependent pathways impacted by age. *Aging Cell. 2021*; 20(5):e13360. doi: 10.1111/acel.13360.

Love M I, Huber W, Anders S. Moderated estimation of fold change and dispersion for RNA-seq data with DESeq2. *Genome Biol*. *2014*; 15(12):550. doi: 10.1186/s13059-014-0550-8.

Luciano A M, Lodde V, Franciosi F, Tessaro I, Corbani D, Modina S C. Large-scale chromatin morpho-functional changes during mammalian oocyte growth and differentiation. *Eur J Histochem. 2012*; 56(3):e37. doi: 10.4081/ejh.2012.e37.

Mamo S, Carter F, Lonergan P, Leal C L, al Naib A, Mcgettigan P, Mehta JP, Evans AC, Fair T. Sequential analysis of global gene expression profiles in immature and in vitro matured bovine oocytes: potential molecular markers of oocyte maturation. *BMC Genomics. 2011*; 12:151. doi: 10.1186/1471-2164-12-151.

Matoulkova E, Michalova E, Vojtesek B, Hrstka R. The role of the 3' untranslated region in post-transcriptional regulation of protein expression in mammalian cells. *RNA Biology*. *2012*; 9(5):563-76. doi: 10.4161/rna.20231.

Mignone F, Gissi C, Liuni S, Pesole G. Untranslated regions of mRNAs. *Genome Biol*. *2002*; 3(3):REVIEWS0004. doi: 10.1186/gb-2002-3-3-reviews0004.

Mihajlović A I & FitzHarris G Segregating Chromosomes in the Mammalian Oocyte. *Curr Biol*. *2018*; 28(16):R895-R907. doi: 10.1016/j.cub.2018.06.057.

Olivennes F, Fanchin R, Bouchard P, Taieb J, Selva J, Frydman R. Scheduled administration of a gonadotrophin-releasing hormone antagonist (Cetrorelix) on day 8 of in-vitro fertilization cycles: a pilot study. *Hum Reprod. 1995*; 10(6):1382-6.

Pühringer T, Hohmann U, Fin L, Pacheco-Fiallos B, Schellhaas U, Brennecke J, Plaschka C. Structure of the human core transcription-export complex reveals a hub for multivalent interactions. *Elife*. *2020*; 9:e61503. doi: 10.7554/eLife.61503.

Reyes J M, Silva E, Chitwood J L, Schoolcraft W B, Krisher R L, Ross P J. Differing molecular response of young and advanced maternal age human oocytes to IVM. *Hum Reprod. 2017*; 32(11):2199-2208. doi: 10.1093/humrep/dex284.

Robinson M D, McCarthy D J, Smyth G K. edgeR: a Bioconductor package for differential expression analysis of digital gene expression data. *Bioinformatics*. *2010*; 26(1):139-40. doi: 10.1093/bioinformatics/btp616.

Schellander K, Hoelker M, Tesfaye D. Selective degradation of transcripts in mammalian oocytes and embryos. *Theriogenology*. *2007*; 68 Suppl 1:S107-15. doi: 10.1016/j.theriogenology.2007.05.054.

Susor A, Jansova D, Cerna R, Danyleversuska A, Anger M, Toralova T, Malik R, Supolijova J, Cook MS, Oh JS, Kubelka M. Temporal and spatial regulation of translation in the mammalian oocyte via the mTOR-eIF4F pathway. *Nat Commun*. *2015*; 6:6078. doi: 10.1038/ncomms7078.

Vassena R, Boué S, González-Roca E, Aran B, Auer H, Veiga A, Izpisua Belmonte JC. Waves of early transcriptional activation and pluripotency program initiation during human preimplantation development. *Development*. *2011*; 138(17):3699-709. doi: 10.1242/dev.064741.

Wartosch L, Schindler K, Schuh M, Gruhn JR, Hoffmann E R, McCoy RC, Xing J. Origins and mechanisms leading to aneuploidy in human eggs. *Prenat Diagn. 2021;* 41(5):620-630. doi: 10.1002/pd.5927.

Wu Z W, Mou Q, Fang T, Wang Y, Liang H, Wang C, Du Z Q, Yang C X. Global 3'-untranslated region landscape mediated by alternative polyadenylation during meiotic maturation of pig oocytes. *Reprod Domest Anim*. *2022*; 57(1):33-44. doi: 10.1111/rda.14026.

Yang F, Wang W, Cetinbas M, Sadreyev R I, Blower M D. Genome-wide analysis identifies cis-acting elements regulating mRNA polyadenylation and translation during vertebrate oocyte maturation. *RNA*. *2020*; 26(3):324-344. doi: 10.1261/rna.073247.119.

Zhao H, Li T, Zhao Y, Tan T, Liu C, Liu Y, Chang L, Huang N, Li C, Fan Y, et al. Single-Cell Transcriptomics of Human Oocytes: Environment-Driven Metabolic Competition and Compensatory Mechanisms During Oocyte Maturation. *Antioxid Redox Signal*. *2019*; 30(4):542-559. doi: 10.1089/ars.2017.7151.

SUPPLEMENTARY INFORMATION CONTENTS:

- **Supplementary Table S1.** Demographic characterization of the patients involved in the study and the related oocytes processed.
- **Supplementary Table S2.** Differentially expressed genes in IVO-MII vs GV.
- **Supplementary Table S3.** Differentially expressed genes in IVM-MII vs GV.
- **Supplementary Table S4.** Differential exon usage in IVO-MII vs GV.
- **Supplementary Table S5.** Differential exon usage in IVM-MII vs GV.
- **Supplementary TableS6.** Comparison between two exons-based software DEXseq and edgeR.
- **Supplementary Table S7.** Differential usage of poly(A) sites in IVO-MII vs GV.
- **Supplementary Table S8.** Differential usage of poly(A) sites in IVM-MII vs GV.
- **Supplementary Table S9.** Differential usage of poly(A) sites in FTM-GV vs GV.
- **Supplementary Table S10.** Genes affected by Alternative splicing in IVO-MII vs GV.
- **Supplementary Table S11.** Genes affected by Alternative splicing in IVM-MII vs GV.
- **Supplementary Table S12.** Genes affected by Alternative splicing in FTM-GV vs GV.
- **Supplementary Table S13.** Differential mRNA processing in IVO-MII vs IVM-MII.
- **Supplementary Table S14.** List of primers used for validation.
- **Supplementary Figure S1.** Genes with differential poly(A) usage are partially correlated with DEGs and genes with differential exon usage.
- **Supplementary Figure S2.** qPCR validation.

Supplementary Table S1-S13 are large Excel files, data available on request from the authors.

Supplementary Table S14. List of primers used for validation.

Gene	Type	Forward Primer sequence (5'-3')	Reverse Primer sequence (5'-3')
PSMC3IP	target	TGGCCTCTCCCATGTCTCA	GGGACTGCAGGATGTCAGAA
	control	CCACCAGCCCTCATCCTCT	AGGAAGTTGGGATAGAGACGG
ESCO1	target	GGTCATAAAAGGCCACAGCAG	TGAACTCAGGACTGGCAACA
	control	AGTGGTGTAGGCAAGAATTTGT	TCCTGATGGAAAGCTGTTTGC
CYP26B1	target	GTGGTGCCCAGAACACAAAC	CCCTCAGACCAGATCCCGTA
	control	TCTTGGGTTAGACTGTGGCG	CCCAAAGGCTGGAGTGTCAT
MAD2L1BP	target	TTCTCCATGTGGCGCTGAAT	AGGACACAGCAAAGAGCAGA
	control	GAAGAAGAAACCTCGGGCCA	AATGTCACTGGTGCCTGGAA
ZAR1L	target	CTAGCCATTTTCCGATGCCAG	TGTACAGTGTGACTTGTAATGGAC
	control	AGCTGTAAATATTGCCACAGGAGA	CCTGCTCAAAGTCTCATTGTTCC
USP49	target	AGCCAGTCTTTGATACATGCCT	TGCAGTGTCGAGGAAGTGTG
	control	CCTCCCTCTGTGTTGTAGCA	GGTCTGGCCGTAATCATCGAG
MDM1	target	ACTTCACACTGGGATCTTAACTT	ACCTAGCTGAGTTGCCTTTATC
	control	TTTTACCCCAGAAATTCTCCTTCCT	AGGACAGATTGTCTGAGATTTCTGC
SNRPC	target	GGGGAGGCCTTATTGTATCGG	TAGGACAGGGGAGCAAGTCT
	control	GCTCCTGGAATGAGGCCG	GAGTCATTCCGGGCCGAG
PAN3	target	AAAAAGCACGCAGGACATGG	TCTTCACAGATAACAGCCTCCA
	control	CTAGATGCTGGTGTGCCAGA	GCAGCTGCAATCAGTTCTTG
KIAA0753	target	TCATCACCAAACTGAGCCAGA	GTCACACTGGAGAAGGGATGG
	control	GGTGAACACAGCTTCTGCAT	CAGAAGAGCTGGTAGATGAAGC
TENT4B	target	TCATGCTCAGGACAGTTGCG	TTTTGCAGCAGGACACAAGG
	control	GCATGGATCAGCAAGGCTCT	TACAGAGGTCTGAGAGGGGC
KIF3C	target	CGAACAGAGCTCCGCGAATA	GTCAGGCTGCCCATCCAATA
	control	CTCATGGTCCGCCACTGTTG	TGCCAGAGTCCTCAGCGG
TAOK1	target	ACATCATCACAGCAGCCTCC	GAACTTTCAGGGCCCCTCTC
	control	TGTTGGAACGTCAAGCCAGA	TGACACTCGTGCTTCTGCTC
ERCC6	target	TCATCCAGGACCGACCGATA	GGGAATCCCCCACTCAAGTC
	control	TCCTGCACTGGCACTTTCTT	CCATCCAGTCTTGGCAGCAT
CENPE	target	AGGTTGCTATGAATTGGTCCCT	TGCTTAGAGTGAAAGAAGATGTCA
	control	TGGTTTCTTGCAGGCTTTCC	ACTTAAGGCAAATGAACATCAACTT
POGZ	target	TGTTGGCAATTAGTGTGACAAGAG	TTTCTGTGAGCCAGCAGCC
	control	ATAATCTTCAACTACAGAGTCCTCA	CGGACACCGACCTGTTCAT
NIPBL	target	ACAGACGTGACTATGCTCTTGT	CTCCTTGAATGACTGCAGTAGG
	control	TGGTAAAGGACAAAAGGAAAGAGA	CCACAAAGATTCTTCAAATGTTGTT
TUBB8	target	AGGTCTTCAGGCCAGACAACT	TGCAAAAGGTCTCATCTGCGT
	control	GGCCTCGTTGTAGTACACGTT	GGTGATCTCTGATGAACATGCC

List of primers used to validate representative genes found differential between immature GVs and matured MIIs.

Supplementary Figure S1.

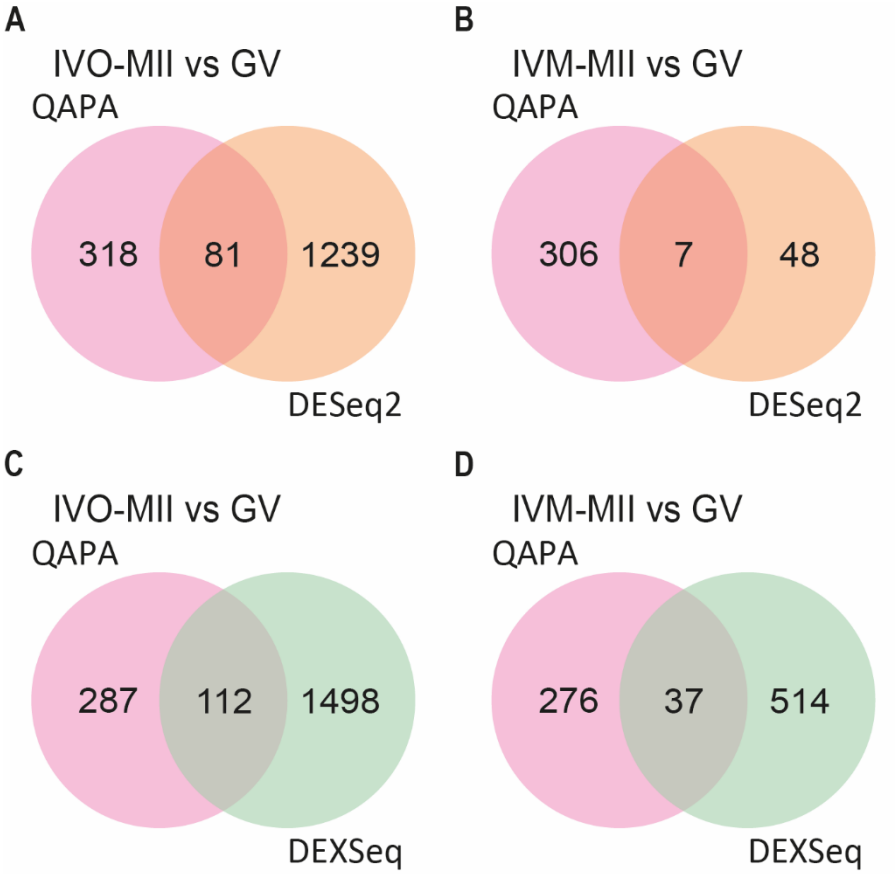

Supplementary Figure S1. Genes with differential poly(A) usage are partially correlated with DEGs and genes with differential exon usage. (A) Comparison between genes with 3'UTR processing during meiotic maturation (ΔPPAU=|10| and p-value <0.05, ranked Wilcoxon paired test) and DEGs (p-adjusted <0.1) in IVO-MII vs GV and **(B)** IVM-MII vs GV. **(C)** Comparison between genes with 3'UTR processing during meiotic maturation (ΔPPAU=|10| and p-value <0.05, ranked Wilcoxon paired test) and genes with differential exons usage (p-adjusted <0.05) in IVO-MII vs GV and **(D)** IVM-MII vs GV. IVO-MII = *in vivo* matured MII oocytes; IVM-MII = *in vitro* matured MII oocytes; GV = germinal vesicles; ΔPPAU = difference in proximal poly(A) usage; DEGs = differentially expressed genes.

Supplementary Figure S2.

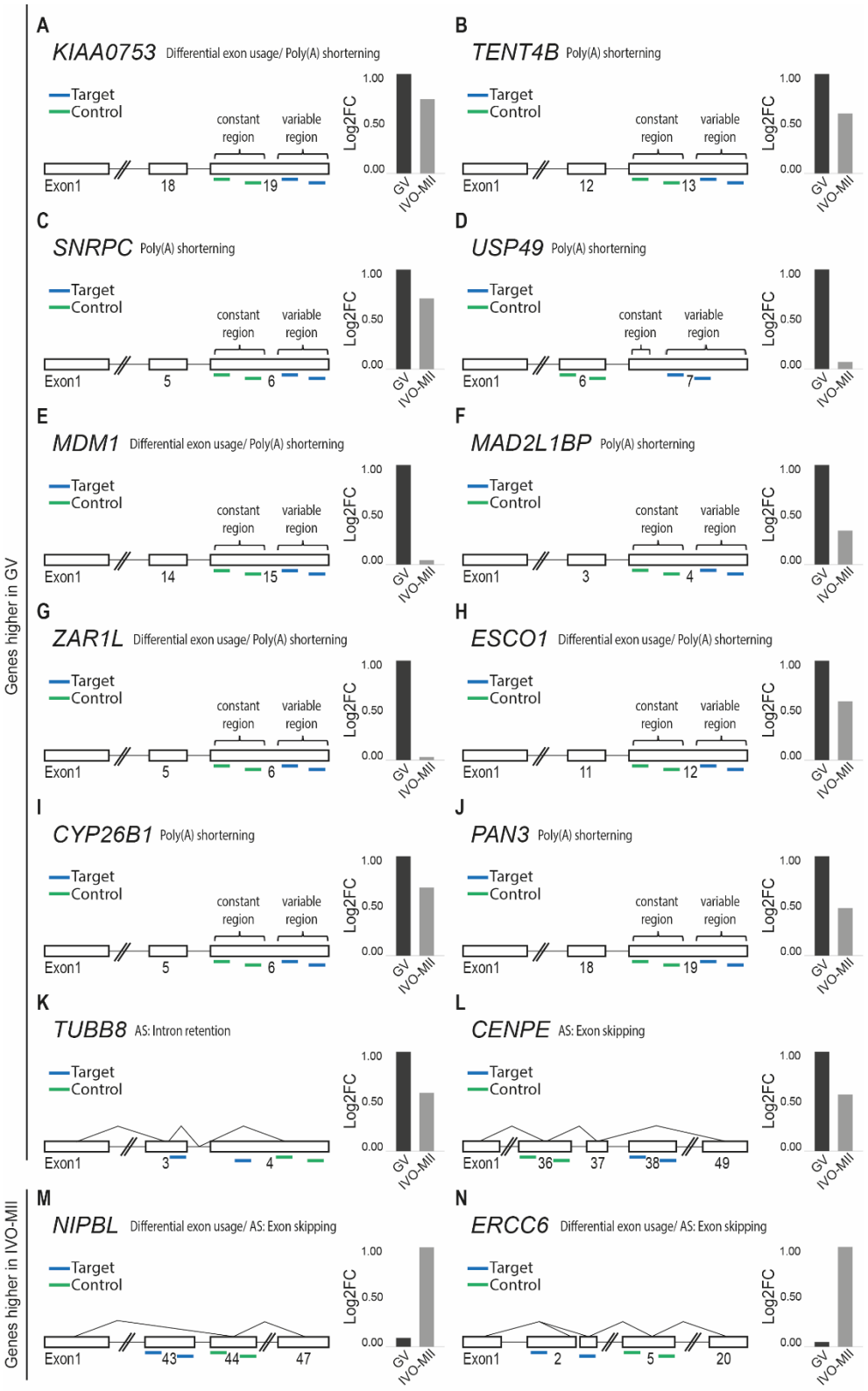

Supplementary Figure S2. qPCR validation. (A-N) Validation of targets identified as differentially processed in GV and in IVO-MII. Primers pairs for control region (green) and target region (blue) are reported for each gene. qPCR results are reported for all the tested genes in the respective graphs. AS = alternative splicing; Log2FC = Log2 Fold Change; IVO-MII = *in vivo* matured MII oocytes; GV = germinal vesicle oocytes.

2. COMPROMISED OOCYTE QUALITY: A BOVINE MODEL TO STUDY EARLY OVARIAN AGING IN HUMANS

Title: Cytoplasmic maturation failure in premature ovarian insufficiency: insights from a bovine model

Authors: Sara Pietroforte[1,2], Pritha Dey[3], Elena Ibáñez[2], Alberto Maria Luciano[3], Valentina Lodde[3], Federica Franciosi[3], Mina Popovic[1], Rita Vassena[1], Filippo Zambelli[1]

Affiliations:

1 - Basic Research Laboratory – Eugin Group, Barcelona 08006, Spain.

2 - Departament of Cell Biology, Physiology and Immunology, Universitat Autònoma de Barcelona, 08193 Bellaterra, Barcelona, Spain.

3 - Reproductive and Developmental Biology Lab., Dipartimento di Scienze Veterinarie per la Salute la Produzione Animale e la Sicurezza Alimentare 'Carlo Cantoni', Università degli Studi di Milano, Lodi, Italy.

ABSTRACT

Poor oocyte quality is one of the hallmarks of oocytes of women suffering from Premature Ovarian Insufficiency (POI). One to ten percent of women <40 years of age are affected by POI, a condition characterized by hormonal alterations and partial follicle deprivation. While oocytes from POI women generate viable embryos with low efficiency, the mechanisms responsible for this phenomenon remain elusive. Due to the scarcity of human oocytes for research, animal models provide a promising way forward. In a recently defined bovine model of low ovarian reserve, young cows presented key hallmarks of human POI, including a specific hormonal profile, reduced antral follicle count and ovarian volume, and overall reduced fertility. We found abundant differentially expressed genes between the germinal vesicle (GV) and metaphase II (MII) stages of oocyte maturation in oocytes collected from cows of 4-8 years either with a normal or low ovarian phenotype. The genes affected were related to RNA processing and transport, protein synthesis, organelle remodeling and reorganization, and metabolism. A comparative analysis with human oocytes from young donors revealed high similarity in global gene expression through the GV-MII transition between cow and human, with partial conservation of global gene expression between species. Furthermore, gene expression analysis between GV and MII of POI-like oocytes showed differences according to cows rather than stages of maturation, a feature that mimics the high number of genetic alterations causing POI in the affected women. We describe a valuable animal model for POI, opening the door to studying the molecular underpinnings of the condition.

Keywords: transcriptome, gene expression, POI, cow, oocyte maturation

INTRODUCTION

A decrease in ovarian reserve and oocyte quality is generally associated with advanced maternal age (AMA) in women over 37 years (Alviggi et al., 2009; Broekmans et al., 2009). However, some women show diminished ovarian function, and low antral follicle counts at a much younger age, with oocytes of lower developmental competence. This condition, premature ovarian insufficiency (POI), affects 1-10% of women (Shestakova et al., 2016; McGlacken-Byrne & Conway, 2022). Women affected by POI present complex systemic symptoms such as amenorrhea, hypoestrogenism, high follicle stimulating hormone (FSH) serum levels, low anti-Mullerian hormone (AMH) levels, and a reduction of estradiol concentration in blood. Furthermore, POI is characterised by accelerated ovarian senescence with a reduction in follicle size and number and, overall, hypofertility (Nelson, 2009; De Vos et al., 2010).

The scarcity of oocytes available from POI women limits direct studies in humans, and animal models are critical tools to understand POI physiopathology. A POI-like phenotype has been described in 5% of 4-8 years old culled dairy cows (Malhi et al., 2005; Luciano et al., 2013; Lodde et al., 2021). These animals have small ovary size (< 2-4 cm length on the major axis), less than 10 antral follicles on both ovaries, normal oocyte *in vitro* maturation rates but reduced developmental competence (about 6% blastocyst rates), high aneuploidy rates in embryos (60%) and, overall, reduced fertility (Luciano et al., 2013). In addition, much like women suffering from POI, these animals also present high FSH serum levels, low AMH, reduced estradiol and increased progesterone in follicular fluid (Lodde et al., 2021).

The molecular characterization of POI-like follicles in these cows showed alterations in mitochondrial distribution and activity, histone modifications, DNA damage, glutathione content and communication between the oocyte and the cumulus cells (Lodde et al., 2021). So far, however, the transcriptome characterization of POI-like cow oocytes is still lacking. Given the similarities in gene expression profiles during oocyte maturation and embryo development between humans and cows (Schall & Latham, 2021a), the study of these oocytes in the bovine model could provide insights into POI in our species. Our aim is to define the transcriptional profile of POI-like oocytes in cows to identify conserved alterations across species linked to this phenotype.

MATERIALS AND METHODS

Oocytes collection and culture

Twenty cumulus-oocytes complexes (COC) from ten cows were collected (Supplementary Table 1) as previously described (Lodde et al., 2021). Briefly, ovaries were recovered at a local abattoir (INALCA, Lodi, Milan, Italy) from pubertal dairy cows (4-8 years old). Ovaries were isolated and characterised in terms of size (length on the major axis) and antral follicles count (AFC) (2-6).

Ovaries were transported to the laboratory at 26ºC, while subsequent procedures were performed at 35-38ºC. COCs were retrieved from medium antral follicles manually with a 0.8 x 40mm syringe and washed in TCM-199 supplemented with 20 mM HEPES buffer, 1.798 U/L heparin and 0.4% fatty acid free bovine serum albumin (BSA) (H-M199). Only follicles of >2 mm were aspirated.

COCs were denuded and either processed immediately at the GV stage or matured *in vitro* (IVM) to the MII stage. Groups of 10-14 COCs were matured for 24 h in TCM-199 supplemented with 0.68 mM L-glutamine, 25 mM NaHCO3, 0.4% fatty acid free BSA, 0.2 mM sodium pyruvate and 0.1 IU/mL recombinant human FSH (Sigma-Aldrich, St. Louis, Missouri, USA) in humidified air under 5% CO2 at 38.5ºC. After IVM, all the COCs were denuded and processed. Only oocytes that extruded the first polar body (PB) were considered mature.

Single cell RNA sequencing

For single cell RNA sequencing, twenty oocytes from 10 cows were included. Oocytes were assigned to the POI-like (n=10) or control (CTRL, n=10) group based on AFC and ovary size of the ovaries they came from. POI-like oocytes were from ovarian pairs with AFC<10 and <2-4 cm in length. Each group included 5 GV and 5 MII oocytes. Each cow provided one GV and one IVM-MII (Supplementary Table S1).

The oocytes' zona pellucida was removed with pronase (Roche Diagnostics, Basel, Switzerland) and zona-free oocytes were lysed individually in 20µL of Extraction Buffer (PicoPure RNA Isolation Kit, Thermo Fisher, Waltham, Massachusetts, USA), incubated at 42°C for 30 min and stored at -80°C. Total RNA extraction was performed following

manufacturer's specifications (PicoPure RNA Isolation Kit, Thermo Fisher, Waltham, Massachusetts, USA).

Single oocyte cDNA libraries were constructed using the Ovation SoLo RNA-Seq System (NuGEN, TECAN, Männedorf, Switzerland). Sequencing of libraries was carried out using a NextSeq500 (Illumina, San Diego, California, USA) with 2x150 bp paired-end reads, with 30 million reads per sample. FastQC (Babraham Bioinformatics, Cambridge, UK) was used to perform the quality control of the sequencing.

Transcriptome analysis

After quality control of raw reads, the clean reads for each sample were aligned to the BosTau8 bovine reference genome using Galaxy (https://usegalaxy.eu/, (Afgan et al., 2022), and bam files were generated. Reads belonging to whole genes or single exons were counted using the function SummarizeOverlaps of the Bioconductor/R package Genomic Features (Lawrence et al., 2013). DESeq2 (Love et al., 2014) was then used to detect differentially expressed genes (DEGs) between experimental groups, and genes with an adjusted p-value <0.1 were considered significant.

Comparative analysis with human public data

The bovine data of the present study were further compared with human transcriptomic data of scRNA sequencing of oocytes at different maturation stages (GSE213267, Pietroforte et al., 2023) obtained from the Gene Expression Omnibus (GEO) at https://www.ncbi.nlm.nih.gov/geo.

To visualize the interaction between proteins in the same pathway, we used the STRING database (Szklarczyk et al., 2019).

Gene set enrichment analysis

Gene set enrichment analysis (GSEA) was performed by WebGestalt (Liao et al., 2019), using the gene ontology (GO) database for biological function selecting the following parameters: Organism: *btaurus*; Enrichment Categories: *geneontology Biological Process noRedundant*; ID type: *ensemble gene id*; Minimum number of IDs in the category: *3*. We then selected the top 20 pathways sorted by False Discovery Rate (FDR).

RESULTS

The transcriptome of control oocytes during meiotic maturation highlights processing of meiosis and female germ cell development genes

The principal component analysis (PCA) showed clear clustering of CTRL group oocytes based on their developmental stage, with a variance of 50% in the first and 17% in the second component (**Figure 1A**). The high variance was caused by one oocyte, as seen also when considering the top 50 variable genes (**Figure 1B**). We considered then this oocyte as outlier and excluded it from further analysis, which were performed on 5 CTRL GV oocytes and 4 CTRL IVM MII oocytes.

We identified 2223 DEGs between oocytes in IVM-MII vs GV (**Figure 1B, 1C;** Supplementary Table S2), 1176 up-regulated and 1047 down-regulated in IVM-MII. Selecting for log2 Fold Change > |±1|, we found 38 up-regulated (7%) and 511 down-regulated (93%) DEGs in IVM-MII oocytes (**Figure 1D**). GSEA highlighted biological processes related to the development of the reproductive system, regulation of hormonal levels, mRNA processing and the meiotic cell cycle, protein transport and localization (**Figure 1E**).

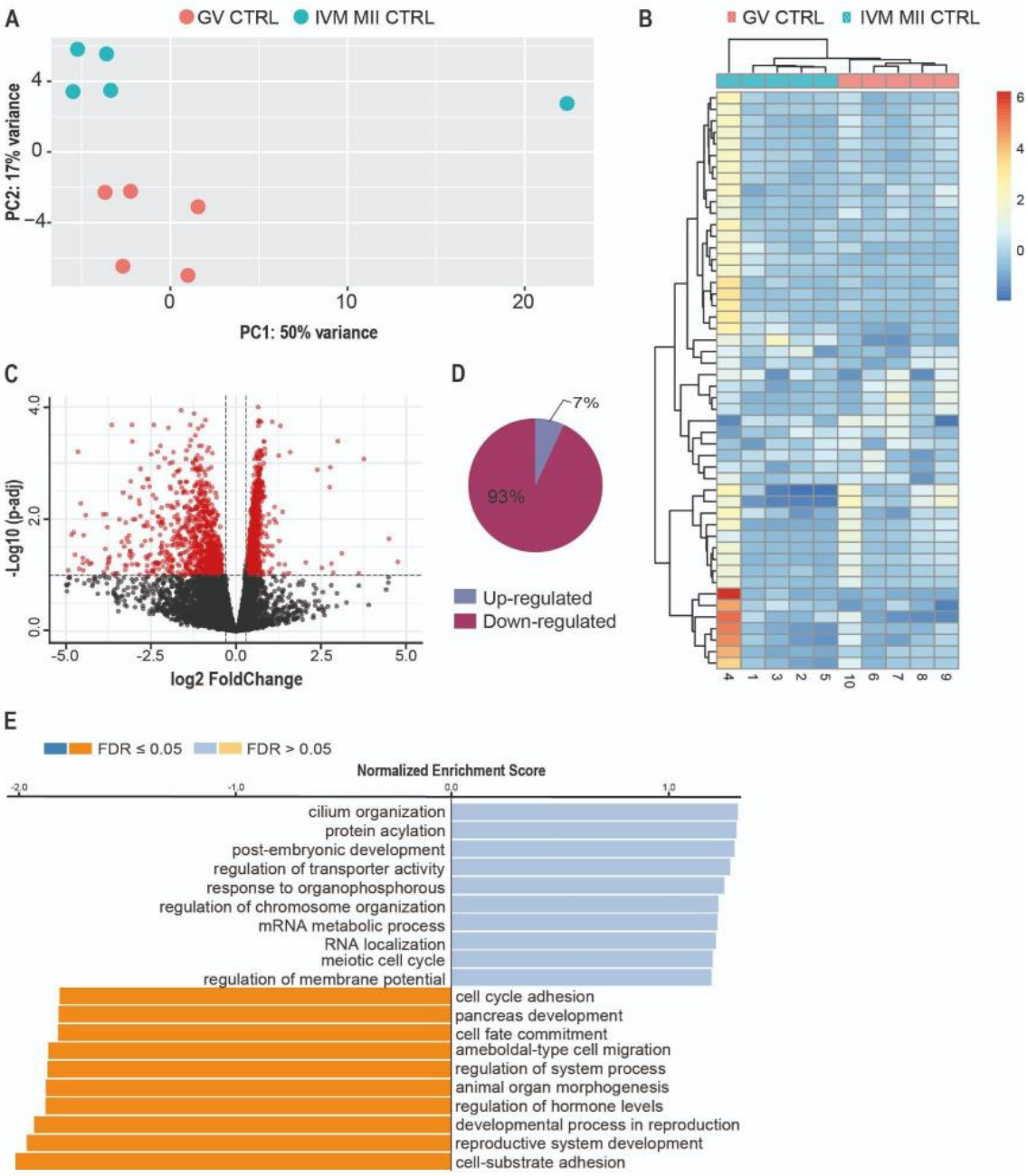

Figure 1. Transcriptomic changes through oocyte meiotic maturation of control bovine oocytes. (**A**) Principal component analysis (PCA) of GV and IVM-MII oocytes from young cows with normal ovarian physiology (CTRL group). (**B**) Heatmap of the top 50 differentially expressed genes (DEGs) between GV and IVM-MII oocytes; the shades of colours represent the counts per million. (**C**) Volcano plot of the DEGs found in the comparison IVM-MII versus GV oocytes. Red dots represent the genes with p-value<0.1, considered statistically significant (**D**) Proportion of up- and down-regulated genes in IVM-MII versus GV oocytes. (**E**) Gene Set Enrichment Analysis (GSEA) of the most affected pathways in the IVM-MII versus GV comparison. The affected pathways with FDR ≤ 0.05 are reported in orange and blue. In our analysis we detected only affected pathways with FDR ≤ 0.05.

Transcriptome convergence of human and bovine oocytes during meiosis

To evaluate the degree of transcriptome similarity between human and bovine oocytes, we processed the RNAseq data of oocytes from young oocyte donors, 10 GV and 10 MII. (GSE213267). We found 1675 DEGs between GV and MII oocytes, mostly related to translation initiation, protein transport, RNA metabolism, RNA transport and splicing pathways, with about 30 DEGs specifically involved in the spliceosome machinery, in agreement with the original report (Pietroforte et al., 2023). We then compared those data with the DEGs identified in bovine CTRL group IVM-MII vs GV and observed an overlap of 285 genes (**Figure 2A**). GSEA of the common DEGs highlighted RNA processing, cell cycle and oocyte meiosis pathways as the biological processes most affected across species (**Figure 2B**). Moreover, we analysed how the proteins interact with each other using STRING database (**Figure 2C, 2D**). DEGs through meiotic maturation and conserved between human and cow include *FRG1* (FSHD Region Gene 1), *RNF20* (Ring Finger Protein 20), *KIF4A* (Kinesin Family Member 4A), *NIPBL* (NIPBL Cohesin Loading Factor), *CDC40* (Cell Division Cycle 40), *TUBB* (Tubulin Beta Class I), *SASS6* (SAS-6 Centriolar Assembly Protein) involved in cell cycle and sister chromatid segregation (Supplementary Figure S1A and zoom on the central area of the interactions in **Figure 2C**) and *MAGOH* (Mago Homolog, Exon Junction Complex Subunit), *SREK1* (Splicing Regulatory Glutamic Acid And Lysine Rich Protein 1), *YTHDC1* (YTH N6-Methyladenosine RNA Binding Protein C1), *THOC1* (THO Complex Subunit 1), *THOC7* (THO Complex Subunit 7), *SRSF4* (Serine And Arginine Rich Splicing Factor 4), *PAPOLG* (Poly(A) Polymerase Gamma), *PRPF18* (Pre-MRNA Processing Factor 18), involved in mRNA processing, transport and degradation (Supplementary Figure S1B and zoom on the central are of the interactions in **Figure 2D**).

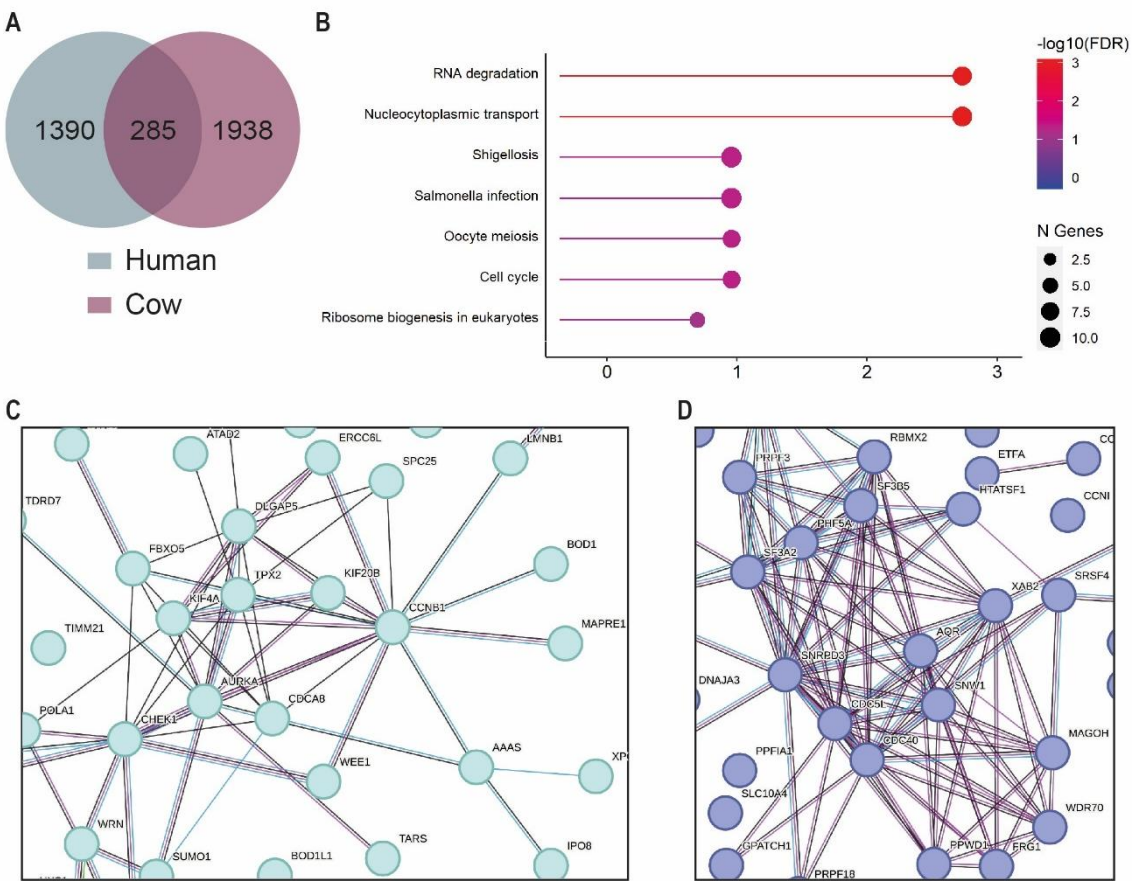

Figure 2. Human-Cow cross-species comparison of the different genes expressed through meiosis. (**A**) Comparison between human (GSE213267) and bovine differentially expressed genes (DEGs) in mature versus immature oocytes. (**B**) Most significant biological processes involved in the transition from immature to mature oocytes in common DEGs between human and bovine. In the lollipop diagram, the significance -log10 (False Discovery Rate, FDR) is represented in red to blue shades and the dot of each pathway is proportional to the number of genes affected. (**C**) Selected network interactions of DEGs involved in oocyte meiosis and (**D**) mRNA processing and transport.

POI-like bovine oocytes fail to remodel their transcriptome after *in vitro* maturation

The PCA analysis showed a stronger clustering of POI-like samples by cow than by meiotic maturation stage (**Figure 3A**), with a variance of 57% in the first and 11% in the second component. Even when considering the top 50 variable genes, the separation of the oocytes continued to be associated with the individual rather than the oocyte's meiotic stage (**Figure 3B**). Given that two samples from the same cow were further away from the bulk of other samples, and PC1 was accounting for 57% of the variance, a very high value, we consider the two oocytes as outliers and proceeded with 4 GV versus 4 IVM-MII oocytes. This clustering of oocytes, both GV and IVM-MII, was specific to the POI-like group, while oocytes in the CTRL group clustered per meiotic stage, as discussed.

The comparison of IVM-MII vs GV oocytes yielded only 18 DEGs, indicating a failure to achieve a correct cytoplasmic maturation (**Figure 3C**). The low number of genes did not allow for the identification of specific biological processes affected in this comparison.

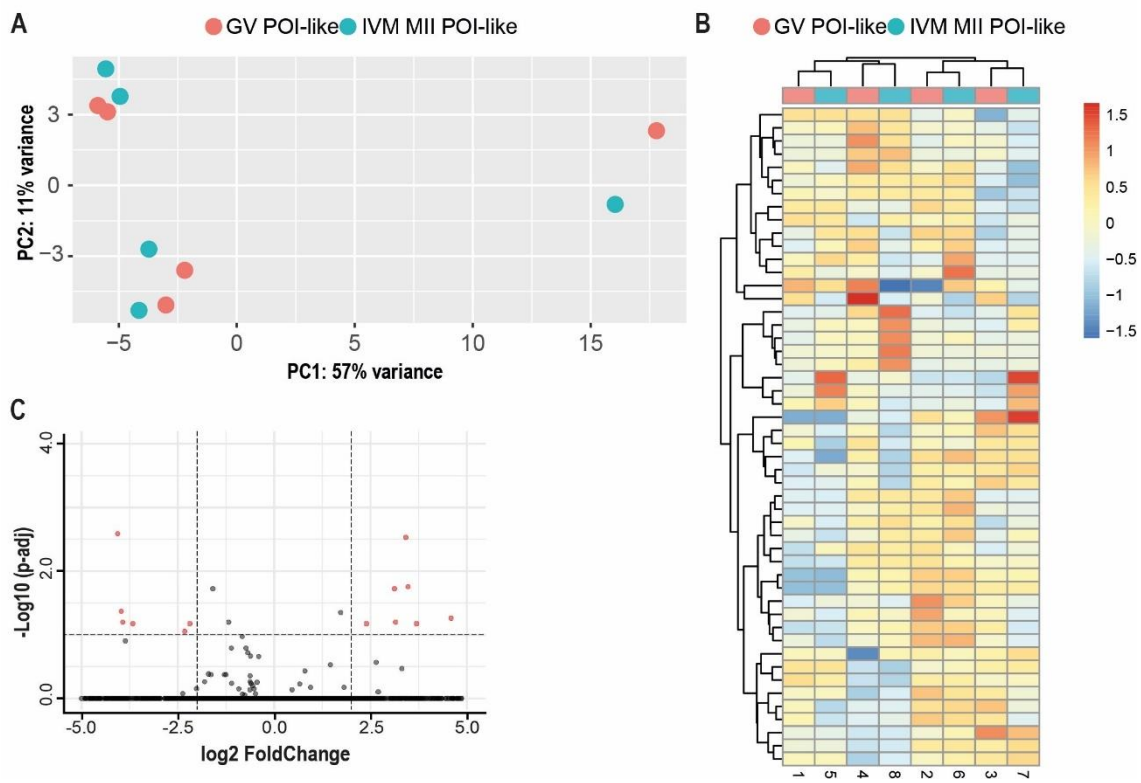

Figure 3. Transcriptional characterization of maturing oocytes from POI-like group. (**A**) Principal component analysis (PCA) of immature GV oocytes and IVM-MII oocytes in the POI-like group. (**B**) Heatmap of the top 50 differentially expressed genes (DEGs) between GV and IVM-MII oocytes. The shades of colours represent the counts per million. (**C**) Volcano plot of the DEGs found with p-adjusted<0.1 (red dots) in the comparison IVM-MII versus GV oocytes in POI-like group.

Oocytes from POI-like cow ovaries fail to undergo a complete nuclear and cytoplasmic maturation

To understand the characteristics of the low number of DEGs observed in the POI-like group, we performed a comparison between CTRL and POI-like groups. When comparing the same meiotic stages, we found 67 and 156 DEGs in GV POI-like versus GV CTRL oocytes (**Table 1**), and IVM-MIIs POI-like versus IVM-MII CTRL oocytes (**Table 2**), respectively. The DEGs in GV oocytes were too few to identify any affected pathway, however those genes were mostly related to cumulus-oocyte complex communication and microtubule organisation, such as *GJA1*, *CEP120*, *NUP35* and *NEK9* (**Table 1**). Furthermore, DEGs in IVM-MII oocytes were primarily involved in biological

processes related to cell cycle, chromosome segregation and spindle organisation (**Table 2**).

Table 1. List of DEGs in GV POI-like versus GV CTRL oocytes

SYMBOL	log2FoldChange	pvalue	padj
HDDC2	1.279659615	4.9114E-05	0.02807903
DEUP1	1.132159598	0.00065535	0.09834173
ALDH7A1	0.787814629	1.285E-05	0.01818158
TCHP	0.780711083	5.1032E-05	0.02807903
FANK1	0.715156812	0.00014368	0.05473007
ATF7IP	0.638467535	0.00024013	0.0612655
FXR2	0.605151324	0.00027109	0.06466259
DCUN1D4	0.546778565	7.1766E-06	0.01776916
CEP120	0.520873457	0.0006123	0.09329492
CDCA7	0.505481275	0.00017774	0.05527177
GOSR1	0.494529525	7.9894E-05	0.03767933
EYA3	0.484029572	7.207E-05	0.03568923
CYB5B	0.42464097	0.00044496	0.08160961
CNOT10	0.393892433	0.0005079	0.08504353
BTBD9	0.361209825	0.00051521	0.08504353
DNAJB6	0.337136023	3.6188E-05	0.02362295
NUP35	0.329023505	0.00042455	0.08127918
STAM	-0.598259193	0.00026866	0.06466259
ZP3	-0.625430917	0.00046164	0.08304941
GRAMD1A	-0.656283479	0.00044138	0.08160961
PEG10	-0.697688584	0.0005356	0.08597631
ERCC2	-0.705635783	0.00046958	0.08304941
MGRN1	-0.737574908	0.00022797	0.0612655
GLRX	-0.757775133	3.3492E-05	0.02362295
NEK9	-0.775637174	3.8163E-05	0.02362295
ITGB4	-0.777774781	2.0401E-05	0.02244972
LPCAT1	-0.899747573	0.00042675	0.08127918
PRKCSH	-0.916179222	0.00028128	0.0647858
DHCR7	-0.944333266	0.00016584	0.05527177

SCAMP4	-0.962569951	0.00066711	0.09861305
ZMYM1	-0.969684353	0.00030763	0.0692443
GJA1	-1.037610869	2.8457E-05	0.02362295
CTSD	-1.03806735	1.4748E-05	0.01825754
SPRED1	-1.041964553	0.00042522	0.08127918
C1GALT1	-1.094780982	0.0001387	0.05473007
PDCD4	-1.100002618	0.00048362	0.0835201
SLC39A14	-1.201827221	0.00021552	0.0612655
AMDHD1	-1.226563163	1.2324E-06	0.00610306
CHD9	-1.269815328	0.00048911	0.0835201
DUSP1	-1.330554293	0.00016841	0.05527177
PIP5K1A	-1.331842234	0.00038977	0.08127918
E2F6	-1.354073565	0.00040439	0.08127918
MAP3K1	-1.359021234	0.0002127	0.0612655
GGCX	-1.397929083	3.3964E-05	0.02362295
SLC4A11	-1.430898346	0.00058178	0.09145979
CTH	-1.45847246	1.8132E-07	0.00179578
ADPGK	-1.516319362	0.00053822	0.08597631
FBXO11	-1.562897184	0.00011333	0.04816474
SPART	-1.621098713	0.00039992	0.08127918
TNN	-1.682831641	0.00024125	0.0612655
TMEM14A	-1.88217857	0.00017203	0.05527177
MACIR	-1.982187788	0.00032814	0.07221957
HERPUD1	-1.989981844	0.00023404	0.0612655
KCTD20	-2.009360651	2.2982E-05	0.02276101
SLC25A19	-2.025123589	5.4738E-06	0.01776916
TMED5	-2.11344858	6.8881E-05	0.03568923
STRA6	-2.154327835	0.00017858	0.05527177
SLC30A6	-2.246417143	3.2699E-05	0.02362295
C23H6orf62	-2.282316063	0.00010022	0.04511766
LIMS1	-2.298554441	0.00038651	0.08127918
PTP4A3	-2.49307743	0.0006041	0.09329492
INHBB	-2.528860728	1.244E-05	0.01818158
SLC33A1	-2.597701111	0.00027422	0.06466259
CCNF	-3.009066694	0.00011672	0.04816474
RMRP	-3.382965739	1.0815E-05	0.01818158

LRRC2	-3.561228816	0.00021926	0.0612655
ARMT1	-6.157723994	0.00016784	0.05527177

List of 67 genes found differentially expressed (DEGs) in the comparison between GV POI-like versus GV CTRL oocytes.

Table 2. List of DEGs in IVM-MIIs POI-like versus IVM-MII CTRL oocytes

SYMBOL	log2FoldChange	pvalue	padj
CEP83	0.820396737	3.6255E-05	0.02710136
MTUS1	0.780589393	8.5719E-05	0.02710136
CENPC	0.777649581	0.00097875	0.06876618
LAMC1	0.738843485	0.0018298	0.07563834
SBDS	0.695037455	0.00028446	0.04496908
CLIP1	0.683188083	5.5777E-05	0.02710136
ARID4A	0.67896374	0.00034849	0.05085272
BAZ1A	0.668497617	0.00107499	0.07031926
KIF11	0.643712321	0.00160887	0.07563834
MSANTD4	0.642525229	0.00693249	0.0968875
LARP7	0.639222357	0.00173969	0.07563834
SMARCAD1	0.635940213	0.0056023	0.09114424
APC	0.62892955	0.00451318	0.08923738
CEP57L1	0.62362901	0.00024137	0.04496908
EIF4G2	0.618447956	0.00696753	0.0968875
CASC4	0.616197743	0.00050144	0.05108729
NRDC	0.615105864	0.00186779	0.07563834
NEMF	0.608534052	0.00649453	0.0968875
SMC3	0.604934209	0.00021586	0.04496908
MAP4K5	0.594092682	0.00051168	0.05108729
CETN3	0.582039949	0.00233315	0.07642222
PHTF1	0.580485279	0.00094453	0.06876618
AGPS	0.578864736	0.00069957	0.05916259
KIF15	0.573097973	0.00207623	0.07642222
ORC2	0.569885663	0.0021481	0.07642222
PALB2	0.569420507	0.00167729	0.07563834
HMMR	0.56925836	0.0010506	0.07031926
ZNF181	0.567713709	0.00489619	0.08923738
SGO1	0.56647643	7.9476E-05	0.02710136
PKP4	0.561166928	3.8674E-05	0.02710136
CCDC88A	0.559458939	0.00718141	0.0968875
BRIX1	0.557342936	6.4644E-05	0.02710136

SAFB	0.556080245	0.00330141	0.08834848
UACA	0.55345391	0.00555	0.09114424
BAZ1B	0.55095891	0.00396261	0.08834848
ZCWPW1	0.549196466	0.00492849	0.08923738
CLSPN	0.547639047	0.00457286	0.08923738
CEP95	0.547185107	0.00311064	0.08677768
DSCC1	0.546956123	0.00440978	0.08923738
DDX10	0.545801945	0.00405555	0.08834848
SSX2IP	0.545351941	0.00521543	0.08923738
SPDL1	0.544738608	0.00683173	0.0968875
PSIP1	0.541324342	0.00455169	0.08923738
RPS6KA3	0.539884384	0.00177519	0.07563834
ATP8A1	0.539540104	0.00291796	0.08534564
DHX29	0.538654702	0.00187401	0.07563834
IFRD1	0.538346306	0.00724083	0.0968875
CFAP97	0.537280958	0.00024075	0.04496908
FNDC3B	0.532981673	0.00753515	0.0979053
CLK4	0.532348931	0.00462346	0.08923738
ZNF292	0.530809157	0.00504308	0.08923738
ZMYND11	0.530565004	0.00160118	0.07563834
SF3B1	0.530099371	0.00071731	0.05916259
NCAPG	0.529225346	0.0080737	0.09977068
RPAP2	0.527908626	0.00279444	0.08414362
KIF23	0.525321534	0.00298344	0.08575143
SYNE2	0.523199961	0.00292434	0.08534564
FANCD2	0.521567591	0.00330972	0.08834848
MFAP1	0.521513899	0.00338397	0.08834848
IK	0.520466118	0.0009006	0.06833774
KTN1	0.520008715	0.00817153	0.09977068
NSF	0.515786754	0.00445434	0.08923738
CSPP1	0.515516941	0.00487334	0.08923738
NASP	0.51359029	0.00345511	0.08834848
CDC5L	0.511714408	0.00043407	0.05108729
ESF1	0.511672465	0.0049887	0.08923738
NCL	0.511095637	0.00813229	0.09977068
KMT2E	0.507945411	0.0005084	0.05108729

POLA1	0.507775598	0.00027667	0.04496908
RBBP8	0.50364441	0.00385807	0.08834848
PPFIBP1	0.50336031	0.00409921	0.08834848
MRE11	0.501406774	0.00061637	0.05846302
CDC42BPA	0.497877666	0.00163136	0.07563834
AP3B1	0.497167825	0.00566949	0.09114424
WDHD1	0.494962815	0.00309963	0.08677768
CEP170	0.49395497	0.00146299	0.07563834
RSL1D1	0.490032291	0.00667532	0.0968875
ATAD5	0.488319546	0.00252754	0.07860222
FRA10AC1	0.484537336	0.00717783	0.0968875
FKBP5	0.483785465	0.00243117	0.07686536
KIF18A	0.483123288	0.00047273	0.05108729
GNAI1	0.482671757	0.00038719	0.05108729
VPS45	0.482276351	0.00521929	0.08923738
USP8	0.482226741	0.00378809	0.08834848
TRIP12	0.482086865	0.00224057	0.07642222
ARHGEF28	0.480098485	0.00330919	0.08834848
SSB	0.479517232	0.00433978	0.08923738
SREK1IP1	0.476594021	0.0037246	0.08834848
ADD3	0.476299919	0.00143816	0.07563834
PPWD1	0.475615893	0.00781798	0.09953501
NUDT9	0.471297509	0.00153946	0.07563834
ARFGEF1	0.471018049	0.00557425	0.09114424
KRIT1	0.469616962	0.00695216	0.0968875
BRD7	0.461400981	0.00162984	0.07563834
EPRS	0.46074893	0.00655699	0.0968875
MAPK8	0.460575041	0.00017314	0.04496908
IQCB1	0.455414039	0.00508722	0.08923738
KIF5B	0.454052808	0.00705777	0.0968875
SNW1	0.453030088	0.00697085	0.0968875
USO1	0.450074318	0.00556754	0.09114424
USP1	0.449876546	0.00533372	0.09033984
ERBIN	0.448831934	0.0049282	0.08923738
FAM169A	0.448217832	0.0008292	0.06554136
NFXL1	0.445872006	0.00131699	0.07563834

POLR3C	0.442155059	0.00388054	0.08834848
IDE	0.437991799	0.00185416	0.07563834
ADAM10	0.43469485	0.00666421	0.0968875
TDRD7	0.426195676	0.00237686	0.07642222
TTC9C	0.425457642	0.00388699	0.08834848
ZC2HC1A	0.424113731	0.0015306	0.07563834
XIAP	0.416376053	0.00790089	0.09977068
CIP2A	0.415680466	0.00662018	0.0968875
TANK	0.414072067	0.00366161	0.08834848
PRC1	0.410241759	0.00258574	0.07911526
CKAP5	0.406316622	0.00688744	0.0968875
SVIL	0.400270198	0.00405608	0.08834848
TAOK1	0.397859744	0.0070023	0.0968875
TMEM14C	0.394968016	0.00768716	0.09853074
NUP160	0.394771264	0.00225923	0.07642222
TAOK3	0.391542076	0.00500317	0.08923738
CHSY1	0.391485743	0.00595662	0.0949556
WDR48	0.390923457	0.0023445	0.07642222
SEC62	0.389856858	0.00795221	0.09977068
ITPRID2	0.389466296	0.00356011	0.08834848
MTF2	0.387820277	0.00493353	0.08923738
RB1CC1	0.385644497	0.00750356	0.0979053
MIA3	0.384009928	0.00619097	0.09626444
GOPC	0.381128184	0.00740749	0.09758343
PDXDC1	0.380542781	0.00171421	0.07563834
KNSTRN	0.379646984	0.00348035	0.08834848
CSDE1	0.378563212	0.00403812	0.08834848
SMARCA5	0.377707048	0.00610779	0.09575598
GKAP1	0.3772953	0.00820465	0.09977068
TARS1	0.373849899	0.00738057	0.09758343
LIN7C	0.373410445	0.00674321	0.0968875
SEH1L	0.367409099	0.00414497	0.08834848
SPAST	0.367024381	0.00371012	0.08834848
TBL1XR1	0.364838456	0.00226057	0.07642222
MORF4L2	0.36480643	0.00522159	0.08923738
MARCHF7	0.364365893	0.00477169	0.08923738

TAB2	0.357502264	0.00204804	0.07642222
ME1	0.346722023	0.00725252	0.0968875
RALGPS2	0.346172599	0.00768589	0.09853074
DR1	0.343793881	0.0056377	0.09114424
RPRD2	0.337087436	0.0022807	0.07642222
NOL10	0.33546611	0.00349682	0.08834848
SASS6	0.320854828	0.00816988	0.09977068
ATF2	0.308884928	0.00608141	0.09575598
ARNTL	0.30797382	0.0069674	0.0968875
OCLN	0.302625139	0.00470518	0.08923738
CNOT4	0.299753932	0.00212363	0.07642222
DRC7	-0.491187614	0.00201079	0.07642222
TUFM	-0.577447982	0.00518049	0.08923738
RPS5	-0.598185917	0.0069785	0.0968875
NOS2	-0.672962915	0.00067032	0.05916259
UNC119	-0.835487169	0.00174078	0.07563834

List of 156 genes found differentially expressed (DEGs) in the comparison between IVM-MIIs POI-like versus IVM-MII CTRL oocytes.

DISCUSSION

We identified changes in gene expression during the transition between GV and MII stages in oocytes from cows of 4-8 years old with normal reproductive physiology, mainly affecting genes related to reproductive system development, regulation of hormonal levels, mRNA processing and meiotic cell cycle, protein transport and localization. Interestingly, these results suggest a failure to properly achieve cytoplasmic maturation in POI-like bovine oocytes.

Gene expression in *in vitro* maturing bovine oocytes has already been investigated with different techniques, from pooled oocytes analysed with microarray (Fair et al., 2007; Mamo et al., 2011) to single oocytes sequenced with massive parallel sequencing (Reyes et al., 2015). Despite the technical differences, these studies consistently identified changes during the transition from GV to MII in the expression of genes involved in cell cycle regulation (MAPK activity), translation initiation, and transcription. In all reports, including ours, most transcripts are downregulated in MII oocytes, as are in other species including humans (Hendrickson et al., 2017; Reyes et al., 2017; Cornet-Bartolomé et al., 2021; Pietroforte et al., 2023), monkeys (Ruebel et al., 2021) and mice, showing a remarkably conserved feature of oocyte transcriptional control across mammals.

In spite of the overall consistent results, it is known that *in vitro* maturation affects the gene expression profiles, in processes related to metabolism and development (Adona et al., 2016), therefore the transcriptome remodelling in *in vivo* mature oocytes might differ.

Our study evaluates the whole transcriptome with massive parallel sequencing, while Reyes and colleagues focused on polyadenylated transcripts (Reyes et al., 2015). However, when comparing the results in terms of DEGs, we found 224 genes in common between the two studies, all related to cell cycle, spindle organisation and regulation of chromosome organisation, RNA degradation, progesterone-mediated oocyte maturation, and metabolism. These results support the hypothesis that the biological processes identified in both studies are robust and consistent, despite significant technical variations.

The comparison with a dataset previously generated in our laboratory on a set of 20 human oocytes (Pietroforte et al., 2023), collected and processed in the exact same way, allowed us to perform an accurate between-species comparison, and control for several

technical confounding factors such as the kits for library preparation and sequencing platform. We found in fact a high level of overlap between the genes that are differentially expressed between human young and CTRL bovine GV and MII oocytes, with RNA degradation, nucleo-cytoplasmic transport and oocyte meiosis being the most relevant biological processes. However, we also observed several differences, as most genes did not overlap, in agreement with another recent report (Schall & Latham, 2021).

Our findings in the POI-like cow model suggest that failure to execute a correct cytoplasmic maturation could cause the very low oocyte competence observed in these cows. We found few DEGs when comparing GV and MII POI-like oocytes, to the point that the only clustering we found was due to the cow background, something not observed in the control group and that highlights the lack of differences between developmental stages. When comparing the same developmental stage between CTRL and POI-like oocytes, we found DEGs in line with the hypothesis that POI-like oocytes fail to complete maturation, both nuclear and cytoplasmic. Comparing MII oocytes, we observed DEGs in pathways related to chromosome organization and spindle assembly. This is analogous to previous observations in *in vitro* matured MII oocytes from aged patients in different studies (Reyes et al., 2017; Llonch et al., 2021). In GV oocytes, on the contrary, we found differences in genes related to cumulus oocyte complex communication and microtubule organization, which is in contrast with the fewer to no differences between GV oocytes from aged and young women (Reyes et al., 2017).

This might suggest that POI-like cow oocytes share some common features with aged oocytes, but their maturation incompetence, not observed in aged oocytes, might be related to a more pervasive effect, perhaps reflecting altered follicular development at the time of oocyte growth and transcriptional activity.

This hypothesis is supported by previous reports characterising the cross talk between the follicle and the oocyte, mainly achieved through trans zonal projections transporting a plethora of signals and molecules required for growth and meiotic maturation, and critical for cytoplasmic maturation (Reyes et al., 2015; Lodde et al., 2021). In such model of poor quality oocytes over 50% of the gap junction are closed, compared to the normal condition, where the majority are open (Lodde et al., 2021). In addition, all the hormone receptors are present in cumulus cells, and the failure to communicate with the oocyte

could compromise the oocyte response to the correct hormonal signalling, which in turn would uncouple nuclear from cytoplasmic maturation.

In conclusion, our study provides clues for the possible mechanism of oocyte quality decrease in POI-like cows through impaired cytoplasmic maturation, providing a valuable animal model to study the human condition of POI.

Data availability

The data underlying this article are available on request from the authors.

Acknowledgements

We would like to thank the laboratory staff from EUGIN (Barcelona, Spain) for their help in sample handling and the IRB Barcelona Functional Genomics Core Facility (Barcelona, Spain) for the technical support.

Authors' roles

SP contributed to design the study, processed the samples, analysed and interpreted the data and drafted the manuscript; PD contributed to samples collection and data analysis; EI and MP revised the manuscript; AML contributed to design the study and to the interpretation of the data; VL and FF contributed to sample collection and to interpretation of the data; RV designed the study, contributed to the interpretation of the data and substantially revised the manuscript; FZ designed the study, analysed and interpreted the data and substantially revised the manuscript.

Funding

This project received intramural funding from the Eugin Group and funding from the European Union's Horizon 2020 research and innovation program under the Marie Skłodowska-Curie grant agreement No 860960.

Conflict of interest

The authors declare that they have no competing interests.

REFERENCES

Afgan, E., Nekrutenko, A., Grüning, B. A., Blankenberg, D., Goecks, J., Schatz, M. C., Ostrovsky, A. E., Mahmoud, A., Lonie, A. J., Syme, A., Fouilloux, A., Bretaudeau, A., Nekrutenko, A., Kumar, A., Eschenlauer, A. C., Desanto, A. D., Guerler, A., Serrano-Solano, B., Batut, B., … Briggs, P. J. (2022). The Galaxy platform for accessible, reproducible and collaborative biomedical analyses: 2022 update. *Nucleic Acids Research*, *50*(W1), W345–W351. https://doi.org/10.1093/NAR/GKAC247

Almansa-Ordonez, A., Bellido, R., Vassena, R., Barragan, M., & Zambelli, F. (2020). Oxidative stress in reproduction: A mitochondrial perspective. In *Biology* (Vol. 9, Issue 9, pp. 1–21). MDPI AG. https://doi.org/10.3390/biology9090269

Alviggi, C., Humaidan, P., Howles, C. M., Tredway, D., & Hillier, S. G. (2009). Biological versus chronological ovarian age: implications for assisted reproductive technology. *Reproductive Biology and Endocrinology : RB&E*, *7*, 101. https://doi.org/10.1186/1477-7827-7-101

Amoushahi, M., Salehnia, M., & Ghorbanmehr, N. (2018). The mitochondrial DNA copy number, cytochrome c oxidase activity and reactive oxygen species level in metaphase II oocytes obtained from in vitro culture of cryopreserved ovarian tissue in comparison with in vivo-obtained oocyte. *Journal of Obstetrics and Gynaecology Research*, *44*(10), 1937–1946. https://doi.org/10.1111/jog.13747

Ben-Meir, A., Burstein, E., Borrego-Alvarez, A., Chong, J., Wong, E., Yavorska, T., Naranian, T., Chi, M., Wang, Y., Bentov, Y., Alexis, J., Meriano, J., Sung, H. K., Gasser, D. L., Moley, K. H., Hekimi, S., Casper, R. F., & Jurisicova, A. (2015). Coenzyme Q10 restores oocyte mitochondrial function and fertility during reproductive aging. *Aging Cell*, *14*(5), 887–895. https://doi.org/10.1111/ACEL.12368

Blazquez, A., Guillén, J. J., Colomé, C., Coll, O., Vassena, R., & Vernaeve, V. (2014). Empty follicle syndrome prevalence and management in oocyte donors. *Human Reproduction (Oxford, England)*, *29*(10), 2221–2227. https://doi.org/10.1093/HUMREP/DEU203

Broekmans, F. J., Soules, M. R., & Fauser, B. C. (2009). Ovarian aging: Mechanisms and clinical consequences. *Endocrine Reviews*, *30*(5), 465–493. https://doi.org/10.1210/er.2009-0006

Cagnone, G. L. M., Tsai, T. S., Makanji, Y., Matthews, P., Gould, J., Bonkowski, M. S., Elgass, K. D., Wong, A. S. A., Wu, L. E., McKenzie, M., Sinclair, D. A., & John, J. C. S. (2016). Restoration of normal embryogenesis by mitochondrial supplementation in pig oocytes exhibiting mitochondrial DNA deficiency. *Scientific Reports*, *6*. https://doi.org/10.1038/SREP23229

Cimadomo, D., Fabozzi, G., Vaiarelli, A., Ubaldi, N., Ubaldi, F. M., & Rienzi, L. (2018). Impact of Maternal Age on Oocyte and Embryo Competence. *Frontiers in Endocrinology*, *9*(JUL), 1. https://doi.org/10.3389/FENDO.2018.00327

Cornet-Bartolomé, D., Barragán, M., Zambelli, F., Ferrer-Vaquer, A., Tiscornia, G., Balcells, S., Rodriguez, A., Grinberg, D., & Vassena, R. (2021). Human oocyte meiotic maturation is associated with a specific profile of alternatively spliced transcript isoforms. *Molecular Reproduction and Development*, *88*(9), 605–617. https://doi.org/10.1002/MRD.23526

De Vos, M., Devroey, P., & Fauser, B. C. (2010). Primary ovarian insufficiency. *Lancet (London, England)*, *376*(9744), 911–921. https://doi.org/10.1016/S0140-6736(10)60355-8

Fair, T., Carter, F., Park, S., Evans, A. C. O., & Lonergan, P. (2007). Global gene expression analysis during bovine oocyte in vitro maturation. *Theriogenology*, *68 Suppl 1*(SUPPL. 1). https://doi.org/10.1016/J.THERIOGENOLOGY.2007.04.018

Heikal, A. A. (2010). Intracellular coenzymes as natural biomarkers for metabolic activities and mitochondrial anomalies. *Biomarkers in Medicine*, *4*(2), 241–263. https://doi.org/10.2217/BMM.10.1

Hendrickson, P. G., Doráis, J. A., Grow, E. J., Whiddon, J. L., Lim, J. W., Wike, C. L., Weaver, B. D., Pflueger, C., Emery, B. R., Wilcox, A. L., Nix, D. A., Peterson, C. M., Tapscott, S. J., Carrell, D. T., & Cairns, B. R. (2017). Conserved roles of mouse DUX and human DUX4 in activating cleavage-stage genes and MERVL/HERVL retrotransposons. *Nature Genetics*, *49*(6), 925–934. https://doi.org/10.1038/NG.3844

Kirillova, A., Smitz, J. E. J., Sukhikh, G. T., & Mazunin, I. (2021). The Role of Mitochondria in Oocyte Maturation. *Cells*, *10*(9). https://doi.org/10.3390/CELLS10092484

Klaidman, L. K., Leung, A. C., & Adams, J. D. (1995). High-performance liquid chromatography analysis of oxidized and reduced pyridine dinucleotides in specific brain regions. *Analytical Biochemistry*, *228*(2), 312–317. https://doi.org/10.1006/ABIO.1995.1356

Krisher, R. L., Brad, A. M., Herrick, J. R., Sparman, M. L., & Swain, J. E. (2007). A comparative analysis of metabolism and viability in porcine oocytes during in vitro maturation. *Animal Reproduction Science*, *98*(1–2), 72–96. https://doi.org/10.1016/J.ANIREPROSCI.2006.10.006

Lawrence, M., Huber, W., Pagès, H., Aboyoun, P., Carlson, M., Gentleman, R., Morgan, M. T., & Carey, V. J. (2013). Software for computing and annotating genomic ranges. *PLoS Computational Biology*, *9*(8). https://doi.org/10.1371/JOURNAL.PCBI.1003118

Leese, H. J., Brison, D. R., & Sturmey, R. G. (2022). The Quiet Embryo Hypothesis: 20 years on. *Frontiers in Physiology*, *13*. https://doi.org/10.3389/FPHYS.2022.899485

Liao, Y., Wang, J., Jaehnig, E. J., Shi, Z., & Zhang, B. (2019). WebGestalt 2019: gene set analysis toolkit with revamped UIs and APIs. *Nucleic Acids Research*, *47*(W1), W199–W205. https://doi.org/10.1093/NAR/GKZ401

Llonch, S., Barragán, M., Nieto, P., Mallol, A., Elosua-Bayes, M., Lorden, P., Ruiz, S., Zambelli, F., Heyn, H., Vassena, R., & Payer, B. (2021). Single human oocyte transcriptome analysis reveals distinct maturation stage-dependent pathways impacted by age. *Aging Cell*, *20*(5). https://doi.org/10.1111/ACEL.13360

Lodde, V., Luciano, A. M., Musmeci, G., Miclea, I., Tessaro, I., Aru, M., Albertini, D. F., & Franciosi, F. (2021). A Nuclear and Cytoplasmic Characterization of Bovine Oocytes Reveals That Cysteamine Partially Rescues the Embryo Development in a Model of Low Ovarian Reserve. *Animals : An Open Access Journal from MDPI*, *11*(7). https://doi.org/10.3390/ANI11071936

Love, M. I., Huber, W., & Anders, S. (2014). Moderated estimation of fold change and dispersion for RNA-seq data with DESeq2. *Genome Biology*, *15*(12). https://doi.org/10.1186/S13059-014-0550-8

Luciano, A. M., Franciosi, F., Lodde, V., Tessaro, I., Corbani, D., Modina, S. C., & Peluso, J. J. (2013). Oocytes isolated from dairy cows with reduced ovarian reserve have a high frequency of aneuploidy and alterations in the localization of progesterone receptor membrane component 1 and aurora kinase B. *Biology of Reproduction*, *88*(3). https://doi.org/10.1095/BIOLREPROD.112.106856

Malhi, P. S., Adams, G. P., & Singh, J. (2005). Bovine model for the study of reproductive aging in women: follicular, luteal, and endocrine characteristics. *Biology of Reproduction*, *73*(1), 45–53. https://doi.org/10.1095/BIOLREPROD.104.038745

Mamo, S., Carter, F., Lonergan, P., Leal, C. L., Al Naib, A., Mcgettigan, P., Mehta, J. P., Co Evans, A., & Fair, T. (2011). *Sequential analysis of global gene expression profiles in immature and in vitro matured bovine oocytes: potential molecular markers of oocyte maturation*. https://doi.org/10.1186/1471-2164-12-151

Marchant, J. S., Ramos, V., & Parker, I. (2002). Structural and functional relationships between Ca2+ puffs and mitochondria in Xenopus oocytes. *American Journal of Physiology. Cell Physiology*, *282*(6). https://doi.org/10.1152/AJPCELL.00446.2001

Martín-Romero, F. J., Miguel-Lasobras, E. M., Domínguez-Arroyo, J. A., Gonzélez-Carrera, E., & Álvarez, I. S. (2008). Contribution of culture media to oxidative stress and its effect on human oocytes. *Reproductive BioMedicine Online*, *17*(5), 652–661. https://doi.org/10.1016/S1472-6483(10)60312-4

McGlacken-Byrne, S. M., & Conway, G. S. (2022). Premature ovarian insufficiency. *Best Practice & Research. Clinical Obstetrics & Gynaecology*, *81*, 98–110. https://doi.org/10.1016/J.BPOBGYN.2021.09.011

McLennan, H. J., Saini, A., Dunning, K. R., & Thompson, J. G. (2020). Oocyte and embryo evaluation by AI and multi-spectral auto-fluorescence imaging: Livestock

embryology needs to catch-up to clinical practice. *Theriogenology*, *150*, 255–262. https://doi.org/10.1016/J.THERIOGENOLOGY.2020.01.061

Muller, B., Lewis, N., Adeniyi, T., Leese, H. J., Brison, D. R., & Sturmey, R. G. (2019). Application of extracellular flux analysis for determining mitochondrial function in mammalian oocytes and early embryos. *Scientific Reports 2019 9:1*, *9*(1), 1–14. https://doi.org/10.1038/s41598-019-53066-9

Nelson, L. M. (2009). Clinical practice. Primary ovarian insufficiency. *The New England Journal of Medicine*, *360*(6), 606–614. https://doi.org/10.1056/NEJMCP0808697

Nicholls, D. G. (2002). Mitochondrial function and dysfunction in the cell: Its relevance to aging and aging-related disease. *International Journal of Biochemistry and Cell Biology*, *34*(11), 1372–1381. https://doi.org/10.1016/S1357-2725(02)00077-8

Pasquariello, R., Ermisch, A. F., Silva, E., McCormick, S., Logsdon, D., Barfield, J. P., Schoolcraft, W. B., & Krisher, R. L. (2019). Alterations in oocyte mitochondrial number and function are related to spindle defects and occur with maternal aging in mice and humans†. *Biology of Reproduction*, *100*(4), 971–981. https://doi.org/10.1093/BIOLRE/IOY248

Pietroforte, S., Monasterio, M. B., Ferrer-Vaquer, A., Irimia, M., Ibáñez, E., Popovic, M., Vassena, R., & Zambelli, F. (2023). Specific processing of meiosis-related transcript is linked to final maturation in human oocytes. *Molecular Human Reproduction*. https://doi.org/10.1093/MOLEHR/GAAD021

Qi, L., Chen, X., Wang, J., Lv, B., Zhang, J., Ni, B., & Xue, Z. (2019). Mitochondria: the panacea to improve oocyte quality? *Annals of Translational Medicine*, *7*(23), 789–789. https://doi.org/10.21037/ATM.2019.12.02

Reyes, J. M., Chitwood, J. L., & Ross, P. J. (2015). RNA-Seq profiling of single bovine oocyte transcript abundance and its modulation by cytoplasmic polyadenylation. *Molecular Reproduction and Development*, *82*(2), 103–114. https://doi.org/10.1002/MRD.22445

Reyes, J. M., Silva, E., Chitwood, J. L., Schoolcraft, W. B., Krisher, R. L., & Ross, P. J. (2017). Differing molecular response of young and advanced maternal age human oocytes to IVM. *Human Reproduction (Oxford, England)*, *32*(11), 2199–2208. https://doi.org/10.1093/HUMREP/DEX284

Ruebel, M. L., Zambelli, F., Schall, P. Z., Barragan, M., Vandevoort, C. A., Vassena, R., & Latham, K. E. (2021). Shared aspects of mRNA expression associated with oocyte maturation failure in humans and rhesus monkeys indicating compromised oocyte quality. *Physiological Genomics*, *53*(4), 137–149. https://doi.org/10.1152/PHYSIOLGENOMICS.00155.2020

Sanchez, T., Venturas, M., Aghvami, S. A., Yang, X., Fraden, S., Sakkas, D., & Needleman, D. J. (2019). Combined noninvasive metabolic and spindle imaging as

potential tools for embryo and oocyte assessment. *Human Reproduction (Oxford, England)*, *34*(12), 2349–2361. https://doi.org/10.1093/HUMREP/DEZ210

Sanchez, T., Zhang, M., Needleman, D., & Seli, E. (2019). Metabolic imaging via fluorescence lifetime imaging microscopy for egg and embryo assessment. *Fertility and Sterility*, *111*(2), 212–218. https://doi.org/10.1016/j.fertnstert.2018.12.014

Schall, P. Z., & Latham, K. E. (2021a). Cross-species meta-analysis of transcriptome changes during the morula-to-blastocyst transition: metabolic and physiological changes take center stage. *American Journal of Physiology. Cell Physiology*, *321*(6), C913–C931. https://doi.org/10.1152/AJPCELL.00318.2021

Schall, P. Z., & Latham, K. E. (2021b). Cross-species meta-analysis of transcriptome changes during the morula-to-blastocyst transition: metabolic and physiological changes take center stage. *American Journal of Physiology. Cell Physiology*, *321*(6), C913–C931. https://doi.org/10.1152/AJPCELL.00318.2021

Schneider, C. A., Rasband, W. S., & Eliceiri, K. W. (2012). NIH Image to ImageJ: 25 years of image analysis. *Nature Methods*, *9*(7), 671–675. https://doi.org/10.1038/NMETH.2089

Seidler, E. A., Sanchez, T., Venturas, M., Sakkas, D., & Needleman, D. J. (2020). Non-invasive imaging of mouse embryo metabolism in response to induced hypoxia. *Journal of Assisted Reproduction and Genetics*, *37*(8), 1797–1805. https://doi.org/10.1007/s10815-020-01872-w

Shah, J. S., Venturas, M., Sanchez, T. H., Penzias, A. S., Needleman, D. J., & Sakkas, D. (2022). Fluorescence lifetime imaging microscopy (FLIM) detects differences in metabolic signatures between euploid and aneuploid human blastocysts. *Human Reproduction*, *37*(3), 400–410. https://doi.org/10.1093/humrep/deac016

Shestakova, I. G., Radzinsky, V. E., & Khamoshina, M. B. (2016). Occult form of premature ovarian insufficiency. *Gynecological Endocrinology*, *32*, 30–32. https://doi.org/10.1080/09513590.2016.1232676

Szklarczyk, D., Gable, A. L., Lyon, D., Junge, A., Wyder, S., Huerta-Cepas, J., Simonovic, M., Doncheva, N. T., Morris, J. H., Bork, P., Jensen, L. J., & Von Mering, C. (2019). STRING v11: protein-protein association networks with increased coverage, supporting functional discovery in genome-wide experimental datasets. *Nucleic Acids Research*, *47*(D1), D607–D613. https://doi.org/10.1093/NAR/GKY1131

Tan, T. C. Y., Brown, H. M., Thompson, J. G., Mustafa, S., & Dunning, K. R. (2022). Optical imaging detects metabolic signatures associated with oocyte quality†. *Biology of Reproduction*, *107*(4), 1014–1025. https://doi.org/10.1093/BIOLRE/IOAC145

Tan, T. C. Y., Mahbub, S. B., Campbell, J. M., Habibalahi, A., Campugan, C. A., Rose, R. D., Chow, D. J. X., Mustafa, S., Goldys, E. M., & Dunning, K. R. (2021). Non-invasive, label-free optical analysis to detect aneuploidy within the inner cell mass of the

preimplantation embryo. *Human Reproduction (Oxford, England)*, *37*(1), 14–29. https://doi.org/10.1093/HUMREP/DEAB233

Truong, T., & Gardner, D. K. (2017). Antioxidants improve IVF outcome and subsequent embryo development in the mouse. *Human Reproduction (Oxford, England)*, *32*(12), 2404–2413. https://doi.org/10.1093/HUMREP/DEX330

van der Reest, J., Nardini Cecchino, G., Haigis, M. C., & Kordowitzki, P. (2021). Mitochondria: Their relevance during oocyte ageing. *Ageing Research Reviews*, *70*. https://doi.org/10.1016/J.ARR.2021.101378

Venturas, M., Shah, J. S., Yang, X., Sanchez, T. H., Conway, W., Sakkas, D., & Needleman, D. J. (2022). Metabolic state of human blastocysts measured by fluorescence lifetime imaging microscopy. *Human Reproduction*, *37*(3), 411–427. https://doi.org/10.1093/humrep/deab283

Venturas, M., Yang, X., Sakkas, D., & Needleman, D. (2023). Noninvasive metabolic profiling of cumulus cells, oocytes, and embryos via fluorescence lifetime imaging microscopy: a mini-review. *Human Reproduction (Oxford, England)*, *38*(5), 799–810. https://doi.org/10.1093/humrep/dead063

Wakai, T., & Fissore, R. A. (2019). Constitutive IP3R1-mediated Ca2+ release reduces Ca2+ store content and stimulates mitochondrial metabolism in mouse GV oocytes. *Journal of Cell Science*, *132*(3). https://doi.org/10.1242/JCS.225441

Wartosch, L., Schindler, K., Schuh, M., Gruhn, J. R., Hoffmann, E. R., McCoy, R. C., & Xing, J. (2021). Origins and mechanisms leading to aneuploidy in human eggs. *Prenatal Diagnosis*, *41*(5), 620–630. https://doi.org/10.1002/PD.5927

Wilding, M., Dale, B., Marino, M., Di Matteo, L., Alviggi, C., Pisaturo, M. L., Lombardi, L., & De Placido, G. (2001). Mitochondrial aggregation patterns and activity in human oocytes and preimplantation embryos. *Human Reproduction (Oxford, England)*, *16*(5), 909–917. https://doi.org/10.1093/HUMREP/16.5.909

Yang, X., Ha, G., & Needleman, D. J. (2021). A coarse-grained NADH redox model enables inference of subcellular metabolic fluxes from fluorescence lifetime imaging. *ELife*, *10*. https://doi.org/10.7554/ELIFE.73808

Zander-Fox, D. L., Fullston, T., McPherson, N. O., Sandeman, L., Kang, W. X., Good, S. B., Spillane, M., & Lane, M. (2015). Reduction of mitochondrial function by FCCP during mouse cleavage stage embryo culture reduces birth weight and impairs the metabolic health of offspring. *Biology of Reproduction*, *92*(5), 124–125. https://doi.org/10.1095/BIOLREPROD.114.123489/2434066

Zeng, H. tao, Yeung, W. S. B., Cheung, M. P. L., Ho, P. C., Lee, C. K. F., Zhuang, G. lun, Liang, X. yan, & O, W. S. (2009). In vitro–matured rat oocytes have low mitochondrial deoxyribonucleic acid and adenosine triphosphate contents and have abnormal mitochondrial redistribution. *Fertility and Sterility*, *91*(3), 900–907. https://doi.org/10.1016/J.FERTNSTERT.2007.12.008

SUPPLEMENTARY INFORMATION CONTENTS:

- **Supplementary Table S1.** Sample table.
- **Supplementary Table S2.** Differentially expressed genes in IVM-MII vs GV in CTRL group.
- **Supplementary Table S3.** Differentially expressed genes in IVM-MII vs GV in POI-like group.
- **Supplementary Figure S1.** Network interactions of DEGs through meiosis identified in Human-Cow cross-species comparison.

Supplementary Table S1. Sample table.

Cow ID	Ovary size (A;B) cm	AFC (A+B)	n. COC	GV ID	IVM-MII ID	Group
1	2.5;3.5	4;4	6	BOV 16	BOV 25	POI-like
2	2.5;3	6;9	14	BOV 18	BOV 27	POI-like
3	3;3.5	4;4	7	BOV 19	BOV 30	POI-like
4	5;3.5	25;17	24	BOV 21	BOV 32	CTRL
5	6;6	27;23	21	BOV 23	BOV 34	CTRL
6	5;3.5	43;28	40	BOV 38	BOV 45	CTRL
7	4;4.5	23;17	20	BOV 39	BOV 47	CTRL
8	3.5;4.5	27;23	30	BOV 40	BOV 48	CTRL
9	4;3.5	5;4	6	BOV 53	BOV 60	POI-like
10	2.5;3	5;6	6	BOV 54	BOV 61	POI-like

List of the collected oocytes from ten cows, five in the CTRL group and five in the POI-like group, divided per maturation stage, GV and IVM-MII. Ovary size (right, A, and left, B), Antral Follicle Count (AFC; right, A, and left, B) and number of the retrieved cumulus-oocytes complex (COC) are reported.

Supplementary Table S2-S3 are large Excel files, data available on request from the authors.

Supplementary Figure S1.

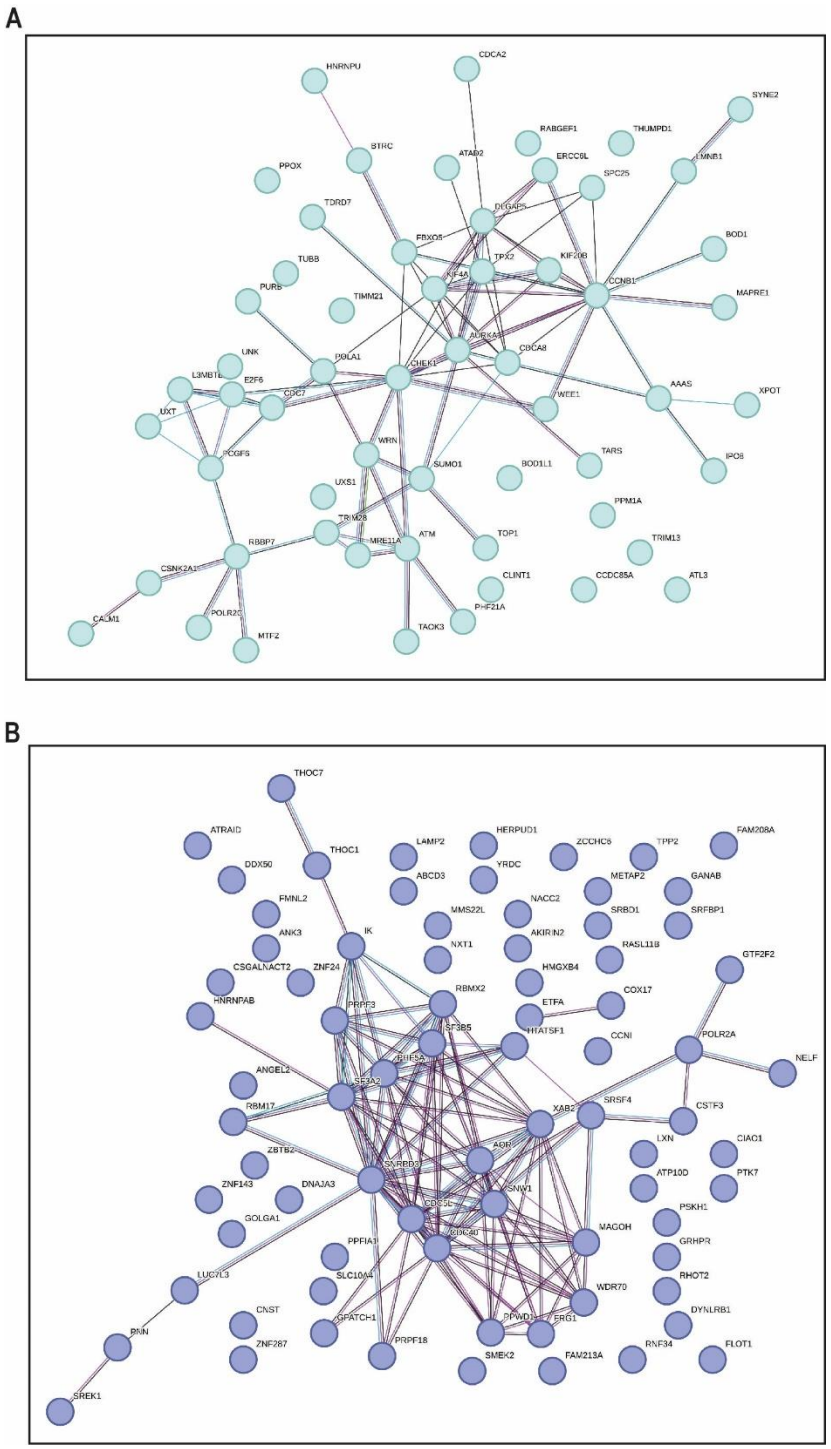

Figure S1. Network interactions of DEGs through meiosis identified in Human-Cow cross-species comparison. STRING database graphical representation of the interactions between DEGs through meiotic maturation and conserved between human and cow. These DEGs are involved in (**A**) cell cycle, meiosis, and sister chromatid segregation, and (**B**) in mRNA processing, transport, and degradation. The different protein-protein interactions are marked with different lines: known interactions from curated databases (light blue) and experimentally determined (pink); predicted interaction by gene neighbourhood (green), gene fusion (red) and gene co-occurrence (dark blue).

3. METABOLIC DYNAMICS DURING HUMAN MEIOSIS AND CHANGES OCCURING WITH AGE

Title: Mitochondrial metabolism influences the capacity to progress through meiotic maturation in human oocytes of young and advanced maternal age women

Authors: Sara Pietroforte[1,2,3], Marion Martins[3], Elena Ibañez[2], Tim Sanchez[4], Rita Vassena[1], Mina Popovic[1], Denny Sakkas[3], Filippo Zambelli[1]

Affiliations:

1 - Research and Development, Eugin Group, Barcelona, Spain

2 - Department of Cell Biology, Physiology and Immunology, Universitat Autonoma de Barcelona, Bellaterra, Barcelona, Spain

3 - Boston IVF – Eugin Group, Waltham, MA, USA

4 - OPTIVA, Boston, MA, USA

ABSTRACT

Advanced maternal age (AMA) oocytes are characterized by poor quality, mostly due to the higher rates of chromosomal segregation errors occurring during meiosis I. Another hallmark of AMA oocytes is an impaired mitochondrial metabolism. Studies in mice have suggested a link between metabolic dysfunction and meiotic failure, but this relationship has not been fully dissected in humans. Here, we explored mitochondrial distribution and activity in oocytes at the germinal vesicle (GV) and metaphase II (MII) stages using high resolution microscopy and revealed that active mitochondria are specifically localized in the subcortex, although mitochondria in general are distributed across the whole oocyte. This pattern was lost in AMA oocytes, which were also characterized by low mitochondrial activity compared to the young group (intensity of 78614±58534 AU in young, 12517±10187 AU in AMA, p=0.003), while no differences in terms of total mitochondria abundance were observed (intensity of 61674±24322 AU in young, 32186±33414 AU in AMA, p=0.195). Using non-invasive Fluorescence Lifetime Imaging Microscopy (FLIM) we assessed the metabolic dynamics of maturing oocytes and confirmed the same pattern observed by immunofluorescence (Redox ratio in young 2e+00±0.15, in AMA 1e+00 ± 0.16, p=2.969e-05). Moreover, young oocytes matured at a significantly higher rate (86.3%; 63/73) than AMA oocytes (62.3%; 38/61; p=0.002).

FLIM imaging revealed that young GV oocytes increased their metabolism by 4% on average after the germinal vesicle break down, whereas in AMA maturing oocytes little to no increase was observed. Furthermore, we compared the metabolic profile of maturing young versus AMA oocytes and observed higher variability among samples in the AMA group, that was also much higher in the AMA oocytes unable to successfully reach MII stage. The impairment of metabolic activity in young oocytes reveal the functional link between adequate metabolic levels and successful meiosis progression. Overall, we show a functional link between mitochondrial metabolism and meiosis progression, contributing to explain the biological mechanisms driving oocyte quality decay in oocytes from advanced maternal age women.

Keywords: mitochondria, mitochondrial activity, mitochondrial metabolism, advanced maternal age, oocyte maturation, oocyte competence, live imaging, non-invasive technique

INTRODUCTION

The role of mitochondrial metabolism during final oocyte maturation has so far been somewhat controversial. Recent studies have found that oocytes with low developmental competence showed compromised mitochondrial activity (Kirillova et al., 2021), and that mitochondrial function is key for meiotic progression (Krisher et al., 2007; Amoushahi et al., 2018). Specifically, mitochondrial function is vital for cytoplasmic calcium regulation (Marchant et al., 2002; Nicholls, 2002; Tiwari et al., 2017; Wang et al., 2018; Wakai & Fissore, 2019), reactive oxygen species (ROS) production and scavenging, intracellular redox potential regulation, and spindle formation during cell division (Liu et al., 2016).

In humans, the final steps of meiotic maturation are triggered by a luteinizing hormone surge, which leads to germinal vesicle breakdown (GVBD) and chromosome condensation. After GVBD, the oocyte progresses through the Metaphase I (MI) stage and completes meiosis I by extruding the polar body and goes on to reach the Metaphase II (MII) stage, ready for fertilisation. Boosting mitochondrial function by supplementing the culture media with antioxidant could lead to an improved maturation rate, and better embryo development (Martín-Romero et al., 2008; Truong & Gardner, 2017; Pasquariello et al., 2019). Accordingly, supplementation of pig oocytes with an autologous population of mitochondrial isolate at fertilization resulted in increased blastocyst rates and an increase in mitochondrial DNA replication prior to embryonic genome activation (Cagnone et al., 2016). Co-enzyme Q10 (CoQ10) was also used to improve mitochondrial function in oocytes and could represent an alternative for increasing oocyte quality especially in advanced maternal age (AMA) women (Ben-Meir et al., 2015; Qi et al., 2019). Most studies so far have focused on the detoxification of cells from excessive amounts of ROS, rather than on evaluating the role of mitochondria and oxidative phosphorylation (OXPHOS) during oocyte growth. Whether oocyte aerobic metabolism changes during oocyte maturation, and to what extent it may affect meiosis progression remains to be explored, and studies on the impairment of metabolic activity to prove its direct involvement in meiotic progression are lacking.

Mitochondrial dysfunction is one of the main features of AMA oocytes, where different studies found a significant decrease in membrane polarization and mtDNA copy number (Pasquariello et al., 2019). The concomitant presence in such oocytes of a decrease in mitochondrial metabolism (van der Reest et al., 2021) and a high level of aneuploidies

(Ma et al., 2020), mostly happening during meiosis I (Wartosch et al., 2021), point toward a possible functional link between the two phenomena, but direct evidence in human oocytes of a direct role of mitochondria in supporting meiotic progression are lacking.

Nicotinamide adenine dinucleotide (NADH), nicotinamide adenine phosphate dinucleotide (NADPH) and flavin adenine dinucleotide (FAD+) are naturally fluorescent metabolic coenzymes (Heikal, 2010). These are electron carriers that have essential roles in the electron transport chain and glycolysis (Chance and Williams, 1995), and are therefore biomarkers of a cell's metabolic state (Klaidman et al., 1995; McLennan et al., 2020; Tan et al., 2021, 2022). The fluorescence *spectra* of NADH and NADPH are almost indistinguishable (Sanchez et al., 2019; Zhang, et al., 2019) and therefore the combined fluorescence of NADH and NADPH is often referred to as the NAD(P)H signal. Fluorescence lifetime imaging microscopy (FLIM) of NAD(P)H and FAD+ provides a means to measure the fluorescence intensity and fluorescence lifetime of these molecules (Sanchez et al., 2019a; Venturas, et al., 2019; Sanchez et al., 2019b; Zhang, et al., 2019; Seidler et al., 2020; Shah et al., 2022; Tan et al., 2021; Tan et al., 2022; Venturas et al., 2022; Venturas et al., 2023). The fluorescence intensity is related to the concentrations of the coenzymes, whereas the fluorescence lifetime depends on the local environment of the coenzymes, varying drastically according to whether the coenzymes are bound to an enzyme or free (Sanchez et al., 2019; Zhang, et al., 2019; Shah et al., 2022; Venturas et al., 2022). Using FLIM, is it possible to generate timelapse profiling of the metabolic state of cumulus cells (Venturas et al., 2022) oocytes (Sanchez et al., 2019; Zhang, et al., 2019; Shah et al., 2022; Venturas et al., 2022) and embryos (Sanchez et al., 2019a; Venturas, et al., 2019; Sanchez et al., 2019b; Zhang, et al., 2019; Seidler et al., 2020; Shah et al., 2022; Venturas et al., 2022; Venturas et al., 2023) without additional markers or dyes. Moreover, FLIM generates three parameters (fraction bound, long and short lifetime) that are sensitive to metabolic shifts for NADH and FAD+.

Recent studies in mice (Sanchez et al., 2019a; Venturas, et al., 2019; Sanchez et al., 2019b; Zhang, et al., 2019; Seidler et al., 2020; Yang et al., 2021) have shown that metabolic imaging is a valuable method for measuring live metabolism in both oocytes and embryos. FLIM was successfully used to distinguish the metabolic state of young and aged mouse oocytes (Sanchez et al., 2019a; Venturas, et al., 2019; Sanchez et al., 2019b; Zhang, et al., 2019). Furthermore, the ability to distinguish mitochondrial metabolism and

positioning of the germinal vesicle (GV) through oocyte's progression to MII will provide valuable insights on their metabolic needs during this critical phase.

In the present study, we evaluated the metabolic changes during the final meiotic maturation stages of human oocyte. Moreover, we assessed the association between mitochondrial metabolism and the ability to complete the meiotic maturation, and the changes occurring to metabolic regulation in oocytes from AMA women.

MATERIALS AND METHODS

Ethical approval

Approval to conduct this study was obtained from the Ethics Committee for Clinical Research (CEIm) of Clinica Eugin and all research was performed in accordance with relevant guidelines and regulations. At Boston IVF the study was approved by the Beth Israel Deacon and was conducted under an institutional review board approval. All women participating in this study gave their written informed consent prior to inclusion.

Study population

Sixty-five women undergoing clinical procedures at BostonIVF (Eugin Group, Waltham, MA, USA) from the beginning of February to the end of March 2022 and 110 women at Eugin (Eugin Group, Barcelona, Spain) were enrolled in the study. Eighty oocytes were used for mitochondrial proteins imaging, 22 oocytes for live staining, 171 oocytes for live imaging, and 89 oocytes for the loss of function study.

Ovarian stimulation, oocyte retrieval and *in vitro* maturation

Women enrolled were stimulated with highly purified urinary human menopausal gonadotrophin (hMG; Menopur®, Ferring, Saint-Prex, Switzerland) or follitropin alpha (Gonal®, Merck Serono, Darmstadt, Germany), with daily injections of 150 to 300 IU (Blazquez et al., 2014). Gonadotropin hormone-releasing hormone (GnRH) antagonist (0.25 mg of cetrorelix acetate, Cetrotide®; Merck Serono, Darmstadt, Germany; or 0.25 mg of ganirelix, Orgalutran®; Merck Sharp & Dohme, Kenilworth, New Jersey, USA) was administered daily for pituitary suppression (Oliviennes et al., 1995) from day 6 of ovarian stimulation. Ovulation was triggered with 0.2 mg of the GnRH agonist triptorelin (Decapeptyl®; Ipsen Pharma, Paris, France) when three or more follicles of ≥18 mm of diameter on both ovaries were observed by transvaginal ultrasound.

The oocytes were retrieved 36 h after trigger by ultrasound-guided transvaginal follicular aspiration.

Sample preparation

Oocytes were denuded in a Hyaluronidase solution (80 IU/ml) (Hyase-10x, Vitrolife, Gothenburg, Sweden) in G-MOPS (Vitrolife, Gothenburg, Sweden) with the aid of manual pipetting and scored. Immature oocytes with a visible GV were *in vitro* matured either in a conventional incubator in a humidified atmosphere of 6% CO_2 at 37°C or in Micro well group culture dish, 9 well (Vitrolife, Gothenburg, Sweden) in 30 µL of G2-plus media (Vitrolife, Gothenburg, Sweden) covered with oil (Oil for Embyo Culture, FUJIFILM Irvine Scientific, Santa Ana, California, USA) in a small chamber in a humidified atmosphere of 6% CO_2 at 37°C for 30 h under the microscope. After *in vitro* maturation, the oocytes were classified as successfully *in vitro* matured MII oocytes (IVM-MII) if the first polar body was visible, whereas if the GV was still present, the oocyte was classified as GV that failed to mature, retaining the germinal vesicle (FTM-GV). If the oocyte underwent germinal vesicle breakdown (GVBD) without extruding the first polar body, it was classified as MI stage.

Metabolic imaging by Fluorescence Lifetime Imaging Microscope analysis

FLIM measurements were performed with a Nikon Eclipse Ti microscope using two-photon excitation from a Ti:Sapphire pulsed laser (Mai-Tai, Spectral-Physics). Imaging was performed with a 40X Nikon objective with 0.2 numerical aperture. Each NAD(P)H and FAD+ FLIM image was acquired within 60 seconds of integration time. Objective piezo stage and motorized stage were used to perform multidimensional acquisition. Three images were acquired per stack on x, y and z axis. A histogram of the fluorescence decay of NAD(P)H and FAD+ was then created. Specifically, eight parameters were measured: short and long lifetimes and the fraction of engaged molecules, for both NAD(P)H and FAD+. In addition, we computed NAD(P)H intensity, FAD+ intensity and redox ratio, providing a total of nine quantitative metabolic parameters.

Mitochondrial imaging

Oocytes for immunofluorescence analysis were fixed in 4% paraformaldehyde (PFA) for 15 min at 37ºC. The proteins Dihydrolipoamide S-Acetyltransferase (D-LAT, 1:100, ab110333; secondary antibody anti-Mouse AlexaFluor488, 1:500) and Translocase of

outer mitochondrial membrane (TOMM20, 1:100, ab186734; secondary antibody anti-Rabbit AlexaFluor568, 1:500) were analysed by immunofluorescence in oocytes at different maturation stages to assess mitochondrial activity and localization, respectively. The 80 stained oocytes were imaged by Dragonfly spinning disk confocal microscope with a 60X oil objective. Fluorescent mean intensities were quantified with ImageJ software (Schneideret al., 2012) and compared by t-test. For D-LAT, we assessed an area of approximately 30 µm inward from the oocyte cortex, while for TOMM20, the whole oocyte diameter was used.

Mitochondrial membrane potential evaluation

The fluorescent dye JC-1 (Calbiochem, USA) was used as a live ratio metric indicator of ΔΨm (Wilding et al., 2001). For the experiment, we prepared a 10 mg/ml stock solution of the dye in DMSO and stored it at -20°C. For mitochondrial staining, the stock solution was diluted first at 1:100 in DMSO and finally at 1:100 in a pre-equilibrated G2-plus medium (Vitrolife, Gothenburg, Sweden) to achieve a working concentration of 1 µg/ml. A total of 22 living oocytes were placed into JC-1 solution and incubated for 30 min in a drop covered by mineral oil (Ovoil, Vitrolife, Gothenburg, Sweden). Samples were then imaged immediately in a glass bottom dish. Oocytes were imaged in a Zeiss Lsm780 laser scanning confocal microscope with a 40X water objective. Confocal imaging was performed using an argon laser to produce an excitation at 488 nm. Emission wavelength detection was set at 508–530 nm (green emission) and 585 nm (red emission). A single equatorial scan was used for the analysis. All samples were imaged and stained on the same day. Imaging data were analysed using the open-source image processing software ImageJ (Schneider et al., 2012).

Inhibition of mitochondrial membrane potential

Eighty-nine immature oocytes were treated for 30 min with 1µM of the mitochondria oxidative phosphorylation uncoupler, Trifluoromethoxy-carbonylcyanide-phenylhydrazone (FCCP, Sigma, St. Louis, Missouri, USA). Then, they were washed in G2-plus culture media (Vitrolife, Gothenburg, Sweden) to remove any drug residual and finally cultured in 30 µL drops of G2-plus media (Vitrolife, Gothenburg, Sweden)

covered with oil (Ovoil, Vitrolife, Gothenburg, Sweden) in a humidified atmosphere of 6% CO_2 at 37°C. After 30 hours of *in vitro* maturation the oocytes were checked, and the maturation stage was assessed. The experiment was optimized by testing different FCCP concentrations with different exposure times to ensure the use of the minimum dosage and avoid side toxicity. Moreover, since the FCCP stock solution was prepared in DMSO, we tested the correspondent concentration of DMSO and verified that it did not alter either mitochondrial metabolism or maturation rates *in vitro*.

After fixation in 4% PFA in PBS, the oocytes were processed for mitochondrial imaging.

Statistical analysis

Comparison of fluorescence intensities between groups of JC-1 stained or immunostained oocytes was performed by t-test. Differences in maturation rates were analysed by Chi-Square test. Significance was considered at $p<0.05$.

RESULTS

NADH in human oocytes predominantly originates from mitochondria

We first examined the extent of NAD(P)H and FAD+ metabolism generated from mitochondria in GV oocytes.

We performed non-invasive FLIM imaging, and once the acquisition was completed, oocytes were fixed and evaluated with mitochondrial markers. In addition, we performed live measurements on a different set of oocytes with JC-1. When comparing the FLIM NAD(P)H signal with IF staining of TOMM20 and D-LAT and the live JC-1 staining, we were able to confirm that the majority of NAD(P)H signal was associated with mitochondria. The higher intensity of NAD(P)H correlated with the areas where mitochondria had more pyruvate dehydrogenase (D-LAT) and a polarised membrane (red signal from JC-1), supporting the hypothesis that more NAD(P)H is produced by more active mitochondria (**Figure 1A-E**). However, the NADH signal was more homogeneously spread in the cell, indicating that most NADH is bound.

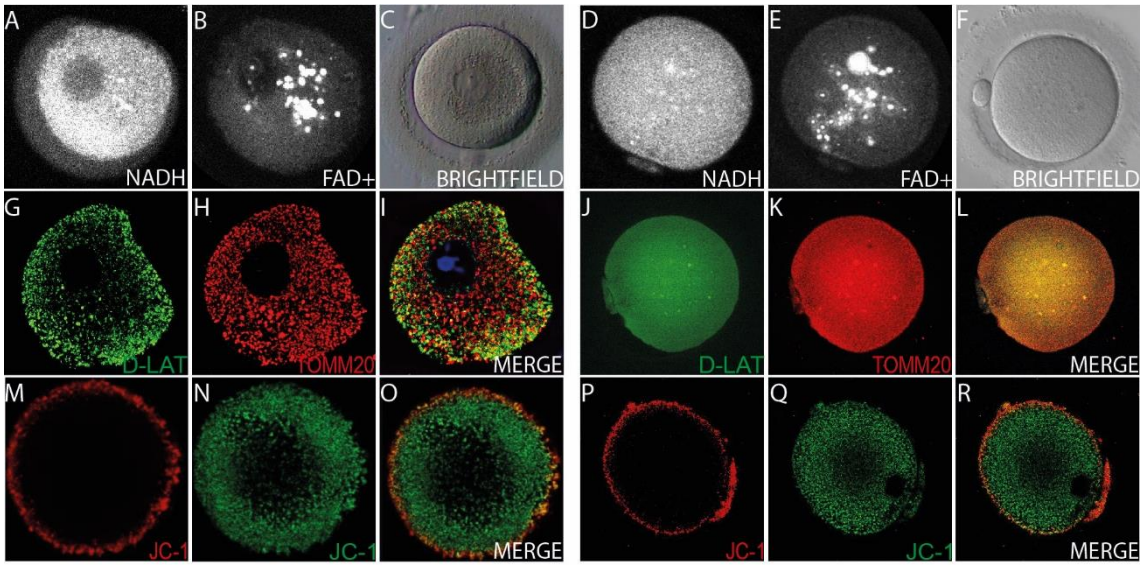

Figure 1. Differences between immature oocytes with a visible germinal vesicle and matured MII oocytes. (**A**) Images from FLIM acquisition of NADH and (**B**) FAD in immature germinal vesicle (GV) and in matured Metaphase II (MII) oocytes (MII) (**D, E**), respectively. Brightfield images of GV (**C**) and MII (**F**) stage oocytes. Images of the immunofluorescence staining (IF) of two mitochondrial proteins, Dihydrolipoamide-S-Acetyltransferase (D-LAT, 1:200, ab110333; secondary antibody anti-Mouse AlexaFluor488, 1:500) to estimate mitochondrial activity, and Translocase-of-outer mitochondrial-membrane (TOMM20, 1:200, ab186734; secondary antibody anti-Rabbit AlexaFluor568, 1:500) to assess mitochondrial localization and, overall abundance in GV (**G, H**) and MII (**J, K**) oocytes, respectively. Merge of the IF staining of GV (**I**) and MII (**L**) oocytes. Images of JC-1 staining at GV (**M, N, O**) and MII stages (**P, Q, R**), where active mitochondria appear in red (**M, P**) and the non-active ones in green (**N, Q**).

Mitochondria rearrange their shape and their position in the subcortical region while metabolite concentration increases during final oocyte maturation

In GV oocytes, mitochondria were located throughout the ooplasm but showed a different shape depending on their location. In the central region, they have a smaller and rounder shape, and in the subcortical area, they appear more clustered and/or bigger ("tubular"). (**Figure 1**). In addition, we detected a high presence of D-LAT in the outermost part of the oocytes, suggesting that that active mitochondria are mostly concentrated in the subcortex area (**Figure 2**).

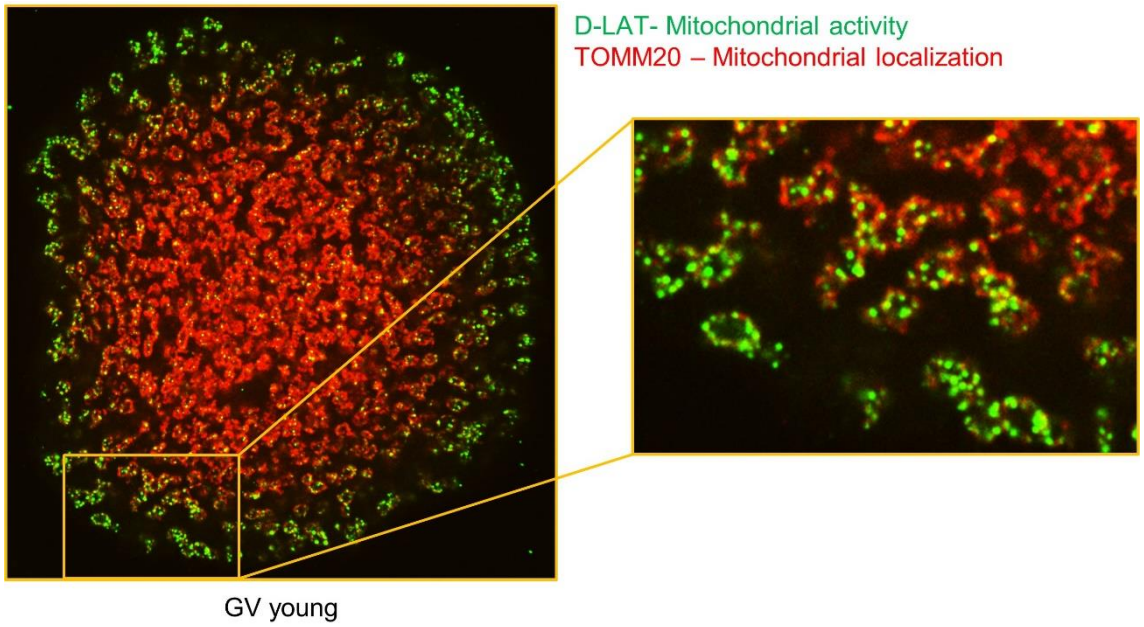

Figure 2. High-resolution image of an immature oocyte obtained from a young healthy donor. Immunofluorescence staining (IF) of two mitochondrial proteins, Dihydrolipoamide-S-Acetyltransferase (D-LAT) to estimate mitochondrial activity and Translocase-of-outer mitochondrial-membrane (TOMM20) to assess mitochondrial localization and, overall, abundance. On the left, selection of one of the stacks acquired to highlight mitochondria, the circular/elongated structures in the images. On the right, magnification of the subcortical area of the oocyte shows the localization of the signals: red on the outside, as the protein is located in the outer mitochondrial membrane, and green on the inside, coherent with a protein of the respiratory chain. Moreover, the abundance of the green (D-LAT) signal compared to the red (TOMM20) is higher in the subcortical area than in the innermost part of the oocyte, suggesting that active mitochondria in immature oocytes are more localized in the outermost part of the cell.

In mature oocytes at MII stage, we observed a spatial reorganization of mitochondria. Indeed, the area occupied by mitochondria expanded to the oolemma and the organelles distributed homogeneously (**Figure 1**). Active mitochondria remained in the outermost part of the oocytes, pushed outward by the cytoplasmic expansion, and active mitochondria were also observed in the polar body. The quantification of the fluorescence intensity of D-LAT and TOMM20 signals revealed no significant differences in mitochondrial activity and number between GV and MII stages, respectively (intensity of D-LAT 78614±58534 AU in GV, 2332.8±26357 AU in MII, p=0.818; intensity of TOMM20 57581±30606 AU in GV, 36413±25915 AU in MII, p=0.143).

JC-1 analysis yielded only small differences between GV (n = 11) and MII (n = 11) stages, with an average of red/green ratio of 1.127 and 0.639, respectively (p = 0.033).

When analysing the number of metabolites in a time-course experiment on 22 GV oocytes that successfully achieved maturation, we observed a small but consistent increase in the NADH intensity of 4% in the hours after GVBD. Interestingly, all maturing samples showed a similar trend and a small variability among them (**Figure 3**).

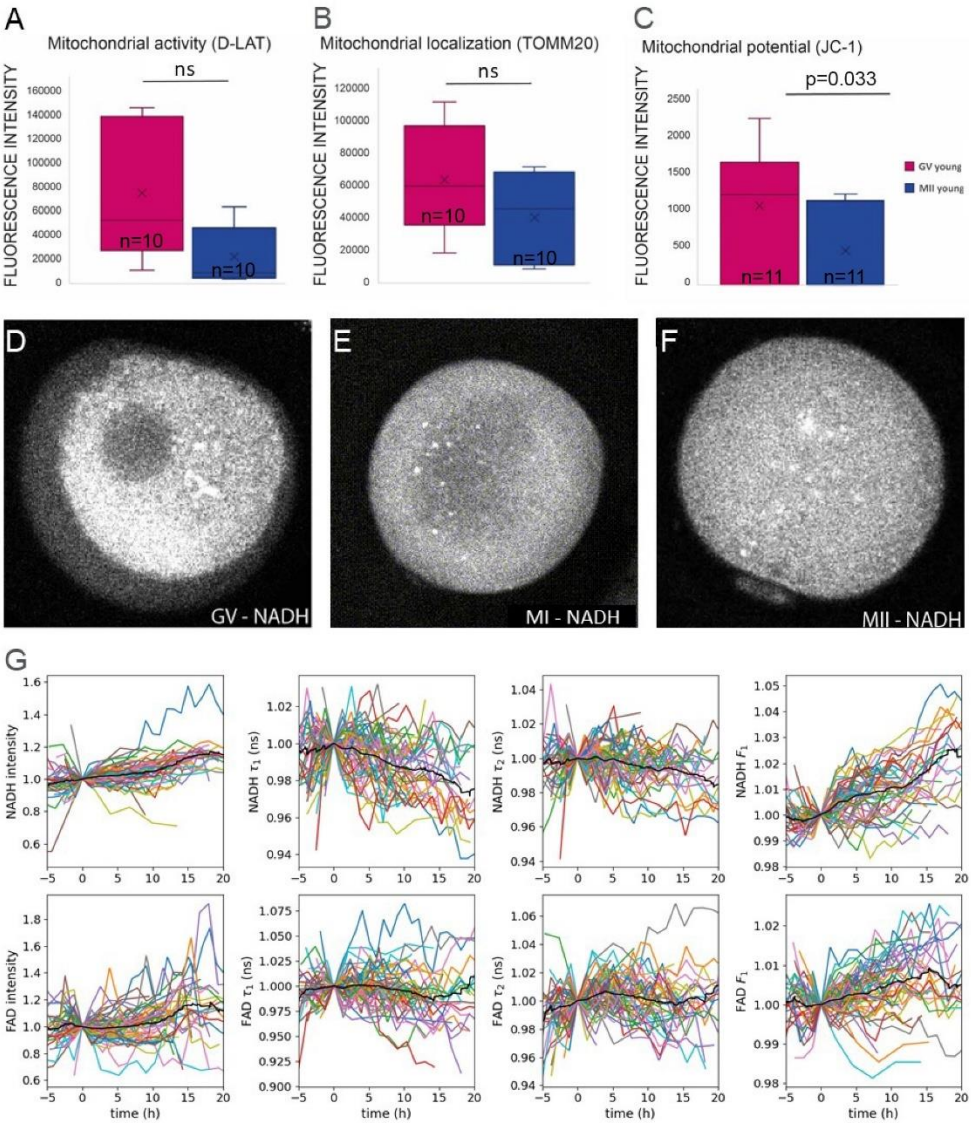

Figure 3. Changes in mitochondria and NADH through meiotic maturation. (**A**) Quantification of the fluorescence intensity of mitochondrial proteins to assess activity, (**B**) localization and (**C**) membrane potential between GV and matured MII oocytes. Selection of the frame during the FLIM acquisition at different maturation stages, (**D**) GV, (**E**) MI and (**F**) MII. (**G**) Time course of the metabolic changes of four FLIM parameters assessed for NADH (graphs on the top) and FAD (graphs on the bottom) through the *in vitro* maturation.

Metabolic basal level and its variation during maturation correlate with the ability to successfully progress through meiosis

We examined whether there were differences in the basal metabolism between GV oocytes that successfully achieved *in vitro* meiotic maturation and the ones that failed (Supplementary Figure S1). When performing cross validation between all the FLIM parameters measured, we found that five of them could distinguish between GV oocytes that would mature and GV oocytes that could not, with an AUC of 70% (**Figure 4**). However, the basal level of intensity alone was not sufficient to discriminate between the two groups of oocytes. We then compared the time-course of NADH of the two classes of GV oocytes and found that the ones unable to mature had higher variations in their metabolic levels (**Figure 4**).

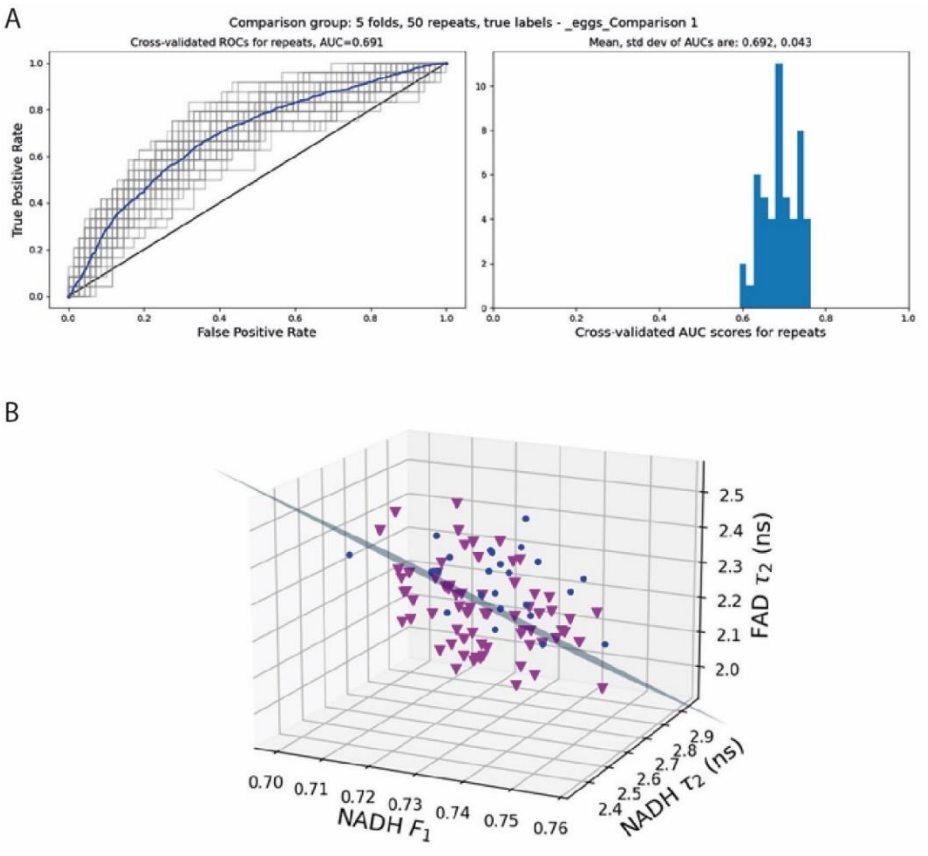

Figure 4. Discriminative power of the basal metabolic levels detected in GV oocytes to predict their maturation fate. (A) Cross validation showing the capacity to predict the successful or failed maturation based on the basal metabolic levels recorded in GV oocytes. **(B)** PCA of the top three parameters for discriminating between oocytes that could and could not extrude the first polar body.

Maturation rates in oocytes from young women

We evaluated the mitochondrial and metabolic dynamics in the GV to MII transition in a cohort of oocytes from young oocyte donors, and associated it with their maturation potential, measured by polar body extrusion after 30 h of *in vitro* maturation in G2-plus media (starting from the GV stage, as oocytes collected as MI at retrieval were not considered). In this cohort, 86.3% (63/73) of GV oocytes matured *in vitro* to MII (**Figure 5C**).

Poor mitochondrial activity and metabolism in oocytes from advanced maternal age women correlate with lower maturation rates

We further compared oocytes collected from young and AMA women. We observed significant changes in terms of global mitochondrial shape. The mitochondria appeared in fact smaller and more rounded in AMA oocytes, compared to those of the young ones, where they were bigger and more tubular-shaped (**Figure 5A-B**).

The evaluation of the metabolic levels of GV oocytes a revealed differences in the intensity of the immunofluorescent staining of mitochondria (D-LAT quantification intensity 78614±58534 AU in young, 12517±10187 AU in AMA, p=0.003, TOMM20 quantification intensity of 61674±24322 AU in young, 32186±33414 AU in AMA, p=0.195, **Figure 5**) and in the metabolite FLIM analysis (Redox ratio in young 2e+00±0.15, in AMA 1e+00 ± 0.16, p=2.969e-05) showing a lower mitochondrial activity without a concomitant significant decrease in mitochondrial number, and a lower redox ratio, indicating also a reduced metabolic activity. At the same time, we also observed a significantly lower meiotic maturation potential, with only 62.3% of AMA oocytes able to mature (38/61), compared to the 86.3% (63/73) of the young cohort (**Figure 5C**).

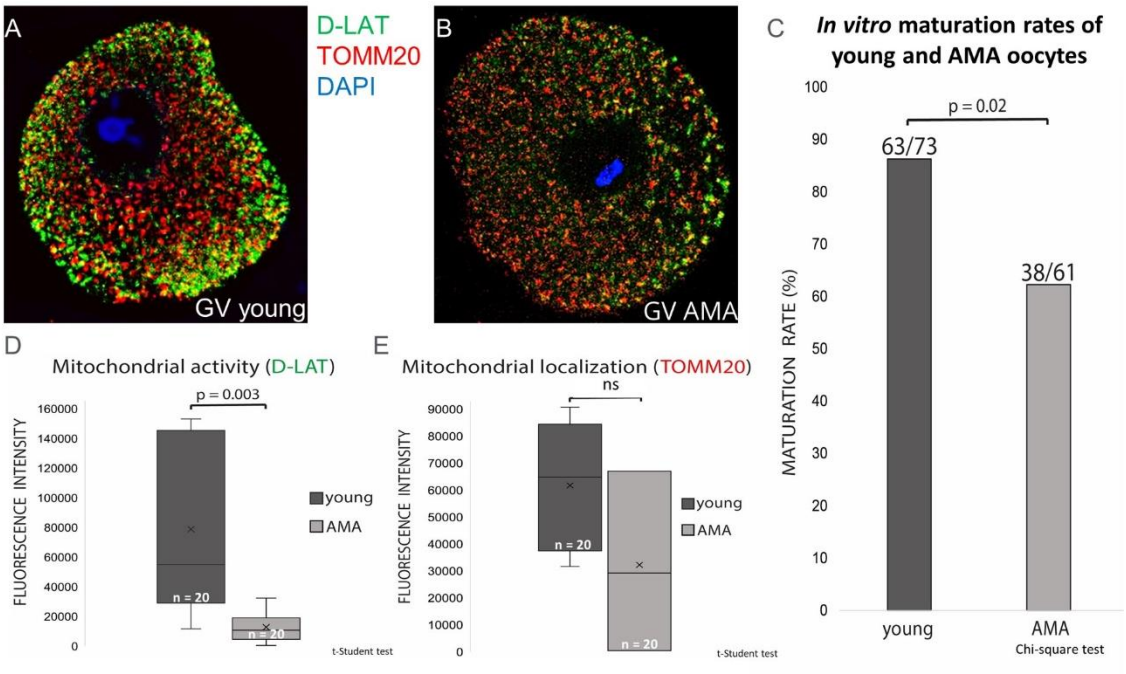

Figure 5. Comparison of the mitochondrial activity and localization between young and AMA oocytes. (**A**) Young GV oocyte stained with D-LAT (green), TOMM20 (red) and DAPI (blue) to estimate mitochondrial activity and assess mitochondrial localization, respectively. The typical pattern of more active mitochondria in the subcortex area is present. (**B**) GV oocytes obtained from advanced maternal age woman stained with D-LAT (green), TOMM20 (red) and DAPI (blue) to estimate mitochondrial activity and assess mitochondrial localization, respectively. D-LAT and TOMM20 patterns are like "points", different from the "tubular" aspects observed in young oocytes. Low D-LAT signal. (**C**) *In vitro* maturation rates of young and AMA groups. (**D**) Quantification of D-LAT and (**E**) TOMM20 fluorescence performed using the open-source image processing software ImageJ.

Time course imaging reveals higher metabolic variations in oocytes that do not achieve maturation

Finally, we performed a live time-course of ten maturing GV AMA oocytes and observed little to no increase in metabolism through GV-MII transition in each oocyte. Interestingly, in GV oocytes that reached the MII stage, we detected a higher variability of the oocyte's metabolic profiles among all the samples, compared to the young group (**Figure 3G**, **Figure 6A**).

The time-course of five AMA oocytes unable to mature, in line with the previous experiments, exhibited an impressive variation in the relative levels of NADH intensity through maturation, with most of the oocytes greatly increasing their metabolism, up to

almost twofold, with only two oocytes diminishing their NADH relative concentrations (**Figure 6B**).

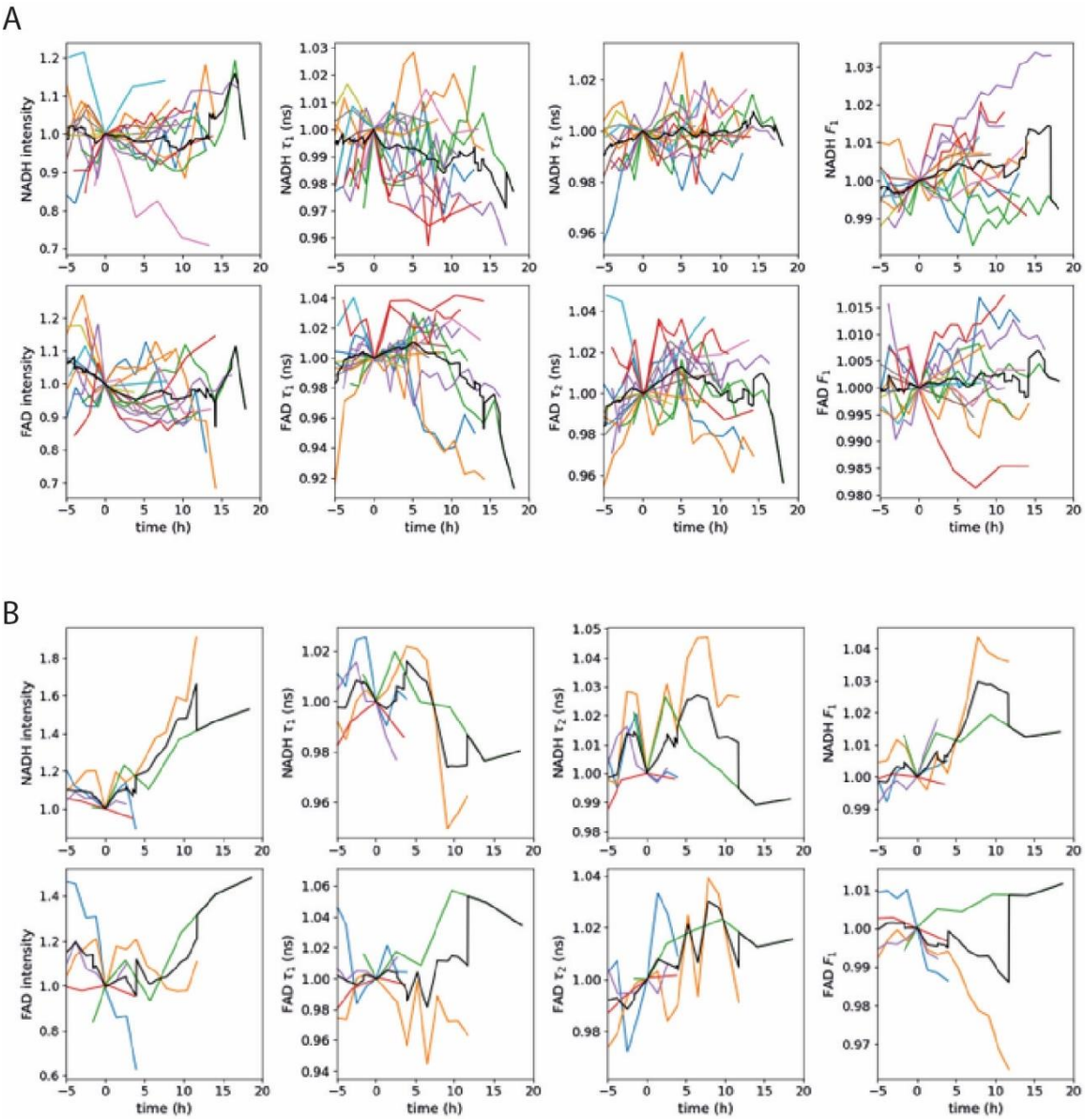

Figure 6. Time course of changes in metabolism through meiotic maturation of oocytes from advanced maternal age women. (**A**) Time course of the metabolic changes of four FLIM parameters assessed for NADH (graphs on the top) and FAD (graphs on the bottom) through the *in vitro* maturation of AMA oocytes able to successfully accomplish meiotic maturation and (**B**) the ones that failed meiosis progression.

Lowering mitochondrial metabolism in young oocytes reduces their meiotic maturation capacity

We then tested the hypothesis that a compromised metabolic function could cause a decreased *in vitro* maturation capacity. We suppressed mitochondrial activity temporarily in young oocytes by exposure to FCCP, followed by culture to the MII stage (**Figure 7A**). We first confirmed that FCCP was effectively inhibiting mitochondrial metabolism (**Figure 7A**) but induced only a transient uncoupling of the oxidative phosphorylation, without inducing cell toxicity. GV oocytes treated with FCCP presented a significant decrease of D-LAT (intensity of 78614±58534 IU in untreated and 11554±16131 IU in treated GVs, p=0.019), indicating a decrease in mitochondrial activity, but similar level of TOMM20, indicating no effect on mitochondria number. GV oocytes from young healthy donors (<30 years) showed an *in vitro* maturation rate of 86% (63/73), while FCCP treated immature oocytes exhibited a significant lower maturation rate, with only 39.5% (17/43) of treated oocytes reaching MII stage (**Figure 7B**).

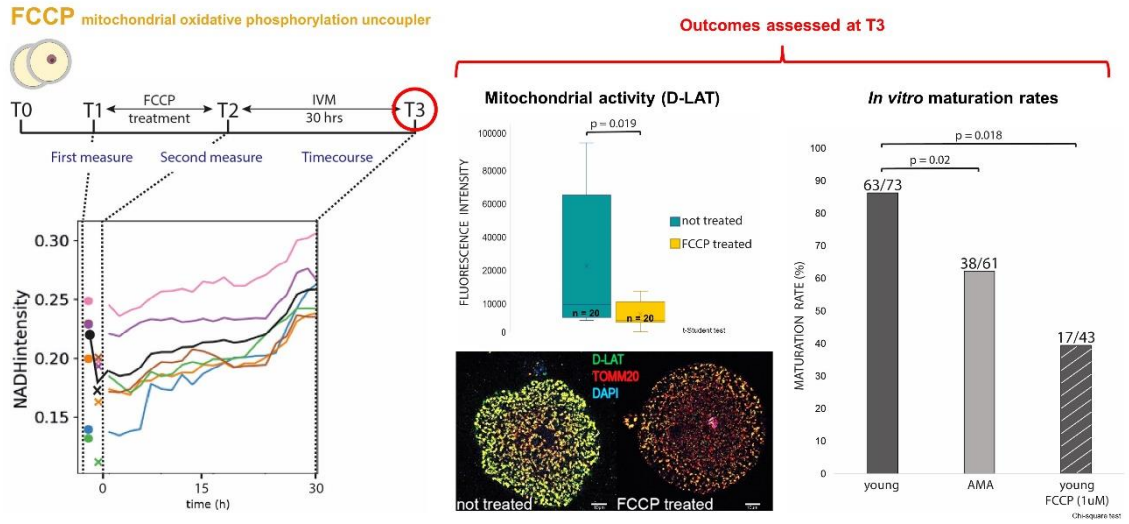

Figure 7. Pharmacological inhibition of mitochondria in young oocytes. (**A**) A sub-set of immature oocytes were collected from young healthy women and used for mitochondrial inhibition. The metabolism of these oocyte was checked prior to treatment ("First measure" at Time1, T1), then, oocytes were treated with 1µM of FCCP (Carbonyl cyanide-p-trifluoromethoxyphenylhydrazone) for 30 min and the "Second measure" was performed (T2). After several washes to remove the drug, the treated oocytes were matured *in vitro* (IVM) for 30 h until T3; oocytes' metabolic profile was measured throughout IVM. In the graph of NADH intensity per time of IVM, the metabolic profiles of the six oocytes included in the experiment are reported (each oocyte in a different colour) while in black we showed the average across samples. (**B**) Outcomes assessed at T3 are mitochondrial activity (left panel) and *in vitro* maturation rate (right panel).

DISCUSSION

Meiotic maturation of human oocytes is orchestrated by several nuclear and cytoplasmic factors (Hassold et al., 2007; Gosden et al., 2010). Studies conducted in mice suggests that impaired metabolic activity and successful meiotic progression might be functionally linked (Mainigi et al., 2011; Li et al., 2020). However, this relationship has not been extensively addressed in humans. In the present study, we aimed at characterising the relationship between mitochondrial activity, abundance and metabolism, with meiotic progression in human oocytes and to understand whether an impaired metabolism can explain the poor developmental competence of AMA oocytes.

In our set of human oocytes, we observed that mitochondria localize in throughout oocyte, while a subset of active ones are located preferentially in the subcortex area. This distribution is more pronounced at the GV stage, while in MII oocytes we found a more homogeneous spread of mitochondria, and the "ring" of active mitochondria was flattened toward the oocyte's membrane. The spatial distribution and organization of mitochondria in the oocyte during maturation are dynamic, and these changes were considered related to mitochondrial function (Hoshino et al., 2018) and, finally, to the achievement of oocyte competence (Hoshino et al., 2018; Lemseffer, 2022; Karillova et al., 2022; van der Reest, 2021). For these reasons, mitochondria have been abundantly explored in oocytes of different mammals using various techniques, including immunofluorescent staining, live dyes and, more recently, non-invasive live imaging.

Active mitochondria in murine oocytes are especially abundant and form aggregates close to the GV, disperse throughout cytoplasm through maturation and then distribute close to the oolemma at the time of the polar body extrusion (Van Blerkom and Runner, 1984; Dumollard et al., 2006; Takahashi et al., 2016; Sanchez et al., 2019; Kirillova et al., 2021; Wang and Hutt, 2021). Mitochondria in the cytoplasm of porcine oocytes present a completely different distribution, showing homogeneous localization and movement towards the central area of the cell after GVBD (Sun et al., 2001). Moreover, no marked changes in the distribution of active mitochondria were observed during cow oocyte maturation (Stojkovic et al., 2001; Lodde et al., 2021). Reports of mitochondrial behaviour in human oocytes are still conflicting (Takahashi et al., 2016). However, recent studies, in agreement with the results presented in this study, point toward the specific distribution of active mitochondria in the outermost part of the maturing human oocyte (Van Blerkom, 2004; Liu et al., 2010; Takahashi et al., 2016; Czernik et al., 2022; Cheng

et al., 2022), similar to what has been observed in cow oocytes (Stojkovic et al., 2001; Lodde et al., 2021).

The changes observed in mitochondrial distribution and reorganization may be explained by the process of fusion/fission typical of the final stages of meiotic maturation in healthy oocytes (Almansa-Ordonez et al., 2020), and might reflect a switch in their function, also reflected in a change in the shape of mitochondria through maturation, "tubular" in GV and "point-like" in MII stages. Mitochondria increase in number during oogenesis, and once MII stage is reached, they remain stable through initial preimplantation development (Dumollard et al., 2006; Dumollard et al., 2007). Therefore, it is reasonable to hypothesize that the mitochondrial load in MII oocytes is not necessarily linked to their meiotic capacity, but rather to the embryo needs, since it relies more on glycolysis than OXPHOS for initial cleavages.

The use of fluorescent mitochondrial membrane potential probes to assess mitochondrial activity is controversial due to the variability in the size and shape of these organelles, complicating the direct interpretation of fluorescent signals (Van Blerkom, 2004; Woods et al., 2018). The use of non-invasive FLIM live imaging overcomes these drawbacks because it relies on the quantification of two naturally fluorescent cellular co-enzymes, without the need for additional exogenous probes. The FLIM live imaging of NADH and FAD through final meiotic maturation confirms the spatial changes of maturing GV oocytes observed indirectly by immunofluorescence and suggests that oocytes need a slight and consistent increase in metabolism in the ten hours posterior to GVBD, likely to have enough energy to sustain the nuclear and cytoplasmic cellular events and complete maturation. To reinforce this hypothesis, this technique was already successful in discriminating oocytes able and unable to mature in mice, based on their metabolic profile (Sanchez et al., 2019).

The evaluation of maturing oocytes obtained from AMA women reveals a different pattern in terms of general mitochondrial distribution and, specifically, in terms of active mitochondria. Furthermore, we detected low mitochondrial activity in AMA oocytes compared to oocytes at the same meiotic stage but from young healthy women. These findings are supported by the literature where mitochondrial dysfunction is associated with poor oocyte quality in aging (Cimadomo et al., 2018; van der Reest et al., 2021).

Indeed, mitochondria are one of the biological elements extensively studied to elucidate the causes of the progressive quality decay observed in AMA oocytes (Cimadomo et al., 2018; van der Reest, 2021; Kirillova et al., 2021).

The trend of metabolism observed in AMA oocytes able to mature was divergent from the one detected in the young group, with little to no changes in terms of increase in the ten hours after GVBD. Interestingly, the variability between AMA oocytes unable to successfully progress in meiosis was much higher than among AMA maturing oocytes. This observed variability in terms of metabolic profile during meiosis in aged oocytes unable to mature is supported by the hypothesis that oocyte maturation and embryo development are sustained by an optimum of metabolism, the "*Optimal Goldilocks range*", rather than an increase of metabolic activity (Leese et al., 2022). Therefore, rather than the commonplace "more is better", maturing oocyte seems to need the correct amount of metabolism, not too much to cause cellular imbalance and not too little, insufficient to sustain nuclear and cytoplasmic changes that occur through maturation (Leese et al., 2022). And this is also confirmed by the high variability in the metabolic profile of AMA oocytes that are unable to mature.

As a whole, our data suggest that, rather than being an indicator of successful meiotic progression, the higher variability in the metabolic profile of AMA maturing oocytes, and even more of those that fail to mature, could be interpreted as a cellular response to support an oocyte with poor quality to progress in meiotic maturation.

Following the same line, the pharmacological inhibition of mitochondrial activity using an OXPHOS uncoupler (Zeng et al., 2009; Zander-Fox et al., 2015; Muller et al., 2019) suggests a functional link between impaired metabolic functions and compromised ability of young oocytes to successfully proceed meiosis *in vitro*. Considering the long turnover of the target proteins of this mitochondrial inhibitor (Muller et al., 2019), this treatment decreases mitochondrial activity, without disrupting the cell and triggering apoptosis (Grasmick et al., 2018; Demine et al., 2019; Muller et al., 2019).

Since mitochondrial dysfunction is well characterized in AMA oocytes, the majority of the studies are aimed at increasing mitochondrial function with the addition of antioxidants to the culture media or the supplementation with specific drugs, to ultimately increase (and reverse) the poor quality of AMA oocytes (Ben-Meir et al., 2015; Qi et al., 2019). However, our goal in the present study was to first understand the biological

mechanisms driving this decay and, only subsequently, identify specific targets to act on. Since another feature of AMA oocytes is undoubtedly the high presence of ROS, supplementation to increase mitochondrial metabolism must be targeted, so as not to unbalance the physiological equilibrium and generate side effects, such as increased ROS and subsequent DNA damage (Hoshino et al., 2018: Kirillova et al., 2021; van der Reest et al., 2021).

In conclusion, we revealed a fundamental role of mitochondria during final meiotic maturation of human oocytes. We confirmed that there are no major changes in the activity during this window, but a sufficient level of metabolism needs to be maintained for allowing the completion of meiosis I. Furthermore, we functionally linked impaired metabolism with less ability of oocytes to successfully proceed in meiosis, bearing out that, in order to successfully achieve final meiotic maturation, it is necessary for the oocyte to have a proper level of metabolism and for this to increase slightly during maturation, while still remaining within the tolerable range.

Data availability

The data underlying this article are available on request from the authors.

Acknowledgements

We would like to thank the laboratory staff from EUGIN (Barcelona, Spain) and BostonIVF (Waltham, MA, USA) for their help in sample handling.

Authors' roles

SP contributed to design the study, processed the samples, interpreted the data and drafted the manuscript; MM contributed to samples collection; EI and MP revised the manuscript; TS processed the data and performed statistical analysis RV and DS designed the study, contributed to the interpretation of the data and substantially revised the manuscript; FZ designed the study, contributed to the interpretation of the data and revised the manuscript.

Funding

This project received intramural funding from the Eugin Group and funding from the European Union's Horizon 2020 research and innovation program under the Marie Skłodowska-Curie grant agreement No 860960.

Conflict of interest

The authors declare that they have no competing interests.

REFERENCES

Almansa-Ordonez, A., Bellido, R., Vassena, R., Barragan, M., & Zambelli, F. (2020). Oxidative stress in reproduction: A mitochondrial perspective. In *Biology* (Vol. 9, Issue 9, pp. 1–21). MDPI AG. https://doi.org/10.3390/biology9090269

Amoushahi, M., Salehnia, M., & Ghorbanmehr, N. (2018). The mitochondrial DNA copy number, cytochrome c oxidase activity and reactive oxygen species level in metaphase II oocytes obtained from in vitro culture of cryopreserved ovarian tissue in comparison with in vivo-obtained oocyte. *Journal of Obstetrics and Gynaecology Research*, *44*(10), 1937–1946. https://doi.org/10.1111/jog.13747

Ben-Meir, A., Burstein, E., Borrego-Alvarez, A., Chong, J., Wong, E., Yavorska, T., Naranian, T., Chi, M., Wang, Y., Bentov, Y., Alexis, J., Meriano, J., Sung, H. K., Gasser, D. L., Moley, K. H., Hekimi, S., Casper, R. F., & Jurisicova, A. (2015). Coenzyme Q10 restores oocyte mitochondrial function and fertility during reproductive aging. *Aging Cell*, *14*(5), 887–895. https://doi.org/10.1111/ACEL.12368

Blazquez, A., Guillén, J. J., Colomé, C., Coll, O., Vassena, R., & Vernaeve, V. (2014). Empty follicle syndrome prevalence and management in oocyte donors. *Human Reproduction (Oxford, England)*, *29*(10), 2221–2227. https://doi.org/10.1093/HUMREP/DEU203

Broekmans, F. J., Soules, M. R., & Fauser, B. C. (2009). Ovarian aging: Mechanisms and clinical consequences. *Endocrine Reviews*, *30*(5), 465–493. https://doi.org/10.1210/er.2009-0006

Cagnone, G. L. M., Tsai, T. S., Makanji, Y., Matthews, P., Gould, J., Bonkowski, M. S., Elgass, K. D., Wong, A. S. A., Wu, L. E., McKenzie, M., Sinclair, D. A., & John, J. C. S. (2016). Restoration of normal embryogenesis by mitochondrial supplementation in pig oocytes exhibiting mitochondrial DNA deficiency. *Scientific Reports*, *6*. https://doi.org/10.1038/SREP23229

Cimadomo, D., Fabozzi, G., Vaiarelli, A., Ubaldi, N., Ubaldi, F. M., & Rienzi, L. (2018). Impact of Maternal Age on Oocyte and Embryo Competence. *Frontiers in Endocrinology*, *9*(JUL), 1. https://doi.org/10.3389/FENDO.2018.00327

Heikal, A. A. (2010). Intracellular coenzymes as natural biomarkers for metabolic activities and mitochondrial anomalies. *Biomarkers in Medicine*, *4*(2), 241–263. https://doi.org/10.2217/BMM.10.1

Kirillova, A., Smitz, J. E. J., Sukhikh, G. T., & Mazunin, I. (2021). The Role of Mitochondria in Oocyte Maturation. *Cells*, *10*(9). https://doi.org/10.3390/CELLS10092484

Klaidman, L. K., Leung, A. C., & Adams, J. D. (1995). High-performance liquid chromatography analysis of oxidized and reduced pyridine dinucleotides in specific brain

regions. *Analytical Biochemistry*, *228*(2), 312–317. https://doi.org/10.1006/ABIO.1995.1356

Krisher, R. L., Brad, A. M., Herrick, J. R., Sparman, M. L., & Swain, J. E. (2007). A comparative analysis of metabolism and viability in porcine oocytes during in vitro maturation. *Animal Reproduction Science*, *98*(1–2), 72–96. https://doi.org/10.1016/J.ANIREPROSCI.2006.10.006

Leese, H. J., Brison, D. R., & Sturmey, R. G. (2022). The Quiet Embryo Hypothesis: 20 years on. *Frontiers in Physiology*, *13*. https://doi.org/10.3389/FPHYS.2022.899485

Marchant, J. S., Ramos, V., & Parker, I. (2002). Structural and functional relationships between Ca2+ puffs and mitochondria in Xenopus oocytes. *American Journal of Physiology. Cell Physiology*, *282*(6). https://doi.org/10.1152/AJPCELL.00446.2001

Martín-Romero, F. J., Miguel-Lasobras, E. M., Domínguez-Arroyo, J. A., Gonzélez-Carrera, E., & Álvarez, I. S. (2008). Contribution of culture media to oxidative stress and its effect on human oocytes. *Reproductive BioMedicine Online*, *17*(5), 652–661. https://doi.org/10.1016/S1472-6483(10)60312-4

McLennan, H. J., Saini, A., Dunning, K. R., & Thompson, J. G. (2020). Oocyte and embryo evaluation by AI and multi-spectral auto-fluorescence imaging: Livestock embryology needs to catch-up to clinical practice. *Theriogenology*, *150*, 255–262. https://doi.org/10.1016/J.THERIOGENOLOGY.2020.01.061

Muller, B., Lewis, N., Adeniyi, T., Leese, H. J., Brison, D. R., & Sturmey, R. G. (2019). Application of extracellular flux analysis for determining mitochondrial function in mammalian oocytes and early embryos. *Scientific Reports 2019 9:1*, *9*(1), 1–14. https://doi.org/10.1038/s41598-019-53066-9

Nicholls, D. G. (2002). Mitochondrial function and dysfunction in the cell: Its relevance to aging and aging-related disease. *International Journal of Biochemistry and Cell Biology*, *34*(11), 1372–1381. https://doi.org/10.1016/S1357-2725(02)00077-8

Pasquariello, R., Ermisch, A. F., Silva, E., McCormick, S., Logsdon, D., Barfield, J. P., Schoolcraft, W. B., & Krisher, R. L. (2019). Alterations in oocyte mitochondrial number and function are related to spindle defects and occur with maternal aging in mice and humans†. *Biology of Reproduction*, *100*(4), 971–981. https://doi.org/10.1093/BIOLRE/IOY248

Qi, L., Chen, X., Wang, J., Lv, B., Zhang, J., Ni, B., & Xue, Z. (2019). Mitochondria: the panacea to improve oocyte quality? *Annals of Translational Medicine*, *7*(23), 789–789. https://doi.org/10.21037/ATM.2019.12.02

Sanchez, T., Venturas, M., Aghvami, S. A., Yang, X., Fraden, S., Sakkas, D., & Needleman, D. J. (2019). Combined noninvasive metabolic and spindle imaging as potential tools for embryo and oocyte assessment. *Human Reproduction (Oxford, England)*, *34*(12), 2349–2361. https://doi.org/10.1093/HUMREP/DEZ210

Sanchez, T., Zhang, M., Needleman, D., & Seli, E. (2019). Metabolic imaging via fluorescence lifetime imaging microscopy for egg and embryo assessment. *Fertility and Sterility*, *111*(2), 212–218. https://doi.org/10.1016/j.fertnstert.2018.12.014

Schall, P. Z., & Latham, K. E. (2021a). Cross-species meta-analysis of transcriptome changes during the morula-to-blastocyst transition: metabolic and physiological changes take center stage. *American Journal of Physiology. Cell Physiology*, *321*(6), C913–C931. https://doi.org/10.1152/AJPCELL.00318.2021

Schall, P. Z., & Latham, K. E. (2021b). Cross-species meta-analysis of transcriptome changes during the morula-to-blastocyst transition: metabolic and physiological changes take center stage. *American Journal of Physiology. Cell Physiology*, *321*(6), C913–C931. https://doi.org/10.1152/AJPCELL.00318.2021

Schneider, C. A., Rasband, W. S., & Eliceiri, K. W. (2012). NIH Image to ImageJ: 25 years of image analysis. *Nature Methods*, *9*(7), 671–675. https://doi.org/10.1038/NMETH.2089

Seidler, E. A., Sanchez, T., Venturas, M., Sakkas, D., & Needleman, D. J. (2020). Non-invasive imaging of mouse embryo metabolism in response to induced hypoxia. *Journal of Assisted Reproduction and Genetics*, *37*(8), 1797–1805. https://doi.org/10.1007/s10815-020-01872-w

Shah, J. S., Venturas, M., Sanchez, T. H., Penzias, A. S., Needleman, D. J., & Sakkas, D. (2022). Fluorescence lifetime imaging microscopy (FLIM) detects differences in metabolic signatures between euploid and aneuploid human blastocysts. *Human Reproduction*, *37*(3), 400–410. https://doi.org/10.1093/humrep/deac016

Tan, T. C. Y., Brown, H. M., Thompson, J. G., Mustafa, S., & Dunning, K. R. (2022). Optical imaging detects metabolic signatures associated with oocyte quality†. *Biology of Reproduction*, *107*(4), 1014–1025. https://doi.org/10.1093/BIOLRE/IOAC145

Tan, T. C. Y., Mahbub, S. B., Campbell, J. M., Habibalahi, A., Campugan, C. A., Rose, R. D., Chow, D. J. X., Mustafa, S., Goldys, E. M., & Dunning, K. R. (2021). Non-invasive, label-free optical analysis to detect aneuploidy within the inner cell mass of the preimplantation embryo. *Human Reproduction (Oxford, England)*, *37*(1), 14–29. https://doi.org/10.1093/HUMREP/DEAB233

Truong, T., & Gardner, D. K. (2017). Antioxidants improve IVF outcome and subsequent embryo development in the mouse. *Human Reproduction (Oxford, England)*, *32*(12), 2404–2413. https://doi.org/10.1093/HUMREP/DEX330

van der Reest, J., Nardini Cecchino, G., Haigis, M. C., & Kordowitzki, P. (2021). Mitochondria: Their relevance during oocyte ageing. *Ageing Research Reviews*, *70*. https://doi.org/10.1016/J.ARR.2021.101378

Venturas, M., Shah, J. S., Yang, X., Sanchez, T. H., Conway, W., Sakkas, D., & Needleman, D. J. (2022). Metabolic state of human blastocysts measured by fluorescence

lifetime imaging microscopy. *Human Reproduction*, *37*(3), 411–427. https://doi.org/10.1093/humrep/deab283

Venturas, M., Yang, X., Sakkas, D., & Needleman, D. (2023). Noninvasive metabolic profiling of cumulus cells, oocytes, and embryos via fluorescence lifetime imaging microscopy: a mini-review. *Human Reproduction (Oxford, England)*, *38*(5), 799–810. https://doi.org/10.1093/humrep/dead063

Wakai, T., & Fissore, R. A. (2019). Constitutive IP3R1-mediated Ca2+ release reduces Ca2+ store content and stimulates mitochondrial metabolism in mouse GV oocytes. *Journal of Cell Science*, *132*(3). https://doi.org/10.1242/JCS.225441

Wartosch, L., Schindler, K., Schuh, M., Gruhn, J. R., Hoffmann, E. R., McCoy, R. C., & Xing, J. (2021). Origins and mechanisms leading to aneuploidy in human eggs. *Prenatal Diagnosis*, *41*(5), 620–630. https://doi.org/10.1002/PD.5927

Wilding, M., Dale, B., Marino, M., Di Matteo, L., Alviggi, C., Pisaturo, M. L., Lombardi, L., & De Placido, G. (2001). Mitochondrial aggregation patterns and activity in human oocytes and preimplantation embryos. *Human Reproduction (Oxford, England)*, *16*(5), 909–917. https://doi.org/10.1093/HUMREP/16.5.909

Yang, X., Ha, G., & Needleman, D. J. (2021). A coarse-grained NADH redox model enables inference of subcellular metabolic fluxes from fluorescence lifetime imaging. *ELife*, *10*. https://doi.org/10.7554/ELIFE.73808

Zander-Fox, D. L., Fullston, T., McPherson, N. O., Sandeman, L., Kang, W. X., Good, S. B., Spillane, M., & Lane, M. (2015). Reduction of mitochondrial function by FCCP during mouse cleavage stage embryo culture reduces birth weight and impairs the metabolic health of offspring. *Biology of Reproduction*, *92*(5), 124–125. https://doi.org/10.1095/BIOLREPROD.114.123489/2434066

Zeng, H. tao, Yeung, W. S. B., Cheung, M. P. L., Ho, P. C., Lee, C. K. F., Zhuang, G. lun, Liang, X. yan, & O, W. S. (2009). In vitro–matured rat oocytes have low mitochondrial deoxyribonucleic acid and adenosine triphosphate contents and have abnormal mitochondrial redistribution. *Fertility and Sterility*, *91*(3), 900–907. https://doi.org/10.1016/J.FERTNSTERT.2007.12.008

SUPPLEMENTARY INFORMATION CONTENTS

Supplementary Figure S1.

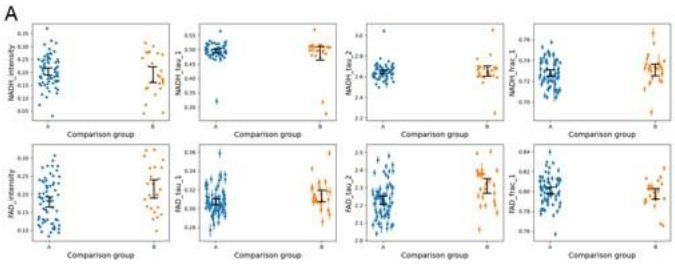

	Comparison group_A	Comparison group_C	p value
N (%)	69 (72%)	27 (28%)	
N_frac_1	0.728 ± 0.002962	0.732 ± 0.005661	0.1696
N_tau_1	0.495 ± 0.006573	0.48 ± 0.0211	0.1672
N_tau_2	2.6 ± 0.0173	2.7 ± 0.0519	0.7715
N_intensity	0.2 ± 0.0138	0.2 ± 0.0273	0.9921
N_num_pix	4e+04 ± 7.2e+02	3e+04 ± 1.6e+03	0.03786
F_frac_1	0.801 ± 0.003397	0.797 ± 0.005621	0.2151
F_tau_1	0.307 ± 0.00335	0.31 ± 0.006631	0.3603
F_tau_2	2.2 ± 0.0236	2.3 ± 0.0386	0.02479
F_intensity	0.18 ± 0.0139	0.21 ± 0.0208	0.01145
F_num_pix	3e+04 ± 1.1e+03	2e+04 ± 2e+03	0.1103
redox_ratio	1.2 ± 0.0872	1e+00 ± 0.13	0.008518

	Comparison group_A	Comparison group_B	p value
N (%)	69 (74%)	24 (26%)	
N_frac_1	0.728 ± 0.002962	0.731 ± 0.005781	0.3459
N_tau_1	0.495 ± 0.006573	0.49 ± 0.0241	0.3401
N_tau_2	2.6 ± 0.0173	2.7 ± 0.0518	0.7929
N_intensity	0.2 ± 0.0138	0.19 ± 0.0304	0.3326
N_num_pix	4e+04 ± 7.2e+02	3e+04 ± 2e+03	0.484
F_frac_1	0.801 ± 0.003397	0.798 ± 0.005188	0.2969
F_tau_1	0.307 ± 0.00335	0.314 ± 0.006128	0.07581
F_tau_2	2.2 ± 0.0236	2.3 ± 0.0414	0.001099
F_intensity	0.18 ± 0.0139	0.21 ± 0.0252	0.01469
F_num_pix	3e+04 ± 1.1e+03	2e+04 ± 1.8e+03	0.005286
redox_ratio	1.2 ± 0.0872	0.9 ± 0.13	0.001091

	Comparison group_D	Comparison group_E	p value
N (%)	6 (43%)	8 (57%)	
N_frac_1	0.74 ± 0.0141	0.739 ± 0.006363	0.6721
N_tau_1	0.494 ± 0.009686	0.491 ± 0.004009	0.5433
N_tau_2	2.6 ± 0.051	2.6 ± 0.0257	0.6077
N_intensity	0.25 ± 0.0313	0.24 ± 0.0283	0.7009
N_num_pix	4e+04 ± 1.2e+03	4e+04 ± 8e+02	0.2532
F_frac_1	0.82 ± 0.0128	0.808 ± 0.006187	0.04383
F_tau_1	0.307 ± 0.009177	0.298 ± 0.005369	0.1304
F_tau_2	2.3 ± 0.0668	2.3 ± 0.0991	0.9178
F_intensity	0.25 ± 0.0513	0.21 ± 0.0269	0.2305
F_num_pix	3e+04 ± 1.5e+03	3e+04 ± 2.8e+03	0.7036
redox_ratio	1e+00 ± 0.18	1e+00 ± 0.15	0.4024

Figure S1. Comparisons of the metabolic profile between oocytes able versus oocytes unable to mature. (**A**) Quantification of the eight FLIM parameters for NADH and FAD indicators of metabolism at GV stage in the comparison between oocytes able to reach MII *in vitro* (Group A in the graphs) and oocytes blocked at MI (Group B in the graphs), (**B**) relative principal

component analysis graph with (**C**) the most significant parameters able to distinguish the two groups and summary table with all the values measured. (**D**) Quantification of the eight FLIM parameters for NADH and FAD indicators of metabolism at GV stage in the comparison between oocytes able to reach MII *in vitro* (Group A in the graphs) and oocytes that failed the maturation retaining the germinal vesicle (Group C in the graphs), (**E**) relative principal component analysis graph with (**F**) the most significant parameters able to distinguish the two groups and summary table with all the values measured. (**G**) Quantification of the eight FLIM parameters for NADH and FAD indicators of metabolism at MI stage in the comparison between oocytes collected as MI (Group D in the graphs) and oocytes collected as MI and able to reach MII (Group E in the graphs), (**H**) relative principal component analysis graph with (**I**) the most significant parameters able to distinguish the two groups and summary table with all the values measured.

DISCUSSION

This thesis characterized the final phases of meiotic maturation in human oocytes, with the aim to understand the biological mechanisms underlying oocyte nuclear and cytoplasmatic maturation, and the acquisition of developmental competence. Specifically, we focused on the transcriptional and post-transcriptional modifications and the metabolic dynamics during meiosis, and on the effects induced by a decline of ovarian function on such processes.

1. THE TRANSCRIPTIONAL PROFILE OF MATURING HUMAN OOCYTES: GENE EXPRESSION

The final stages of meiotic maturation are accompanied by a strong transcriptional control, and this regulation is crucial to establish and sustain oocyte competence and early embryo development, up to EGA. EGA occurs at species specific times; in human, for example, it begins as early as the 4-cell stage, with a small increase in transcriptional activity at 2-cell stage, while the stronger protein expression occurs at the morula stage (Vassena et al. 2011). This is similar to cows, where EGA starts ate the 4-8 cell stage (Graf et al., 2014), while in mouse embryonic transcription is detectable as early as the late 1-cell stage (Shultz, 1993; Wang and Latham, 1997; Ma et al., 2001; Fugaku, 2022).

RNA transcription in the human oocyte is active during the initial follicular growth, when CCs provide the oocyte with the mRNAs necessary for oocyte maturation through their transzonal projections (TZP). During the final steps of oocyte growth and maturation, transcription stops in those GV oocytes that have acquired the SN chromatin conformation (Cornet-Bartolomè et al., 2021). In accordance with a repressed transcription, the processes of meiotic resumption, spindle assembly and cytoplasmic maturation are mainly based on existing transcripts (Hendrinkson et al., 2017). Further, co- and post- transcriptional modifications might also play an important role in meiosis. One of the most important co-transcriptional modifications is constitutive splicing, i.e. the mechanism of intron removal and exon ligation of the majority of the exons in the order in which they are present in a gene. AS is a deviation from this constitutive process, by which it is possible to obtain different isoforms from maturing mRNA through events such as exons skipping, intron retention. and alternative splice sites. AS can produce

different proteins from the same gene, which may have different functions, and this is crucial in maintaining genome variability (Kelemen et al., 2013), contributing to transcriptome complexity (Braunschweig et al., 2013). AS dysregulation results in aberrant phenotypes and diseases (Cooper et al., 2009). While global changes in gene expression have already been investigated in human oocytes (Reyes et al., 2017; Li et al., 2020; Llonch et al., 2020; Cornet-Bartolomè et al., 2021), co- and post- transcriptional regulation have not been extensively addressed yet.

We decided to investigate the transition between GV to MII in terms of transcriptional processing on a high number of oocytes, the highest reported so far for such a purpose, by single cell RNA sequencing.

We observed a set of genes differentially expressed in maturing oocytes mainly related to organelle biogenesis and maintenance, spliceosome, transport to cytoplasm and metabolic pathways. These features were already pointed out by previous studies (Reyes et al., 2017; Li et al., 2020; Llonch et al., 2020; Cornet-Bartolomè et al., 2021) using both massive parallel sequencing and microarrays. There seems to be an expected gene expression profile that characterizes the transition from GV to MII stages, consistent enough to be detected with different technologies and by different groups. The priming employed in our single cell RNA sequencing further allowed us to distinguish, among the high number of DEGs detected between IVO-MII and GV oocytes, 27 DEGs specifically involved in spliceosome machinery and RNA transport. These DEGs include *PRPF8*, involved in the pre-mRNA capping and processing, and splicing factors such as *SF3B* and *SRFS*. Moreover, we found genes involved in other RNA regulatory processes and nuclear export of maturing mRNA, such as the TREX complex factors *MAGOH* and *THOCs*, as well as *eIF4A3*.

For example, TREX is a multiprotein complex evolutionally conserved in both mammalian and non-mammalian species (Katahira, 2012) that plays a central role in orchestrating mRNA biogenesis, including mRNA transcription, processing, and specifically nuclear export (Katahira, 2012; Pühringer et al., 2020). In eukaryotes, protein-coding mRNAs are matured, with the modifications of 5' capping, splicing or AS and 3' polyadenylation in the nucleus, and then exported and translated in the cytoplasm (Pühringer et al., 2020). The TREX complex, containing the multi-subunit THO complex,

RNA helicases and RNA export adaptor (Stäßer et al., 2002), is recruited during transcription (Heath et al., 2016; Viphakone at al., 2019) and it seems to be able to discern mRNAs and selectively export them from the nucleus (Viphakone at al., 2019; Pühringer et al., 2020). This TREX function is conserved across species (Sträßer et al., 2002) and cell types, including oocytes in GVBD, where this complex probably does not need to actively export mature mRNAs.

Moreover, comparing IVO-MII with GV oocytes, we observed an up-regulation of *THOC* and *MAGOH* genes, concomitant with a downregulation of the *eIF* – family genes in GV oocytes, as expected given that the mTOR and eIF4F pathway become active shortly after GVBD (Susor et al., 2015).

The comparison between IVO-MII and GV oocytes showed differences in biological processes such as RNA processing, mitochondrial metabolism, and protein targeting and/or stability; this could be related to the fact that the IVO-MII oocytes were retrieved as fully mature and vitrified. Before being used in the study, the oocytes were thawed and allowed to recover for about 4h in the IVF incubator. This could explain the detection of more DEGs related to metabolism in the comparison of IVM-MII versus GV than in IVO-MII versus GV comparison. Moreover, studies comparing *in vitro* and *in vivo* matured oocytes in mice (Zang et al., 2021), rabbit (Arias-Álvarez et al., 2017), cow (Caetano et al., 2022) and human (Ferrer-Vaquer et al., 2019) have associated the differences in terms of metabolism-related processes to differences in the environment in which the oocytes were cultured.

2. THE TRANSCRIPTIONAL PROFILE OF MATURING HUMAN OOCYTES: EXON USAGE AND UTR PROCESSING

Following the analysis of mRNA expression, we evaluated the processing of maturing transcripts using two exon-based approaches, with more than 60% of overlapping between results. Overall, we found more than one thousand genes with differential exon usage and UTR variants comparing IVO-MII versus GV oocytes and fewer in IVM-MII versus GV ones. Furthermore, it was only looking deeply that we realized that the majority of those events occurred in the 5' or 3' UTR regions of the genes, as reported in Results 1., **Figure 4**. Over representation analysis showed that genes affected by this process were consistent between the two comparisons performed, IVO-MII versus GV and IVM-MII versus GV, and that the biological processes affected were also similar. The functions of these genes are mostly related to chromosome and organelle organization, mitotic cell cycle and nuclear division, as shown in Results 1., **Figure 3** and **Figure 4.**

Some differentially processed genes are related to spindle formation and chromosome segregation, which are closely related processes, as the spindle segregates homologous chromosomes in anaphase I and sister chromatids in anaphase II. One notable example is *AURKA,* differentially processed between mature and immature oocytes. Aurora kinases (AURK) are serine/threonine kinases crucial for both mitosis and meiosis. There are three known isoforms of AURK in mammals: A, B and C. While loss of *AURKB* and *AURKC* can be compensated, loss of *AURKA* is not fully explored. Blengini and colleagues have shown that mice without *AURKA* are sterile, and their oocytes fail to complete meiosis I (Blengini et al., 2021). The most severe phenotypes are induced by pathogenic mutations or by complete protein absence (Biswas et al., 2021), however, also alterations in gene expression or in isoforms abundance can impair AURK function in the regulation of oocyte maturation (Virant-Klun et al., 2013).

Overall, the genes identified in our study and differentially processed through meiosis were functional in processes related to meiotic resumption and specifically cell progression, indicating that the pre-mRNA processing of specific transcripts is connected

to -and perhaps necessary for- successful completion of meiosis I and progression through metaphase II.

As most processing involved the 3'end of the genes, we chose *qapa* (Ha et al., 2018), a bioinformatic tool to detect and characterize Alternative poly(A) (APA) sites usage through final meiotic maturation. In both comparisons, IVO-MII versus GV and IVM-MII versus GV, we found around two hundred genes affected. Specifically, we observed that the majority of the genes identified had shortened UTR through oocyte maturation and were functionally linked to chromosome and chromatin organization and cell cycle process. Fewer genes had lengthened UTR, and the over representation analysis did show any specific pathway affected.

This phenomenon of mRNA processing during oocyte maturation has already been observed in mammals, with analogous observations in pigs (Wu et al., 2022), bovine (Reyes et al., 2015) and mice (He et al., 2021). Wu and colleagues reported a higher level of UTR shortening during final oocyte maturation in genes involved in cell cycle, kinetochore, chromosome and spindle organization (Wu et al., 2022), similar to what both Reyes and colleagues (Reyes et al., 2015) and ourselves have observed. In mice, conversely, a pervasive 3'UTR isoform switch was observed, but with a global abundance of genes with longer 3'UTR isoforms in matured oocytes (He et al., 2021). In this case, the discrepancy could be due to the technology for RNA capture, based on poly(A) capture in the study from He and colleagues (He et al., 2021) versus total RNA-isolation in our study. Genes not undergoing polyadenylation at GV stage might have been missed by the capture method, influencing the total outcome. Another explanation could be the effective diversities between the two species, mice in their study and humans in ours (Schall and Latham, 2021).

Overall, our results and others (Reyes et al., 2015; Wu et al., 2022) point to the conservation of these modifications characteristic of the latest stages of transcription. Transcription in mouse oocytes is indeed repressed in fully grown GV oocytes, as is in other mammalian species. In cow, for example, transcription stops at the periovulatory stage (GV2-GV3). In most mammalian species studied so far, transcription remains active during GV growth, and stops after the LH surge as the oocyte approaches GVBD (Mamo et al., 2011; Luciano et al., 2012; Yang et al., 2020; Wu et al., 2022).

In humans as well, although we analysed fully grown GV oocytes, we know that they still maintain a residual transcriptional activity, and it was reported that a significant proportion of immature oocytes retrieved at GV present an open chromatin configuration NSN rather than chromatin condensed around the nucleolus (SN) or are in the transition stage between NSN-to-SN (Cornet-Bartolomè et al., 2021), and still possess transcriptional activity. As recently shown (Cornet-Bartolomè et al., 2021), the transcription in GV oocytes from stimulated ovaries and retrieved after an ovulatory stimulus, may be active depending on the chromatin configuration. When the chromatin is in an open state, resembling the NSN state of mouse GV oocytes, transcription is still active. When the chromatin compacts around the nucleolus, transcription stops. This is equivalent to the mouse SN conformation.

We performed an additional analysis of exon expression to prove the absence of technical biases. In this new analysis, we compared FTM-GV versus IVO-MII oocytes, to show that the differences were indeed stage-specific and not due to aleatory results influenced by the library prep method in the GV group. The results we found were similar to the GV vs IVO-MII comparison, as 514 differentially expressed exons from 408 genes were found in FTM-GV vs IVO-MII oocytes (89% being underrepresented in IVO-MII oocytes), and pathway analysis revealed again that most of the targets were involved in chromosome organization, microtubule dynamics and nuclear division. The fact that a separate group of 10 oocytes yielded similar results in the same comparison supports the specificity of the results.

3. THE TRANSCRIPTIONAL PROFILE OF MATURING HUMAN OOCYTES: THE OOCYTE NEEDS SPECIFIC RNA ISOFORMS TO EXECUTE MEIOSIS

Regarding AS, we found fewer but specific isoforms switches of genes involved in microtubule dynamics, chromosome condensation and spindle assembly in matured MII oocytes compared to immature GV ones. This finding complements and extends the data in mice, where AS regulates growing oocytes at multiple levels while maintaining

transcriptome integrity (Do et al., 2018), and where the deregulation of this machinery has been associated with aberrant phenotypes and diseases (Cooper et al., 2009), but also with aging (Tollervey et al., 2011) with an increased presence of spliced transcripts found in tissues of old mice (Rodríguez et al., 2016).

We found approximately one hundred differentially spliced genes in both IVO-MII versus GV and IVM-MII versus GV comparisons, mostly related to mitosis, meiosis, nuclear division, chromosome formation and segregation pathways. Furthermore, some of the alternatively spliced genes include key players in the process of meiotic spindle formation such as *CENPE*, *NIPBL*, and *TUBB8* (Results 1., **Table 1** and **Figure 5F, 5G, 5H**), all genes interacting to obtain a functionally active spindle (Wong et al., 2007; Bennabi et al., 2016; Biswas et al., 2021).

The spindle is a central component for chromosome segregation, and alterations in genes encoding spindle components might cause meiotic arrest and infertility. Alpha- and β-tubulin heterodimers form microtubules and TUBB8 is the only primate-specific isotype of the tubulin family, whose mutations have been reported in cases of familiar female fertility (Feng et al., 2016). In these cases, the retrieved oocytes were either morphologically abnormal, arrested in MI or had abnormal or absent spindle (Feng et al., 2016). Women with TUBB8 mutations and oocytes maturation defects are able to conceive through egg donation (Lanuza-Lopez et al., 2020). In the last decades, TUBB8 function was poorly characterized, and this can be perhaps due to the fact that its expression is limited to primate oocytes (Biswas et al., 2021). However, alterations in splicing or isoforms changes through meiotic maturations were already reported by us and others (Li et al., 2020), expanding the possibility in which *TUBB8* can play a central role in the explanation of cases of poor oocyte quality.

We detected minor changes in protein isoforms during final oocyte maturation. However, due to their key role (Biswas et al., 2021) and the consistency of our findings with other reports (Cornet-Bartolomè et al., 2021; Li et al., 2020), we consider these changes to be specific. Indeed, we compared the pathways affected by differential AS in our study with those of two recent reports, and found consistent findings (Li et al., 2020; Cornet-Bartolomè et al., 2021).

The differentially spliced genes in immature and mature oocytes are important for spindle formation. It is known from studies in *Xenopus* that the components of the spliceosome

are involved in the correct formation of the spindle, while non-coding mis-spliced transcripts act on AURK and CENP proteins to produce incorrect spindle formation (Grenfell, Heald, & Strzelecka, 2016). Furthermore, it was reported that an imbalance between protein isoforms induces chromosome mis-segregation during mitosis in cancer cell lines. Sororin and APC2, both involved in chromosome segregation, show mis-spliced variants that can induce incorrect spindle formation when the spliceosome activity is deregulated in HeLa cells (Lelij et al., 2014; Oka et al., 2014; Sundaramoorthy, Vázquez-Novelle, Lekomtsev, Howell, & Petronczki, 2014; Watrin, Demidova, Watrin, Hu, & Prigent, 2014).

The cruciality of a correct AS was recently reported in mouse oocytes (Sun et al., 2023), where the authors identified *SRSF1* (Serine/arginine-rich splicing factor 1) as a pivotal post-transcriptional regulator in meiosis prophase I and showed that SRSF1 knockout mice were unable to resume meiosis and proceed in maturation, elucidating its role in the molecular mechanisms driving primordial follicle formation (Sun et al., 2023).

4. THE TRANSCRIPTIONAL PROFILE OF MATURING HUMAN OOCYTES *IN VIVO* VERSUS *IN VITRO*

As a whole, the significant changes in mRNA processing between oocytes at GV and MII stages were conserved between *in vivo* and *in vitro* matured MII oocytes. Nevertheless, the comparison between IVO-MII and IVM-MII showed differences in genes involved in oocyte meiosis progression. This might highlight the lower ability of IVM-MII oocytes to achieve important milestones of oocyte maturation, like chromosome condensation and spindle assembly, reflecting their lower developmental competence, despite being morphological similar to IVO-MII oocytes.

The debate on whether rescued IVM-MII oocytes have sufficient quality to be employed in a clinical setting is still open (Yang et al., 2021; Strączyńska et al., 2022). What is known so far is that rescued oocytes, despite being correctly fertilized and able to support development to the blastocyst stage, have a reduced competence overall. For example, a

study performed on "rescue" IVM of human GV oocytes showed lower developmental competence and a fertilization rate below 50% in these oocytes (Faramarzi et al., 2018).

We identified little to no differences between oocytes retrieved as immature GV oocytes and oocytes that failed to mature after 30 hours of *in vitro* maturation, retaining the GV (FTM-GV). Moreover, we found that the changes detected are associated with successful meiotic progression, rather than factors as time in culture or overall oocyte quality.

5. HIGH SIMILARITY IN THE TRANSCRIPTOME OF HUMAN AND BOVINE OOCYTES DURING FINAL MEIOTIC MATURATION

Following the main objective of this thesis, after evaluating the transcriptome remodelling during the final meiotic maturation of oocytes from young women, we should have moved on to do the same but in oocytes from AMA women. However, due to the difficulties in collecting such samples, we decided to focus on a similar phenotype in an animal model.

One of the best models to study the female reproductive system is the cow, due to its similarity in reproductive physiology, ovulation, gestation, oocyte maturation, and development of preimplantation embryos (Ménézo and Hérubel, 2002).

We collected oocytes at GV and MII stage from young cows and from cows with an "AMA-like" phenotype, with similar features to those is observed in AMA women and evaluated transcriptome remodelling through meiosis.

In oocytes from young cows, the majority of the mechanisms changing through meiosis were related to RNA processing, cell cycle, meiosis and metabolism, as we discussed in Results 2.. Moreover, the comparison between DEGs in the GV-MII transition in the bovine and human returned a significant overlap. This similarity in global transcriptome has also been reported by Yao (Yao et al., 2022). Specifically, they found that global gene expression and gene co-expression networks are generally conserved between humans and cows across several tissues (Yao et al., 2022). In spite of a general similarity in terms of transcriptome and gene expression of human and bovine oocytes, processing and

regulation of mRNA is likely regulated in a species-specific manner (Schall and Latham, 2021).

6. POI-like OOCYTES: INSIGHT FROM A COW MODEL TO EXPLORE THE HUMAN CONDITION OF EARLY AGING

We then moved forward to analyse our study group, i.e. oocytes from young cows but with an AMA-like ovarian phenotype that mimics aging in human.

Since the early 90s a low ovarian quality phenotype was observed in 5% of culled dairy cows of 4-8 years old (Gandolfi et al., 1997; Malhi et al., 2005; Tessaro et al., 2011; Lodde et al., 2021; Luciano et al., 2013; Modina et al., 2014). Cows with this ovarian phenotype are characterized by small ovary size (< 2-4 cm length on the major axis), low AFC (<10 in both ovaries), normal oocyte maturation rates but reduced developmental competence, with about 6% of blastocyst rates, high percentage of aneuploidies (60%) and, overall, reduced fertility (Luciano et al., 2013). In addition, they present a high serum level of FSH, low AMH, reduced estradiol concentration and increased of progesterone in follicular fluid (Malhi et al., 2005; Luciano et al., 2013; Lodde et al., 2021).

We compared MII versus GV oocytes, where each AMA-like cow provided both a GV and an MII oocyte. Surprisingly, less than 20 DEGs were observed. Such few genes indicate little to no differences in global gene expression between the two maturation stages, in contrast with the observation in the control group. In the transit from GV to MII, the oocyte undergoes an extensive nuclear and cytoplasmic reorganization, and this is supported by data in literature, specifically from the transcriptional studies where we and others (Reyes et al., 2015) found more than 2000 DEGs associated with RNA processing and transport, meiosis, cell cycle and metabolism between maturation stages.

The principal component analysis further indicated a clustering of oocytes by individual rather than maturation stage: each GV oocyte of the GV-MII pair from the same cow was closer to its corresponding MII, and each pair was mostly separated from the others (Results 2., **Figure 3**). This is likely due to the absence of any significant differences in

global expression between maturation stages and the genetic variability among animals (Gao et al., 2004; Severance et al., 2020). Moreover, the lack of detectable differences between GV and MII oocytes in global gene expression may indicate that cytoplasmic and nuclear maturation are profoundly asynchronous.

We concluded that cows with an AMA-like ovarian phenotype may serve as a model of poor oocyte quality rather than a specific model for AMA. Indeed, all the previous studies on the transcriptome of aged oocytes performed in animals and humans showed differences in the global expression of genes involved in several biological processes, including cell cycle and metabolism (Hamatani et al., 2004; Reyes et al., 2017; Mishina et al., 2021; Yuan et al., 2021; Wu et al., 2022; Bebbere et al., 2022; Takahashi et al., 2023), rather than no differences. Therefore, to properly study oocyte aging in a bovine model, it would be better to directly collect oocytes from old animals of 10-12 years, which, however, are harder to find than culled young cows in our environment.

As a whole, these findings suggest that we observed a pattern of poor-quality oocytes typical of the clinical condition of POI, also known to be similar to early aging. POI is a clinical condition affecting 1-10% of women below 40 years of age and characterized by amenorrhea, hypoestrogenism, high serum FSH levels, low AMH, reduction of estradiol concentration, overall hormonal alterations and total or partial follicle deprivation (McGlacken-Byrne & Conway, 2022; Shestakova et al., 2016). Beyond these general systemic alterations, POI is characterized by accelerated ovarian senescence follicular reduction in size and number and, overall, hypofertility (De Vos et al., 2010; Nelson, 2009).

POI causes can be divided in spontaneous, mainly genetics, and induced by toxicants, chemicals, or environmental pollutants. Regarding the genetic causes of POI, at the beginning, this condition was considered only monogenic, but recent studies have reported a synergistic effect of several genes, rather suggesting a polygenic origin (Tucker et al., 2016; Tucker et al., 2022). The main biological processes involved are folliculogenesis, metabolism DNA repair, apoptosis, meiosis and DNA replication, immune function, and hormonal signalling (Tucker et al., 2016; Tucker et al., 2022). Whereas fertility is generally compromised, in cases of POI it is generally not absolute; as up to 25% of women with POI may ovulate, and 5-10% of these will conceive (Tucker et al., 2016).

Overall, oocytes from women diagnosed with POI present an impaired capacity to generate viable embryos, and the mechanisms responsible still remain elusive.

According with our results, we defined the "POI-like" group. In this group, the lack in abundance of genes necessary for meiosis progression can explain why oocytes from this sub-population of young cows with poor ovary phenotype have failed to achieve cytoplasmic and nuclear maturation, resulting in low blastocyst rates, as already reported (Luciano et al., 2013). Actually, the cytoplasmic maturation failure has been explained by the lack of cross talk between the follicle and the oocyte, mainly regulated through TZPs (Lodde et al., 2021; Reyes et al., 2015). Furthermore, the low-quality model studied by Lodde and colleagues showed over 50% of the oocyte's gap junction closed, compared to control oocytes at the same stage, where most gap junctions are open (Lodde et al., 2021). Another factor that might play a crucial role in nuclear and cytoplasmic maturation and that seems to be absent in POI-like oocytes, is mitochondrial activity. In the analysis of MII versus GV oocytes in the control group, we found a proportion of DEGs related to mitochondrial metabolism. However, this was not found in the POI-like group. As recently reported, overall mitochondrial activity is lower in the low-quality oocytes compared to the controls (Lodde et al., 2021).

When comparing the same developmental stages between the CTRL and POI-like groups, we found 67 and 156 DEGs in GV and MII oocytes, respectively. The DEGs in the GV groups were mostly related to cumulus-oocyte-complex communication and microtubule organization, while the DEGs in the IVM-MII groups were primarily related to cell cycle, chromosome segregation and spindle organization.

For example, the presence of *GJA1* as differentially expressed between CTRL and POI-like GV oocytes can explain the poor quality of the oocytes in the POI-like group. In mammals, one of the crucial factors for oocyte development are the gap junctions that regulate the essential intracellular communication between granulosa cells and between CCs and oocyte (El-Hayek and Clarke, 2015). GJA1 is a protein involved in the communications between granulosa cells in the growing follicle (El-Hayek and Clarke, 2015) and, in mouse oocytes, *GJA1* mediates prophase I meiotic arrest (Richard and Baltz, 2014).

7. MITOCHONDRIAL DYNAMICS THROUGH HUMAN FINAL MEIOTIC MATURATION

We then shifted our attention to the mitochondrial dynamics characterizing the GV to MII transition, to test whether a mitochondrial insufficiency could be directly related to meiotic failure possibly by a deregulation of the transcriptional/splicing programme. We investigated mitochondrial activity, abundance, and metabolite production, because these organelles are crucial in providing energy for follicle growth, oocyte maturation and embryo development, sustaining nuclear and cytoplasmic reorganization (May-Panloup et al., 2007).

The evaluation of mitochondrial proteins in immature oocytes confirmed the reports with JC-1 or Mito tracker, which revealed the localization of mitochondria across the ooplasm, while active mitochondria were specifically localized into the subcortex area of the oocyte (Results 3.). Mitochondria of immature oocytes are rounder, whereas in mature oocytes they seem smaller and sharper. Our super resolution images are so far the best characterization of the mitochondria in maturing oocytes, so we cannot compare it to other studies in literature, which use lower resolution techniques. Nonetheless, we can speculate from our images that, rather than the metabolic level, a mechanism which could be involved in this transition is mitochondrial fusion/fission, a process well characterized in maturing oocytes (Van Blerkom, 2004). The shape of the mitochondrion, however, is known to be a reflection of its activity, as tubular and interconnected structures are associated with a higher presence of cristae, and in general a greater number of OXPHOS complexes, whereas a rounder and smaller shape is generally associated to a lack of activity (Van Blerkom, 2004; Almansa-Odoñez et al., 2020; van der Rees, 2021). Taking this into consideration, we may be witnessing the final shutting down of the mitochondrial network that supported the growth of the GV oocyte, to enter the more quiescent metabolic phase that characterize the early embryo development. However, we did not observe such a decrease in membrane potential, NADH concentration or DLAT presence, which indicates that this change may either not reflect an accompanying change in metabolic activity, or that the metabolic shut down will happen later on, at fertilization.

Using non-invasive live imaging we were able to detect the metabolic profile through the *in vitro* maturation, from GV to MII, in each of the investigated oocytes. As reported in Results 3., we observed a small increase of 4% metabolism in the ten hours immediately

after GVBD. The metabolic profile detected was similar across samples, and this increase in metabolism was observed in almost all the oocytes from young women. This is reasonable since after GVBD the oocytes need to accomplish several nuclear and cytoplasmic changes and relocation of organelles and chromosomes (e.g. spindle assembly and chromatid segregation). On the contrary, in oocytes that did not mature, we did not find the same increase. We saw, indeed, a higher variability among these oocytes, with some having a high increase, and some a decrease, which on average resulted in a higher NAD concentration of 14%, significantly more than the "modest" 4% of the ones that matured.

Overall, these observations can be interpreted with the "Goldilocks theory" postulated in the early XXI century by Leese (Leese, 2002). He hypothesized that embryo development was associated with a "*"quiet" rather than "active" metabolism"* (Leese, 2002). A few years later, thanks to new studies on non-invasive evaluation of amino acids metabolic turnover in preimplantation embryos (Houghton et al., 2002; Brison et al., 2004) corroborating the hypothesis, the theory was revisited: we have to distinguish between *"Functional Quietness"*, defined as metabolic activity changes part of the natural developmental behaviour of embryos, and *"Loss of quietness in response to (environmental) stress"* (Leese et al., 2022). As recently reviewed by the main promoters of the theory, the commonplace "more is better" is not appropriate in the case of oocyte maturation and embryo development (Leese et al., 2022). Indeed, they reported that developmental embryos have a *"Optimal Goldilocks range"* in which the metabolic activity is neither too high nor too low, but in the range sufficient for the developing embryo to survive and grow (Leese et al., 2022).

The applicability of this theory has reached beyond human early embryo development. Indeed, in a study on bovine oocytes, it was reported that oocytes with higher and lower developmental potential present different metabolic activity and, specifically, poorer quality was related to higher nucleotide metabolism turnover (Collado-Fernandez et al., 2012).

8. MITOCHONDRIA AND METABOLISM ARE ALTERED IN ADVANCED MATERNAL AGE OOCYTES

We saw significant differences in mitochondrial metabolism in oocytes from AMA women, compared to the ones of younger donors. Specifically, we found a very significant decrease in the presence of the mitochondrial subunit of the pyruvate dehydrogenase in AMA oocytes. Despite being an indirect proxy for the measure of activity, it seems these oocytes have serious impairments in the mitochondria in general, as also observed in several other studies, which pointed out a decrease in the mitochondrial membrane potential and mtDNA (Perry et al., 2015; Pasquariello et al., 2019; van der Reest et al., 2021; Kirillova et al., 2021). We found such a lower enzyme detection that we expected also a significant drop in metabolite presence. However, while we did find some differences in NAD(P)H and FAD concentration, they were not comparable to the mitochondrial protein abundance decrease. In fact, every oocyte showed variations in NADH concentration through *in vitro* culture, some increasing their NADH concentration and others decreasing it. This was evident in oocytes that matured, and even more in oocytes that did not. In oocytes, mitochondrial ATP production is mainly through mitochondrial metabolism, while glycolysis accounts for less than 10% of the total ATP production (Hoshino et al., 2018), so that a decrease in mitochondrial activity should be mostly connected to ATP decrease and a consequent decrease in NADH concentrations (Igarashi et al., 2005). The fact that we did not see a sharp drop in the intensity levels of NADH could be due to the fact that the sources of NADH production are several, including glycolysis and the Krebs Cycle (Pelley, 2012).

9. MITOCHONDRIA AND NUCLEAR MATURATION: CAUSE AND CONSEQUENCE?

One of the main goals of this thesis was to assess the link between meiosis progression and mitochondrial metabolism of the oocyte. We first analysed the physiological status in oocytes from young donors and concluded that a steady metabolism with a slight increase is consistently associated with reaching the MII stage. In our dataset, the

maturation rate of the GV oocytes for these women was ~86%. However, we did not find the same homogeneous increase in oocytes that did not mature, but rather a highly variable pattern, with some oocytes recording a high increase, and some a decrease, which in average resulted in a higher NAD concentration of 14%, significantly more than the "modest" 4% of the ones that matured. This pointed towards an association between a finely tuned metabolic progression and successful maturation. In AMA oocytes, we confirmed a lower abundance of metabolic enzymes associated to a lower maturation rate and highly fluctuating levels of NADH associated to the inability to progress to MII. However, this association by itself was not enough to provide a functional link between metabolism and meiotic progression. Thus, we decided to functionally test the link between metabolism and maturation in young oocytes through the pharmacological inhibition of mitochondrial activity with FCCP, a well-known mitochondrial OXPHOS uncoupler. Interestingly, we found a drop in approximately 40% in maturation rates, similarly to what we had observed in the AMA group. Hence, we showed an association between mitochondrial metabolism and successful meiosis progression.

We can assume that the metabolic profile of young oocytes able to mature in our dataset could be a good reference to identify the *"Optimal Goldilocks range"* (Leese et al., 2022) that healthy human oocytes need to proceed in meiosis. Fluctuations (i.e. increasing metabolism, as we observed in our dataset of young oocytes) through maturation are necessary to proceed, while remaining within the tolerable range. Furthermore, the farther you stray from this reference range, the greater are the chances that metabolic level is too high or too low (i.e. *"metabolic activity too quiescent to support requirements"*, (Leese et al., 2022)), resulting in a decreased ability of these oocytes to progress in meiosis and reach the MII stage.

10. WHO CAME FIRST, THE CHICKEN OR THE EGG?

"Who came first, the chicken or the egg?" or, more to the point: "Who came first, metabolism or transcriptional remodelling?" It is mitochondrial metabolism that drives transcript processing and all downstream changes during oocyte maturation, or is it transcriptome remodelling itself that determines the achievement of nuclear and cytoplasmic maturity?

This project was started to test the hypothesis that mitochondria drive mRNA processing of maturing oocytes and that mitochondrial alterations in metabolism, activity or abundance can influence the remodelling of the transcriptome, resulting in poor quality oocytes with compromised nuclear and cytoplasmic meiotic maturation. And whether this can explain the oocyte quality decay observed in oocytes from AMA women.

At the end of this project, our proposed operating model is that mitochondrial metabolism is a necessary but not sufficient condition to achieve meiotic maturation. The oocyte needs a certain amount of metabolism to correctly resume meiosis, break down the GV, reorganize organelles, assemble a functional spindle, and segregate chromosomes. But the correct mRNA processing of transcripts functionally associated with meiosis and that the oocyte needs immediately to move forward, including the correct isoforms of certain meiosis-related genes, is also critical.

Our data obtained from oocytes that failed to mature after 30 h of IVM (FTM-GV) retaining the GV, suggest that without GVBD those oocytes are unable to remodel the transcriptome (i.e. those oocytes shown the same transcriptional profile of immature GV oocytes). Furthermore, live imaging revealed that mitochondria in FTM-GV try to reorganize themselves several times to sustain the incoming maturation, but, in absence of GVBD, none of the downstream processing can happen. However, mitochondrial metabolism must certainly be in the right range to sustain the transcriptional remodelling of the meiosis-related genes, and mitochondrial dysfunction and/or displacements from the established metabolism range can explain a proportion of the AMA oocytes that fail meiosis progression.

11. FUTURE PERSPECTIVES

In the discussion, some research avenues were identified to further tease apart the intricated synergy between the mechanisms involved during meiotic maturation, and how they are impacted by aging.

The planned follow up experiments are:

- To explore the genes whose splicing pattern changes through maturation as targets in functional studies. For example, the *TUBB8* isoforms ratio between MII and GV stages could be altered with RNA editing, and the oocyte phenotype in terms of meiotic transit and downstream translation could be analysed (Richter and Lasko, 2011; Susor et al., 2015; Jansova et al., 2018; Jansova et al., 2021).

- To inhibit the spliceosome machinery using erythromycin, an antibiotic that acts on the spliceosome B/C complex and inhibits translation (Effenberger et al., 2016). Several molecules can be successfully used to impair splicing (Effenberger et al., 2016), however erythromycin has a lower toxicity and, therefore, fewer side effects. Moreover, the use of erythromycin to cause mis-splicing is well described in the literature (Hertweck et al., 2002; Jenquin et al., 2019), although no studies have been conducted in human oocytes yet. Since the study of the transcriptome of maturing oocytes has revealed the crucial role of the spliceosome machinery that orchestrates the processing of specific meiosis-related genes to achieve meiotic maturation, pharmacological inhibition should help test whether an oocyte with altered splicing is unable to successfully reach the MII stage.

- To produce a single cell RNA transcriptome of oocytes collected from young (4-8 years old) and old (10-12 years old) cows and evaluate the transcriptional remodelling during meiotic maturation. This should provide new insights into the changes brought about by aging, and likely confirmation that the cow is a good model of oocyte maturation in general and, specifically, the progressive decay in oocyte quality associated with age.

- To compare the transcriptomic and metabolic profiles in batches of GV and IVM-MII oocytes from young and AMA women. We have already performed metabolic evaluation of a set of 10 young and 10 AMA oocytes, and the same oocytes were then prepared for single cell RNA-sequencing, with the results pending. This final experiment should identify the link between transcriptome remodelling and mitochondrial metabolism and delineate the decaying trend of mitochondrial metabolism and transcriptome remodelling in aged oocytes. Finally, it will provide the opportunity to identify potential targets for subsequent functional studies.

CONCLUSIONS

1. Human oocytes undergoing meiosis need to remodel their transcriptome in order to successfully progress in maturation. Specifically, key meiosis-associated genes change isoform composition after meiosis resumption, mostly on their 3'UTR, to reach the MII stage, assemble a functional meiotic spindle and, ultimately, achieve meiotic competence.

2. Remodelling of the transcriptome through the GV-MII transition seems to be associated to the generation of shorter 3'UTR isoforms in mature oocytes, as a key feature of transcriptome regulation.

3. Global gene expression changes during oocyte maturation, and genes associated to the spliceosome and RNA transport are the most differentially expressed between immature and matured oocytes.

4. *In vitro* matured MII oocytes present small, but significant, differences in terms of RNA processing compared to *in vivo* matured ones, highlighting an incorrect mRNA processing during maturation *in vitro*. The differences detected were mainly in genes associated to meiotic maturation, spindle assembly and positioning, and chromosome condensation, reflecting the partially mature state of *in vitro* matured MII oocytes, despite being morphologically similar to competent MII oocytes.

5. The gene expression of cow maturing oocytes changes significantly in the transition between immature and matured stages. The genes affected are related to RNA processing and transport, protein synthesis, organelles remodelling and reorganization, and metabolism. The global gene expression and the associated changes through the GV-MII transition are conserved between bovine and humans.

6. Failure to remodel the transcriptome is a possible cause of oocytes quality decay in a cow model of POI. Moreover, this feature seems to mimic the high number of genetic alterations causing POI in women.

7. High-resolution microscopy of mitochondrial proteins in human GV and MII oocytes revealed that while mitochondria are distributed across the ooplasm, active mitochondria are specifically localized mostly in the subcortical area. It also revealed changes in mitochondrial shape and spatial distribution in the oocyte's cytoplasm during final meiotic maturation.

8. The mitochondrial metabolism increases in a controlled fashion in maturing oocytes reaching the MII stage. Moreover, the variability in the metabolic profile is smaller in maturing young oocytes than in AMA oocytes.

9. Immature oocytes from AMA women present lower mitochondrial activity and lower mitochondrial metabolism than oocytes from young woman, concordant with their lower *in vitro* maturation rates.

10. Young oocytes with artificially impaired mitochondrial function mimic AMA oocytes in terms of mitochondrial activity, metabolism, and inability to successfully reach the MII stage and, overall, achieve meiotic competence. This highlights the functional link between mitochondrial metabolism and meiotic progression in human oocytes.

REFERENCES

Albertini, D. F., Combelles, C. M. H., Benecchi, E., & Carabatsos, M. J. (2001). Cellular basis for paracrine regulation of ovarian follicle development. *Reproduction*, *121*(5), 647–653. https://doi.org/10.1530/REP.0.1210647

Almansa-Ordonez, A., Bellido, R., Vassena, R., Barragan, M., & Zambelli, F. (2020). Oxidative stress in reproduction: A mitochondrial perspective. In *Biology* (Vol. 9, Issue 9, pp. 1–21). MDPI AG. https://doi.org/10.3390/biology9090269

Almonacid, M., Terret, M. E., & Verlhac, M. H. (2018). Control of nucleus positioning in mouse oocytes. *Seminars in Cell & Developmental Biology*, *82*, 34–40. https://doi.org/10.1016/J.SEMCDB.2017.08.010

Alushin, G. M., Lander, G. C., Kellogg, E. H., Zhang, R., Baker, D., & Nogales, E. (2014). High-resolution microtubule structures reveal the structural transitions in αβ-tubulin upon GTP hydrolysis. *Cell*, *157*(5), 1117–1129. https://doi.org/10.1016/J.CELL.2014.03.053

Alviggi, C., Humaidan, P., Howles, C. M., Tredway, D., & Hillier, S. G. (2009). Biological versus chronological ovarian age: implications for assisted reproductive technology. *Reproductive Biology and Endocrinology : RB&E*, *7*, 101. https://doi.org/10.1186/1477-7827-7-101

Amjad, S., Nisar, S., Bhat, A. A., Shah, A. R., Frenneaux, M. P., Fakhro, K., Haris, M., Reddy, R., Patay, Z., Baur, J., & Bagga, P. (2021). Role of NAD+ in regulating cellular and metabolic signaling pathways. *Molecular Metabolism*, *49*. https://doi.org/10.1016/J.MOLMET.2021.101195

Angell, R. (1995). Meiosis I in human oocytes. *Cytogenetics and Cell Genetics*, *69*(3–4), 266–272. https://doi.org/10.1159/000133977

Aoki, F. (2022). Zygotic gene activation in mice: profile and regulation. *The Journal of Reproduction and Development*, *68*(2), 79. https://doi.org/10.1262/JRD.2021-129

Arias-Álvarez, M., García-García, R. M., López-Tello, J., Rebollar, P. G., Gutiérrez-Adán, A., & Lorenzo, P. L. (2017). In vivo and in vitro maturation of rabbit oocytes differently affects the gene expression profile, mitochondrial distribution, apoptosis and early embryo development. *Reproduction, Fertility, and Development*, *29*(9), 1667–1679. https://doi.org/10.1071/RD15553

Balaban, B., & Urman, B. (2006). Effect of oocyte morphology on embryo development and implantation. *Reproductive Biomedicine Online*, *12*(5), 608–615. https://doi.org/10.1016/S1472-6483(10)61187-X

Balakier, H., Bouman, D., Sojecki, A., Librach, C., & Squire, J. A. (2002). Morphological and cytogenetic analysis of human giant oocytes and giant embryos. *Human Reproduction (Oxford, England)*, *17*(9), 2394–2401. https://doi.org/10.1093/HUMREP/17.9.2394

Baralle, F. E., & Giudice, J. (2017). Alternative splicing as a regulator of development and tissue identity. *Nature Reviews. Molecular Cell Biology*, *18*(7), 437–451. https://doi.org/10.1038/NRM.2017.27

Beaurepaire, E., & Mertz, J. (2002). Epifluorescence collection in two-photon microscopy. *Applied Optics*, *41*(25), 5376. https://doi.org/10.1364/AO.41.005376

Bebbere, D., Coticchio, G., Borini, A., & Ledda, S. (2022). Oocyte aging: looking beyond chromosome segregation errors. *Journal of Assisted Reproduction and Genetics*, *39*(4), 793. https://doi.org/10.1007/S10815-022-02441-Z

Becker, W. (2012). Fluorescence lifetime imaging--techniques and applications. *Journal of Microscopy*, *247*(2), 119–136. https://doi.org/10.1111/J.1365-2818.2012.03618.X

Bellone, M., Zuccotti, M., Redi, C. A., & Garagna, S. (2009). The position of the germinal vesicle and the chromatin organization together provide a marker of the developmental competence of mouse antral oocytes. *Reproduction (Cambridge, England)*, *138*(4), 639–643. https://doi.org/10.1530/REP-09-0230

Bennabi, I., Quéguiner, I., Kolano, A., Boudier, T., Mailly, P., Verlhac, M., & Terret, M. (2018). Shifting meiotic to mitotic spindle assembly in oocytes disrupts chromosome alignment. *EMBO Reports*, *19*(2), 368. https://doi.org/10.15252/EMBR.201745225

Bennabi, I., Terret, M. E., & Verlhac, M. H. (2016). Meiotic spindle assembly and chromosome segregation in oocytes. *The Journal of Cell Biology*, *215*(5), 611–619. https://doi.org/10.1083/JCB.201607062

Bettegowda, A., Patel, O. V., Ireland, J. J., & Smith, G. W. (2006). Quantitative analysis of messenger RNA abundance for ribosomal protein L-15, cyclophilin-A, phosphoglycerokinase, beta-glucuronidase, glyceraldehyde 3-phosphate dehydrogenase, beta-actin, and histone H2A during bovine oocyte maturation and early embryogenesis in vitro. *Molecular Reproduction and Development*, *73*(3), 267–278. https://doi.org/10.1002/MRD.20333

Bhatti, J. S., Bhatti, G. K., & Reddy, P. H. (2017). Mitochondrial dysfunction and oxidative stress in metabolic disorders - A Step towards mitochondria based therapeutic strategies. *Biochimica et Biophysica Acta*, *1863*(5), 1066. https://doi.org/10.1016/J.BBADIS.2016.11.010

Biswas, L., Tyc, K., El Yakoubi, W., Morgan, K., Xing, J., & Schindler, K. (2021). Meiosis interrupted: the genetics of female infertility via meiotic failure. *Reproduction (Cambridge, England)*, *161*(2), R13–R35. https://doi.org/10.1530/REP-20-0422

Blengini, C. S., Ibrahimian, P., Vaskovicova, M., Drutovic, D., Solc, P., & Schindler, K. (2021). Aurora kinase A is essential for meiosis in mouse oocytes. *PLoS Genetics*, *17*(4). https://doi.org/10.1371/JOURNAL.PGEN.1009327

Boguszewska, K., Szewczuk, M., Kazmierczak-Baranska, J., & Karwowski, B. T. (2020). The Similarities between Human Mitochondria and Bacteria in the Context of Structure,

Genome, and Base Excision Repair System. *Molecules*, *25*(12). https://doi.org/10.3390/MOLECULES25122857

Boke, E., Ruer, M., Wühr, M., Coughlin, M., Lemaitre, R., Gygi, S. P., Alberti, S., Drechsel, D., Hyman, A. A., & Mitchison, T. J. (2016). Amyloid-like Self-Assembly of a Cellular Compartment. *Cell*, *166*(3), 637–650. https://doi.org/10.1016/J.CELL.2016.06.051

Bose, M., Lampe, M., Mahamid, J., & Ephrussi, A. (2022). Liquid-to-solid phase transition of oskar ribonucleoprotein granules is essential for their function in Drosophila embryonic development. *Cell*, *185*(8), 1308-1324.e23. https://doi.org/10.1016/J.CELL.2022.02.022

Bouniol-Baly, C., Hamraoui, L., Guibert, J., Beaujean, N., Szöllösi, M. S., & Debey, P. (1999). Differential transcriptional activity associated with chromatin configuration in fully grown mouse germinal vesicle oocytes. *Biology of Reproduction*, *60*(3), 580–587. https://doi.org/10.1095/BIOLREPROD60.3.580

Bowles, J., Knight, D., Smith, C., Wilhelm, D., Richman, J., Mamiya, S., Yashiro, K., Chawengsaksophak, K., Wilson, M. J., Rossant, J., Hamada, H., & Koopman, P. (2006). Retinoid signaling determines germ cell fate in mice. *Science (New York, N.Y.)*, *312*(5773), 596–600. https://doi.org/10.1126/SCIENCE.1125691

Brangwynne, C. P., Eckmann, C. R., Courson, D. S., Rybarska, A., Hoege, C., Gharakhani, J., Jülicher, F., & Hyman, A. A. (2009). Germline P granules are liquid droplets that localize by controlled dissolution/condensation. *Science (New York, N.Y.)*, *324*(5935), 1729–1732. https://doi.org/10.1126/SCIENCE.1172046

Braunschweig, U., Gueroussov, S., Plocik, A. M., Graveley, B. R., & Blencowe, B. J. (2013). Dynamic integration of splicing within gene regulatory pathways. *Cell*, *152*(6), 1252–1269. https://doi.org/10.1016/J.CELL.2013.02.034

Brinkley, B. R. (1985). Microtubule organizing centers. *Annual Review of Cell Biology*, *1*, 145–172. https://doi.org/10.1146/ANNUREV.CB.01.110185.001045

Brison, D. R., Houghton, F. D., Falconer, D., Roberts, S. A., Hawkhead, J., Humpherson, P. G., Lieberman, B. A., & Leese, H. J. (2004). Identification of viable embryos in IVF by non-invasive measurement of amino acid turnover. *Human Reproduction (Oxford, England)*, *19*(10), 2319–2324. https://doi.org/10.1093/HUMREP/DEH409

Brunet, S., & Maro, B. (2007). Germinal vesicle position and meiotic maturation in mouse oocyte. *Reproduction (Cambridge, England)*, *133*(6), 1069–1072. https://doi.org/10.1530/REP-07-0036

Bryan, J., & Wilson, L. (1971). Are cytoplasmic microtubules heteropolymers? *Proceedings of the National Academy of Sciences of the United States of America*, *68*(8), 1762–1766. https://doi.org/10.1073/PNAS.68.8.1762

Buratini, J., Dellaqua, T. T., de Lima, P. F., Renzini, M. M., Canto, M. D., & Price, C. A. (2023). Oocyte secreted factors control genes regulating FSH signaling and the maturation cascade in cumulus cells: the oocyte is not in a hurry. *Journal of Assisted Reproduction and Genetics*. https://doi.org/10.1007/S10815-023-02822-Y

Burbank, K. S., & Mitchison, T. J. (2006). Microtubule dynamic instability. *Current Biology : CB*, *16*(14). https://doi.org/10.1016/J.CUB.2006.06.044

Burbank, K. S., Groen, A. C., Perlman, Z. E., Fisher, D. S., & Mitchison, T. J. (2006). A new method reveals microtubule minus ends throughout the meiotic spindle. *The Journal of Cell Biology*, *175*(3), 369–375. https://doi.org/10.1083/JCB.200511112

Caetano, L. C., Verruma, C. G., Pinaffi, F. L. V., Jardim, I. B., Furtado, G. P., Silva, L. A., Furtado, C. L. M., & Rosa-E-Silva, A. C. J. D. S. (2023). In vivo and in vitro matured bovine oocytes present a distinct pattern of single-cell gene expression. *Zygote*, *31*(1), 31–43. https://doi.org/10.1017/S0967199422000478

Caley, D. P., Pink, R. C., Trujillano, D., & Carter, D. R. F. (2010). Long noncoding RNAs, chromatin, and development. *TheScientificWorldJournal*, *10*, 90–102. https://doi.org/10.1100/TSW.2010.7

Cavalier-Smith, T. (2006). Origin of mitochondria by intracellular enslavement of a photosynthetic purple bacterium. *Proceedings of the Royal Society B: Biological Sciences*, *273*(1596), 1943. https://doi.org/10.1098/RSPB.2006.3531

Cavazza, T., & Vernos, I. (2016). The RanGTP pathway: From nucleo-cytoplasmic transport to spindle assembly and beyond. *Frontiers in Cell and Developmental Biology*, *3*(JAN), 169805. https://doi.org/10.3389/FCELL.2015.00082/BIBTEX

Chaaban, S., & Brouhard, G. J. (2017). A microtubule bestiary: structural diversity in tubulin polymers. *Molecular Biology of the Cell*, *28*(22), 2924–2931. https://doi.org/10.1091/MBC.E16-05-0271

Charalambous, C., Webster, A., & Schuh, M. (2023). Aneuploidy in mammalian oocytes and the impact of maternal ageing. *Nature Reviews. Molecular Cell Biology*, *24*(1), 27–44. https://doi.org/10.1038/S41580-022-00517-3

Checa, J., & Aran, J. M. (2020). Reactive Oxygen Species: Drivers of Physiological and Pathological Processes. *Journal of Inflammation Research*, *13*, 1057. https://doi.org/10.2147/JIR.S275595

Cheeseman, L. P., Boulanger, J., Bond, L. M., & Schuh, M. (2016). Two pathways regulate cortical granule translocation to prevent polyspermy in mouse oocytes. *Nature Communications 2016 7:1*, *7*(1), 1–13. https://doi.org/10.1038/ncomms13726

Chen, Q., Vazquez, E. J., Moghaddas, S., Hoppel, C. L., & Lesnefsky, E. J. (2003). Production of Reactive Oxygen Species by Mitochondria: CENTRAL ROLE OF COMPLEX III. *Journal of Biological Chemistry*, *278*(38), 36027–36031. https://doi.org/10.1074/JBC.M304854200

Chenevert, J., Roca, M., Besnardeau, L., Ruggiero, A., Nabi, D., McDougall, A., Copley, R. R., Christians, E., & Castagnetti, S. (2020). The Spindle Assembly Checkpoint Functions during Early Development in Non-Chordate Embryos. *Cells*, *9*(5). https://doi.org/10.3390/CELLS9051087

Cheng, S., Altmeppen, G., So, C., Welp, L. M., Penir, S., Ruhwedel, T., Menelaou, K., Harasimov, K., Stützer, A., Blayney, M., Elder, K., Möbius, W., Urlaub, H., & Schuh, M. (2022). Mammalian oocytes store mRNAs in a mitochondria-associated membraneless compartment. *Science (New York, N.Y.)*, *378*(6617). https://doi.org/10.1126/SCIENCE.ABQ4835

Chouinard, L. A. (1975). A light- and electron-microscope study of the oocyte nucleus during development of the antral follicle in the prepubertal mouse. *Journal of Cell Science*, *17*(3), 589–615. https://doi.org/10.1242/JCS.17.3.589

Chrétien, D., & Fuller, S. D. (2000). Microtubules switch occasionally into unfavorable configurations during elongation. *Journal of Molecular Biology*, *298*(4), 663–676. https://doi.org/10.1006/JMBI.2000.3696

Chrétien, D., & Wade, R. H. (1991). New data on the microtubule surface lattice. *Biology of the Cell*, *71*(1–2), 161–174. https://doi.org/10.1016/0248-4900(91)90062-R

Cimadomo, D., Fabozzi, G., Vaiarelli, A., Ubaldi, N., Ubaldi, F. M., & Rienzi, L. (2018). Impact of Maternal Age on Oocyte and Embryo Competence. *Frontiers in Endocrinology*, *9*(JUL), 1. https://doi.org/10.3389/FENDO.2018.00327

Claw, K. G., & Swanson, W. J. (2012). Evolution of the egg: new findings and challenges. *Annual Review of Genomics and Human Genetics*, *13*, 109–125. https://doi.org/10.1146/ANNUREV-GENOM-090711-163745

Clift, D., & Schuh, M. (2013). Restarting life: fertilization and the transition from meiosis to mitosis. *Nature Reviews Molecular Cell Biology 2013 14:9*, *14*(9), 549–562. https://doi.org/10.1038/nrm3643

Clift, D., & Schuh, M. (2015). A three-step MTOC fragmentation mechanism facilitates bipolar spindle assembly in mouse oocytes. *Nature Communications*, *6*. https://doi.org/10.1038/NCOMMS8217

Collado-Fernandez, E., Picton, H. M., & Dumollard, Ré. (2012). Metabolism throughout follicle and oocyte development in mammals. *The International Journal of Developmental Biology*, *56*(10–12), 799–808. https://doi.org/10.1387/IJDB.120140EC

Combelles, C. M. H., & Albertini, D. F. (2001). Microtubule patterning during meiotic maturation in mouse oocytes is determined by cell cycle-specific sorting and redistribution of gamma-tubulin. *Developmental Biology*, *239*(2), 281–294. https://doi.org/10.1006/DBIO.2001.0444

Cooper, T. A., Wan, L., & Dreyfuss, G. (2009). RNA and disease. *Cell*, *136*(4), 777–793. https://doi.org/10.1016/J.CELL.2009.02.011

Cornet-Bartolomé, D., Barragán, M., Zambelli, F., Ferrer-Vaquer, A., Tiscornia, G., Balcells, S., Rodriguez, A., Grinberg, D., & Vassena, R. (2021). Human oocyte meiotic maturation is associated with a specific profile of alternatively spliced transcript isoforms. *Molecular Reproduction and Development*, *88*(9), 605–617. https://doi.org/10.1002/MRD.23526

Coticchio, G., Albertini, D. F., & De Santis, L. (2013). Oogenesis. *Oogenesis*, 1–353. https://doi.org/10.1007/978-0-85729-826-3/COVER

Coticchio, G., Dal Canto, M., Renzini, M. M., Guglielmo, M. C., Brambillasca, F., Turchi, D., Novara, P. V., & Fadini, R. (2014). Oocyte maturation: Gamete-somatic cells interactions, meiotic resumption, cytoskeletal dynamics and cytoplasmic reorganization. *Human Reproduction Update*, *21*(4), 427–454. https://doi.org/10.1093/humupd/dmv011

Coticchio, G., Dal Canto, M., Renzini, M. M., Guglielmo, M. C., Brambillasca, F., Turchi, D., Novara, P. V., & Fadini, R. (2015). Oocyte maturation: gamete-somatic cells interactions, meiotic resumption, cytoskeletal dynamics and cytoplasmic reorganization. *Human Reproduction Update*, *21*(4), 427–454. https://doi.org/10.1093/HUMUPD/DMV011

Das, D., & Arur, S. (2022). Regulation of oocyte maturation: Role of conserved ERK signaling. *Molecular Reproduction and Development*, *89*(9), 353–374. https://doi.org/10.1002/MRD.23637

De La Fuente, R. (2006). Chromatin modifications in the germinal vesicle (GV) of mammalian oocytes. *Developmental Biology*, *292*(1), 1–12. https://doi.org/10.1016/J.YDBIO.2006.01.008

De Vos, M., Devroey, P., & Fauser, B. C. (2010). Primary ovarian insufficiency. *Lancet (London, England)*, *376*(9744), 911–921. https://doi.org/10.1016/S0140-6736(10)60355-8

Derti, A., Garrett-Engele, P., MacIsaac, K. D., Stevens, R. C., Sriram, S., Chen, R., Rohl, C. A., Johnson, J. M., & Babak, T. (2012). A quantitative atlas of polyadenylation in five mammals. *Genome Research*, *22*(6), 1173–1183. https://doi.org/10.1101/GR.132563.111

Dias, A. P., Dufu, K., Lei, H., & Reed, R. (2010). A role for TREX components in the release of spliced mRNA from nuclear speckle domains. *Nature Communications*, *1*(7). https://doi.org/10.1038/NCOMMS1103

Duan, X., & Sun, S. C. (2019). Actin cytoskeleton dynamics in mammalian oocyte meiosis. *Biology of Reproduction*, *100*(1), 15–24. https://doi.org/10.1093/BIOLRE/IOY163

Dumollard, R., Duchen, M., & Carroll, J. (2007). The role of mitochondrial function in the oocyte and embryo. *Current Topics in Developmental Biology*, *77*, 21–49. https://doi.org/10.1016/S0070-2153(06)77002-8

Dumont, J., Petri, S., Pellegrin, F., Terret, M. E., Bohnsack, M. T., Rassinier, P., Georget, V., Kalab, P., Gruss, O. J., & Verlhac, M. H. (2007). A centriole- and RanGTP-independent spindle assembly pathway in meiosis I of vertebrate oocytes. *The Journal of Cell Biology*, *176*(3), 295–305. https://doi.org/10.1083/JCB.200605199

Duran, H. E., Simsek-Duran, F., Oehninger, S. C., Jones, H. W., & Castora, F. J. (2011). The association of reproductive senescence with mitochondrial quantity, function, and DNA integrity in human oocytes at different stages of maturation. *Fertility and Sterility*, *96*(2), 384–388. https://doi.org/10.1016/J.FERTNSTERT.2011.05.056

Ebner, T., Moser, M., & Tews, G. (2006). Is oocyte morphology prognostic of embryo developmental potential after ICSI? *Reproductive Biomedicine Online*, *12*(4), 507–512. https://doi.org/10.1016/S1472-6483(10)62006-8

Effenberger, K. A., Urabe, V. K., & Jurica, M. S. (2017). Modulating splicing with small molecular inhibitors of the spliceosome. *Wiley Interdisciplinary Reviews. RNA*, *8*(2). https://doi.org/10.1002/WRNA.1381

Eichenlaub-Ritter, U., & Peschke, M. (2002). Expression in in-vivo and in-vitro growing and maturing oocytes: focus on regulation of expression at the translational level. *Human Reproduction Update*, *8*(1), 21–41. https://doi.org/10.1093/HUMUPD/8.1.21

EK, M., & B, G. (2006). Asymmetric spindle positioning. *Current Opinion in Cell Biology*, *18*(1), 79–85. https://doi.org/10.1016/J.CEB.2005.12.006

El-Hayek, S., & Clarke, H. J. (2015). Follicle-stimulating hormone increases gap junctional communication between somatic and germ-line follicular compartments during murine oogenesis. *Biology of Reproduction*, *93*(2), 47–48. https://doi.org/10.1095/BIOLREPROD.115.129569/2434266

Evans, J. P., & Janice Evans, C. P. (2020). Preventing polyspermy in mammalian eggs—Contributions of the membrane block and other mechanisms. *Molecular Reproduction and Development*, *87*(3), 341–349. https://doi.org/10.1002/MRD.23331

Evsikov, A. V., & De Evsikova, C. M. (2009). Gene expression during the oocyte-to-embryo transition in mammals. *Molecular Reproduction and Development*, *76*(9), 805–818. https://doi.org/10.1002/MRD.21038

Faramarzi, A., Khalili, M. A., Ashourzadeh, S., & Palmerini, M. G. (2018). Does rescue in vitro maturation of germinal vesicle stage oocytes impair embryo morphokinetics development? *Zygote (Cambridge, England)*, *26*(5), 430–434. https://doi.org/10.1017/S0967199418000515

Fatica, A., & Bozzoni, I. (2014). Long non-coding RNAs: new players in cell differentiation and development. *Nature Reviews. Genetics*, *15*(1), 7–21. https://doi.org/10.1038/NRG3606

FD, H., JA, H., PG, H., JE, H., AH, B., AJ, R., & HJ, L. (2002). Non-invasive amino acid turnover predicts human embryo developmental capacity. *Human Reproduction (Oxford, England)*, *17*(4), 999–1005. https://doi.org/10.1093/HUMREP/17.4.999

Feng, R., Sang, Q., Kuang, Y., Sun, X., Yan, Z., Zhang, S., Shi, J., Tian, G., Luchniak, A., Fukuda, Y., Li, B., Yu, M., Chen, J., Xu, Y., Guo, L., Qu, R., Wang, X., Sun, Z., Liu, M., … Wang, L. (2016). Mutations in TUBB8 and Human Oocyte Meiotic Arrest. *The New England Journal of Medicine*, *374*(3), 223–232. https://doi.org/10.1056/NEJMOA1510791

Ferrarini Zanetti, B., Paes de Almeida Ferreira Braga, D., Souza Setti, A., de Cássia Sávio Figueira, R., Iaconelli, A., & Borges, E. (2018). Is perivitelline space morphology of the oocyte associated with pregnancy outcome in intracytoplasmic sperm injection cycles? *European Journal of Obstetrics, Gynecology, and Reproductive Biology*, *231*, 225–229. https://doi.org/10.1016/J.EJOGRB.2018.10.053

Ferreira, E. M., Vireque, A. A., Adona, P. R., Meirelles, F. V, Ferriani, R. A., & Navarro, P. A. A. S. (n.d.). *Cytoplasmic maturation of bovine oocytes: Structural and biochemical modifications and acquisition of developmental competence*. https://doi.org/10.1016/j.theriogenology.2008.10.023

Ferrer-Vaquer, A., Barragán, M., Rodríguez, A., & Vassena, R. (2019). Altered cytoplasmic maturation in rescued in vitro matured oocytes. *Human Reproduction*, *34*(6), 1095–1105. https://doi.org/10.1093/HUMREP/DEZ052

Figueira, R. D. C. S., De Almeida Ferreira Braga, D. P., Semião-Francisco, L., Madaschi, C., Iaconelli, A., & Borges, E. (2010). Metaphase II human oocyte morphology: contributing factors and effects on fertilization potential and embryo developmental ability in ICSI cycles. *Fertility and Sterility*, *94*(3), 1115–1117. https://doi.org/10.1016/J.FERTNSTERT.2009.11.039

FitzHarris, G., Marangos, P., & Carroll, J. (2007). Changes in endoplasmic reticulum structure during mouse oocyte maturation are controlled by the cytoskeleton and cytoplasmic dynein. *Developmental Biology*, *305*(1), 133–144. https://doi.org/10.1016/J.YDBIO.2007.02.006

Francis, S. E., & Davis, T. N. (1999). The spindle pole body of Saccharomyces cerevisiae: Architecture and assembly of the core components. *Current Topics in Developmental Biology*, *49*, 105–132. https://doi.org/10.1016/S0070-2153(99)49006-4

Gandolfi, F., Luciano, A. M., Modina, S., Ponzini, A., Pocar, P., Armstrong, D. T., & Lauria, A. (1997). The in vitro developmental competence of bovine oocytes can be related to the morphology of the ovary. *Theriogenology*, *48*(7), 1153–1160. https://doi.org/10.1016/S0093-691X(97)00348-8

Gao, S., Czirr, E., Chung, Y. G., Han, Z., & Latham, K. E. (2004). Genetic Variation in Oocyte Phenotype Revealed Through Parthenogenesis and Cloning: Correlation with

Differences in Pronuclear Epigenetic Modification. *Biology of Reproduction*, *70*(4), 1162–1170. https://doi.org/10.1095/BIOLREPROD.103.024216

Gardner, D. K., & Sakkas, D. (2003). Assessment of embryo viability: The ability to select a single embryo for transfer - A review. *Placenta*, *24*(SUPPL. B), S5. https://doi.org/10.1016/S0143-4004(03)00136-X

Ghukasyan, V. V., & Heikal, A. A. (2014). Natural Biomarkers for Cellular Metabolism: Biology, Techniques, and Applications. *Natural Biomarkers for Cellular Metabolism: Biology, Techniques, and Applications*, 1–374. https://doi.org/10.1201/B17427

Goodson, H. V., & Jonasson, E. M. (2018). Microtubules and Microtubule-Associated Proteins. *Cold Spring Harbor Perspectives in Biology*, *10*(6). https://doi.org/10.1101/CSHPERSPECT.A022608

Gorbsky, G. J. (2015). The spindle checkpoint and chromosome segregation in meiosis. *The FEBS Journal*, *282*(13), 2458–2474. https://doi.org/10.1111/FEBS.13166

Gosden, R., & Lee, B. (2010). Portrait of an oocyte: our obscure origin. *The Journal of Clinical Investigation*, *120*(4), 973–983. https://doi.org/10.1172/JCI41294

Goswami, B. N., Venugopal, V., Sangupta, D., Madhusoodanan, M. S., & Xavier, P. K. (2006). Increasing trend of extreme rain events over India in a warming environment. *Science (New York, N.Y.)*, *314*(5804), 1442–1445. https://doi.org/10.1126/SCIENCE.1132027

Gottlieb, S. F., Tupper, C., Kerndt, C. C., & Tegay, D. H. (2022). Genetics, Nondisjunction. *StatPearls*. https://www.ncbi.nlm.nih.gov/books/NBK482240/

Graf, A., Krebs, S., Heininen-Brown, M., Zakhartchenko, V., Blum, H., & Wolf, E. (2014). Genome activation in bovine embryos: review of the literature and new insights from RNA sequencing experiments. *Animal Reproduction Science*, *149*(1–2), 46–58. https://doi.org/10.1016/J.ANIREPROSCI.2014.05.016

Grenfell, A. W., Heald, R., & Strzelecka, M. (2016). Mitotic noncoding RNA processing promotes kinetochore and spindle assembly in Xenopus. *Journal of Cell Biology*, *214*(2), 133–141. https://doi.org/10.1083/jcb.201604029

Grover, A. R., Fegley, B., Duncan, T. V., & Duncan, F. E. (2018). The oocyte. In *Encyclopedia of Reproduction* (pp. 21–28). Elsevier. https://doi.org/10.1016/B978-0-12-801238-3.64390-8

Gruhn, J. R., Zielinska, A. P., Shukla, V., Blanshard, R., Capalbo, A., Cimadomo, D., Nikiforov, D., Chan, A. C. H., Newnham, L. J., Vogel, I., Scarica, C., Krapchev, M., Taylor, D., Kristensen, S. G., Cheng, J., Ernst, E., Bjørn, A. M. B., Colmorn, L. B., Blayney, M., … Hoffmann, E. R. (2019). Chromosome errors in human eggs shape natural fertility over reproductive life span. *Science (New York, N.Y.)*, *365*(6460), 1466–1469. https://doi.org/10.1126/SCIENCE.AAV7321

Gueth-Hallonet, C., Antony, C., Aghion, J., Santa-Maria, A., Lajoie-Mazenc, I., Wright, M., & Maro, B. (1993). gamma-Tubulin is present in acentriolar MTOCs during early mouse development. *Journal of Cell Science*, *105 (Pt 1)*(1), 157–166. https://doi.org/10.1242/JCS.105.1.157

Hamatani, T., Falco, G., Carter, M. G., Akutsu, H., Stagg, C. A., Sharov, A. A., Dudekula, D. B., VanBuren, V., & Ko, M. S. H. (2004). Age-associated alteration of gene expression patterns in mouse oocytes. *Human Molecular Genetics*, *13*(19), 2263–2278. https://doi.org/10.1093/HMG/DDH241

Handyside, A. H. (2012). Molecular origin of female meiotic aneuploidies. *Biochimica et Biophysica Acta (BBA) - Molecular Basis of Disease*, *1822*(12), 1913–1920. https://doi.org/10.1016/J.BBADIS.2012.07.007

Hangauer, M. J., Vaughn, I. W., & McManus, M. T. (2013). Pervasive transcription of the human genome produces thousands of previously unidentified long intergenic noncoding RNAs. *PLoS Genetics*, *9*(6). https://doi.org/10.1371/JOURNAL.PGEN.1003569

Hassa, H., Aydın, Y., & Taplamacıoğlu, F. (2014). The role of perivitelline space abnormalities of oocytes in the developmental potential of embryos. *Journal of the Turkish German Gynecological Association*, *15*(3), 161. https://doi.org/10.5152/JTGGA.2014.13091

Hassold, T., Hall, H., & Hunt, P. (2007). The origin of human aneuploidy: where we have been, where we are going. *Human Molecular Genetics*, *16*(R2), R203–R208. https://doi.org/10.1093/HMG/DDM243

Haverfield, J., Dean, N. L., Nöel, D., Rémillard-Labrosse, G., Paradis, V., Kadoch, I. J., & FitzHarris, G. (2017). Tri-directional anaphases as a novel chromosome segregation defect in human oocytes. *Human Reproduction (Oxford, England)*, *32*(6), 1293–1303. https://doi.org/10.1093/HUMREP/DEX083

He, M., Zhang, T., Yang, Y., & Wang, C. (2021). Mechanisms of Oocyte Maturation and Related Epigenetic Regulation. *Frontiers in Cell and Developmental Biology*, *9*. https://doi.org/10.3389/FCELL.2021.654028

Heald, R., & Khodjakov, A. (2015). Thirty years of search and capture: The complex simplicity of mitotic spindle assembly. *The Journal of Cell Biology*, *211*(6), 1103–1111. https://doi.org/10.1083/JCB.201510015

Heath, C. G., Viphakone, N., & Wilson, S. A. (2016). The role of TREX in gene expression and disease. *Biochemical Journal*, *473*(19), 2911–2935. https://doi.org/10.1042/BCJ20160010

Heikal, A. A. (2010). Intracellular coenzymes as natural biomarkers for metabolic activities and mitochondrial anomalies. *Biomarkers in Medicine*, *4*(2), 241–263. https://doi.org/10.2217/BMM.10.1

Hendrickson, P. G., Doráis, J. A., Grow, E. J., Whiddon, J. L., Lim, J. W., Wike, C. L., Weaver, B. D., Pflueger, C., Emery, B. R., Wilcox, A. L., Nix, D. A., Peterson, C. M., Tapscott, S. J., Carrell, D. T., & Cairns, B. R. (2017). Conserved roles of mouse DUX and human DUX4 in activating cleavage-stage genes and MERVL/HERVL retrotransposons. *Nature Genetics*, *49*(6), 925–934. https://doi.org/10.1038/NG.3844

Hertig, A. T., & Adams, E. C. (1967). Studies on the human oocyte and its follicle. I. Ultrastructural and histochemical observations on the primordial follicle stage. *The Journal of Cell Biology*, *34*(2), 647–675. https://doi.org/10.1083/JCB.34.2.647

Hertweck, M., Hiller, R., & Mueller, M. W. (2002). Inhibition of nuclear pre-mRNA splicing by antibiotics in vitro. *European Journal of Biochemistry*, *269*(1), 175–183. https://doi.org/10.1046/J.0014-2956.2001.02636.X

Holubcová, Z., Blayney, M., Elder, K., & Schuh, M. (2015). Human oocytes. Error-prone chromosome-mediated spindle assembly favors chromosome segregation defects in human oocytes. *Science (New York, N.Y.)*, *348*(6239), 1143–1147. https://doi.org/10.1126/SCIENCE.AAA9529

Huang, Z., & Wells, D. (2010a). The human oocyte and cumulus cells relationship: new insights from the cumulus cell transcriptome. *Molecular Human Reproduction*, *16*(10), 715–725. https://doi.org/10.1093/MOLEHR/GAQ031

Huang, Z., & Wells, D. (2010b). The human oocyte and cumulus cells relationship: new insights from the cumulus cell transcriptome. *Molecular Human Reproduction*, *16*(10), 715–725. https://doi.org/10.1093/MOLEHR/GAQ031

Hutt, K. J., & Albertini, D. F. (2007). An oocentric view of folliculogenesis and embryogenesis. *Reproductive Biomedicine Online*, *14*(6), 758–764. https://doi.org/10.1016/S1472-6483(10)60679-7

Igarashi, H., Takahashi, T., Takahashi, E., Tezuka, N., Nakahara, K., Takahashi, K., & Kurachi, H. (2005). Aged mouse oocytes fail to readjust intracellular adenosine triphosphates at fertilization. *Biology of Reproduction*, *72*(5), 1256–1261. https://doi.org/10.1095/BIOLREPROD.104.034926

Inoue, F., Parvin, M. S., & Yamasu, K. (2008). Transcription of fgf8 is regulated by activating and repressive cis-elements at the midbrain–hindbrain boundary in zebrafish embryos. *Developmental Biology*, *316*(2), 471–486. https://doi.org/10.1016/J.YDBIO.2008.01.013

Jaffe, L. A., & Egbert, J. R. (n.d.). *Regulation of Mammalian Oocyte Meiosis by Intercellular Communication Within the Ovarian Follicle*. https://doi.org/10.1146/annurev-physiol-022516-034102

Jagarlamudi, J., & Daumé, H. (2010). Extracting multilingual topics from unaligned comparable corpora. *Lecture Notes in Computer Science (Including Subseries Lecture Notes in Artificial Intelligence and Lecture Notes in Bioinformatics)*, *5993 LNCS*, 444–456. https://doi.org/10.1007/978-3-642-12275-0_39/COVER

Jagarlamudi, K., Reddy, P., Adhikari, D., & Liu, K. (2010). Genetically modified mouse models for premature ovarian failure (POF). *Molecular and Cellular Endocrinology*, *315*(1–2), 1–10. https://doi.org/10.1016/J.MCE.2009.07.016

Jamieson-Lucy, A., & Mullins, M. C. (2019). The vertebrate Balbiani body, germ plasm, and oocyte polarity. *Current Topics in Developmental Biology*, *135*, 1–34. https://doi.org/10.1016/BS.CTDB.2019.04.003

Jansova, D., Aleshkina, D., Jindrova, A., Iyyappan, R., An, Q., Fan, G., & Susor, A. (2021). Single Molecule RNA Localization and Translation in the Mammalian Oocyte and Embryo. *Journal of Molecular Biology*, *433*(19), 167166. https://doi.org/10.1016/J.JMB.2021.167166

Jansova, D., Tetkova, A., Koncicka, M., Kubelka, M., & Susor, A. (2018). Localization of RNA and translation in the mammalian oocyte and embryo. *PloS One*, *13*(3). https://doi.org/10.1371/JOURNAL.PONE.0192544

Jenquin, J. R., Yang, H., Huigens, R. W., Nakamori, M., & Berglund, J. A. (2019). Combination Treatment of Erythromycin and Furamidine Provides Additive and Synergistic Rescue of Mis-splicing in Myotonic Dystrophy Type 1 Models. *ACS Pharmacology and Translational Science*, *2*(4), 247–263. https://doi.org/10.1021/ACSPTSCI.9B00020/SUPPL_FILE/PT9B00020_SI_001.PDF

Johnson, M. H. (n.d.). *Essential reproduction*. 412. Retrieved July 6, 2023, from https://www.wiley.com/en-gb/Essential+Reproduction%2C+8th+Edition-p-9781119246398

Jones, K. T. (2004). Turning it on and off: M-phase promoting factor during meiotic maturation and fertilization. *Molecular Human Reproduction*, *10*(1), 1–5. https://doi.org/10.1093/MOLEHR/GAH009

Jones, K. T. (2008). Meiosis in oocytes: predisposition to aneuploidy and its increased incidence with age. *Human Reproduction Update*, *14*(2), 143–158. https://doi.org/10.1093/HUMUPD/DMM043

Kalab, P., & Heald, R. (2008). The RanGTP gradient – a GPS for the mitotic spindle. *Journal of Cell Science*, *121*(Pt 10), 1577. https://doi.org/10.1242/JCS.005959

Katahira, J. (2012). mRNA export and the TREX complex. *Biochimica et Biophysica Acta*, *1819*(6), 507–513. https://doi.org/10.1016/J.BBAGRM.2011.12.001

Kelemen, O., Convertini, P., Zhang, Z., Wen, Y., Shen, M., Falaleeva, M., & Stamm, S. (2013). Function of alternative splicing. *Gene*, *514*(1), 1–30. https://doi.org/10.1016/J.GENE.2012.07.083

Khan, S., Luck, H., Winer, S., & Winer, D. A. (2021). Emerging concepts in intestinal immune control of obesity-related metabolic disease. *Nature Communications*, *12*(1). https://doi.org/10.1038/S41467-021-22727-7

Kiewisz, R., Fabig, G., Conway, W., Baum, D., Needleman, D., & Müller-Reichert, T. (2022). Three-dimensional structure of kinetochore-fibers in human mitotic spindles. *ELife*, *11*, 75459. https://doi.org/10.7554/ELIFE.75459

Kim, J., Gupta, R., Blanco, L. P., Yang, S., Shteinfer-Kuzmine, A., Wang, K., Zhu, J., Yoon, H. E., Wang, X., Kerkhofs, M., Kang, H., Brown, A. L., Park, S. J., Xu, X., van Rilland, E. Z., Kim, M. K., Cohen, J. I., Kaplan, M. J., Shoshan-Barmatz, V., & Chung, J. H. (2019). VDAC oligomers form mitochondrial pores to release mtDNA fragments and promote lupus-like disease. *Science (New York, N.Y.)*, *366*(6472), 1531–1536. https://doi.org/10.1126/SCIENCE.AAV4011

Kincade, J. N., Hlavacek, A., Akera, T., & Balboula, A. Z. (2023). Initial spindle positioning at the oocyte center protects against incorrect kinetochore-microtubule attachment and aneuploidy in mice. *Science Advances*, *9*(7), eadd7397. https://doi.org/10.1126/SCIADV.ADD7397/SUPPL_FILE/SCIADV.ADD7397_MOVIES_S1_TO_S3.ZIP

Kirillova, A., Smitz, J. E. J., Sukhikh, G. T., & Mazunin, I. (2021). The Role of Mitochondria in Oocyte Maturation. *Cells*, *10*(9). https://doi.org/10.3390/CELLS10092484

Kirkegaard, K., Ahlström, A., Ingerslev, H. J., & Hardarson, T. (2015). Choosing the best embryo by time lapse versus standard morphology. *Fertility and Sterility*, *103*(2), 323–332. https://doi.org/10.1016/J.FERTNSTERT.2014.11.003

Kirschner, M. W., & Mitchison, T. (1986). Microtubule dynamics. *Nature*, *324*(6098), 621. https://doi.org/10.1038/324621A0

Kirschner, M., & Mitchison, T. (1986). Beyond self-assembly: from microtubules to morphogenesis. *Cell*, *45*(3), 329–342. https://doi.org/10.1016/0092-8674(86)90318-1

Kistler, K. E., Trcek, T., Hurd, T. R., Chen, R., Liang, F. X., Sall, J., Kato, M., & Lehmann, R. (2018). Phase transitioned nuclear Oskar promotes cell division of Drosophila primordial germ cells. *ELife*, *7*. https://doi.org/10.7554/ELIFE.37949

Koubova, J., Menke, D. B., Zhou, Q., Cape, B., Griswold, M. D., & Page, D. C. (2006). Retinoic acid regulates sex-specific timing of meiotic initiation in mice. *Proceedings of the National Academy of Sciences of the United States of America*, *103*(8), 2474–2479. https://doi.org/10.1073/PNAS.0510813103

Kouznetsova, A., Lister, L., Nordenskjöld, M., Herbert, M., & Höög, C. (2007). Bi-orientation of achiasmatic chromosomes in meiosis I oocytes contributes to aneuploidy in mice. *Nature Genetics*, *39*(8), 966–968. https://doi.org/10.1038/NG2065

Kovacs, P., & Lieman, H. J. (2019). Which embryo selection method should be offered to the patients? *Journal of Assisted Reproduction and Genetics*, *36*(4), 603–605. https://doi.org/10.1007/S10815-019-01443-8

Krauhs, E., Little, M., Kempf, T., Hofer-Warbinek, R., Ade, W., & Ponstingl, H. (1981). Complete amino acid sequence of beta-tubulin from porcine brain. *Proceedings of the National Academy of Sciences of the United States of America*, *78*(7), 4156–4160. https://doi.org/10.1073/PNAS.78.7.4156

Krisher, R. L. (2004). The effect of oocyte quality on development. *Journal of Animal Science*, *82 E-Suppl*. https://doi.org/10.2527/2004.8213_supplE14x

Krisher, R. L., & Bavister, B. D. (1998). Responses of oocytes and embryos to the culture environment. *Theriogenology*, *49*(1), 103–114. https://doi.org/10.1016/S0093-691X(97)00405-6

Kues, W. A., Sudheer, S., Herrmann, D., Carnwath, J. W., Havlicek, V., Besenfelder, U., Lehrach, H., Adjaye, J., & Niemann, H. (2008). Genome-wide expression profiling reveals distinct clusters of transcriptional regulation during bovine preimplantation development in vivo. *Proceedings of the National Academy of Sciences of the United States of America*, *105*(50), 19768–19773. https://doi.org/10.1073/PNAS.0805616105/SUPPL_FILE/ST1.XLS

Kyogoku, H., & Kitajima, T. S. (2017). Large Cytoplasm Is Linked to the Error-Prone Nature of Oocytes. *Developmental Cell*, *41*(3), 287-298.e4. https://doi.org/10.1016/J.DEVCEL.2017.04.009

Lakowicz, J. R. (2006). Principles of fluorescence spectroscopy. *Principles of Fluorescence Spectroscopy*, 1–954. https://doi.org/10.1007/978-0-387-46312-4/COVER

Lanuza-López, M. C., Martínez-Garza, S. G., Solórzano-Vázquez, J. F., Paz-Cervantes, D., González-Ortega, C., Maldonado-Rosas, I., Villegas-Moreno, G., Villar-Muñoz, L. G., Arroyo-Méndez, F. A., Gutiérrez-Gutiérrez, A. M., & Piña-Aguilar, R. E. (2020). Oocyte maturation arrest produced by TUBB8 mutations: impact of genetic disorders in infertility treatment. *Gynecological Endocrinology : The Official Journal of the International Society of Gynecological Endocrinology*, *36*(9), 829–834. https://doi.org/10.1080/09513590.2020.1725968

Leese, H. J. (2002). Quiet please, do not disturb: a hypothesis of embryo metabolism and viability. *BioEssays : News and Reviews in Molecular, Cellular and Developmental Biology*, *24*(9), 845–849. https://doi.org/10.1002/BIES.10137

Leese, H. J., Brison, D. R., & Sturmey, R. G. (2022). The Quiet Embryo Hypothesis: 20 years on. *Frontiers in Physiology*, *13*. https://doi.org/10.3389/FPHYS.2022.899485

Lelij, P., Stocsits, R. R., Ladurner, R., Petzold, G., Kreidl, E., Koch, B., Schmitz, J., Neumann, B., Ellenberg, J., & Peters, J. (2014). SNW1 enables sister chromatid cohesion by mediating the splicing of sororin and APC2 pre-mRNAs. *The EMBO Journal*, *33*(22), 2643–2658. https://doi.org/10.15252/EMBJ.201488202

Lemseffer, Y., Terret, M.-E., Campillo, C., & Labrune, E. (2022). Methods for Assessing Oocyte Quality: A Review of Literature. *Biomedicines*, *10*(9). https://doi.org/10.3390/biomedicines10092184

Leonard Huskins, C. (1933). Mitosis and Meiosis. *Nature 1933 132:3323*, *132*(3323), 62–63. https://doi.org/10.1038/132062a0

Leppek, K., Das, R., & Barna, M. (2018). Functional 5' UTR mRNA structures in eukaryotic translation regulation and how to find them. *Nature Reviews. Molecular Cell Biology*, *19*(3), 158–174. https://doi.org/10.1038/NRM.2017.103

Lequarre, A. S., Traverso, J. M., Marchandise, J., & Donnay, I. (2004). Poly(A) RNA is reduced by half during bovine oocyte maturation but increases when meiotic arrest is maintained with CDK inhibitors. *Biology of Reproduction*, *71*(2), 425–431. https://doi.org/10.1095/BIOLREPROD.103.026724

Li, H., Guo, F., Rubinstein, B., & Li, R. (2008). Actin-driven chromosomal motility leads to symmetry breaking in mammalian meiotic oocytes. *Nature Cell Biology*, *10*(11), 1301–1308. https://doi.org/10.1038/NCB1788

Li, J., Lu, M., Zhang, P., Hou, E., Li, T., Liu, X., Xu, X., Wang, Z., Fan, Y., Zhen, X., Li, R., Liu, P., Yu, Y., Hang, J., & Qiao, J. (2020). Aberrant spliceosome expression and altered alternative splicing events correlate with maturation deficiency in human oocytes. *Cell Cycle (Georgetown, Tex.)*, *19*(17), 2182–2194. https://doi.org/10.1080/15384101.2020.1799295

Li, R., & Albertini, D. F. (2013). The road to maturation: somatic cell interaction and self-organization of the mammalian oocyte. *Nature Reviews. Molecular Cell Biology*, *14*(3), 141–152. https://doi.org/10.1038/NRM3531

Li, R., Phillips, D. M., & Mather, J. P. (1995). Activin promotes ovarian follicle development in vitro. *Endocrinology*, *136*(3), 849–856. https://doi.org/10.1210/ENDO.136.3.7867593

Litscher, E. S., Williams, Z., & Wassarman, P. M. (2009). Zona pellucida glycoprotein ZP3 and fertilization in mammals. *Molecular Reproduction and Development*, *76*(10), 933–941. https://doi.org/10.1002/mrd.21046

Little, M., Krauhs, E., & Ponstingl, H. (1981). Tubulin sequence conservation. *Bio Systems*, *14*(3–4), 239–246. https://doi.org/10.1016/0303-2647(81)90031-9

Liu, M. (2011). The biology and dynamics of mammalian cortical granules. *Reproductive Biology and Endocrinology : RB&E*, *9*. https://doi.org/10.1186/1477-7827-9-149

Lodde, V., Luciano, A. M., Musmeci, G., Miclea, I., Tessaro, I., Aru, M., Albertini, D. F., & Franciosi, F. (2021). A Nuclear and Cytoplasmic Characterization of Bovine Oocytes Reveals That Cysteamine Partially Rescues the Embryo Development in a Model of Low Ovarian Reserve. *Animals : An Open Access Journal from MDPI*, *11*(7). https://doi.org/10.3390/ANI11071936

Lodde, V., Modina, S., Galbusera, C., Franciosi, F., & Luciano, A. M. (2007). Large-scale chromatin remodeling in germinal vesicle bovine oocytes: Interplay with gap

junction functionality and developmental competence. *Molecular Reproduction and Development*, *74*(6), 740–749. https://doi.org/10.1002/MRD.20639

Lodge, C., & Herbert, M. (2020). Oocyte aneuploidy-more tools to tackle an old problem. *Proceedings of the National Academy of Sciences of the United States of America*, *117*(22), 11850–11852. https://doi.org/10.1073/PNAS.2005739117/ASSET/C07385A8-9429-4A10-85D4-75892883B020/ASSETS/GRAPHIC/PNAS.2005739117FIG01.JPEG

Longo, F. J., & Chen, D. Y. (1985). Development of cortical polarity in mouse eggs: involvement of the meiotic apparatus. *Developmental Biology*, *107*(2), 382–394. https://doi.org/10.1016/0012-1606(85)90320-3

Lu, Q., Moore, G. D., Walss, C., & Ludueña, R. F. (1999). Structural and functional properties of tubulin isotypes. *Advances in Structural Biology*, *5*(C), 203–227. https://doi.org/10.1016/S1064-6000(98)80012-4

Luchniak, A., Kuo, Y. W., McGuinness, C., Sutradhar, S., Orbach, R., Mahamdeh, M., & Howard, J. (2023). Dynamic microtubules slow down during their shrinkage phase. *Biophysical Journal*, *122*(4), 616–623. https://doi.org/10.1016/j.bpj.2023.01.020

Luciano, A. M., Franciosi, F., Lodde, V., Tessaro, I., Corbani, D., Modina, S. C., & Peluso, J. J. (2013). Oocytes isolated from dairy cows with reduced ovarian reserve have a high frequency of aneuploidy and alterations in the localization of progesterone receptor membrane component 1 and aurora kinase B. *Biology of Reproduction*, *88*(3). https://doi.org/10.1095/BIOLREPROD.112.106856

Luduena, R. F., & Little, M. (1981). Comparative structure and chemistry of tubulins from different eukaryotes. *Biosystems*, *14*(3–4), 231–238. https://doi.org/10.1016/0303-2647(81)90030-7

Ma, N., Mochel, N. R. de, Pham, P. D., Yoo, T. Y., Cho, K. W. Y., & Digman, M. A. (2019). Label-free assessment of pre-implantation embryo quality by the Fluorescence Lifetime Imaging Microscopy (FLIM)-phasor approach. *Scientific Reports*, *9*(1). https://doi.org/10.1038/S41598-019-48107-2

Machaty, Z. (2016). Signal transduction in mammalian oocytes during fertilization. *Cell and Tissue Research*, *363*(1), 169–183. https://doi.org/10.1007/S00441-015-2291-8

Mailloux, R. J. (2020). An Update on Mitochondrial Reactive Oxygen Species Production. *Antioxidants 2020, Vol. 9, Page 472*, *9*(6), 472. https://doi.org/10.3390/ANTIOX9060472

Malhi, P. S., Adams, G. P., & Singh, J. (2005). Bovine model for the study of reproductive aging in women: follicular, luteal, and endocrine characteristics. *Biology of Reproduction*, *73*(1), 45–53. https://doi.org/10.1095/BIOLREPROD.104.038745

Mamo, S., Carter, F., Lonergan, P., Leal, C. L., Al Naib, A., Mcgettigan, P., Mehta, J. P., Co Evans, A., & Fair, T. (2011). *Sequential analysis of global gene expression profiles*

in immature and in vitro matured bovine oocytes: potential molecular markers of oocyte maturation. https://doi.org/10.1186/1471-2164-12-151

Mann, J. S., Lowther, K. M., & Mehlmann, L. M. (2010). Reorganization of the endoplasmic reticulum and development of Ca2+ release mechanisms during meiotic maturation of human oocytes. *Biology of Reproduction*, *83*(4), 578–583. https://doi.org/10.1095/BIOLREPROD.110.085985

Mao, L., Lou, H., Lou, Y., Wang, N., & Jin, F. (2014). Behaviour of cytoplasmic organelles and cytoskeleton during oocyte maturation. *Reproductive Biomedicine Online*, *28*(3), 284–299. https://doi.org/10.1016/J.RBMO.2013.10.016

Mascarenhas, M. N., Flaxman, S. R., Boerma, T., Vanderpoel, S., & Stevens, G. A. (2012). National, Regional, and Global Trends in Infertility Prevalence Since 1990: A Systematic Analysis of 277 Health Surveys. *PLoS Medicine*, *9*(12). https://doi.org/10.1371/journal.pmed.1001356

Matković, J., Ghosh, S., Ćosić, M., Eibes, S., Barišić, M., Pavin, N., & Tolić, I. M. (2022). Kinetochore- and chromosome-driven transition of microtubules into bundles promotes spindle assembly. *Nature Communications 2022 13:1*, *13*(1), 1–18. https://doi.org/10.1038/s41467-022-34957-4

Matoulkova, E., Michalova, E., Vojtesek, B., & Hrstka, R. (2012). *RNA Biology The role of the 3' untranslated region in post-transcriptional regulation of protein expression in mammalian cells*. https://doi.org/10.4161/rna.20231

Mattson, B. A., & Albertini, D. F. (1990). Oogenesis: chromatin and microtubule dynamics during meiotic prophase. *Molecular Reproduction and Development*, *25*(4), 374–383. https://doi.org/10.1002/MRD.1080250411

May-Panloup, P., Chretien, M. F., Malthiery, Y., & Reynier, P. (2007). Mitochondrial DNA in the oocyte and the developing embryo. *Current Topics in Developmental Biology*, *77*, 51–83. https://doi.org/10.1016/S0070-2153(06)77003-X

McBride, H. M., Neuspiel, M., & Wasiak, S. (2006). Mitochondria: More Than Just a Powerhouse. *Current Biology*, *16*(14). https://doi.org/10.1016/J.CUB.2006.06.054

McGlacken-Byrne, S. M., & Conway, G. S. (2022). Premature ovarian insufficiency. *Best Practice & Research. Clinical Obstetrics & Gynaecology*, *81*, 98–110. https://doi.org/10.1016/J.BPOBGYN.2021.09.011

Ménézo, Y. J. R., & Hérubel, F. (2002). Mouse and bovine models for human IVF. *Reproductive Biomedicine Online*, *4*(2), 170–175. https://doi.org/10.1016/S1472-6483(10)61936-0

Mercer, T. R., Dinger, M. E., & Mattick, J. S. (2009). Long non-coding RNAs: insights into functions. *Nature Reviews. Genetics*, *10*(3), 155–159. https://doi.org/10.1038/NRG2521

Metchat, A., Eguren, M., Hossain, J. M., Politi, A. Z., Huet, S., & Ellenberg, J. (2015). An actin-dependent spindle position checkpoint ensures the asymmetric division in mouse oocytes. *Nature Communications 2015 6:1*, *6*(1), 1–10. https://doi.org/10.1038/ncomms8784

Mignone, F., Gissi, C., Liuni, S., & Pesole, G. (2002). Untranslated regions of mRNAs. *Genome Biology*, *3*(3), 1–10. https://doi.org/10.1186/GB-2002-3-3-REVIEWS0004/TABLES/6

Mihajlović, A. I., & FitzHarris, G. (2018). Segregating Chromosomes in the Mammalian Oocyte. *Current Biology*, *28*(16), R895–R907. https://doi.org/10.1016/J.CUB.2018.06.057

Mikkelsen, A. L., & Lindenberg, S. (2001). Morphology of in-vitro matured oocytes: impact on fertility potential and embryo quality. *Human Reproduction (Oxford, England)*, *16*(8), 1714–1718. https://doi.org/10.1093/HUMREP/16.8.1714

Mikwar, M., MacFarlane, A. J., & Marchetti, F. (2020). Mechanisms of oocyte aneuploidy associated with advanced maternal age. In *Mutation Research - Reviews in Mutation Research* (Vol. 785). Elsevier B.V. https://doi.org/10.1016/j.mrrev.2020.108320

Mirre, C., Hartung, M., & Stahl, A. (1980). Association of ribosomal genes in the fibrillar center of the nucleolus: a factor influencing translocation and nondisjunction in the human meiotic oocyte. *Proceedings of the National Academy of Sciences of the United States of America*, *77*(10), 6017–6021. https://doi.org/10.1073/PNAS.77.10.6017

Mishina, T., Tabata, N., Hayashi, T., Yoshimura, M., Umeda, M., Mori, M., Ikawa, Y., Hamada, H., Nikaido, I., & Kitajima, T. S. (2021). Single-oocyte transcriptome analysis reveals aging-associated effects influenced by life stage and calorie restriction. *Aging Cell*, *20*(8), e13428. https://doi.org/10.1111/ACEL.13428

Mitchison, T. J. (2014). The engine of microtubule dynamics comes into focus. *Cell*, *157*(5), 1008–1010. https://doi.org/10.1016/j.cell.2014.05.001

Modina, S. C., Tessaro, I., Lodde, V., Franciosi, F., Corbani, D., & Luciano, A. M. (2014). Reductions in the number of mid-sized antral follicles are associated with markers of premature ovarian senescence in dairy cows. *Reproduction, Fertility, and Development*, *26*(2), 235–244. https://doi.org/10.1071/RD12295

Modrek, B., & Lee, C. (2002). A genomic view of alternative splicing. *Nature Genetics*, *30*(1), 13–19. https://doi.org/10.1038/NG0102-13

Molecular Biology of the Cell - NCBI Bookshelf. (n.d.). Retrieved July 6, 2023, from https://www.ncbi.nlm.nih.gov/books/NBK21054/

Moreno, R. D., Schatten, G., & Ramalho-Santos, J. (2002). Golgi Apparatus Dynamics During Mouse Oocyte In Vitro Maturation: Effect of the Membrane Trafficking Inhibitor

Brefeldin A. *Biology of Reproduction*, *66*(5), 1259–1266. https://doi.org/10.1095/BIOLREPROD66.5.1259

Motta, P. M., Nottola, S. A., Makabe, S., Heyn, R., & Jansen, R. (2000). Mitochondrial morphology in human fetal and adult female germ cells. *Human Reproduction (Oxford, England)*, *15 Suppl 2*(SUPPL. 2), 129–147. https://doi.org/10.1093/HUMREP/15.SUPPL_2.129

Musacchio, A. (2015). The Molecular Biology of Spindle Assembly Checkpoint Signaling Dynamics. *Current Biology*, *25*(20), R1002–R1018.

Musacchio, A., & Salmon, E. D. (2007). The spindle-assembly checkpoint in space and time. *Nature Reviews Molecular Cell Biology 2007 8:5*, *8*(5), 379–393. https://doi.org/10.1038/nrm2163

Nachury, M. V., Maresca, T. J., Salmon, W. C., Waterman-Storer, C. M., Heald, R., & Weis, K. (2001). Importin beta is a mitotic target of the small GTPase Ran in spindle assembly. *Cell*, *104*(1), 95–106. https://doi.org/10.1016/S0092-8674(01)00194-5

Nardelli, A. A., Stafinski, T., Motan, T., Klein, K., & Menon, D. (2014). Assisted reproductive technologies (ARTs): Evaluation of evidence to support public policy development. *Reproductive Health*, *11*(1), 1–14. https://doi.org/10.1186/1742-4755-11-76/FIGURES/3

Nelson, L. M. (2009). Clinical practice. Primary ovarian insufficiency. *The New England Journal of Medicine*, *360*(6), 606–614. https://doi.org/10.1056/NEJMCP0808697

Nogales, E. (2015). An electron microscopy journey in the study of microtubule structure and dynamics. *Protein Science : A Publication of the Protein Society*, *24*(12), 1912. https://doi.org/10.1002/PRO.2808

Nogales, E. (2016). Dear microtubule, I see you. *Molecular Biology of the Cell*, *27*(21), 3202. https://doi.org/10.1091/MBC.E16-06-0372

Oka, Y., Varmark, H., Vitting-Seerup, K., Beli, P., Waage, J., Hakobyan, A., Mistrik, M., Choudhary, C., Rohde, M., Bekker-Jensen, S., & Mailand, N. (2014). UBL5 is essential for pre-mRNA splicing and sister chromatid cohesion in human cells. *EMBO Reports*, *15*(9), 956–964. https://doi.org/10.15252/EMBR.201438679

Oktay, K., Briggs, D., & Gosden, R. G. (1997). Ontogeny of follicle-stimulating hormone receptor gene expression in isolated human ovarian follicles. *The Journal of Clinical Endocrinology and Metabolism*, *82*(11), 3748–3751. https://doi.org/10.1210/JCEM.82.11.4346

Onukwufor, J. O., Berry, B. J., & Wojtovich, A. P. (2019). Physiologic Implications of Reactive Oxygen Species Production by Mitochondrial Complex I Reverse Electron Transport. *Antioxidants*, *8*(8). https://doi.org/10.3390/ANTIOX8080285

Ozturk, S. (2020). Selection of competent oocytes by morphological criteria for assisted reproductive technologies. *Molecular Reproduction and Development*, *87*(10), 1021–1036. https://doi.org/10.1002/MRD.23420

Pacchiarotti, A., Selman, H., Valeri, C., Napoletano, S., Sbracia, M., Antonini, G., Biagiotti, G., & Pacchiarotti, A. (2016). Ovarian Stimulation Protocol in IVF: An Up-to-Date Review of the Literature. *Current Pharmaceutical Biotechnology*, *17*(4), 303–315. https://doi.org/10.2174/1389201017666160118103147

Pailas, A., Niaka, K., Zorzompokou, C., & Marangos, P. (2022). The DNA Damage Response in Fully Grown Mammalian Oocytes. *Cells*, *11*(5). https://doi.org/10.3390/CELLS11050798

Palacios, M. J., Joshi, H. C., Simerly, C., & Schatten, G. (1993). Gamma-tubulin reorganization during mouse fertilization and early development. *Journal of Cell Science*, *104 (Pt 2)*(2), 383–389. https://doi.org/10.1242/JCS.104.2.383

Palermo, R. (2007). Differential actions of FSH and LH during folliculogenesis. *Reproductive Biomedicine Online*, *15*(3), 326–337. https://doi.org/10.1016/S1472-6483(10)60347-1

Pan, B., & Li, J. (2019). The art of oocyte meiotic arrest regulation. *Reproductive Biology and Endocrinology 2019 17:1*, *17*(1), 1–12. https://doi.org/10.1186/S12958-018-0445-8

Pang, P. C., Chiu, P. C. N., Lee, C. L., Chang, L. Y., Panico, M., Morris, H. R., Haslam, S. M., Khoo, K. H., Clark, G. F., Yeung, W. S. B., & Dell, A. (2011). Human sperm binding is mediated by the sialyl-Lewis(x) oligosaccharide on the zona pellucida. *Science (New York, N.Y.)*, *333*(6050), 1761–1764. https://doi.org/10.1126/SCIENCE.1207438

Parfenov, V., Potchukalina, G., Dudina, L., Kostyuchek, D., & Gruzova, M. (1989). Human antral follicles: oocyte nucleus and the karyosphere formation (electron microscopic and autoradiographic data). *Gamete Research*, *22*(2), 219–231. https://doi.org/10.1002/MRD.1120220209

Pasquariello, R., Ermisch, A. F., Silva, E., McCormick, S., Logsdon, D., Barfield, J. P., Schoolcraft, W. B., & Krisher, R. L. (2019). Alterations in oocyte mitochondrial number and function are related to spindle defects and occur with maternal aging in mice and humans†. *Biology of Reproduction*, *100*(4), 971–981. https://doi.org/10.1093/BIOLRE/IOY248

Patrizio, P., & Sakkas, D. (2009). From oocyte to baby: a clinical evaluation of the biological efficiency of in vitro fertilization. *Fertility and Sterility*, *91*(4), 1061–1066. https://doi.org/10.1016/j.fertnstert.2008.01.003

Payne, C., & Schatten, G. (2003). Golgi dynamics during meiosis are distinct from mitosis and are coupled to endoplasmic reticulum dynamics until fertilization. *Developmental Biology*, *264*(1), 50–63. https://doi.org/10.1016/J.YDBIO.2003.08.004

Pelley, J. W. (2012). Citric Acid Cycle, Electron Transport Chain, and Oxidative Phosphorylation. *Elsevier's Integrated Review Biochemistry*, 57–65. https://doi.org/10.1016/B978-0-323-07446-9.00007-6

Pietroforte, S., Monasterio, M. B., Ferrer-Vaquer, A., Irimia, M., Ibáñez, E., Popovic, M., Vassena, R., & Zambelli, F. (2023). Specific processing of meiosis-related transcript is linked to final maturation in human oocytes. *Molecular Human Reproduction*. https://doi.org/10.1093/MOLEHR/GAAD021

Plachot, M., Selva, J., Wolf, J. P., Bastit, P., & De Mouzon, J. (2002). [Consequences of oocyte dysmorphy on the fertilization rate and embryo development after intracytoplasmic sperm injection. A prospective multicenter study]. *Gynecologie, Obstetrique & Fertilite*, *30*(10), 772–779. https://doi.org/10.1016/S1297-9589(02)00437-X

Pühringer, T., Hohmann, U., Fin, L., Pacheco-Fiallos, B., Schellhaas, U., Brennecke, J., & Plaschka, C. (2020). Structure of the human core transcription-export complex reveals a hub for multivalent interactions. *ELife*, *9*, 1–65. https://doi.org/10.7554/ELIFE.61503

Rama Raju, G. A., Prakash, G. J., Krishna, K. M., & Madan, K. (2007). Meiotic spindle and zona pellucida characteristics as predictors of embryonic development: a preliminary study using PolScope imaging. *Reproductive Biomedicine Online*, *14*(2), 166–174. https://doi.org/10.1016/S1472-6483(10)60784-5

Rémillard-Labrosse, G., Dean, N. L., Allais, A., Mihajlović, A. I., Jin, S. G., Son, W. Y., Chung, J. T., Pansera, M., Henderson, S., Mahfoudh, A., Steiner, N., Agapitou, K., Marangos, P., Buckett, W., Ligeti-Ruiter, J., & FitzHarris, G. (2020). Human oocytes harboring damaged DNA can complete meiosis I. *Fertility and Sterility*, *113*(5), 1080-1089.e2. https://doi.org/10.1016/J.FERTNSTERT.2019.12.029

Revenkova, E., Herrmann, K., Adelfalk, C., & Jessberger, R. (2010). Oocyte cohesin expression restricted to predictyate stages provides full fertility and prevents aneuploidy. *Current Biology : CB*, *20*(17), 1529–1533. https://doi.org/10.1016/J.CUB.2010.08.024

Reyes, J. M., Silva, E., Chitwood, J. L., Schoolcraft, W. B., Krisher, R. L., & Ross, P. J. (2017). Differing molecular response of young and advanced maternal age human oocytes to IVM. *Human Reproduction (Oxford, England)*, *32*(11), 2199–2208. https://doi.org/10.1093/HUMREP/DEX284

Reynier, P., May-Panloup, P., Chrétien, M. F., Morgan, C. J., Jean, M., Savagner, F., Barrière, P., & Malthièry, Y. (2001). Mitochondrial DNA content affects the fertilizability of human oocytes. *Molecular Human Reproduction*, *7*(5), 425–429. https://doi.org/10.1093/MOLEHR/7.5.425

Richard, S., & Baltz, J. M. (2014). Prophase I arrest of mouse oocytes mediated by natriuretic peptide precursor C requires GJA1 (connexin-43) and GJA4 (connexin-37) gap junctions in the antral follicle and cumulus-oocyte complex. *Biology of Reproduction*, *90*(6), 137–138. https://doi.org/10.1095/BIOLREPROD.114.118505/2514359

Richter, J. D., & Lasko, P. (2011). Translational Control in Oocyte Development. *Cold Spring Harbor Perspectives in Biology*, *3*(9), 1–14. https://doi.org/10.1101/CSHPERSPECT.A002758

Rienzi, L., Balaban, B., Ebner, T., & Mandelbaum, J. (2012). The oocyte. *Human Reproduction*, *27*(suppl_1), i2–i21. https://doi.org/10.1093/HUMREP/DES200

Rodríguez, S. A., Grochová, D., Mckenna, T., Borate, B., Trivedi, N. S., Erdos, M. R., & Eriksson, M. (2016). Global genome splicing analysis reveals an increased number of alternatively spliced genes with aging. *Aging Cell*, *15*(2), 267–278. https://doi.org/10.1111/acel.12433

Roeles, J., & Tsiavaliaris, G. (2019). Actin-microtubule interplay coordinates spindle assembly in human oocytes. *Nature Communications*, *10*(1). https://doi.org/10.1038/S41467-019-12674-9

Rosenbusch, B., Schneider, M., Gläser, B., & Brucker, C. (2002). Cytogenetic analysis of giant oocytes and zygotes to assess their relevance for the development of digynic triploidy. *Human Reproduction*, *17*(9), 2388–2393. https://doi.org/10.1093/HUMREP/17.9.2388

Ruebel, M. L., Schall, P. Z., Midic, U., Vincent, K. A., Goheen, B., & Vandevoort, C. A. (2018). Transcriptome analysis of rhesus monkey failed-to-mature oocytes: deficiencies in transcriptional regulation and cytoplasmic maturation of the oocyte mRNA population. *Molecular Human Reproduction*, *24*(10), 478–494. https://doi.org/10.1093/MOLEHR/GAY032

Ruebel, M. L., Zambelli, F., Schall, P. Z., Barragan, M., Vandevoort, C. A., Vassena, R., & Latham, K. E. (2021). Shared aspects of mRNA expression associated with oocyte maturation failure in humans and rhesus monkeys indicating compromised oocyte quality. *Physiological Genomics*, *53*(4), 137–149. https://doi.org/10.1152/PHYSIOLGENOMICS.00155.2020

Ruggeri, E., Deluca, K. F., Galli, C., Lazzari, G., Deluca, J. G., & Carnevale, E. M. (2015). Cytoskeletal alterations associated with donor age and culture interval for equine oocytes and potential zygotes that failed to cleave after ICSI. *Reproduction, Fertility, and Development*, *27*(6), 944. https://doi.org/10.1071/RD14468

Salisbury, J., Hutchison, K. W., Wigglesworth, K., Eppig, J. J., & Graber, J. H. (2009). Probe-level analysis of expression microarrays characterizes isoform-specific degradation during mouse oocyte maturation. *PloS One*, *4*(10). https://doi.org/10.1371/JOURNAL.PONE.0007479

Samura, O., Nakaoka, Y., & Miharu, N. (2023). Sperm and Oocyte Chromosomal Abnormalities. *Biomolecules 2023, Vol. 13, Page 1010*, *13*(6), 1010. https://doi.org/10.3390/BIOM13061010

Sánchez, F., & Smitz, J. (2012). Molecular control of oogenesis. *Biochimica et Biophysica Acta (BBA) - Molecular Basis of Disease*, *1822*(12), 1896–1912. https://doi.org/10.1016/J.BBADIS.2012.05.013

Sanchez, T., Venturas, M., Aghvami, S. A., Yang, X., Fraden, S., Sakkas, D., & Needleman, D. J. (2019). Combined noninvasive metabolic and spindle imaging as potential tools for embryo and oocyte assessment. *Human Reproduction (Oxford, England)*, *34*(12), 2349–2361. https://doi.org/10.1093/HUMREP/DEZ210

Sanchez, T., Zhang, M., Needleman, D., & Seli, E. (2019). Metabolic imaging via fluorescence lifetime imaging microscopy for egg and embryo assessment. *Fertility and Sterility*, *111*(2), 212–218. https://doi.org/10.1016/j.fertnstert.2018.12.014

Santos, T. A., El Shourbagy, S., & St. John, J. C. (2006). Mitochondrial content reflects oocyte variability and fertilization outcome. *Fertility and Sterility*, *85*(3), 584–591. https://doi.org/10.1016/J.FERTNSTERT.2005.09.017

Sathananthan, A. H. (1994). Ultrastructural changes during meiotic maturation in mammalian oocytes: unique aspects of the human oocyte. *Microscopy Research and Technique*, *27*(2), 145–164. https://doi.org/10.1002/JEMT.1070270208

SATHANANTHAN, A. H., NG, S. C., CHIA, C. M., LAW, H. Y., EDIRISINGHE, W. R., & RATNAM, S. S. (1985). The origin and distribution of cortical granules in human oocytes with reference to Golgi, nucleolar, and microfilament activity. *Annals of the New York Academy of Sciences*, *442*(1), 251–264. https://doi.org/10.1111/J.1749-6632.1985.TB37526.X

Schieber, M., & Chandel, N. S. (2014). ROS Function in Redox Signaling and Oxidative Stress. *Current Biology : CB*, *24*(10), R453. https://doi.org/10.1016/J.CUB.2014.03.034

Schon, E. A., Kim, S. H., Ferreira, J. C., Magalhães, P., Grace, M., Warburton, D., & Gross, S. J. (2000). Mitochondrial distribution and function in oocytes and early embryos. *Human Reproduction (Oxford, England)*, *15 Suppl 2*, 189–198. https://doi.org/10.1093/HUMREP/15.SUPPL_2.189

Schuh, M., & Ellenberg, J. (2007). Self-Organization of MTOCs Replaces Centrosome Function during Acentrosomal Spindle Assembly in Live Mouse Oocytes. *Cell*, *130*(3), 484–498. https://doi.org/10.1016/j.cell.2007.06.025

Schultz, R. M. (1993). Regulation of zygotic gene activation in the mouse. *BioEssays*, *15*(8), 531–538. https://doi.org/10.1002/bies.950150806

Scott, I., & Youle, R. J. (2010). Mitochondrial fission and fusion. *Essays in Biochemistry*, *47*, 85–98. https://doi.org/10.1042/BSE0470085

Severance, A. L., Midic, U., & Latham, K. E. (2020). Genotypic divergence in mouse oocyte transcriptomes: Possible pathways to hybrid vigor impacting fertility and embryogenesis. *Physiological Genomics*, *52*(2), 96–109.

https://doi.org/10.1152/PHYSIOLGENOMICS.00078.2019/ASSET/IMAGES/LARGE/ZH70012044010006.JPEG

Seydoux, G. (2018). The P Granules of C. elegans: A Genetic Model for the Study of RNA-Protein Condensates. *Journal of Molecular Biology*, *430*(23), 4702–4710. https://doi.org/10.1016/J.JMB.2018.08.007

Shestakova, I. G., Radzinsky, V. E., & Khamoshina, M. B. (2016). Occult form of premature ovarian insufficiency. *Gynecological Endocrinology*, *32*, 30–32. https://doi.org/10.1080/09513590.2016.1232676

Siomi, M. C., Sato, K., Pezic, D., & Aravin, A. A. (2011). PIWI-interacting small RNAs: the vanguard of genome defence. *Nature Reviews. Molecular Cell Biology*, *12*(4), 246–258. https://doi.org/10.1038/NRM3089

Sirard, M. A., Richard, F., Blondin, P., & Robert, C. (2006). Contribution of the oocyte to embryo quality. *Theriogenology*, *65*(1), 126–136. https://doi.org/10.1016/J.THERIOGENOLOGY.2005.09.020

Skala, M. C., Riching, K. M., Bird, D. K., Gendron-Fitzpatrick, A., Eickhoff, J., Eliceiri, K. W., Keely, P. J., & Ramanujam, N. (2007). In vivo multiphoton fluorescence lifetime imaging of protein-bound and free nicotinamide adenine dinucleotide in normal and precancerous epithelia. *Journal of Biomedical Optics*, *12*(2), 024014. https://doi.org/10.1117/1.2717503

So, C., Menelaou, K., Uraji, J., Harasimov, K., Steyer, A. M., Seres, K. B., Bucevičius, J., Lukinavičius, G., Möbius, W., Sibold, C., Tandler-Schneider, A., Eckel, H., Moltrecht, R., Blayney, M., Elder, K., & Schuh, M. (2022). Mechanism of spindle pole organization and instability in human oocytes. *Science (New York, N.Y.)*, *375*(6581). https://doi.org/10.1126/SCIENCE.ABJ3944

Stäßer, K., Masuda, S., Mason, P., Pfannstiel, J., Oppizzi, M., Rodriguez-Navarro, S., Rondón, A. G., Aguilera, A., Struhl, K., Reed, R., & Hurt, E. (2002). TREX is a conserved complex coupling transcription with messenger RNA export. *Nature*, *417*(6886), 304–308. https://doi.org/10.1038/NATURE746

Stein, L. R., & Imai, S. I. (2012). The dynamic regulation of NAD metabolism in mitochondria. *Trends in Endocrinology and Metabolism: TEM*, *23*(9), 420–428. https://doi.org/10.1016/J.TEM.2012.06.005

Stojkovic, M., Machado, S. A., Stojkovic, P., Zakhartchenko, V., Hutzler, P., Gonçalves, P. B., & Wolf, E. (2001). Mitochondrial distribution and adenosine triphosphate content of bovine oocytes before and after in vitro maturation: correlation with morphological criteria and developmental capacity after in vitro fertilization and culture. *Biology of Reproduction*, *64*(3), 904–909. https://doi.org/10.1095/BIOLREPROD64.3.904

Strączyńska, P., Papis, K., Morawiec, E., Czerwiński, M., Gajewski, Z., Olejek, A., & Bednarska-Czerwińska, A. (2022). Signaling mechanisms and their regulation during in

vivo or in vitro maturation of mammalian oocytes. *Reproductive Biology and Endocrinology 2022 20:1*, *20*(1), 1–12. https://doi.org/10.1186/S12958-022-00906-5

Su, A. I., Cooke, M. P., Ching, K. A., Hakak, Y., Walker, J. R., Wiltshire, T., Orth, A. P., Vega, R. G., Sapinoso, L. M., Moqrich, A., Patapoutian, A., Hampton, G. M., Schultz, P. G., & Hogenesch, J. B. (2002). Large-scale analysis of the human and mouse transcriptomes. *Proceedings of the National Academy of Sciences of the United States of America*, *99*(7), 4465–4470. https://doi.org/10.1073/PNAS.012025199

Su, Y. Q., Sugiura, K., Woo, Y., Wigglesworth, K., Kamdar, S., Affourtit, J., & Eppig, J. J. (2007). Selective degradation of transcripts during meiotic maturation of mouse oocytes. *Developmental Biology*, *302*(1), 104–117. https://doi.org/10.1016/J.YDBIO.2006.09.008

Sun, M., Jia, M., Ren, H., Yang, B., Chi, W., Xin, G., Jiang, Q., & Zhang, C. (2021). NuMA regulates mitotic spindle assembly, structural dynamics and function via phase separation. *Nature Communications*, *12*(1). https://doi.org/10.1038/S41467-021-27528-6

Sun, Q. Y., Wu, G. M., Lai, L., Park, K. W., Cabot, R., Cheong, H. T., Day, B. N., Prather, R. S., & Schatten, H. (2001). Translocation of active mitochondria during pig oocyte maturation, fertilization and early embryo development in vitro. *Reproduction*, *122*(1), 155–163. https://doi.org/10.1530/REP.0.1220155

Sundaramoorthy, S., Vázquez-Novelle, M. D., Lekomtsev, S., Howell, M., & Petronczki, M. (2014). Functional genomics identifies a requirement of pre-mRNA splicing factors for sister chromatid cohesion. *The EMBO Journal*, *33*(22), 2623–2642. https://doi.org/10.15252/EMBJ.201488244

Susor, A., Jansova, D., Cerna, R., Danylevska, A., Anger, M., Toralova, T., Malik, R., Supolikova, J., Cook, M. S., Oh, J. S., & Kubelka, M. (2015). Temporal and spatial regulation of translation in the mammalian oocyte via the mTOR-eIF4F pathway. *Nature Communications*, *6*. https://doi.org/10.1038/NCOMMS7078

Szollosi, D. (1967). Development of cortical granules and the cortical reaction in rat and hamster eggs. *The Anatomical Record*, *159*(4), 431–446. https://doi.org/10.1002/AR.1091590412

Takahashi, N., Franciosi, F., Daldello, E. M., Luong, X. G., Althoff, P., Wang, X., & Conti, M. (2023). CPEB1-dependent disruption of the mRNA translation program in oocytes during maternal aging. *Nature Communications 2023 14:1*, *14*(1), 1–17. https://doi.org/10.1038/s41467-023-35994-3

Takahashi, Y., Hashimoto, S., Yamochi, T., Goto, H., Yamanaka, M., Amo, A., Matsumoto, H., Inoue, M., Ito, K., Nakaoka, Y., Suzuki, N., & Morimoto, Y. (2016). Dynamic changes in mitochondrial distribution in human oocytes during meiotic maturation. *Journal of Assisted Reproduction and Genetics*, *33*(7), 929. https://doi.org/10.1007/S10815-016-0716-2

Tan, T. C. Y., Brown, H. M., Thompson, J. G., Mustafa, S., & Dunning, K. R. (2022). Optical imaging detects metabolic signatures associated with oocyte quality†. *Biology of Reproduction*, *107*(4), 1014–1025. https://doi.org/10.1093/BIOLRE/IOAC145

Tang, F., Barbacioru, C., Nordman, E., Bao, S., Lee, C., Wang, X., Tuch, B. B., Heard, E., Lao, K., & Surani, M. A. (2011). Deterministic and stochastic allele specific gene expression in single mouse blastomeres. *PloS One*, *6*(6). https://doi.org/10.1371/JOURNAL.PONE.0021208

Taylor, D. H., Chu, E. T. J., Spektor, R., & Soloway, P. D. (2015). Long non-coding RNA regulation of reproduction and development. *Molecular Reproduction and Development*, *82*(12), 932–956. https://doi.org/10.1002/MRD.22581

Tessaro, I., Luciano, A. M., Franciosi, F., Lodde, V., Corbani, D., & Modina, S. C. (2011). The endothelial nitric oxide synthase/nitric oxide system is involved in the defective quality of bovine oocytes from low mid-antral follicle count ovaries. *Journal of Animal Science*, *89*(8), 2389–2396. https://doi.org/10.2527/JAS.2010-3714

Thomas, C., Cavazza, T., & Schuh, M. (2021). Aneuploidy in human eggs: contributions of the meiotic spindle. *Biochemical Society Transactions*, *49*(1), 107–118. https://doi.org/10.1042/BST20200043

Tilokani, L., Nagashima, S., Paupe, V., & Prudent, J. (2018). Mitochondrial dynamics: overview of molecular mechanisms. *Essays in Biochemistry*, *62*(3), 341. https://doi.org/10.1042/EBC20170104

Tirnauer, J. S., Salmon, E. D., & Mitchison, T. J. (2004). Microtubule Plus-End Dynamics in Xenopus Egg Extract Spindles. *Molecular Biology of the Cell*, *15*(4), 1776. https://doi.org/10.1091/MBC.E03-11-0824

Tollervey, J. R., Wang, Z., Hortobágyi, T., Witten, J. T., Zarnack, K., Kayikci, M., Clark, T. A., Schweitzer, A. C., Rot, G., Curk, T., Zupan, B., Rogelj, B., Shaw, C. E., & Ule, J. (2011). Analysis of alternative splicing associated with aging and neurodegeneration in the human brain. *Genome Research*, *21*(10), 1572–1582. https://doi.org/10.1101/gr.122226.111

Tora, L., & Vincent, S. D. (2021). What defines the maternal transcriptome? *Biochemical Society Transactions*, *49*(5), 2051. https://doi.org/10.1042/BST20201125

Trcek, T., & Lehmann, R. (2019). Germ granules in Drosophila. *Traffic*, *20*(9), 650–660. https://doi.org/10.1111/TRA.12674/

Trebichalská, Z., Kyjovská, D., Kloudová, S., Otevřel, P., Hampl, A., & Holubcová, Z. (2021). Cytoplasmic maturation in human oocytes: an ultrastructural study †. *Biology of Reproduction*, *104*(1), 106–116. https://doi.org/10.1093/BIOLRE/IOAA174

Tucker, E. J., Grover, S. R., Bachelot, A., Touraine, P., & Sinclair, A. H. (2016). Premature Ovarian Insufficiency: New Perspectives on Genetic Cause and Phenotypic Spectrum. *Endocrine Reviews*, *37*(6), 609–635. https://doi.org/10.1210/ER.2016-1047

Tucker, E. J., Tan, T. Y., Stark, Z., & Sinclair, A. H. (2022). Genomic testing in premature ovarian insufficiency: proceed with caution. *Biology of Reproduction*, *107*(5), 1155–1158. https://doi.org/10.1093/BIOLRE/IOAC153

Turathum, B., Gao, E. M., & Chian, R. C. (2021a). The Function of Cumulus Cells in Oocyte Growth and Maturation and in Subsequent Ovulation and Fertilization. *Cells*, *10*(9). https://doi.org/10.3390/CELLS10092292

Turathum, B., Gao, E. M., & Chian, R. C. (2021b). The Function of Cumulus Cells in Oocyte Growth and Maturation and in Subsequent Ovulation and Fertilization. *Cells*, *10*(9). https://doi.org/10.3390/CELLS10092292

Ultrastructure of the human egg - PubMed. (n.d.). Retrieved July 6, 2023, from https://pubmed.ncbi.nlm.nih.gov/9234062/

Van Blerkom, J. (2004). Mitochondria in human oogenesis and preimplantation embryogenesis: engines of metabolism, ionic regulation and developmental competence. *Reproduction (Cambridge, England)*, *128*(3), 269–280. https://doi.org/10.1530/REP.1.00240

van der Reest, J., Nardini Cecchino, G., Haigis, M. C., & Kordowitzki, P. (2021). Mitochondria: Their relevance during oocyte ageing. *Ageing Research Reviews*, *70*. https://doi.org/10.1016/J.ARR.2021.101378

Van Soom, A., Tanghe, S., De Pauw, I., Maes, D., & De Kruif, A. (2002). Function of the cumulus oophorus before and during mammalian fertilization. *Reproduction in Domestic Animals = Zuchthygiene*, *37*(3), 144–151. https://doi.org/10.1046/J.1439-0531.2002.00345.X

Vassena, R., Boué, S., González-Roca, E., Aran, B., Auer, H., Veiga, A., & Belmonte, J. C. I. (2011). Waves of early transcriptional activation and pluripotency program initiation during human preimplantation development. *Development*, *138*(17), 3699–3709. https://doi.org/10.1242/DEV.064741

Vassena, R., Han, Z., Gao, S., Baldwin, D. A., Schultz, R. M., & Latham, K. E. (2007). Tough beginnings: Alterations in the transcriptome of cloned embryos during the first two cell cycles. *Developmental Biology*, *304*(1), 75–89. https://doi.org/10.1016/J.YDBIO.2006.12.015

Venturas, M., Yang, X., Sakkas, D., & Needleman, D. (2023). Noninvasive metabolic profiling of cumulus cells, oocytes, and embryos via fluorescence lifetime imaging microscopy: a mini-review. *Human Reproduction (Oxford, England)*, *38*(5), 799–810. https://doi.org/10.1093/humrep/dead063

Verlhac, M. H., Lefebvre, C., Guillaud, P., Rassinier, P., & Maro, B. (2000). Asymmetric division in mouse oocytes: with or without Mos. *Current Biology : CB*, *10*(20), 1303–1306. https://doi.org/10.1016/S0960-9822(00)00753-3

Viphakone, N., Sudbery, I., Griffith, L., Heath, C. G., Sims, D., & Wilson, S. A. (2019). Co-transcriptional Loading of RNA Export Factors Shapes the Human Transcriptome. *Molecular Cell*, *75*(2), 310-323.e8. https://doi.org/10.1016/j.molcel.2019.04.034

Virant-Klun, I., Knez, K., Tomazevic, T., & Skutella, T. (2013). Gene expression profiling of human oocytes developed and matured in vivo or in vitro. *BioMed Research International*, *2013*. https://doi.org/10.1155/2013/879489

Viste, K., Kopperud, R. K., Christensen, A. E., & Døskeland, S. O. (2005). Substrate enhances the sensitivity of type I protein kinase a to cAMP. *The Journal of Biological Chemistry*, *280*(14), 13279–13284. https://doi.org/10.1074/JBC.M413065200

Vivarelli, E., Conti, M., De Felici, M., & Siracusa, G. (1983). Meiotic resumption and intracellular cAMP levels in mouse oocytes treated with compounds which act on cAMP metabolism. *Cell Differentiation*, *12*(5), 271–276. https://doi.org/10.1016/0045-6039(83)90023-4

Wade, R. H. (2009). On and around microtubules: an overview. *Molecular Biotechnology*, *43*(2), 177–191. https://doi.org/10.1007/S12033-009-9193-5

Wallace, W. H. B., & Kelsey, T. W. (2010). Human ovarian reserve from conception to the menopause. *PloS One*, *5*(1). https://doi.org/10.1371/JOURNAL.PONE.0008772

Wasielak-Politowska, M., & Kordowitzki, P. (2022). Chromosome Segregation in the Oocyte: What Goes Wrong during Aging. *International Journal of Molecular Sciences*, *23*(5). https://doi.org/10.3390/IJMS23052880

Watrin, E., Demidova, M., Watrin, T., Hu, Z., & Prigent, C. (2014). Sororin pre-mRNA splicing is required for proper sister chromatid cohesion in human cells. *EMBO Reports*, *15*(9), 948–955. https://doi.org/10.15252/EMBR.201438640

WHO. (2023). Retrieved June 30, 2023, from https://www.who.int/news/item/04-04-2023-1-in-6-people-globally-affected-by-infertility

Winata, C. L., & Korzh, V. (2018). The translational regulation of maternal mRNAs in time and space. *Febs Letters*, *592*(17), 3007. https://doi.org/10.1002/1873-3468.13183

Wong, J., Nakajima, Y., Westermann, S., Shang, C., Kang, J. S., Goodner, C., Houshmand, P., Fields, S., Chan, C. S. M., Drubin, D., Barnes, G., & Hazbun, T. (2007). A Protein Interaction Map of the Mitotic Spindle. *Molecular Biology of the Cell*, *18*(10), 3800. https://doi.org/10.1091/MBC.E07-06-0536

Wu, J., Liu, Y., Song, Y., Wang, L., Ai, J., & Li, K. (2022). Aging conundrum: A perspective for ovarian aging. *Frontiers in Endocrinology*, *13*. https://doi.org/10.3389/FENDO.2022.952471

Wu, J., Xu, J., Liu, B., Yao, G., Wang, P., Lin, Z., Huang, B., Wang, X., Li, T., Shi, S., Zhang, N., Duan, F., Ming, J., Zhang, X., Niu, W., Song, W., Jin, H., Guo, Y., Dai, S., … Sun, Y. (2018). Chromatin analysis in human early development reveals epigenetic

transition during ZGA. *Nature*, *557*(7704), 256–260. https://doi.org/10.1038/S41586-018-0080-8

Wu, Y. W., Li, S., Zheng, W., Li, Y. C., Chen, L., Zhou, Y., Deng, Z. Q., Lin, G., Fan, H. Y., & Sha, Q. Q. (2022). Dynamic mRNA degradome analyses indicate a role of histone H3K4 trimethylation in association with meiosis-coupled mRNA decay in oocyte aging. *Nature Communications 2022 13:1*, *13*(1), 1–17. https://doi.org/10.1038/s41467-022-30928-x

Wu, Z. W., Mou, Q., Fang, T., Wang, Y., Liang, H., Wang, C., Du, Z. Q., & Yang, C. X. (2022). Global 3'-untranslated region landscape mediated by alternative polyadenylation during meiotic maturation of pig oocytes. *Reproduction in Domestic Animals = Zuchthygiene*, *57*(1), 33–44. https://doi.org/10.1111/RDA.14026

Xiao, W., Wang, R. S., Handy, D. E., & Loscalzo, J. (2018). NAD(H) and NADP(H) Redox Couples and Cellular Energy Metabolism. *Antioxidants & Redox Signaling*, *28*(3), 251. https://doi.org/10.1089/ARS.2017.7216

Xu, X. F., Li, J., Cao, Y. X., Chen, D. W., Zhang, Z. G., He, X. J., Ji, D. M., & Chen, B. L. (2015). Differential Expression of Long Noncoding RNAs in Human Cumulus Cells Related to Embryo Developmental Potential: A Microarray Analysis. *Reproductive Sciences (Thousand Oaks, Calif.)*, *22*(6), 672–678. https://doi.org/10.1177/1933719114561562

Xue, Z., Huang, K., Cai, C., Cai, L., Jiang, C. Y., Feng, Y., Liu, Z., Zeng, Q., Cheng, L., Sun, Y. E., Liu, J. Y., Horvath, S., & Fan, G. (2013). Genetic programs in human and mouse early embryos revealed by single-cell RNA sequencing. *Nature*, *500*(7464), 593–597. https://doi.org/10.1038/NATURE12364

Yamoto, M., Shima, K., & Nakano, R. (1992). Gonadotropin receptors in human ovarian follicles and corpora lutea throughout the menstrual cycle. *Hormone Research*, *37 Suppl 1*, 5–11. https://doi.org/10.1159/000182335

Yan, L., Yang, M., Guo, H., Yang, L., Wu, J., Li, R., Liu, P., Lian, Y., Zheng, X., Yan, J., Huang, J., Li, M., Wu, X., Wen, L., Lao, K., Li, R., Qiao, J., & Tang, F. (2013). Single-cell RNA-Seq profiling of human preimplantation embryos and embryonic stem cells. *Nature Structural & Molecular Biology*, *20*(9), 1131–1139. https://doi.org/10.1038/NSMB.2660

Yan, W., Diao, S., & Fan, Z. (2021). The role and mechanism of mitochondrial functions and energy metabolism in the function regulation of the mesenchymal stem cells. *Stem Cell Research & Therapy*, *12*(1). https://doi.org/10.1186/S13287-021-02194-Z

Yang, F., Wang, W., Cetinbas, M., Sadreyev, R. I., & Blower, M. D. (2020). Genome-wide analysis identifies cis-acting elements regulating mRNA polyadenylation and translation during vertebrate oocyte maturation. *RNA (New York, N.Y.)*, *26*(3), 324–344. https://doi.org/10.1261/RNA.073247.119

Yang, H., Kolben, T., Meister, S., Paul, C., van Dorp, J., Eren, S., Kuhn, C., Rahmeh, M., Mahner, S., Jeschke, U., & von Schönfeldt, V. (2021). Factors Influencing the In Vitro Maturation (IVM) of Human Oocyte. *Biomedicines*, *9*(12). https://doi.org/10.3390/BIOMEDICINES9121904

Yang, Y. jie, Zhang, Y. jun, & Li, Y. (2009). Ultrastructure of human oocytes of different maturity stages and the alteration during in vitro maturation. *Fertility and Sterility*, *92*(1), 396.e1-396.e6. https://doi.org/10.1016/j.fertnstert.2009.02.010

Yao, Y., Liu, S., Xia, C., Gao, Y., Pan, Z., Canela-Xandri, O., Khamseh, A., Rawlik, K., Wang, S., Li, B., Zhang, Y., Pairo-Castineira, E., D'Mellow, K., Li, X., Yan, Z., Li, C. jun, Yu, Y., Zhang, S., Ma, L., … Tenesa, A. (2022). Comparative transcriptome in large-scale human and cattle populations. *Genome Biology*, *23*(1), 1–24. https://doi.org/10.1186/S13059-022-02745-4/FIGURES/8

Yoshida, H., Takakura, N., Kataoka, H., Kunisada, T., Okamura, H., & Nishikawa, S. I. (1997). Stepwise requirement of c-kit tyrosine kinase in mouse ovarian follicle development. *Developmental Biology*, *184*(1), 122–137. https://doi.org/10.1006/DBIO.1997.8503

Yuan, L., Yin, P., Yan, H., Zhong, X., Ren, C., Li, K., Chin Heng, B., Zhang, W., & Tong, G. (2021). Single-cell transcriptome analysis of human oocyte ageing. *Journal of Cellular and Molecular Medicine*, *25*(13), 6289. https://doi.org/10.1111/JCMM.16594

Zaninovic, N., & Rosenwaks, Z. (2020). Artificial intelligence in human in vitro fertilization and embryology. *Fertility and Sterility*, *114*(5), 914–920. https://doi.org/10.1016/J.FERTNSTERT.2020.09.157

Zhang, L., & Jiang, X. H. (2010). Ultrastructure of unfertilized human oocytes and undivided human zygoytes. *Journal of Sichuan University (Medical Science)*, *41*(5), 810–813.

Zhao, H., Li, T., Zhao, Y., Tan, T., Liu, C., Liu, Y., Chang, L., Huang, N., Li, C., Fan, Y., Yu, Y., Li, R., & Qiao, J. (2019). Single-Cell Transcriptomics of Human Oocytes: Environment-Driven Metabolic Competition and Compensatory Mechanisms During Oocyte Maturation. *Antioxidants & Redox Signaling*, *30*(4), 542–559. https://doi.org/10.1089/ARS.2017.7151

Zhao, J., Zhang, J., Yu, M., Xie, Y., Huang, Y., Wolff, D. W., Abel, P. W., & Tu, Y. (2013). Mitochondrial dynamics regulates migration and invasion of breast cancer cells. *Oncogene*, *32*(40), 4814–4824. https://doi.org/10.1038/ONC.2012.494

Zielinska, A. P., Holubcova, Z., Blayney, M., Elder, K., & Schuh, M. (2015). Sister kinetochore splitting and precocious disintegration of bivalents could explain the maternal age effect. *ELife*, *4*(DECEMBER2015). https://doi.org/10.7554/ELIFE.11389

Zuccotti, M., Giorgi Rossi, P., Martinez, A., Garagna, S., Forabosco, A., & Redi, C. A. (1998). Meiotic and developmental competence of mouse antral oocytes. *Biology of Reproduction*, *58*(3), 700–704. https://doi.org/10.1095/BIOLREPROD58.3.700

Zuccotti, M., Merico, V., Cecconi, S., Redi, C. A., & Garagna, S. (2011). What does it take to make a developmentally competent mammalian egg? *Human Reproduction Update*, *17*(4), 525–540. https://doi.org/10.1093/HUMUPD/DMR009

DISSEMINATION

- **Metabolic timelapse reveals that an impaired mitochondrial metabolism contributes to reduce the oocyte maturation rates in women of advanced maternal age.**

  Pietroforte S, Martins M, Ibañez E, Popovic M, Vassena R, Sanchez T, Sakkas D, Zambelli F

  Selected for oral presentation at the Spanish Association for the Study of Reproductive Biology Congress, Palma de Mallorca, Spain, 15-17 November 2023, ASEBIR2023

- **Mitochondrial dynamics drive meiosis and contribute to the development of high quality human oocytes.**

  Pietroforte S, Martins M, Ibañez E, Popovic M, Vassena R, Sanchez T, Sakkas D, Zambelli F

  Selected for oral presentation at the Gordon Research Seminar and Conference Fertilization and Activation of Development – "The Basics of Gamete Biology and Early Development and Their Clinical Implications", Holderness, NH, 22-28 July 2023

- **Poor mitochondrial metabolism impairs meiosis and contributes to reduced oocyte maturation rates in patients with advanced maternal age.**

  Pietroforte S, Martins M, Ibañez E, Popovic M, Vassena R, Sanchez T, Sakkas D, Zambelli F.

  Selected for oral presentation at the 39º European Society of Human Reproduction and Embryology Congress, Copenhagen, Denmark 25-28 July 2023, ESHRE2023

- **Meiosis and maturation of human oocytes are influenced by mitochondrial metabolism.**

  Pietroforte S, Martins M, Ibañez E, Popovic M, Vassena R, Sanchez T, Sakkas D, Zambelli F.

  Selected for oral presentation at the XVIII Biology of Reproduction Symposium, Barcelona, Spain 24 May 2023

- **Non-invasive prediction of oocyte maturation to Metaphase II (MII) from Germinal Vesicle (GV) by mitochondrial function markers using Fluorescence Lifetime Imaging Microscopy (FLIM).**
  Pietroforte S, Martins M, Zambelli F, Vassena R, Gulliford C, Sanchez T, Sakkas D
  Selected for poster presentation at the 78º American Society for Reproductive Medicine Congress, Anaheim, CA, 22-26 October 2022, ASRM2022

- **Meiotic progression of human oocytes is characterized by mRNA splicing events of specific meiosis and spindle associated transcripts.**
  Pietroforte S, Barragan M, Ferrer A, Ibañez E, Vassena R, Zambelli F
  Selected for oral presentation at the 38º European Society of Human Reproduction and Embryology Congress, Milan, Italy 3-6 July 2022, ESHRE2022

- **Low meiotic progression rates in oocytes from older women are due to impaired mitochondrial metabolism.**
  Zambelli F, Pietroforte S, Ibañez E, Vassena R
  Selected for poster presentation at the 38º European Society of Human Reproduction and Embryology Congress, Milan, Italy 3-6 July 2022, ESHRE2022

- **Decreased mitochondrial activity is related to lower *in vitro* maturation rates in oocytes from advanced maternal age women** (Una baja actividad mitocondrial se correlaciona con una tasa reducida de maduración *in vitro* en ovocitos de mujeres de edad materna avanzada).
  Pietroforte S, Ibañez E, Vassena R, Zambelli F
  Selected for oral presentation at the 33º National Spanish Fertility Society Congress, Bilbao, Spain 4-6 May 2022, SEF2022